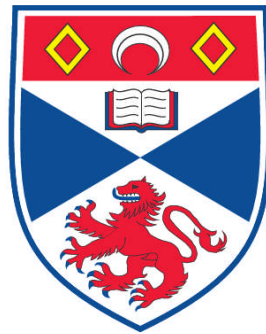


**MORPHOGENESIS IN DROSOPHILA MELANOGASTER : AN IN
VITRO ANALYSIS**

Julie Scarborough

**A Thesis Submitted for the Degree of PhD
at the
University of St. Andrews**



2007

**Full metadata for this item is available in
Research@StAndrews:FullText
at:**

<http://research-repository.st-andrews.ac.uk/>

Please use this identifier to cite or link to this item:

<http://hdl.handle.net/10023/337>

This item is protected by original copyright

**This item is licensed under a
Creative Commons License**

Morphogenesis in
Drosophila melanogaster:
An *in vitro* analysis

Julie Scarborough

Ph.D Thesis submitted for the degree of Doctor of
Philosophy to the University of St Andrews, January 2007

Acknowledgements

Without the help and support of the following people this thesis would not have made its way to the binders.

My Ph.D supervisor Dr. Martin Milner, who was always very supportive and gave me lots of encouragement. I could not have completed so many imaginal disc dissections and observations without his help and technical expertise in microdissection. Martin - thank you for introducing me to the wonderful world of *Drosophila melanogaster*, for giving me free reign in the lab, for carrying out any dissection requests I made and for reading this manuscript. It has been a pleasure to work in your lab.

Dr Deborah Cottam, treasured friend and colleague who always gave me good advice. Thank you for introducing me to the black arts (antibody staining) for asking me the most important questions 'How are you going to assay for that?' and 'Where are your controls?' and for maintaining a perspective when things went wrong in the lab 'lets get some chocolate'. Thank you for reading this manuscript, I couldn't have finished this thesis without your help.

Mr. John Mackintyre, friend and colleague who always gave expert technical help when required. John, thank you listening to my moans about children and life in general, I will miss your good humour and kind words.

Ms Jill McVee, another treasured friend, thank you for your friendship over the past years and the expert technical advice which was thrown in during lunches. I will miss you.

Messrs, Dave Roche and Jim Allan in photography, thanks for the friendship and attempts at humour over the past few years! A special thank you to Jim who helped out with printing when I was coming to the end of this thesis.

Mr. Murray Coutts for coming to my rescue when computers did strange things.

All the staff in the Schools of Biology and Medicine who have become good friends, particularly Jim, Steve, Sue, the two Sandra's and Morven. My friends, John and Neda, who have given long distance advice, support and friendship over the last years.

My family who tried to look interested when I talked about my work.

And lastly but not least, to my best friend and partner, Crichton, who continues to make a significant contribution to my sanity, happiness and well-being, thank you for everything over the past few years.

Contents

Declaration	1
Acknowledgements	2
Contents	3
Abbreviations	10
Abstract	12
Chapter 1: Introduction	15
1.1: Morphogenesis	15
1.2: Background	16
1.3: Primary Cell and Tissue Cultures	18
1.4: Cell types in Primary Culture	19
1.5: Larval Cell types	19
Figure 1.1: Primary embryonic cells in culture	22
1.6: Adult cell types in <i>Drosophila</i>	23
1.7: Cell Lines	25
1.8: The role of moulting hormone, ecdysone, in cell cultures	26
1.9: Morphogenesis in primary embryonic cultures	28
1.10: Morphogenesis in a <i>Drosophila</i> cell line	29
1.11: Morphogenesis in <i>Drosophila</i> imaginal discs	29
Figure 1.2: Evagination in imaginal discs	30
1.12: Aims of thesis	30
Chapter 2: Materials and Methods	32
2.1: <i>Drosophila</i> Primary Embryonic Cultures	33
2.2: Medium	33
2.3: Egg collection	33
2.3.1: Washing and sterilisation of the eggs	34
2.3.2: Column drops	35
Figure 2.1: Column drop slides	35
2.4: <i>Drosophila</i> Imaginal Disc Cell Lines (Clone 8+)	36
2.4.1: Medium	36
2.4.2: Cell lines	36
Table 2.1: List of Clone 8+ cell lines	36
2.4.3: Routine sub-culture of imaginal disc cell lines	37

2.5: <i>Drosophila</i> Imaginal Disc Dissection	37
2.5.1: Medium	37
2.5.2: Micro-Dissection Technique	38
2.6: Fly lines	38
2.7: Moulting hormone (ecdysone)	38
2.8: Microscopy	39
Chapter 3: Primary embryonic tissue culture	40
3.1: Introduction	41
3.2: Materials and Methods	42
3.2.1: Egg collection	43
3.2.2: Primary embryonic cultures	43
3.3: Results	45
3.3.1: Standard embryo cultures	45
3.3.2: Early embryo cultures	46
3.3.3: Older embryo cultures	48
3.4: Discussion	49
Figure 3.1: Chordotonal organ	53
Figures	57
Chapter 4: RNAi analysis in primary embryonic cultures	64
4.1: Introduction	65
4.2: Materials and Methods	67
4.2.1: Optimization of RNAi in primary embryonic cultures	67
4.2.2: Direct incubation of dsRNA and primary embryonic cells	69
4.2.3: Transfection agent	70
4.2.4: Electroporation	71
4.2.5: Immunohistochemistry	72
4.3: Results	73
4.3.1: Control cultures	73
Table 4.1: The effect of dsRNA and transfection agents on primary embryonic cultures	74
4.3.2: Soaking of dsRNA directly	74
4.3.3: FuGENE	75
4.3.4: Electroporation	76
4.4: Discussion	76

4.4.1: Incubation and dsRNA concentration	76
4.4.2: Transfection agents	77
4.4.3: EB1	78
4.4.4: Thread	79
4.4.5: dsRNA-GFP	80
4.4.6: Resistance to dsRNA	80
Figures	82
Chapter 5 : Statistical analysis of cell adhesion in Clone 8+ cell lines	85
5:1 Introduction	86
5.2: Materials and Methods	87
5.2.1: Passage numbers (<i>in vitro</i> age)	87
5.2.2: Growth rate and effect of ecdysone	87
5.2.3: Data analysis	88
5.2.4: Cell adhesion	88
5.2.5: Data analysis	89
5.3: Results	90
5.3.1: YCl.8+ and Cl.8R cells in culture	90
5.3.2: OCl.8+ and ZfeCl.8+ cells in culture	91
5.3.3: Morphological response to ecdysone	91
5.3.4: Rate of growth (proliferation)	92
5.3.5: Adhesion	93
5.3.6: Ecdysone effect	93
5.3.7: Observations	94
5.3.8: Data analysis	95
5.3.9: YCl.8+ cells and OCl.8+ substrate	95
5.3.10: OCl.8+ cells and YCl.8+ substrate	96
5.3.11: Ecdysone response	96
5.3.12: Rate of growth (proliferation)	97
5.3.13: Adhesion	97
5.3.14: Adhesion and proliferation of YCl.8+ and OCl.8+ on used substrate with conditioned medium.	97
5.4: Discussion	97
5.4.1: Clone 8R	98
5.4.2: ZfeClone 8+ cell line, cell proliferation and adhesion	99

5.4.3: Old Clone 8+ cell line compared to Young Clone 8+	101
5.4.4: Old Clone 8+ cells	101
5.4.5: Young Clone 8+ cells	102
Tables and Figures	104
Chapter 6: Microarray Analysis in Clone 8+ cell lines	110
6.1: Introduction	111
6.2: Materials and Methods	112
6.2.1: Experimental design	112
6.2.2: Sample preparation	113
6.2.3: Microarray	114
6.2.4: Scanning and Analysis	114
6.2.5: Data analysis	114
6.3: Results	116
6.3.1: Individual data sets analysed by SAM	116
6.3.2: No threshold (Table 6.1a).	116
6.3.3: Two fold threshold (Table 6.1b).	116
6.3.4: Young Clone 8+ hybridised with Clone 8R (Table 6.3 a,b).	117
6.3.5: Young Clone 8+ cells after ecdysone hybridised with Clone 8R cells after ecdysone (Table 6.4 a,b).	117
6.3.6: Young Clone 8+ cells hybridised with Old Clone 8+ cells (Table 6.5 a,b).	118
6.3.7: Gene expression differences between cell lines lines of high passage	118
6.3.8: Gene expression differences between cell lines before and after ecdysone (Table 6.6 a).	118
6.3.9: Old Clone 8+ cells after ecdysone hybridised with ZfeClone 8+ cells after ecdysone (Table 6.7 a,b).	119
6.3.10: Young Clone 8+ cells no ecdysone, hybridised with Young Clone 8+ cells after ecdysone (Table 6.8 a,b).	119
6.3.11: Clone 8R no ecdysone hybridised with Clone 8R after ecdysone	119

6.3.12: Old Clone 8+ no ecdysone hybridised with Old Clone 8+ after ecdysone (Table 6.9 a,b).	120
6.3.13: ZfeClone 8+ no ecdysone hybridised with ZfeClone 8+ after ecdysone	120
6.3.14: Genes increased two fold or more in Clone 8R, Old Clone 8+ and ZfeClone 8+ cells	120
6.3.15: Genes decreased in expression in Clone 8R, Old Clone 8+ and ZfeClone 8+ when compared to Young Clone 8+ cells.	123
6.3.16: Pairwise comparison of Young Clone 8+ before and after ecdysone and Clone 8R before and after ecdysone	126
6.4: Discussion	127
6.4.1: Statistical data analysis helpful or not?	127
6.4.2: Clone 8R	129
6.4.3: ZfeClone 8+ cells	130
6.4.4: Old Clone 8+ cells	131
Tables	136
Chapter 7: Expression of Glutactin in Clone 8+ cells	146
7.1: Introduction	147
7.2: Materials and Methods	148
7.2.1: Immunohistochemistry	148
7.2.2: Glutactin and f-actin	148
7.2.3: α -tubulin and Glutactin	149
7.2.4: Microscopy	150
Figure 7.1	151
7.3: Results	152
7.3.1: 24 hours after culture initiation	152
7.3.2: The cytoskeleton	152
7.3.3: Filopodia and cell aggregates	154
7.3.4: Day 5 after culture initiation	155
7.3.5: After ecdysone treatment	155
7.4: Discussion	156

7.4.1: Young Clone 8+ cell line	157
7.4.2: The cytoskeleton	159
7.4.3: Filopodia	160
7.4.4: After ecdysone	161
7.4.5: How do the cell line derivatives Clone 8R, Old Clone 8+ and ZfeClone 8+ differ from Young Clone 8+?	162
Figures	165
Chapter 8: Cell polarity in Clone 8+ cell lines	178
8.1: Introduction	179
8.2: Materials and Methods	180
8.2.1: Genes of interest	181
8.3: Results	182
8.3.1: Young Clone 8+ hybridised with Old Clone 8+ (table 8.1a,1b).	182
8.3.2: Old Clone 8+ cells hybridised with ZfeClone 8+ cells (table 8.2a,2b)	182
8.3.3: Young Clone 8+ hybridised with Clone 8R (table 8.3a,3b).	182
8.3.4: Young Clone 8+ hybridised with Young Clone 8+ after ecdysone (data not shown see appendix, table 8.4a,4b).	183
8.3.5: Old Clone 8+ hybridised with Old Clone 8+ after ecdysone (data not shown see appendix, table 8.5a,5b).	183
8.3.6: ZfeClone 8+ hybridised with ZfeClone 8+ after ecdysone (data not shown see appendix, table 8.6a,6b).	184
8.3.7: Clone 8R hybridised with Clone 8R after ecdysone (data not shown see appendix, table 8.7a,7b).	184
8.3.8: Young Clone 8+ cells after ecdysone hybridised with Old Clone 8+ cells after ecdysone (data not shown see appendix, table 8.8a,8b).	184
8.3.9: Old Clone 8+ after ecdysone hybridised with ZfeClone 8+ after ecdysone (data not shown see	185

appendix, table 8.9a,9b).	
8.3.10: Young Clone 8+ after ecdysone hybridised with Clone 8R after ecdysone (data not shown see appendix, table 8.10a,10b).	185
8.3.11: Decreased expression in Old Clone 8+ cells (table 8.11a,11b)	185
8.3.12: No change in expression in Old Clone 8+ when compared to Young Clone 8+ cells (table 8.12).	186
8.3.13: Positive change in expression in Old Clone 8+ cells when compared to Young Clone 8+ cells (tables 8.13a,b,c).	186
8.4: Discussion	187
8.4.1: Genes downregulated in the Old Clone 8+ cells	188
8.4.2: How do the Old Clone 8+ cells differ from ZfeClone 8+?	193
8.4.2: Age difference	194
Tables	199
Chapter 9: Peripodial epithelium	213
9.1: Introduction	214
Figure 9.1: Third instar wing disc.	214
9.2: Materials and Methods	215
9.2.1: Fly stocks	215
9.2.2: Dissection	216
9.2.3: Microscopy	216
9.2.4: Histochemical staining	216
9.2.5: Immunohistochemistry	217
9.2.6: Peripodial epithelium	217
Figures 9.2 and 9.3: Peripodial epithelium	218
9.3: Results	220
9.3.1: Wild-type flies	220
9.3.2: Transgenic fly strain actin-GFP	220
9.3.3: Transgenic fly strain actin- <i>lacZ</i>	221
9.3.4: Wild-type flies stained for f-actin	221

9.3.5: Transgenic fly strains CD8-GFP	222
9.4: Discussion	222
Figure 9.4: Wound healing in zebra fish embryo	224
Figures	227
Chapter 10: The actin ring	231
10.1: Introduction	232
Figure 10.1: Dorsal closure during <i>Drosophila</i> embryogenesis	232
10.2: Materials and Methods	233
10.2.1: Imaginal Disc Dissection	233
10.2.2: Microscopy and image analysis	234
10.3: Results	234
10.3.1: Actin expression moesin-GFP wing discs	234
10.3.2: Wing disc one	235
10.3.3: Cell morphology and size analysis	236
10.3.4: Wing disc two	237
10.3.5: Cell morphology and size analysis	238
10.4: Discussion	239
10.4.1: The lumen	239
Figure 10.2: Convergent extension in the peripodial epithelium	242
Figure 10.3: Accumulation of actin in the amnioserosa	244
10.4.2: What evidence is there to support the hypothesis that peripodial cells invaginate?	246
Figures	252
Summary	263
References	275
Appendices	304

Abbreviations List

Ca ²⁺	Calcium ions
DAPI	4'6-diamidino-2-phenylindole
Cl.8+	Clone 8+ cell line
Cl.8R	Clone 8R cell line (r-resistant)
cDNA	Complementary deoxyribonucleic acid
DNA	Deoxyribonucleic acid
<i>Drosophila</i>	<i>Drosophila melanogaster</i>
dsRNA	Double stranded Ribonucleic acid
EcR	Ecdysone receptor protein
JNK s/ pathway	Jun-N-terminal Kinase signalling pathway
Ecdysone	Moulting hormone, 20-hydroxyecdysone
mRNA	Messenger RNA
OC1.8+	Old Clone 8+ cell line
PBS	Phosphate buffered saline
PCP	Planar Cell Polarity
shRNAs	short hairpin RNA
USP	Ultraspiracle
YCl.8+	Young Clone 8+ cell line
Zfe	Zero fly extract
ZfeCl.8+	ZfeClone 8+ cell line.

Abstract

The aim of this thesis was to investigate morphogenesis in the fruit fly *Drosophila melanogaster* using three *in vitro* tissue culture systems.

Primary embryonic cultures derived from *Drosophila melanogaster* were used to study the effect of the moulting hormone ecdysone on cells in culture. The hypothesis was that the effect of ecdysone on these primary embryonic cells would parallel events which occur during metamorphosis *in vivo* and therefore the primary embryonic cultures could be used as an '*in vitro*' model system. Transgenic fly lines expressing GFP were used to visualise and identify specific cell types and it was shown that cells in primary embryonic cultures respond to ecdysone morphologically. However due to the variability of cultures it was concluded that this culture system was not suitable for use as a model system. As defined cell types were observed the development of a protocol suitable for use with the primary embryonic culture system using dsRNA in order to demonstrate RNA interference was undertaken. Although this was unsuccessful, as cells in the primary embryonic cultures appeared to be resistant to dsRNA, some technical avenues remain to be explored.

The *Drosophila melanogaster* cell line, Clone 8+, was used to investigate cell adhesion in tissue culture. Statistical analyses were carried out and it was established that derivatives of the parent cell line, Clone 8+, showed differential adhesion and proliferation characteristics. Analysis of microarray data was carried out in order to identify genes which may be responsible for the loss of cell adhesion in Clone 8+ cell lines and the potential roles of these genes in adhesion were discussed. A gene of interest, *glutactin*, was identified

which may be responsible for loss of cell adhesion. Antibody staining was used to establish the expression of the protein glutactin in the Clone 8+ cell lines. The expression of glutactin suggested that the Clone 8+ cell line had maintained properties of the wing disc epithelial cell-type and disruption of cell polarity was considered as a possible mechanism. It was shown that f-actin colocalised with glutactin and the role of the cytoskeleton in glutactin secretion was discussed. It was concluded that glutactin was not responsible for loss of cell adhesion in the Clone 8+ cell lines. Further analysis of the microarray data revealed potential genes that could be responsible for the loss of cell polarity in the Clone 8+ cell lines and the possibility of cellular senescence was considered. It was hypothesised that the properties of adhesion and proliferation related to their '*in vitro*' age.

In the final investigation the movement of epithelial cells in *Drosophila melanogaster* third instar larval imaginal discs during morphogenesis was investigated. Firstly a lumen was identified in fixed imaginal disc tissue in association with cells expressing f-actin. This result was discussed in relation to the process of dorsal closure and wound healing. Further investigations involved live imaging of the dynamic process of evagination in the imaginal wing disc using transgenic flies expressing moesin-GFP. It was concluded that the lumen was not associated with the process of wound healing and it was concluded that the lumen appeared to be the mechanism directing peripodial epithelium contraction during morphogenesis of the imaginal wing disc. Dorsal closure and the process of invagination in relation to morphogenesis of the imaginal wing disc were discussed.

Chapter 1

Introduction

1: Introduction

1:1 Morphogenesis

Morphogenesis, the shaping of an organism, is accomplished by formation of complex tissues and involves cell adhesion and movement of these cells.

These processes are the subject of the following studies carried out in *Drosophila melanogaster*.

The fruit fly *Drosophila melanogaster* (herein referred to as *Drosophila*) has been and still is one of the most useful model systems in which to study morphogenesis. The use of insect tissue culture to study *Drosophila* tissues and cells *in vitro* has been of major importance in the field of biology. Since the establishment of the first *Drosophila* cell line by Echalier et al (1965) cell lines, along with *Drosophila* primary cultures and whole tissue explants have been used for countless studies on morphogenesis (Cherbas et al., 1980; Milner et al., 1983; Cottam and Milner, 1997; Currie et al., 1988; Agnes et al., 1999; Kozlova and Thummel, 2002; Lee et al., 2002; McClure and Schubiger, 2005). The culture of insect cells and tissues is an invaluable tool for studying insect physiology, endocrinology, development processes, genetics and biochemistry.

In the recent past tissue culture in *Drosophila* had largely been used as a secondary approach to the study of morphogenesis and many studies have concentrated on the whole organism (Schubiger et al., 1998; Kiehart et al., 2000; Bloor and Kiehart., 2002; Jacinto et al., 2002). Whilst it may be preferable to use whole embryos, larvae or adult flies to examine the dynamic processes of development, subsequent visualisation *in vivo* and interpretation of results

may often be difficult. There has recently been resurgence in the use of cell culture *in vitro* as individual cells and whole tissue explants are easier to manipulate when exploiting techniques such as RNAi and Microarray analysis. In this study three tissue culture systems, using *Drosophila* cells and tissue have been used to explore morphogenesis in *Drosophila*.

1.2: Background

In order to grow cells successfully in culture a suitable biochemical environment, which mimics *in vivo* conditions in the insect, must be available. In insects there is a single body fluid, the blood or haemolymph, which is not enclosed within tubes but flows through sinuses in the head, thorax, abdomen and appendages, bathing the tissues directly. As one would expect the composition of insect haemolymph varies from species to species. Moreover there is also variability between the different stages of development i.e. larval and adult, and between the microenvironments to which different tissues are exposed such as the imaginal wing disc and leg disc environments (Echalier, 1980).

The initial attempt to culture insect tissue was made in 1915 by Goldschmidt, who was able to maintain living insect tissue in culture for three weeks bathed in the haemolymph of the insect. Due to the inherent difficulties associated with the formulation of an adequate medium in which to sustain healthy, growing cells and tissue, little progress was made in the field until the 1950's. Detailed analysis of the haemolymph in several different insects revealed that there are many factors relevant to the design of culture medium such as osmotic pressure, pH, inorganic ion ratios, concentration of carbohydrates, amino acids, organic acids, proteins, sugars and fatty acids. In

an ideal situation individual culture media to suit every insect species at every stage of their development would be preferable.

A detailed analysis of the larval haemolymph of the Lepidopteran, *Bombyx mori* resulted in the development of a medium by Wyatts (Wyatts, 1956). Modification of this medium by Grace (1962) established the first permanent cell lines from the ovarian tissue of the Lepidopteran *Antheraea eucalypti* followed by the Dipteran mosquito larvae *Aedes aegypti* (1966). A major contribution to the study of development in insects has been made by studies on the fruit fly *Drosophila*. Analysis of the third instar larval haemolymph of *Drosophila* in 1963 by Begg and Cruickshank led to the successful culture of the first *Drosophila* cell line by Echalièr et al in 1965.

Several media have now been designed and successful adaptations of these have been made. For example Grace's medium was originally designed to culture moth cells, but has been modified and used to culture other Lepidopteran larvae and leaf hoppers (Mitsuhashi, 1969, 1976). Landureau-Jollès medium was originally designed to culture cockroach cells and has been found to suit several species of the insect with only changes in the osmotic pressure required (Landureau and Jollès, 1969). Several media have been designed to grow *Drosophila* tissue and cells including Schneiders (1967) and Shields and Sang's (1970). Modifications of media have been carried out for individual insects. These modifications include the addition of serum, usually fetal calf serum, and in some cases the appropriate insect haemolymph (fly extract) which is thought to contain other factors (such as growth factors) essential for successful cultures (Lynn and Oberlander, 1982).

1.3: Primary Cell and Tissue Cultures (figure 1.1, pg. 8)

The term 'Primary Culture' has been used to describe the limited survival and possible proliferation of cells and tissues newly explanted from an organism. Primary cultures have been initiated from whole embryos and individual tissues such as the ovaries, neural tissue and imaginal discs (Mitsuhashi, 1972, 1976; Eide, 1975; Shields and Sang, 1970; Milner et al., 1983). However since the first cell line was established in 1965, researchers using *Drosophila* primary cultures have been primarily interested in establishing cell lines and primary cultures from *Drosophila* have mainly been taken from single embryos (Sang, 1981). But for a period during the 1960's and 70's there was much interest in using the cultures to identify certain cell types, to study their differentiation *in vitro* and the effect of moulting hormones on these cells (Shields and Sang, 1970; Dübendorfer et al., 1978; Dübendorfer and Eichenberger-Glinz, 1980). Traditionally cells are cultured on a flat surface, but this is a poor substitute for their normal growth which is inherently 3-dimensional. In order to carry out these studies a technique named the column drop technique was developed (Shields et al., 1975). Using this technique it was discovered that when *Drosophila* gastrulae were dissociated, and the resulting cells cultured in an appropriate medium, a range of cell types would grow and differentiate. These cell types included larval muscle and nerve, larval fat, larval epidermal cells and imaginal disc cells. If ecdysone was added to such cultures, adult tubular and fibrillar muscle, adult cuticle with bristles and trichomes and adult fat formed, whilst their larval counterparts broke down.

Studies have shown that primary embryonic cultures contain two types of cells with different fates, namely larval and adult. In order to observe cells from embryos that were competent to differentiate *in vitro* a series of experiments was undertaken by Seecof and Donady (1971). They discovered

that cells taken from pre-gastrula embryos did not survive *in vitro*. Very little, if any differentiation was seen and the cells became granular and eventually disintegrated (Seecof and Donady, 1972). However after the onset of gastrulation, at about 3 hours and 15 minutes into embryogenesis, the number of surviving cells capable of differentiating *in vitro* was shown to increase progressively. A near maximum was reached with cells cultured from embryos about 4 -5 hours after oviposition (Seecof and Donady, 1972). Researchers have since used several different approaches in the number of hours after oviposition to set up their cultures and make observations. The number of hours has varied from 1-3 hours, 6-8 hours, 10-12 and 20-24 hours (Echalier, 1965; Shields and Sang, 1970; Schneider, 1972; Shields et al., 1975).

1.4: Cell types in Primary Culture

There are several cell types which have been observed in *Drosophila* primary embryonic cultures. The description of observed cell types *in vitro* has been documented by several researchers (Rizki, 1957; Shields and Sang, 1970; Seecof et al., 1971; Shields et al., 1975; Dübendorfer, 1976; Milner and Dübendorfer, 1982; Dübendorfer and Eichenberger-Glinz, 1980). These cell types have been mainly categorised as larval or adult depending on their morphology and their appearance in time in the cultures. A third category of undifferentiated cell types has also been described. The following descriptions are from observations made on *Drosophila* primary embryonic cultures 6-8 hours after oviposition.

1.5: Larval Cell types

Early observations of the cells in culture describe the cells as being similar in morphology showing only variation in size. During the first few hours cells

were observed to be fairly active, putting out cell processes and changing shape. This was followed by rounding up and degeneration of some cells and by about 12 hours the cultures appeared thinner, although a high proportion of cells were still viable (Shields and Sang, 1970). Early nerve cells or neurocytes appear in cultures in the first 6-12 hours. They were described as being easily identifiable in cultures because of the length of their cytoplasmic extensions in comparison to their cell body (Seecof et al., 1971, 1973). As the cultures matured the cells have been described as being 'small round greyish looking cells with complex networks of threads, often with varicosities, which may cluster together forming thicker tracts' (Shields and Sang, 1970).

Myoblasts were described as small cells approximately 5 μ m in diameter. They begin to appear in cultures in the first 6-12 hours. The putative muscle cells have been described as long spindle shaped cells with narrow elongated attachment processes at either end, an ovoid nucleus and a prominent nucleolus. Individual myoblast cells often divided into 2 smaller cells called myocytes. The myocytes changed morphology, elongating and adopting a bipolar configuration. They have been observed to aggregate with neighbouring myocytes into parallel arrays, some cells aligning and then fusing to form syncytial myotubes or sheet muscle (Seecof et al., 1973). The final form was usually achieved in the first 15 hours of culture and contractile movement of the muscle was observed at about 36 hours after culture initiation (Shields and Sang, 1970; Seecof et al., 1971).

In the larva the fat body is a relatively loosely organised tissue with a large surface area in contact with the haemolymph, performing functions such as lipid and glycogen storage (figure 1.1a). In *Drosophila* primary embryonic cultures, larval fat body cells appeared in the first 24 hours and developed from flattened epithelial-like cells. These cells rounded up and showed

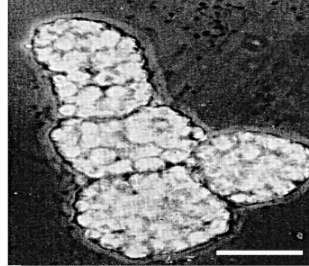
granulation in the cytoplasm. Once rounding was completed, about day four, the accumulated lipid droplets started to swell rapidly which increased their size up to four fold. They tended to become more loosely attached to the substrate and associate with one another in small groups.

Three types of macrophages have been described which are also found in *Drosophila* haemolymph (Dübendorfer and Eichenburger-Glinz, 1980) (figure 1.1b). In primary cultures these have been described and named as plasmocytes, podocytes and lamellocytes (Rizki, 1957, 1961). Plasmocytes have been described as the most frequently observed cell type. These cells have been observed to appear during the first 24 hours of culture from unknown precursors, as bulky, shapeless cells with large vacuoles the cells gradually flatten. The peripheral border of clear cytoplasm has been observed to contract and extend giving the cell an irregular outline. Melanization of these cells has also been observed and is thought to be a result of deleterious culture conditions, such as overcrowding and cell death (Shields and Sang, 1970).

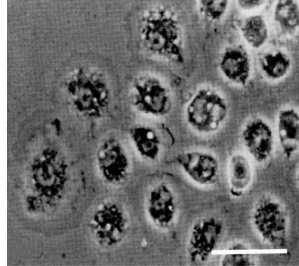
The epidermis in the larva is one cell thick and secretes a flexible cuticle, which allows movement, provides protection, insulation and sensory information. In primary embryonic cultures, epidermal cells have been described as small, round, clear cells possessing a refractile body. These cells arise in the cultures during the first 24 hours, often occurring in tight groups. By the middle of the second week these cells have been observed to secrete one or more layers of chitin, which sometimes melanizes and may be smooth or textured (figure 1.1c). Short stubby hairs similar to denticles on the larval denticle belt have also been observed and very occasionally tooth-like structures that have been described as possible mouth parts of the larva (Shields et al., 1975; Dübendorfer and Eichenburger-Glinz, 1980).

Figure 1.1: Primary embryonic cells in culture from a variety of sources, the number of days in culture has been listed. Scale bar represents 20 μ m.

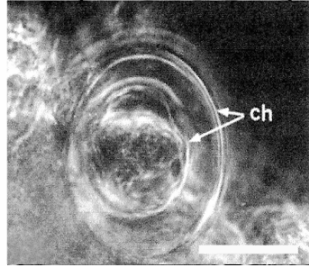
1.1a: Fat cells, 10 days



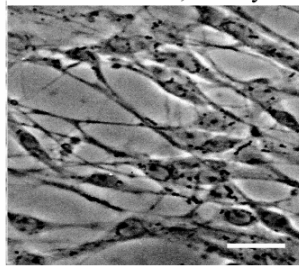
1.1b: Macrophages, 3 days



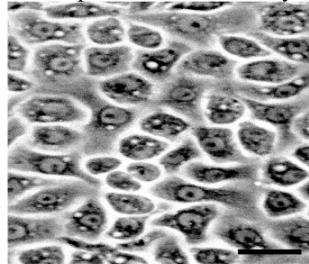
1.1c: Epidermal cell, 21 days



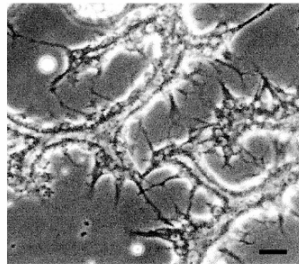
1.1d: Fibroblasts, 21 days



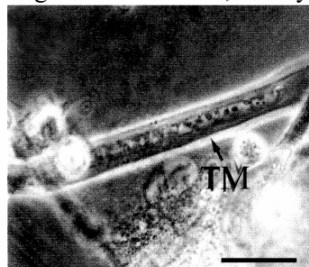
1.1e: Epithelial-like, 21 days



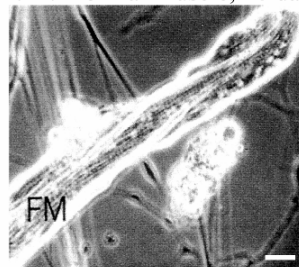
1.1f: Trachea, 21 days



1.1g: Tubular muscle, 28 days



1.1h: Fibrillar muscle, 28 days



(Shields, Dübendorfer and Sang, 1975, figures 1.1a, 1.1b, 1.1d, 1.1e)

(Milner and Dübendorfer, 1982, figures 1.1g, 1.1h)

(Dübendorfer and Eichenberger-Glinz, 1980, figures 1.1c, 1.1f)

TM-tubular muscle, FM-fibrillar muscle

The imaginal discs are hollow sacs of cells that develop into adult structures during metamorphosis. They have been described in primary cultures as small monolayered, hollow vesicles that appear in the cultures within the first 24 hours and then disappear. Growing vesicles of about 20 cells usually appear towards the end of the first week. Cell multiplication takes place and by the end of the third week the vesicles may have reached a very large size and contain hundreds of cells (Shields et al., 1975).

There were two types of undifferentiated cell types found in cultures towards the end of the second week. Fibroblast like cells assumed an elongated cell form with large nuclei and prominent nucleolus (figure 1.1d). Epithelial-like cells have a rounded appearance initially but have been observed to alter their morphology to a fibroblastic form (figure 1.1e). Both types of cell have been observed to form open networks or sheets and generally maintain contact with each other (Shields et al., 1975; Dübendorfer, 1976).

The tracheal system is the respiratory organ in *Drosophila* and consists of a complex branched epithelial network that is derived from the ectoderm. Tracheal cells were not normally observed until the primary embryonic cultures were more mature, about two to three weeks, and their appearance has been more rare (Shields et al., 1975) (figure 1.1f).

1.6: Adult cell types in *Drosophila*

The differentiation of adult cell types and tissue in primary embryonic cultures can be observed when metamorphosis is induced by the addition of moulting hormone, 20-hydroxyecdysone (herein referred to as ecdysone). Ecdysteroids were normally added after two weeks of culture (Shields and Sang, 1970; Dübendorfer, 1976).

The observed response of most larval fat body cells on addition of ecdysone was degeneration of the cells and release of their lipid vacuoles into the culture medium, resembling the fate of larval fat body *in vivo* (Dübendorfer and Eichenberger-Glinz, 1985). Degeneration of larval muscle was observed and deterioration of some of the haemocyte cell types which appeared to detach and deteriorate. However there are two larval cell types on which the addition of the ecdysone had a more positive affect. The larval epidermal cells secreted several new layers of chitin and wrinkled pupal-like cuticle was formed. Trachea, which were not observed until later cultures, appeared to grow out and form tubes (Dübendorfer and Eichenberger-Glinz, 1980).

Two types of adult muscle have been described after ecdysone addition; tubular muscle and fibrillar or indirect adult flight muscle. Tubular muscle appeared to develop from precursor fibroblast-like cells which fused to form striated muscle cylinders (figure 1.1g). Single rows of nuclei were observed along their central axis, accompanied by visible contraction of the muscle (Dübendorfer et al, 1978). Less is known about fibrillar precursor cells. Fibrillar muscle cells appeared in cultures as isolated fibres with blunt ends and many small nuclei scattered throughout the sarcoplasm (Dübendorfer et al., 1978) (figure 1.1h).

Vesicles of imaginal disc cells, the future adult epidermis, have been observed to secrete cuticle after ecdysone addition, which may be smooth and tanned. These vesicles contained one specific sort of trichome or/and bristles with fully developed sockets and shafts. However specialised structures such as claws, eye facets or sex combs have never been observed to develop in primary embryonic cultures (Dübendorfer et al., 1975; Dübendorfer, 1976). Pre-cursors of adult fat body have been observed as fibroblast type cells, which aggregate and gradually draw in their processes. These cells start to

swell and accumulate many lipid vacuoles (Dübendorfer and Eichenberger-Glinz, 1985).

1.7: Cell Lines

The definition of a cell line, which may be described as continuous, permanent or established, refers to any line that 'can be cultured for such a long time that it has apparently developed the potential to be subcultured indefinitely *in vitro*'.

Since the establishment of the first continuous cell line in 1962 by Grace, insect cell lines have become extremely important in many areas of research. This is reflected in the number of cell lines that have been established in the last forty years of over 400 cell lines from over 100 insect species (Lynn et al., 1998). The advances which have been made in molecular and biochemical techniques has meant that primary tissue culture has become an important resource for establishing a cell line (Lynn, 2001). Insect cell lines have been derived from primary cultures of embryonic, larval and adult tissues of many insect orders such as Lepidoptera, Hemiptera, Coleoptera, Diptera and Hymenoptera (Mitsuhashi, 1972, 1973; Kurtti and Brooks, 1976; Eide, 1975; Echaliier and Ohanessian, 1970; Schneider, 1972; Lynn and Hung, 1991).

One advantage of using cell lines is that researchers are able to use homogenous populations of cells, which generate greater amounts of identical cellular tissue and therefore a more convenient source of material for the characterisation and isolation of genes and proteins (Lynn et al., 1998).

Understandably there are limitations in using established cell lines, one is that many of the lines have been derived from primary cultures in which a range of cell types may grow and so the tissue of origin from which the cell line is

derived remains unknown. Cells have been transformed and their genetic and biochemical properties may no longer be a true representation of their *in vivo* counterparts. In addition it has been found that the properties of a cell line may not remain constant and change over time (Dinan et al., 1990; Cottam and Milner, 1997). This problem has been alleviated to some extent by cloning groups of cells on a regular basis, in order to maintain a more stable cell population. Many of the cell lines derived from *Drosophila* are from primary cultures for example Schneiders S2 line and Echalier's Kc line, these lines have been around since the 1960's and are of very high, unknown passage number. The imaginal disc cell line Clone 8+ is derived from a single defined tissue, third instar imaginal disc epithelia, and is of known passage number (Currie et al., 1988).

1.8: The role of moulting hormone, ecdysone, in cell cultures

Drosophila is a holometabolous insect and many changes which take place during morphogenesis are governed by the moulting hormone ecdysone. Experiments undertaken by Kopec between 1917 and 1922 lead to the proposal that the insect brain secreted a hormone responsible for metamorphosis. In 1934 Wigglesworth began his investigations on the control of moulting and metamorphosis in *Rhodnius prolixus*, and eventually traced the moult inducing activity to the exact location in the brain. He then showed evidence that the 'brain hormone' did not act directly or alone on the epidermis which was substantiated in many different insects during the 1950's. These elegant experiments by Wigglesworth and further studies by other researchers have eventually resulted in the recovery and identification of the insect moulting hormones. Their subsequent purification and synthesis has made it possible to investigate their mode of action, metabolism and degradation on tissues *in vitro*, giving biologists an insight into insect growth

and development. *In vitro* studies on insect cuticle have been carried out on *Drosophila*, various lepidopteran species including the tobacco hornworm *Manduca sexta*, Orthopterans and Coleopterans (Schneider, 1972; Milner and Sang, 1974; Riddiford et al., 1980; Dutkowski et al., 1977; Marks and Ward, 1987). *Drosophila* cells in tissue culture have been used extensively to study the mechanisms of actions of the insect moulting hormones. For example, cell lines that were shown to differ in their response to ecdysone have facilitated the characterisation of a typical hormone response of cells in culture. These are; changes in morphology, cell aggregation, arrest of cell division and protein synthesis (Best-Belpomme et al., 1980; Cherbas et al., 1980; Stevens et al., 1980).

Ecdysone exerts its effects via members of the nuclear receptor superfamily which act as ligand-regulated transcription factors. The ecdysone receptor is a heterodimer of two nuclear receptors, the ecdysone receptor (EcR) and ultraspiracle receptor (USP) (Koelle et al., 1991; Yao et al., 1993). The ecdysone/EcR/USP complex directly regulates primary-response gene expression, including the induction of a small set of transcription factor-encoding early genes such as *Broad Complex (BRC)* and *E74* (Di Bello et al., 1991; Thummel et al., 1990). These transcription factors then act to transduce and amplify the hormonal signal by regulating late secondary-response target genes. Studies suggest that ecdysone directs cell death, proliferation and differentiation responses at multiple stages of the life cycle of *Drosophila* through the coordinated induction of specific genes (Riddiford, 1993; Jiang et al., 1997; Jiang et al., 2000; Yin et al., 2005)

1.9: Morphogenesis in primary embryonic cultures

In the first part of this study in morphogenesis in *Drosophila* cell death, cell proliferation and differentiation during metamorphosis will be examined. Pulses of ecdysone signal moulting of the cuticle in first and second instar larvae. The pulse of ecdysone towards the end of the third instar larval stage signals puparium formation, followed by a second pulse about 10-12 hours later which initiates pupariation, the prepupal to pupal transition and adult head eversion. At these times, the larval tissues which will no longer be required in the adult degenerate, and adult precursor cells proliferate to form the adult tissue. 'In vitro' studies on primary cultures have found that tissues show a differential response to ecdysone, for example the larval anterior muscle and midgut degenerate after the pulse signalling puparium formation (Robertson., 1936; Jiang et al., 1997). The salivary glands do not degenerate until the second pulse some 10 hours later (Jiang et al., 2000).

At the onset of metamorphosis larval cells respond to ecdysone by degenerating in a 'stage-specific sequence'. The larval midgut for example is no longer needed at the time it degenerates along with the anterior muscle groups which are associated with it. The larval nerve network also begins a remodelling programme in order to innervate future adult musculature. Premature destruction of larval muscle or nerve tissue would leave the larva immobile. In the imaginal precursors, delays in proliferation and differentiation of adult muscle may lead to their being inappropriately innervated. Therefore stage specific cell death, proliferation and differentiation are extremely important during morphogenesis in *Drosophila*.

1.10: Morphogenesis in a *Drosophila* cell line

The *Drosophila* Clone 8+ cell line will be used in the second part of this study to examine cell-matrix adhesion '*in vitro*'. Maintenance of adhesion and the control of proliferation in epithelium are a prerequisite for successful morphogenesis *in vivo*, disruption of adhesive properties and uncontrolled proliferation can lead to tissue dissemination, tissue overgrowth and tumour progression (Roote and Zusman, 1995, Bloor and Kiehart, 2002, Bilder, 2004, Bokel et al., 2004). The extracellular matrix plays an important role during morphogenesis in all organisms, maintaining tissue integrity, facilitating the action of signalling molecules and the remodelling of tissue during development (Brower et al., 1987, Adams and Watt, 1993, Fessler et al., 1994). Mutations in *Drosophila* laminin for example have been shown to cause a wing blistering phenotype in adult flies due to the separation of epithelial layers (Martin et al., 1999, Brown et al., 2000). Basal membrane matrix interactions are also important in regulating cell re-arrangement and migration of cells which occurs during oogenesis and wing expansion in *Drosophila* (Medioni and Noselli, 2005, Kiger et al., 2007). Cell-matrix adhesion is of vital importance during development maintaining structural integrity of the tissue and cell-cell, cell-matrix communication in order for morphogenesis to occur precisely.

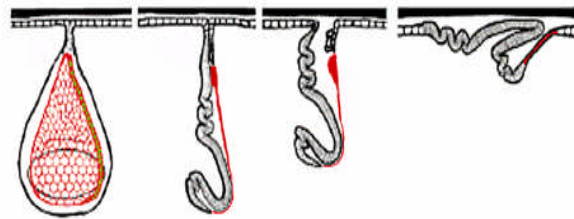
1.11: Morphogenesis in *Drosophila* imaginal discs

In the final part of this study *Drosophila* imaginal discs which have been dissected from late third instar larvae will be used to study the contraction of the peripodial epithelium during evagination. In *Drosophila* there are 19 discs, 9 pairs form the head and thorax and a single medial disc forms the genitalia. They arise as pockets in the embryonic ectoderm and grow inside the body

cavity until the larva pupates at which point they evaginate to form the body wall and appendages in the adult (Oberlander, 1985; Bate and Martinez-Arias, 1991). During embryogenesis the disc cells divide and the discs grow until the end of the third instar larval stage. At this time the imaginal discs consist of two opposing surfaces; small columnar epithelial cells which form the appendages and larger, squamous, peripodial cells (Auerbach, 1936). During metamorphosis, in response to changing levels of ecdysone, the discs undergo dramatic transformations resulting in the formation of the adult exoskeleton.

The initial stage of disc transformation is called evagination and is composed of two processes, elongation and eversion (figure 1.2).

Figure 1.2: Diagrammatic overview: evagination in *Drosophila* imaginal discs. The peripodial epithelium is outlined in red (adapted from Fristrom, 1993).



Elongation comprises the lengthening and shaping of the columnar epithelia to form the adult appendage. Eversion is the process whereby contraction of the peripodial epithelium drives the appendage to the external surface of the developing fly (Milner, 1977; Milner et al., 1987). Fusion of the adjacent disc derivatives follows to form the contiguous adult epidermis (Fristrom and Fristrom, 1993).

1.12: Aims of thesis

Drosophila primary embryonic cultures will be examined to explore the possibility that these cultures could be used as an 'in vitro' model system to

study metamorphosis *in vivo*. The effect of the addition of ecdysone to the larval cells which are present in *Drosophila* primary embryonic cultures *in vitro* will be visualised and correlated with events which place *in vivo*.

The *Drosophila* cell line Clone 8+ will be used to study cell adhesion in tissue culture. Statistical analyses will be undertaken to establish whether there are differences between the parent line and the derivatives of the parent line with regard to adhesion, proliferation and ecdysone response. Microarray analysis of the cell lines will also be undertaken to compare differential gene expression between these cell lines.

In the final study the process of evagination which occurs during metamorphosis of the adult precursors cells, imaginal discs, will be investigated using *Drosophila* third instar larval imaginal discs. In particular, the role of the peripodial epithelium and the cytoskeleton during this process will be explored.

Chapter 2

Materials and Methods

2: Materials and Methods

The general methods and materials which have been employed throughout this study are described in this section. Techniques which were more specific in their application are detailed within the relevant chapters.

2.1: *Drosophila* Primary Embryonic Cultures

The method of homogenising large numbers of *Drosophila* embryos and successfully growing and characterising the differentiated cells *in vitro* was based on a technique called the 'column drop' method was originally devised by Shields and Sang (1970). The following method is based on the modified column drop method (Shields et al., 1975).

2.2: Medium

Primary embryonic cultures were grown in a Shields and Sang modified MM3 medium (Shields and Sang, 1977), the constituents of which are listed in the appendix. The medium was further modified for growth of the cells through the addition of 10 % foetal bovine serum (FBS). The medium plus additive was filter sterilized through a 0.22 μ m filter before use and is referred to as primary (1°) medium.

2.3: Egg collection

Wild-type Oregon-S flies from 7-21 days of age were used as controls for this procedure. The flies, which were kept in food bottles at 25°C, were transferred to a special egg-laying plastic bottle. A square of agar jelly was placed on a watch-glass, and the square smeared with a paste of ground, autoclaved dried

yeast and water. The watch-glass was used to cover the bottle which was then inverted to stand on the watch-glass and incubated at 25°C for 1-2 hours. The watch-glass was removed and these eggs discarded, this is termed the pre-collection. The pre-collection was discarded as it may contain retained embryos further on in development than desired. The watch-glass was replaced with a fresh one, which was left for 1-2 hours. Eggs were sometimes collected for a short a time as possible so that all the embryos were comparable in terms of development. Several bottles were used at one collection to ensure adequate numbers of eggs were collected and the eggs were incubated at 25°C until the required stage for processing was reached.

2.3.1: Washing and sterilisation of the eggs

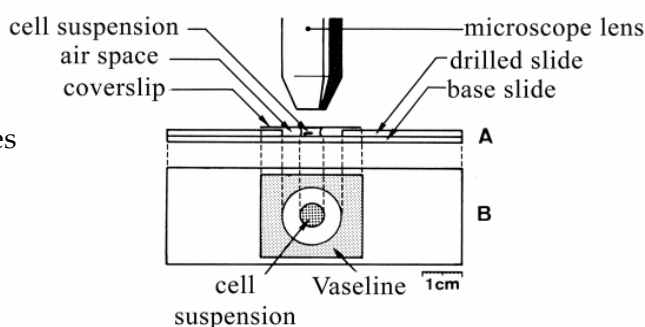
Saturated sugar solution was used to wash the eggs, and as little of the yeast as possible, off the agar squares at which point the eggs float and the yeast sinks. Examination of the embryos floating on the surface of the sucrose solution was made under a dissecting microscope and any hatched larvae were removed. Repeated washing was carried out until all trace of the yeast had been removed. The eggs were finally rinsed with distilled water and transferred into a glass boiling tube with freshly prepared and filtered 3% calcium hypochlorite solution. The eggs were coated with the calcium hypochlorite solution by inversion and left for 7 minutes, mixing occasionally. Aseptic technique was employed from this point onward. The eggs were poured into a sterile 100µm sieve and washed with plenty of sterile distilled water, then rinsed with 5 mls of primary (1°) embryonic medium. The eggs were then poured into a sterile homogeniser tube and rinsed with 5mls of fresh medium, allowed to settle and most of the medium removed. This was repeated twice more and finally 2ml fresh 1° medium added. Homogenisation was carried out by inserting a pestle slowly into the tube twisting at the

bottom and withdrawing. This was repeated once or twice until no whole embryos or large clumps of tissue were visible. The suspension was pipetted into a sterile universal and centrifuged at 1600rpm for 1 minute, the supernatant was removed and the pellet resuspended in 2ml fresh 1° medium. This step was repeated twice more. The pellet was resuspended in 1ml 1° medium, a haemocytometer count was carried out and sufficient medium was added to the remaining 0.9ml to give a final suspension of 3.5×10^6 cells/ml.

2.3.2: Column drops

Sterile drilled slides (figure 2.1) were prepared by putting petroleum jelly around the well. A 50µl drop of suspension was aliquoted onto a sterile 24x24 coverslip and a drilled slide was inverted with the well placed over the suspension so a column drop was formed. Slides were left inverted for up to 1 hour to enable cells to adhere to the coverslip. Once turned over the cells become suspended into the medium and grow in a three-dimensional network. The cultures were examined, the slides labelled with date and number and incubated at 25°C in a 5% CO₂ atmosphere.

Figure 2.1: Column drop slides
(Shields and Sang, 1975)



2.4: *Drosophila* Imaginal Disc Cell Lines (Clone 8+)

The cell lines used in these studies were *Drosophila* Clone 8+ (Cl.8+) cell lines which were originally derived from late third instar imaginal wing discs dissected from *Drosophila* larvae (Currie et al., 1988).

2.4.1: Medium

Clone 8+ cell lines were grown in Shields and Sang modified MM3 medium (Shields and Sang, 1977) the constituents of which are listed in the appendix. The medium was further modified for growth of the cells through the addition of 2% heat inactivated foetal bovine serum (FBS), 12.5IU/100ml insulin and 2.5% fly extract (FE2). The medium plus additives was filtered sterilized through 0.22µm filter and was referred to as complete sterile medium (CSM).

2.4.2: Cell lines

The cell line, Clone 8+ (Cl.8+), and derivatives of the Clone 8+ line which were used in this study are listed in the table below (table 2.1).

Name	Characteristics	Passage number	Comments
YCl.8+	20-HE responsive	30 (20-24)	Young
OCl.8+	20-HE responsive	30 (70-134)	Old
Cl.8R	20-HE unresponsive	30 (21-24)	Resistant to ecdysone
ZfeCl.8+	20-HE responsive	30 (68-72)	No FE2 in medium

Table 2.1: List of Clone 8+ cell line and derivatives with passage numbers. Passage number 30 refers to the age at which the cell line was cloned and the numbers in brackets are the number of passages past cloning.

2.4.3: Routine sub-culture of imaginal disc cell lines

Clone 8+ cells were passaged once every 7 days when in culture. Passaging is a term which denotes the splitting of the cells once confluence is reached and before overgrowth, usually on a weekly basis. Cells were pipetted off the tissue culture dish surface and centrifuged at 1200rpm for 5 minutes. The supernatant was removed and the pellet resuspended in 1ml of fresh CSM. Cells were normally seeded at a density of 3×10^6 per 5ml CSM onto a 50mm Petri dish. Dishes were dated and marked with the passage number and cell line name and placed in a humidified incubator with a 5% CO₂ atmosphere and set at 25°C. In most laboratories it is not usual practice to take note of the passage number of *Drosophila* cell lines. The passage number is often taken as an indication of their '*in vitro*' age (Cottam and Milner, 1997). For long term storage Clone 8+ cells were preserved in a liquid nitrogen freezer.

2.5: *Drosophila* Imaginal Disc Dissection

The imaginal disc structures dissected in these studies and used as controls were taken from Oregon-S late third instar *Drosophila* larvae. The dissection technique and culture *in vitro* was based on a technique previously described by Milner and Sang, 1974.

2.5.1: Medium

Imaginal discs were cultured in Shields and Sang modified MM3 medium (Shields and Sang, 1977) the constituents of which are listed in the appendix. The medium was further modified for growth of the discs through the addition of 2% heat inactivated foetal bovine serum (FBS). The medium plus foetal bovine serum was filtered through a 0.22µm filter to sterilize.

2.5.2: Micro-Dissection Technique

All dissections took place in a sterilised U.V. hood with a microscope window for a Wild M5 dissecting microscope. All dissecting instruments were swabbed with alcohol and flamed before use. Cavity slides were pre-prepared by applying petroleum jelly around the cavity. Drops of culture medium were placed onto a siliconised slide and sterile 3rd instar larvae placed into a drop to wash. Larvae were dissected, the imaginal discs removed and placed into a single drop. Each disc was placed onto a coverslip in a 5µl drop of medium or medium with 0.1µg/ml 20 hydroxyecdysone (herein referred to as ecdysone). A cavity slide was lowered gently onto the coverslip, the medium and disc becoming suspended between the coverslip and the bottom of the cavity slide. The discs were viewed immediately or placed in the incubator at 16°C overnight until the stage of development required. Further experimental procedures were carried out, such as fixation and antibody staining, which are described with the appropriate chapter.

2.6: Fly lines

Transgenic fly stocks used in many these studies, unless stated, were obtained from the Bloomington stock centre (<http://flybase.bio.indianna>)

2.7: Moulting hormone (ecdysone)

The hormone used in all the Clone 8+ cell line experiments and imaginal disc dissection was the insect moulting hormone, ecdysone (20-hydroxyecdysone Northern Biochemical Company). For experiments using 10ng/ml of ecdysone:100µg ecdysone was weighed out onto a foil boat, 5 ml of the appropriate medium added (under sterile conditions) and serial dilutions

made. Filter sterilisation was not carried out as this appeared to affect the activity of the hormone in cultures.

2.8: Microscopy

During routine observations cells were monitored and photographed using a Leitz Diavert photomicroscope or a Nikon inverted photo microscope. Cells treated for visualisation by immunofluorescence were examined using a Zeiss (Oberkochen Ltd) Axioplan 2ie microscope fitted with accessories for indirect fluorescence, differential interference contrast, and phase microscopy. Images were captured using x10, x20, x40, x63 (NA 1.4) oil immersion, Planapo objectives, and an Orca ER cooled CCD camera (Hamamatsu Photonics UK Ltd). Analysis and image management were conducted using OpenLab software version 3.09 (Improvision Co. Ltd) and Adobe photoshop version 5.5 (Adobe Systems Incorporated) for Apple Mackintosh. Figures which are found within the Introduction, Materials and Methods and Discussion sections have been given a numerical prefix and suffix. Figures which are listed in the Results sections have been given a numerical prefix and an alphabetical suffix.

Chapter 3

Primary embryonic cultures

3.1: Introduction

Cell death, proliferation and differentiation play an important role during metamorphosis in holometabolous insects. However the changes which take place are difficult to study in whole organisms, due to the rapid degeneration of the cells undergoing the process (Jacobson et al., 1997). In *Manduca sexta*, neurons that are fated to die appear to contain higher levels of an ecdysone receptor than those that survive (Fahrback and Truman, 1989). In *Drosophila* there are three isoforms of the EcR receptor, EcR-A, EcR-B1 and EcR-B2 and it has been shown that these EcR receptors are expressed in different tissues at different times during development (Talbot et al., 1993). The response of many tissues to ecdysone during metamorphosis however has not been ascertained. Primary cultures of larval salivary glands have been used to study the ecdysone response due to their longevity, they may be cultured for several hours (Jiang et al., 2000). However maintaining cell types such as the larval midgut have proved more difficult due to their complexity (Jiang et al., 2000; Lee et al., 2002).

Primary embryonic cultures have been used infrequently since the 1980's, and would at this time seem to be an ideal *in vitro* culture system to examine the response of *Drosophila* cells to ecdysone using modern imaging techniques and it has previously been stated that there is some organisation into higher structures of these cells during development (Shields et al., 1975). Studies on whole *Drosophila* prepupae and pupae during metamorphosis have been difficult and to some extent the primary embryonic culture system appears to parallel what occurs during metamorphosis *in vivo*. After initiation, development proceeds and larval cell types are observed; addition of ecdysone elicits the programmed cell death of obsolete larval tissue and

signals the proliferation and differentiation of adult precursor cells into adult cell types. There is an added advantage of using primary embryonic cultures as they may continue to develop over a longer period of time, several weeks in many cases. Previous studies have found that cells which are competent to differentiate *in vitro* should be obtained from embryos after the initiation of gastrulation, stage 7. For these studies an early primary culture was initiated from embryos post gastrulation, 3½ –4½ hours after oviposition, stage 8, and a later primary culture initiated from 11-13 hour embryos, stage 12, in order to compare them with the standard 6-8 hour embryo, stage 10.

Initial investigations were to observe the similarities and differences between cell death, proliferation and differentiation of the cells *in vitro* and compare them with development *in vivo*. To what extent does the morphogenesis of primary embryonic cultures mirror *in vivo* development? Could the primary embryonic cultures be used as a 'model system' to investigate the role ecdysone plays during larval cell death and subsequent proliferation and differentiation of adult precursor cells, which occurs during metamorphosis *in vivo*?

3.2: Materials and Methods

Primary cultures were initiated following the protocol described in Chapter 2 (Materials and Methods). To aid with identification of some cell types and to follow their subsequent development in the cultures it was decided to utilise transgenic fly strains expressing GFP as well as wild-type flies (Sun et al., 1999; Ward et al., 2002).

3.2.1: Egg collection

Early embryos were collected for ½-1 hour and dissociated 3½-4½hrs after oviposition. Standard embryos were collected for 1 hour and dissociated 6-8 hrs after oviposition. Late embryos (pre-collection 4 hours) were collected for 1 hour and dissociated 11-13 hrs after oviposition.

3.2.2: Primary embryonic cultures

Primary embryonic cultures were initiated from dissociated *Drosophila* wild-type embryos and from fly strains expressing GFP in living cells using cultures derived from a GAL4 enhancer detection technique (Brand and Perrimon 1993). Fly strains used for GFP decoration of microtubules and nerve were 24B and 458 respectively. The 24B fly line, expresses GAL4 in presumptive mesoderm tissue which was crossed with a line carrying the UAS-tau-MGFP6 insert (Kaltschmidt et al., 2000). Cells of mesodermal origin, muscle, blood and fat, express the tau-GFP construct which decorates the microtubule network. Virgins were collected from both fly strains, crossed and the resulting F1 embryos were used to prepare primary embryonic cultures (chapter 2). The 458 fly line, expressing *GawB*elav (embryonic lethal abnormal vision) in the embryonic nervous system was crossed with a UAS-GFP.S65T2. Gal4 is expressed in all tissues of the embryonic nervous system (Lin and Goodman, 1994).

Column drop cultures were established and partial medium changes were made weekly. In order to dissect out the developmental stages α -ecdysone was added to the cultures on days 14 and 21 (mimicking the high titre peaks of ecdysone which occur at the end of the third instar larval stage and after puparium formation). α -ecdysone was chosen as the hormone, as the reaction

of cells in cultures to the pro-hormone, α -ecdysone, occurs at a much slower rate than adding ecdysone directly, therefore it would be easier to observe the development of the cultures.

Medium changes were:

All slides day 7:

25 μ l of medium was removed from the cultures and replaced with 25 μ l of fresh 1 $^\circ$ medium.

Control – No medium change

All slides day 14 and 21:

25 μ l of medium was removed from the cultures and replaced with 25 μ l of 4 μ g/ml α -ecdysone made in 1 $^\circ$ medium, which gave a final concentration of 2 μ g/ml.

Controls – No medium change

1 $^\circ$ medium change only.

Slides were examined on a daily basis, observations recorded and images taken. The following general observations were based on 8 (5 wild-type and 3 elav-GFP) successful culture initiations for each embryonic stage. The total number of slides used for observation of standard cultures was 163; early embryo cultures 128 slides and older embryos, 87 slides. As tau-GFP has been shown to have an adverse effect on normal neuron morphology these cultures were only used to identify defined cell types (Williams, 2000).

Note: There is no figure 3l or 3o

3.3 Results

3.3.1: Standard embryo cultures

Immediately after initiation of the culture, many different cell morphologies were present (figure 3a). In the first 24 hours there was a rounding up of some cells, cell death, differentiation and proliferation. Groups of myoblasts fused to form muscle and contraction of muscle was observed as early as 9 hours after initiation. Neural-like cells divided and either remained as single cells or aggregated into groups of 6 to 8 cell bodies. By the end of day 1 these groups and single cells had put out fine processes, and were identified as nerve, which was confirmed by the expression of *elav* in *elav*-GFP cultures. Fat like cells had also begun to aggregate around the nerve cell clusters (figure 3b).

By day 2 macrophage-type cells, larval fat, epidermal cells and imaginal disc cells were all identified. During days 2-7 further aggregation of cells occurred and association of muscle, nerve and fat cells was evident. Muscle was observed firmly attached to the coverslip, either in isolation or close to and under nerve cell clusters, the fat cells tending to surround and cover these clusters. The cultures were mobile, new attachments were made from nerve, muscle and fat aggregates to other aggregates and the appearance of the cultures changed daily. During the first week there was no evidence of further differentiation of defined cell types after day 4. By day 7, the 3-dimensional network of cells and tissues covered the cover-slip, with some cells, such as macrophages, adhering to the cover-slip and aggregates of cells, including fat cells and nerve, becoming suspended into the medium (figure 3c). Undifferentiated cells of a round or fibroblast like appearance were observed on day 12.

α -ecdysone was added to the cultures on day 14. By day 15, epidermal type cells had secreted 3-4 layers of chitin, cell blebbing was observed in some cells and small clusters of phase bright cells appeared in the cultures. By day 17 larval muscle contraction had largely stopped, though isolated muscle contractions were observed in some cultures. The amount of cell debris observed increased. The products of larval fat cell degeneration from day 17 obscured further observation for the following 2-3 days. By day 21 the neural network did not appear to be affected by the hormone, but the larval fat cells which had aggregated around the nerve cell bodies had disappeared, and larval muscle had degenerated (figure 3d).

One day after α -ecdysone addition on day 21, the cultures appeared to be less crowded. Macrophage-type cells increased in number and adult fat cells were observed on day 22 (figures 3e, 3f). Tissue recognisable as adult tubular and fibrillar muscle was observed by day 24 (figures 3g, 3h). Adult cuticle with bristles and trichomes, was also observed in these cultures. Trachea was observed briefly only on two slides in all the culture preparations, once on days 22-23 and once on day 28 -29 (figure 3i). No further changes were noted after day 28 and cultures began to degenerate around week 7.

3.3.2: Early embryo cultures

Initially early embryo cultures had different cell types present represented by a difference in cell morphology (figure 3j). The cells were extremely motile and as differentiation proceeded some cells began to aggregate, flatten down and put out processes. After 24 hours many cells were lost, rounding up and falling off the cover-slip and the cultures became sparse. The majority of surviving cells were pro-neural in appearance (Seecof et al., 1971). Small,

round, dark cells measuring 3-5 μ m in diameter sent out long thin processes which at intervals contained small nodules or varicosities. These cells and processes were identified as nerve, confirmed by the presence of elav, a protein expressed in neurons of *Drosophila* (Robinow and White, 1991) (figure 3k). As development proceeded small neural aggregates containing 4 -12 cell bodies developed, nerve processes extending from some neural cells became longer and more complex. By the end of week one, nerve cells were the dominant cell type and the neural networks which developed in the medium and on the coverslip were complex (figure 3m).

During the second week of culture axons grew alongside one another, giving the appearance of a single thickened tract, joining two or more neural cell clusters together. Single nerve cells connected to other axons or clusters until the nerve network was completely connected as one tissue (figure 3n). Larval muscle was observed in these cultures, although infrequently and the form was normally of a shortened type containing only a few nuclei. Larval fat cells, macrophage-type cells and epidermal cells (phase bright) were also present, again in small numbers. Imaginal disc vesicles and cells of unknown origin were never observed.

Addition of α -ecdysone on day 14 was followed by degeneration of individual axons (figures 3p, 3q). By day 19 the nerve tracts began to thicken and the aggregates of nerve cell bodies increased in number, large neural cells were also identified close to axons. Further thickening of nerve tracts and aggregation of nerve cell bodies was observed after the addition of α -ecdysone on day 21 (figures 3r, 3s). There was no change in the cultures after day 25, no adult tissue or cells, such as trachea, adult muscle or adult fat cells were observed in these cultures. Degeneration of the cultures took place around week 6.

3.3.3: Older embryo cultures

Older embryo cultures were distinguished by the presence of small, phase bright clusters of tightly bound undissociated cells which were identified as nerve cells (figure 3t). Larger aggregates of tissue were also present. Cuticle and undifferentiated single cells with different morphologies were present in small numbers. During the first 24 hours there was elongation, flattening and movement of cells to form complex tissue aggregates covering and surrounding the neural clusters (figure 3u). Cultures contained very few single cells. Imaginal disc vesicles reaching a diameter up to 130 μm were apparent from day 1 and in greater numbers than had been observed in the standard cultures. Filopodia (cytonemes) were observed stretching across the imaginal disc vesicles (figure 3v).

The imaginal disc vesicles remained in the cultures for up to six days and then disappeared. Single cell types such as macrophages and fat cells were present but in small numbers by comparison with standard cultures. During the second week flattened sheets of larval-like muscle were observed lying on top of tissue aggregates. The flattened sheets of larval-like muscles were attached to the coverslip on either side of the tissue (figure 3w). The complex tissue put out long processes thereby aggregating with other tissue (figure 3x).

Contraction of muscle cells was never observed in these cultures.

With the addition of ecdysone on day 14 the tight complex tissue structures in the older embryo cultures began to spread out. By day 19 degeneration of tissue revealed underlying clusters of neural cells from which the outward migration of single nerve cells was observed (figure 3y). Groups of elongated nerve cells also appeared in the cultures, attached to muscle (figure 3z). Many

of the single cells became flattened with long cell processes which were invaded by macrophage-type cells (figure 3aa).

After the addition of ecdysone on day 21 macrophages increased in number and melanization of many cells obscured any further observations on the development of these cultures (figure 3bb). However many cells also appeared to lose their cell processes and detach from the coverslip. Trachea, adult muscle (fibrillar or tubular) or adult fat cells were never observed in these cultures after the addition of hormone. Degeneration of the cultures occurred rapidly during week 4.

3.4: Discussion

The pattern of development in the primary embryonic cultures *in vitro* does not mirror the pattern of embryo development *in vivo*. This was to be expected as embryogenesis is a complex process. Cells and tissues require an assortment of developmental cues which are received spatially and temporally, these are implicit to the normal development of the embryo. Unfortunately during the dissociation of the embryos *in vitro* these cues have been permanently lost.

The degeneration of *Drosophila* cells and tissue *in vitro* shares similarities with the stage-specific response found *in vivo* to ecdysone. However the precise timing of the degeneration of the majority of cells after ecdysone was impossible to pinpoint. The larval fat body responded to the early pulse unfortunately the products of this degeneration prevented further observations. Similarly the proliferation and differentiation of adult precursor cells was elusive. This was due in part to the variability of development

observed in all culture preparations and even every slide. During the homogenisation process and subsequent aliquoting, the cells are plated in a random mix and not every cell type may have been represented adequately on every slide.

Cultures initiated from stage 10 embryos 6-8 hours after oviposition were comparable with observations made by other investigators (see Introduction) (Shields and Sang, 1970; Shields et al., 1975; Dübendorfer et al., 1975). Primary embryonic cultured cells aggregated to form tissues that were recognisable as larval, such as fat body, muscle and nerve (Dübendorfer and Eichenburger-Glinz, 1980). However this tissue did not aggregate in an anatomically correct way which would be recognisable as a functioning tissue in larvae. For example aggregations of nerve cells did not form structures which could be compared to the ventral nerve cord *in vivo* (Broadie et al., 1992). Solitary larval muscle was observed to contract spontaneously, with no input from nerve present or attachment to epidermal cell types. Epidermis is essential to the further development of the muscle after muscle differentiation (Bate, 1990).

Degeneration of the larval tissue *in vivo* occurs in a stage-specific sequence, anterior muscle and the midgut breakdown in response to the late third instar ecdysone pulse. The larval salivary glands degenerate in response to the prepupal ecdysone pulse (Robertson, 1936; Jiang et al., 2000). Standard cultures responded to the first peak of ecdysone by the degradation of the fat body, the by-products obscuring many other cells undergoing cell death at this time. Cells and tissue undergoing degeneration were also obscured by other cells lying across or over them. Muscle breakdown was evident after the first application of ecdysone was given, as muscle contractions ceased in the cultures around day 17 and sheet muscle was observed to disintegrate. Without further characterisation of the larval muscle which had developed in

these cultures it is not known whether the muscle was specifically anterior but this seems unlikely. If all the muscle present in these cultures degenerates after the first peak of α -ecdysone this serves as an indication that their developmental response to ecdysone may have become inappropriate. *In vivo* the total loss of musculature after the first peak of ecdysone does not occur. The muscle cells response to α -ecdysone may have been affected by the initiation process or as a response to neighbouring cells and tissues which they would not normally be in contact with.

Adult precursor cells were present in the standard cultures, as during the fourth week of culture adult fat, adult muscle, tubular and fibrillar were observed (figure 3f,h,i). Every effort was taken to follow the progress of small nests of cells present in the cultures which may have been adult precursors cells. However the active migration of cells and remodelling of tissue which took place during the morphogenesis of the cultures prevented this. Adult fat body was observed by day 22 and it is possible that these precursors responded to the first peak of ecdysone. It is impossible to predict when the adult muscle precursor cells first responded to the ecdysone and began to differentiate, as they were only recognisable in their final adult form and appeared around days 26-32, several days after the second application of ecdysone.

Primary embryonic cultures initiated from early embryos consistently produced cultures which were almost entirely nerve (figures 3n). The observation that neuron-like cells formed a high proportion of the surviving cell population in cultures initiated from early embryo cultures was also made by Shields and Sang (1970). As dissociation of the early embryo takes place shortly after gastrulation, it is likely that other cell types do not survive in these cultures because they need other inductive signals from the developing

embryo which are lost once the embryos are dissociated. The neural cells may be the first cells to acquire the competence to differentiate *in vivo* and therefore need no more positional input in order to proceed with development *in vitro*. Other cell types present such as macrophages and muscle may be an indication that older embryos were present in the egg collection.

The persistence of the early embryonic cultures is possibly due to the fact that *in vivo* some neural cells (neuroblasts), such as those associated with the mushroom body, divide continuously throughout embryonic and larval life, while the daughter cells differentiate into neurones and glial cells (Lee et al., 1999). Neural cells such as thoracic neuroblasts divide from the second instar larval stage until the pupal stage and abdominal neuroblasts divide during the third instar larval stage (Ito and Hotta, 1992; Tissot and Stocker, 2000). If any, or all, of these neural cell types are present in the early embryonic cultures this would account for the continued neurogenesis observed in these cultures.

When α -ecdysone was added to these cultures there appeared to be remodelling of the neural network. Some cell processes (axons and dendrites) degenerated, other nerve processes became thickened and the nerve network became more complex. To some degree this echoes the initial remodelling of the larval nervous system *in vivo*. During metamorphosis neurons act in one of two ways, either responding to ecdysone by undergoing programmed cell death or persisting into the adult nervous system (Truman, 1990; Gendre et al., 2004). Pruning of excess neuronal cell processes by retraction or by degeneration of the axons and dendrites during metamorphosis has been shown in *Drosophila* (Lee et al., 1999; Watts et al., 2003). In the mushroom bodies, glial cells are thought to have a role in the pruning process by

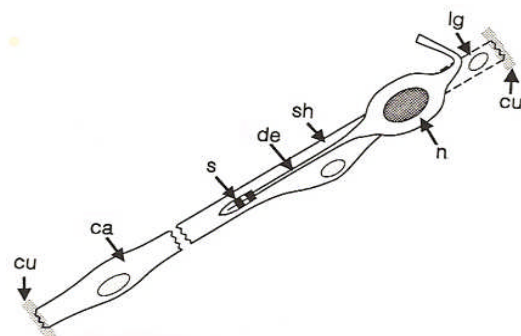
invading and engulfing the degenerating processes (Watts et al., 2004; Awasaki and Ito, 2004). In contrast remodelling of the thoracic ventral neurosecretory cells was found to be by axon retraction (Brown et al., 2006). The remodelling identified in the early embryo cultures appeared to be by axon degeneration (figures 3p 3q). Axon retraction was not observed, this does not mean that it did not take place but that it would be more difficult to identify. The presence of varicosities along the nerve cell processes is possibly an aberrant morphology, varicosities found on other neural cell processes *in vitro* have been found to contain randomly ordered microtubule organisation. This contrasts to neurites *in vivo*, in which microtubules are uniformly distributed and longitudinally oriented (Jacobs and Stevens, 1986 cited in Brown et al., 2006).

Identification of specific nerve cell types, such as the chordotonal organs, and their individual response to ecdysone in these cultures would be difficult without continuous observations. Larval chordotonal organs are located in the body wall attached to cuticle and are made up of a single neuron and three support cells (figure 3.1). Large nerve cells which resembled chordotonal organs were observed after ecdysone addition (figure 3r). It is possible that these nerve cells were adult fly chordotonal organs, although there is little morphological difference between larval and adult and they may have been present before ecdysone addition (Jan and Jan, 2003). Unfortunately these cell types were observed infrequently.

Figure 3.1: Chordotonal organ

cu, cuticle; ca, Cap cell; s, scolopale;
de, dendrite; sh, sheath cell; n, neuron;
lg, ligament cell.

(adapted from Jan and Jan, 1993).



As few cell types, other than neuronal, were present in the early embryo cultures it is unfeasible to truly compare these observations with remodelling of the central nervous system which takes place during metamorphosis *in vivo*.

The late embryos were extremely difficult to dissociate and the culture preparations were often a mass of undissociated tissue (figure 3t). As these embryos are further on in developmental time (stage 12) we would expect that the cells and tissues would be more firmly adhered to each other. In the cultures, tissue aggregation was rapid and the tissue was very complex, with few recognisable previously defined cells or tissue present. Nerve cell clusters were identified using elav-GFP. Late embryo cultures responded to the first pulse of ecdysone by cell spreading and flattening, a characteristic shared by some cell lines *in vitro*. Migration of nerve cells was also observed. Adult muscle and fat precursor cells may have been present but, contrary to expectations, there was no evidence for this as tissue recognisable as adult was not observed after ecdysone. One possible explanation for this is that stage 12 embryos have already been exposed to a high level of ecdysone *in vivo* during germ band retraction (Kozlova and Thummel, 2003). This may have affected the cells' subsequent response to ecdysone *in vitro*.

Macrophages were present in all of the primary embryonic cultures although to varying degrees. In the standard embryo cultures the appearance of macrophages to areas where cells were undergoing apoptosis was apparent (figure 3e). The sudden appearance of increased numbers of macrophages in the standard cultures may have been due to the degeneration of larval fat body and muscle which may have obscured macrophage cells already present. In the early embryo cultures, few macrophages were present. On the addition of α -ecdysone their numbers did not appear to increase unlike the

standard or late embryo cultures. Cellular debris was seen in all of the cultures and the size of macrophages varied from 20 μ m up to 60+ μ m in diameter. This compares with findings which have suggested that the numbers of macrophages *in vivo* does not increase with the increase of cell death, but that macrophage cells may increase in size as cellular debris accumulates in the haemolymph (Tepass et al., 1994).

The rate and pattern of cell development and subsequent cell death and degeneration was variable from culture to culture and slide to slide. This was despite improvements made to the conditions for the culture of cells *in vitro*, such as the homogenisation technique, which was adjusted to minimise cell damage. Egg collection times were shortened to reduce the variability in embryo development and an increase in the number of medium changes was also included. Removal of ecdysone was also carried out, to echo the low levels found between the peaks found *in vivo*. Due to this variability, further procedures such as the use of transgenic fly lines and immunohistochemistry to identify specific cell types and EcR receptor expression during metamorphosis were not pursued (Abrams et al., 1993; Talbot et al., 1993; Schubiger and Trueman, 2000; Li and White, 2003).

Although these cultures may not give any insight into how ecdysteroids regulate stage-specific cell death, proliferation and differentiation there are many cell types which are clearly identifiable, such as muscle, macrophages and nerve. Recently this culture system has been used successfully in investigations on the cytoskeleton in association with defined cell types (Tucker et al., 2004; Cottam et al., 2006). Using wild-type and transgenic fly lines, it would be of interest to exploit these cultures to examine the effect of RNA Interference (RNAi) on a defined cell type. At this time only cell lines and primary cultures, using single embryos albeit rarely, are used to

investigate the effects of dsRNA on cells. Cell lines although useful, do not contain cells of a defined cell type and primary cultures have a very short life span, just a few days in many cases. Development of the primary embryonic culture system in order to assess the effect of specific dsRNA would give an added insight into the roles of genes and proteins on cell morphology, adhesion and migration in defined cell types.

Figures

Figure 3a: Standard embryo primary culture, 3 hours after initiation
 Phase contrast image of undifferentiated cell types with different morphologies which are normally present in these cultures. Aggregation of cells can be seen beginning to take place.
 n, neural type cells; p, process;
 e, epidermal cell.
 Scale bar represents:20µm

Figure 3a: Standard embryo culture, 3 hours after initiation

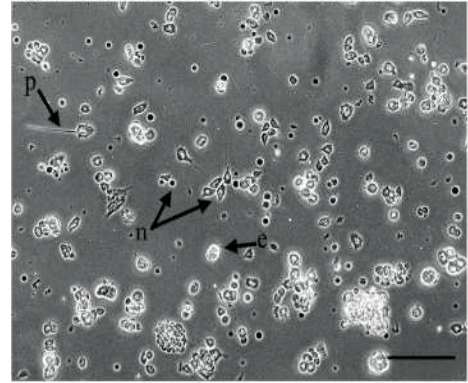


Figure 3b: Standard embryo culture 24 hours after initiation
 Phase contrast image one day after initiation, muscle cells have fused and elongated. Contraction of muscle has already begun. Nerve cells have aggregated and long processes can be seen. This image was taken focused below the plane of the coverslip as cultures were already beginning to hang in a 3-dimensional network.
 a, aggregate of various cells; m, muscle;
 p, nerve cell process; e, epidermal cell.
 Scale bar represents:20µm

Figure 3b: Standard embryo culture 24 hours after initiation

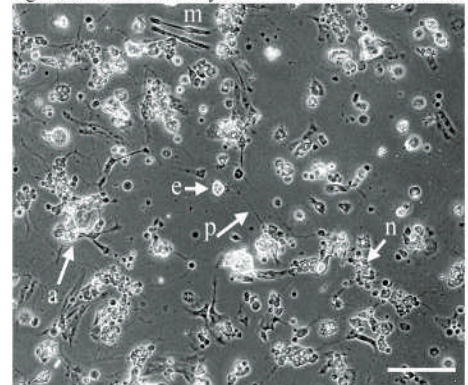


Figure 3c: Standard embryo culture day 7
 Phase contrast image showing an overview of one small area of the standard culture. Aggregates of nerve, muscle and fat body hang from the coverslip into the medium. A hollow epidermal vesicle is attached to an aggregate of tissue. The dark processes extend from the nerve cell aggregate to other aggregates. Fat cells can be seen covering nerve cells and nerve processes.
 a, aggregate; p, nerve process; v, vesicle; f, fat cells
 Scale bar represents 20µm

Figure 3c: Standard embryo culture day 7

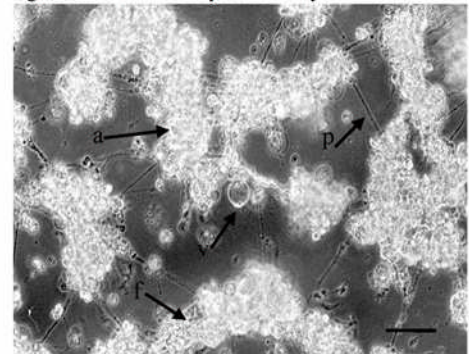


Figure 3d: Standard embryo culture after ecdysone week 3.
 DIC image showing the standard culture approximately 3 days after ecdysone. Larval muscle and fat body have degenerated and the products of the degenerating cells has dispersed revealing the clusters of nerve cells underneath. The nerve tracts appear thicker and more complex.
 p, nerve process; n, nerve cell
 Scale bar represents 20µm

Figure 3d: Standard embryo culture, after ecdysone, week 3.

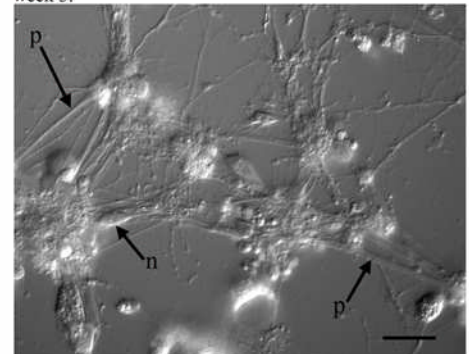


Figure 3e: Standard embryo culture, day 22,
1 day after 2nd ecdysone addition
Phase contrast image of macrophages firmly attached
to the coverslip.
m, macrophages; af, adult fat body
Scale bar represents:20µm

Figure 3e: Standard embryo culture, day 22, 1 day after 2nd ecdysone addition

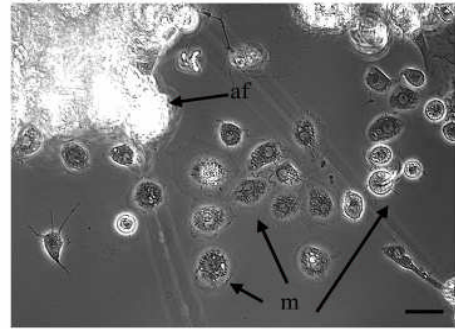


Figure 3f: Standard embryo culture, after ecdysone, day 22
Phase contrast image of adult fat body which was
observed after cultures had been exposed to ecdysone.
The adult fat has already begun to cover nerve cell
aggregates.
af, adult fat body; n, nerve cell
Scale bar represents:20µm

Figure 3f: Standard embryo culture, after ecdysone, day 22

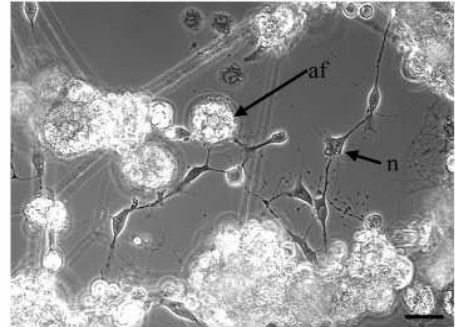


Figure 3g: Standard embryo culture after ecdysone,
day 29, fibrillar muscle.
DIC image of differentiated adult fibrillar muscle which
was observed after 2nd exposure of ecdysone around days
28-30. The fibrils extended from aggregates of nerve
tissue into the medium. Rapid muscle contraction of the
fibrillar was observed although infrequently.
Fm, fibrillar muscle; af, adult fat body
Scale bar represents:20µm

Figure 3g: Standard embryo culture day 29 after ecdysone, fibrillar muscle.

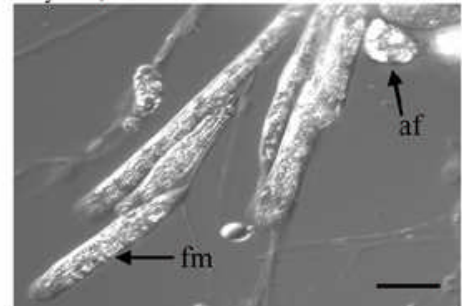


Figure 3h: Standard embryo culture after ecdysone
day 29, tubular muscle
Phase contrast image of fully differentiated adult tubular
muscle observed around days 27-30, after of ecdysone on
days 14 and 21. The tubular muscle extended from aggregates
of nerve tissue and the muscles were attached to the coverslip
or other aggregates via large nerve cells. Slow muscle
contraction was observed.
t, tubular muscle; n, nerve cell
Scale bar represents:20µm

Figure 3h: Standard embryo culture after ecdysone, tubular muscle.

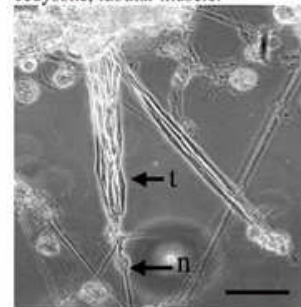


Figure 3i: Standard embryo culture after ecdysone day 28.
Phase contrast image of trachea which was observed
infrequently, easily identified by the large nuclei and
the long filopodial extensions which grew outwardly
from the main body into the medium.
af, adult fat body; t, trachea; m, macrophage
Scale bar represents:20µm

Figure 3i: Standard embryo culture after ecdysone, trachea.

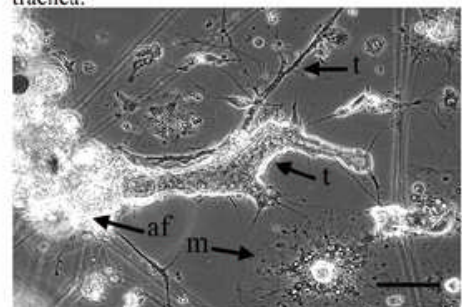


Figure 3j: Early embryo culture 3 hours after initiation
Phase contrast image of undifferentiated cells with different morphologies, many phase bright epidermal-like and small dark neural-like cells were found in these cultures just after initiation
n, putative undifferentiated nerve cell; e, epidermal cell
Scale bar represents:20µm

Figure 3j: Early embryo culture 3 hours after initiation

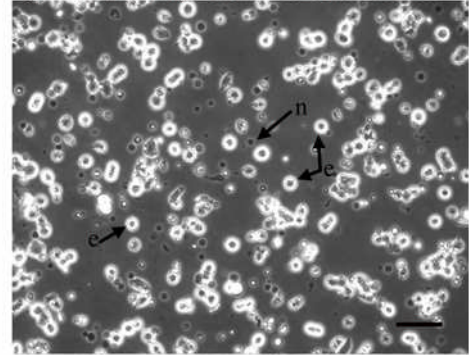


Figure 3k: Early embryo culture 24 hours after initiation
DIC image showing nerve cells which are the dominant cell type, lots of nerve processes (axons) are growing out from the small aggregates and single nerve cells and can be seen covering the coverslip.
Muscle and macrophages were rarely observed in these cultures.
e, epidermal cell; n, nerve cell; p, nerve processes;
v, varicosity
Scale bar represents:20µm

Figure 3k: Early embryo culture 24 hours after initiation

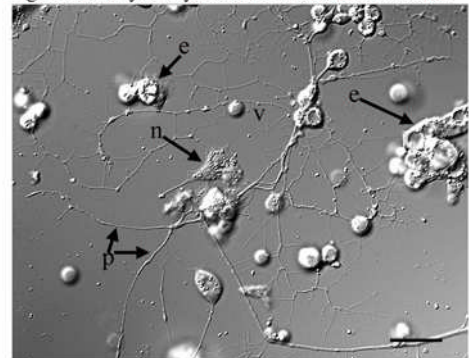


Figure 3m: Early embryo culture 1 week.
Phase contrast image of a typical culture at this time.
Cultures look sparse when compared to the 1 week standard culture. Very little muscle is observed, epidermal cells and fat body is present surrounding nerve cell aggregates.
n, nerve; p, processes;
Scale bar represents:20µm

Figure 3m: Early embryo culture 1 week

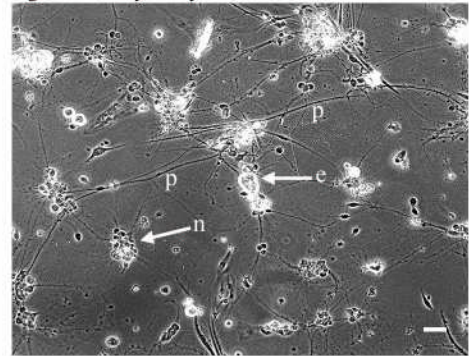


Figure 3n: Early embryo culture 2 weeks.
Phase contrast image showing the complex development of nerve tissue present in these cultures just before the addition of ecdysone. The number of nerve cells in the aggregates has increased. Axons have grown alongside one another giving the appearance of a single thickened tract. All the neural cell clusters are joined together and the nerve network is completely connected as one tissue.
a, aggregates; e, epidermal cell; n, nerve cells;
p, nerve cell processes; tnt, thickened nerve tract.
Scale bar represents:20µm

Figure 3n: Early embryo culture 2 weeks

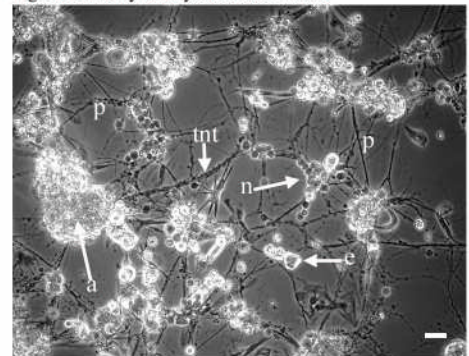


Figure 3p: Early embryo culture day 14 (before hormone)

Phase contrast image before the addition of ecdysone of one area in a culture which was sparse and therefore easier to track changes. Many of the nerve processes have small nodule attachments, or varicosities, and form extensive networks in the medium.

a, aggregate of nerve cells; v, varicosities
Scale bar represents:20µm

Figure 3p: Early embryo culture day 14 (before ecdysone)

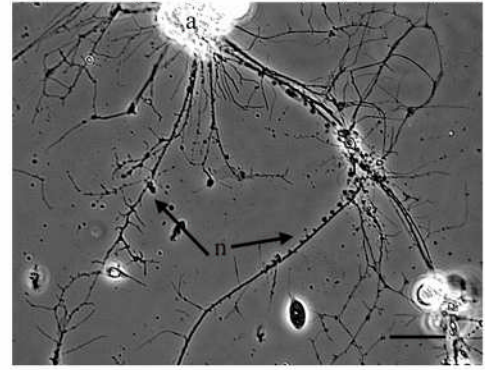


Figure 3q: Early embryo culture day 15 (after hormone)
Phase contrast image of the same area as in figure 3p but 24 hours after ecdysone. The processes appear to be responding to ecdysone by degeneration of the axons, the nerve cell aggregates do not appear to be affected. Macrophages, usually present when cells degenerate were not observed to be in the immediate vicinity when this was taking place.

a, aggregate of nerve cells; d, degenerating nerve
Scale bar represents:20µm

Figure 3q : Early embryo culture day 15 (after ecdysone)

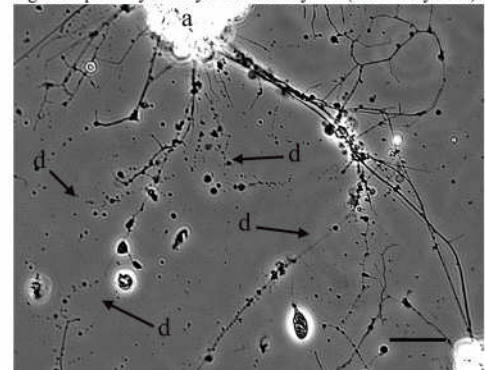


Figure 3r: Early embryo culture elav-GFP after ecdysone, day 25.

This DIC image shows further thickening of nerve tracts and aggregation of nerve cell bodies was observed after the addition of moulting hormone on day 21 (figures 3r, 3s). There was no change in the cultures after day 25, no adult tissue or cells, such as trachea, adult muscle or adult fat cells were observed in these cultures.

a, aggregate; f, fat body; tnt, thickened nerve tract; un, unknown nerve cell

Scale bar represents:20µm

Figure 3r: Early embryo culture, elav-GFP, day 25, after ecdysone

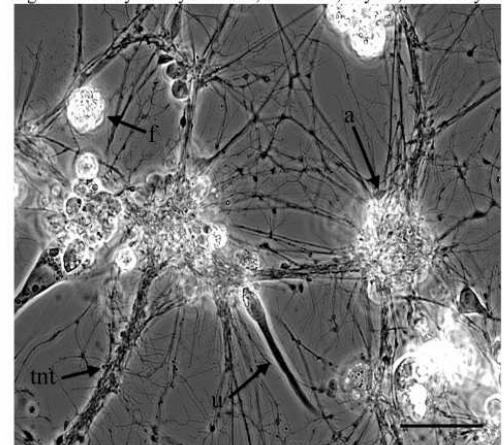


Figure 3s: Early embryo culture, elav-GFP

Fluorescent image of figure 3r, showing the expression of elav-GFP confirming the observations that the majority of cells and processes are nerve. There are also cells present in the cultures identified as putative sensory nerve cells (the chordotonal organ).

n, nerve cell

Scale bar represents:20µm

Figure 3s: Early embryo culture, elav-GFP

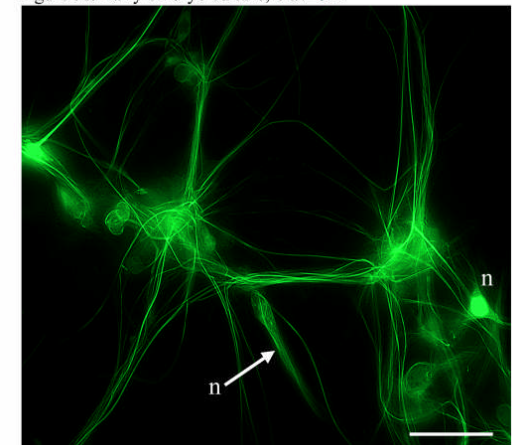


Figure 3t: Late embryo culture 3 hours after initiation
Phase contrast image showing the undissociated tissue which was present in these cultures soon after initiation. Single cells were rarely observed.
f, fat body; u, undissociated cells; n, nerve cell
Scale bar represents:20µm

Figure 3t: Late embryo culture 3 hours after initiation

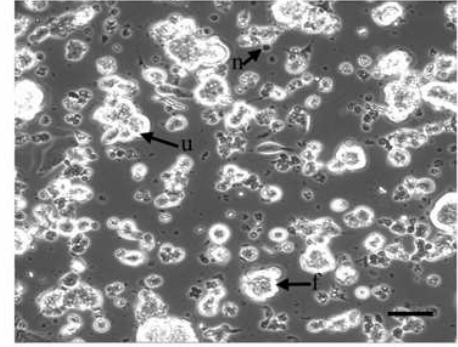


Figure 3u: Late embryo culture 24 hours.
DIC image of undissociated tissue in the older embryo cultures which aggregated to form complex structures. Nerve cell processes were not in evidence, unlike in the young and standard cultures. However isolated muscle and groups of nerve cells could be identified.
m, muscle; n, nerve aggregate
Scale bar represents:20µm

Figure 3u: Late embryo culture 24 hours after initiation

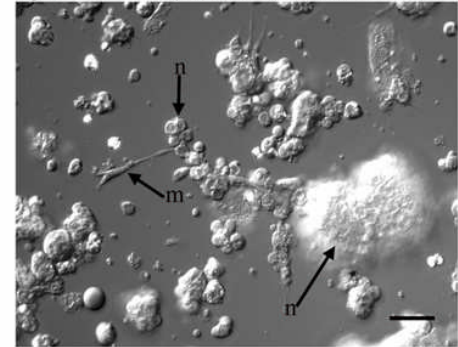


Figure 3v: Late embryo culture, week 1, Imaginal disc vesicle
DIC image showing an imaginal disc vesicles. Imaginal disc vesicles reached up to 130µm in diameter, filopodia or cytonemes were observed stretching from one side of a vesicle to another.
i, imaginal disc vesicle; c, cytoneme
Scale bar represents:20µm

Figure 3v: Late embryo culture, week 1
Imaginal Disc vesicle.

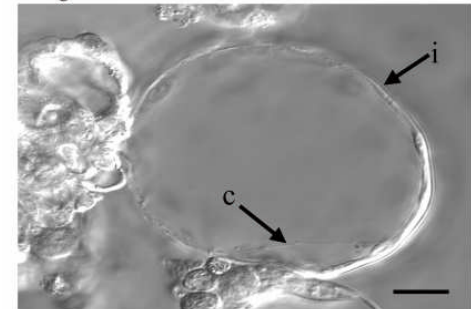


Figure 3w: Late embryo culture, week 2 complex tissue aggregates
DIC image of two aggregates of tissue, many individual aggregates eventually made connections with others by nerve processes.
a, aggregate of nerve and unidentified tissue; p, nerve cell process; v, vesicles.
Scale bar represents:20µm

Figure 3w: Late embryo culture, week 2
complex tissue aggregates.

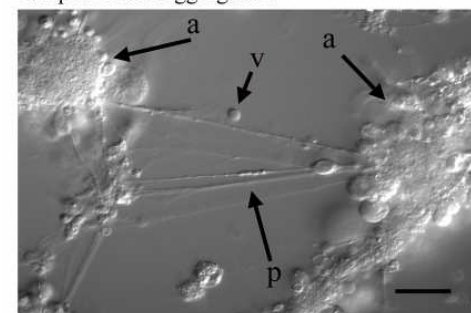


Figure 3x: Late embryo culture week 2, flattened muscle-like cells.
DIC image of flattened tissue, muscle-like in appearance which attached to the floor of the coverslip at various points and covering the nerve tissue. The nerve tissue is seen here out of focus underneath.
a, aggregate; m, muscle-like cells; n, nerve cell
Scale bar represents:20µm

Figure 3x: Late embryo culture week 2,
flattened muscle-like cells.

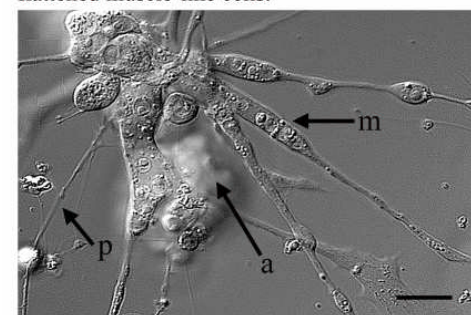


Figure 3y: Late embryo culture, day 17, 3 days after ecdysone.

DIC image of nerve cells (identified by the presence of elav-GFP) migrating away from a slowly degenerating aggregation of nerve and unidentified tissue after the initial exposure of the cultures to ecdysone.

n, nerve cells; m, muscle

Scale bar represents:20µm

Figure 3y: Late embryo culture day 17, 3 days after ecdysone, nerve cell migration.

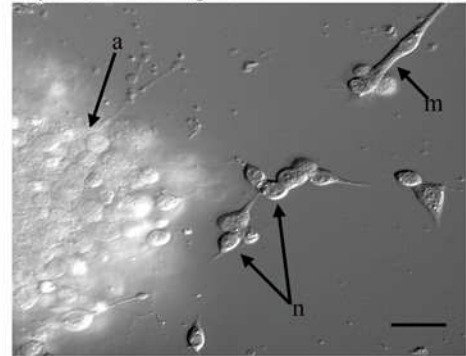


Figure 3z: Late embryo culture, day 17, 5 days after ecdysone.

DIC image of the same region as 3y above, but 2 days later. Cells have differentiated to form elongate cells with different morphologies. In this culture the migrating nerve cells observed made attachments to muscle cells.

a, aggregate; n, nerve cell; m, muscle

Scale bar represents:20µm

Figure 3z: Late embryo culture, 5 days after ecdysone, nerve cells attached to muscle.

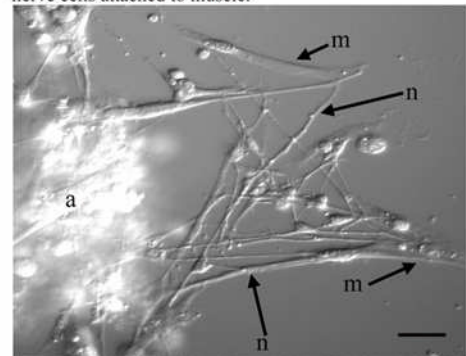


Figure 3aa: Late embryo culture day 19, 4 days after ecdysone.

DIC image of a cell, possibly a nerve cell, which has flattened and spread after the first exposure to ecdysone. Macrophages can be seen starting to invade the nerve tissue.

m, macrophage; s, spreading of the cell

Scale bar represents:20µm

Figure 3aa: Late embryo culture day 19, 4 days after ecdysone, cell spreading.

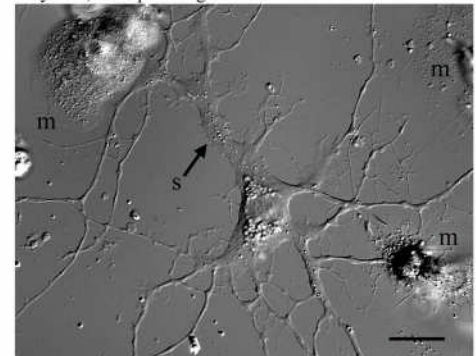


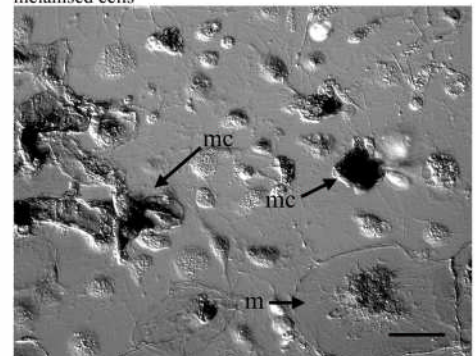
Figure 3bb: Late embryo culture day 25, after ecdysone.

DIC image showing areas commonly found in these cultures after the second exposure to ecdysone. Most of the tissue has degenerated, cells are spread out onto the culture surface and melanised cells can be seen. These cultures were full of macrophages

m, macrophage; mc, melanised cells

Scale bar represents:20µm

Figure 3bb: Late embryo culture, day 25, after ecdysone melanised cells



Chapter 4

RNAi analysis in primary embryonic cultures

4.1: Introduction

It was discovered that injecting the nematode *Caenorhabditis elegans* with double stranded RNA (dsRNA) directed against a specific gene, caused a powerful effect resulting in loss-of-function phenotypes (Fire et al., 1998; Montgomery et al., 1998). Since the initial discovery RNA interference (RNAi) has become a technique which is proving to be an extremely useful tool in dissecting out the roles played by genes of interest in many organisms including *Drosophila*.

Early studies on *Drosophila* and RNAi mostly involved the use of embryos which were injected with dsRNA (Misquitta and Paterson, 1999). The results of these studies were useful but the techniques employed proved to be time-consuming (Perrimon, 2002). Clemens et al (2000) using the well characterised insulin signal transduction pathway, showed that dsRNA could be added to directly to *Drosophila* cells in culture and specifically abolish the protein product of the gene they targeted. Since that experiment RNAi studies have mainly been carried out using *Drosophila* Schneider S2 cells in culture (Lum et al., 2003; Goshima and Vale, 2003; Roignant et al., 2003; Baeg et al., 2005; Guertin et al., 2006).

The ease and success of RNAi in *Drosophila* cell lines has been instrumental in the development of the method called 'High-throughput' RNAi screening (Armknecht et al., 2005; Echeverri and Perrimon, 2006). Multiple genes expressed in a cell line are systematically down regulated by RNAi to reduce the mRNA levels of that gene. Delivery of cells and RNAi into 384 well plates, microscopy and image acquisition, is almost entirely automated, which means that visual phenotypes can be screened very quickly (Kiger et al., 2003). Examples of loss-of-function phenotypes from genes that have been screened

so far include those that affect cell growth and viability and morphological defects (Kiger et al., 2003; Boutros et al., 2004). Important findings on a large scale have been made, such as the identification of more than 50 previously unidentified genes which have now been shown to play a role in cytoskeletal organisation and cell shape in morphologically distinct cells from cell lines (Kiger et al., 2003).

Cell lines chosen to perform RNAi studies normally express a particular gene of interest or have morphologically distinct features (Clemens et al., 2000; Kiger et al., 2003). However the interpretation of results may be difficult as the cells affected by the RNAi do not have a distinct phenotype. In addition many cell line populations although seemingly homogeneous are by nature heterogeneous. Cell lines are transformed and their genetic and biochemical properties may no longer be a true representation of their *in vivo* counterparts. It also has been suggested that the properties of a cell line may not remain constant and do in fact change over time (Dinan et al., 1990; Cottam and Milner, 1997). This was demonstrated recently in an RNAi study using a derivative of S2 cells which during the course of the study exhibited a change in morphology and no longer responded to the peptidoglycan treatment (Baeg et al., 2005).

At the present time few studies on the effect of RNAi involving primary cultures of *Drosophila* have been undertaken, as in most instances cells from primary cultures do not survive for many days. The primary embryonic culture system therefore, in which cells may survive for many weeks, would be an ideal additional *in vitro* system in which to explore the effect of RNAi. Many of the primary embryonic cells found in *in vitro* cultures have been characterised and are recognisable as cells derived from larval and adult tissue (Rizki 1957; Shields and Sang, 1970; Seecof et al., 1971; Shields et al.,

1975; Dübendorfer, 1976; Milner and Dübendorfer, 1982; Dübendorfer and Eichenberger-Glinz, 1980). Muscle, fat, nerve and macrophages are all represented in these cultures.

Preliminary experiments were carried out to examine the possibility that the primary embryonic culture system would be compatible with the addition of dsRNA and that RNAi could be demonstrated. Hopefully this would lead to devising an experimental protocol which could easily be implemented by other researchers and be used in this instance to examine specific dsRNA targeting protein *DmEb1* which may be involved in cell adhesion and migration.

4.2: Material and Methods

4.2.1: Optimization of RNAi in primary embryonic cultures

In *Drosophila* cell lines long dsRNA of around 500-700 bp can be introduced directly to cells and once inside the cell they are cleaved by a ribonuclease called Dicer, into small (21-25 nucleotides) interfering RNA's (siRNA's) (Tuschl et al., 1999; Zamore et al., 2000). The short siRNA's assemble with protein complexes into an RNA-induced silencing complex (RISC). Activated RISC then binds to complementary transcripts by base pairing interactions between the siRNA antisense strand and the mRNA. The bound mRNA is then cleaved and sequence specific degradation of mRNA results in gene silencing (Bernstein et al., 2001; Zamore, 2002).

The dsRNA used for these experiments were *Drosophila thread* (*th*) also known as DIAP1, EB1 and GFP which were between 500-700bp in length (supplied

by Buzz Baum). Experiments were based on a protocol provided by B. Baum, and scaled up from a 384 well plate (Kiger et al., 2003). As preliminary experiments indicated that direct exposure to dsRNA was insufficient in primary embryonic cells it was decided to approach RNA interference using alternative transfection methods at the same time.

Primary embryonic cultures were initiated from dissociated *Drosophila* wild-type (Oregon-S) embryos and from fly strains expressing EB1-GFP (FC29A1), a microtubule-associated protein which localises to the plus end tips of microtubules (Elliot et al., 2005). Cultures were initiated from embryos 5-7 hours after oviposition (the standard culture) following the protocol described in Chapter 2, with the following modifications:

The cells were homogenised and rinsed in SS3 (Sigma) medium, centrifuged at 4°C and re-suspended in SS3 medium. Shields and Sang medium was used as it was serum and antibiotic free, both serum and antibiotics have been known to impede the successful transfection of dsRNA. Cells were counted and control slides were made at 3.5×10^6 cells/ml in SS3 + 10% FCS.

Three experiments were set up in parallel:

Addition of dsRNA into the cells directly by soaking.

dsRNA transfection of cells using a transfection agent, FuGENE 6 (Roche).

Transfection of cells with dsRNA via electroporation (Multiporator, Amaxa biosystems).

Wild-type and EB1 Standard cells were prepared and given the following treatments:

- Cells only
- Cells + dsRNA
- Cells + FuGENE
- Cells + dsRNA + FuGENE
- Cells + Electroporation
- Cells + dsRNA + electroporation

The quantity of dsRNA used for a 384-well plate was 0.4µg per 1.4×10^4 cells/ml. This was adjusted for each dsRNA for example *thread* is at 0.5µg/µl, and for the number of cells, 1.4×10^5 cells per 40µl suspension drop. The dsRNA amounts in the following procedures are described for dsRNA *thread*. Slides were set up in the following ways:

4.2.2: Direct incubation of dsRNA and primary embryonic cells

To optimise the amount of dsRNA that would be effective 2µg, 4 µg and 6µg of each of the dsRNA's was used and cells were incubated with only one dsRNA at a time. As an additional control the Clone 8+ cell line was also used in the direct incubation of dsRNA onto cells. Clone 8+ cells have previously been used successfully in RNAi studies using transfection agents in 96 and 384 well plates (Baum, unpublished).

Sterile coverslips were placed on dampened filter paper.

10µl of 1.4×10^5 cells in SS3 medium were pipetted onto each coverslip.

3.2µl (4µg) dsRNA was added to the drop and mixed evenly.

Cells were covered and left to incubate for 2 hours (22°C) or overnight at 25°C or 16°C. Following incubation 30 µl of SS3 + 15%FCS was added to each drop,

the cells were covered with a drilled microscope slide, sealed with petroleum jelly and left inverted for several hours. Slides were kept in a 25°C incubator for the duration of the study. Standard cell suspension only was added to control coverslips in the same way to compare for evaporation and subsequent development.

4.2.3: Transfection agents

dsRNA transfection by FuGENE, a lipid-based transfection agent, was chosen as it had been known to be successful in RNAi assays (Baum, unpublished). To ascertain the optimum amount of FuGENE which may be required, experiments were carried out using 1:1 ($\mu\text{l}:\mu\text{g}$) 3:1 and 6:1 FuGENE: dsRNA.

For the 1:1 ratio the following components were aliquoted into small sterile eppendorf tubes, in the order and amounts listed;

SS3 medium, 15.6 μl

FuGENE: 4 μl

dsRNA: 3.2 μl (4 μg)

Cells: 22 μl

Total: 44.8 μl

FuGENE (at room temperature) was added to the medium, ensuring that FuGENE did not touch the plastic walls of the tube, and vortexed for 1 minute. After a 5 minute incubation period dsRNA was added.

dsRNA, medium and FuGENE were incubated for 45 minutes, before being added dropwise to the cells and mixed gently.

10 μl of treated cells, were pipetted onto sterile coverslips covered with sterile lids and incubated for two hours (22°C) or overnight at 16°C or 25°C

Following incubation 30 μ l SS3 + 15% FCS was added to each drop and the cells covered with a drilled microscope slide, sealed with petroleum jelly and left inverted for several hours. Slides were kept in a 25°C incubator for the duration of the study. Standard cell suspension with and without FuGENE, were set up as controls to compare for evaporation and development.

4.2.4: Electroporation

dsRNA cell transfection via electroporation uses electrical pulses to open up the cell membranes, allowing the passage of dsRNA into the cells.

Electroporation has previously been used successfully for transfection of plasmids into *Drosophila* S2 cells.

Cells were counted and resuspended at 5×10^6 cells/ml in 2mls SS3 medium. Cell numbers were increased to allow for any cell death which electroporation has been found to cause. The cell suspension was subdivided and centrifuged at 1600rpm for 1 minute. Supernatant was removed and the cells were resuspended in 1 ml Optimum electroporation buffer (Eppendorf) or 1 ml SS3 medium.

Cuvettes used for electroporation held 100 μ l of cell suspension.

The following were set up:

100 μ l Cells in SS3 medium

100 μ l Cells in Optimum

92 μ l cells in Optimum + 8 μ l dsRNA

92 μ l cells in SS3 medium + 8 μ l dsRNA

100 μ l Cells in Optimum no electroporation.

dsRNA (0.1 μ g/ μ l) was added to the cuvette just before electroporation.

The cells were electroporated immediately, as Optimisation buffer has been shown to have an adverse affect on successful electroporation if left in the buffer for too long. For all samples 2 programmes were used, programmes T-01, U-01 for 1 minute (Amaza). After electroporation 40µl cells were pipetted onto a coverslip, half of the medium was removed and replaced with SS3 medium + 15% FCS. Slides were placed on top, left inverted for several hours and incubated at 25°C for the duration of the study.

dsRNA has been known to take 2-3 days before taking effect (Clemens et al., 2000). The cultures were examined on a daily basis, images taken and observations noted.

4.2.5: Immunohistochemistry

Antibody staining was carried out using anti- α -tubulin (Sigma T9026) and anti-*DmEB1* (Diagnostic Scotland) to study the effect of dsRNA-EB1 in wild-type primary embryonic cultures.

Slides were fixed on days 4 and 10 after incubation with 6µg dsRNA *DmEB1*. Coverslips were removed from the slides and cells were rinsed briefly in PBS to remove any medium. Cells were fixed in ice-cold methanol 0°C for 4 minutes and rinsed gently in PBS three x 5 minutes then incubated for 2 hours at 25°C with primary antibody monoclonal mouse anti- α -tubulin diluted 1:1000 in PBS. Followed by rinsing with agitation 4 x 5 minutes in PBS and incubation with secondary antibody, anti-mouse fluorescein (Vector) 1:200 for 2 hrs at 25°C. After incubation the cells were rinsed with agitation 4 x 5 minutes in PBS. Cells were then incubated for 2 hours at 25°C with primary antibody rabbit anti-*DmEB1* used at 1:1500 diluted in PBS (Cottam et al., 2006).

Followed by rinsing with agitation 4 x 5 minutes in PBS and incubated with secondary antibody anti-rabbit-Texas red 1:200 for 2 hrs at 25°C.

After incubation cells were rinsed with agitation 4 x 5 minutes in PBS.

Nuclear DNA was stained by incubation with 0.125µg/ml DAPI solution for 10 minutes at room temperature, followed by rinsing in PBS, with agitation, 4 x 5 minutes.

Controls were set up as follows:

Cells from wild-type primary embryonic culture day 4 no dsRNA

Cells were fixed but not stained to monitor autofluorescence

Cells were fixed and incubated with secondary antibodies to monitor non specific binding.

Coverslips were mounted using Vectashield mounting medium, sealed with nail varnish and placed at 4°C and viewed the following day.

4.3: Results

4.3.1: Control cultures

Standard primary embryonic cultures derived from wild-type flies developed as expected (Chapter 3). Primary embryonic cultures derived from the EB1-GFP fly strain, using the standard timing, developed as the controls. Larval muscle, nerve and fat body were all identified and aggregation of these cells and development over a 2 week period were comparable to the wild type cultures (figure 4a). EB1 was found to be expressed primarily at the tips of microtubules (figure 4b) (Tirnauer and Bierer, 2000).

Table 4.1: The effect of dsRNA and transfection agents on primary embryonic cultures

Culture	DsRNA	FuGENE	Electroporation	Observations over 2 week period
Control/EB1	no	no	no	Cultures developed as normal
Control/EB1	<i>Th</i>	no	no	Cell death, recovery, contamination
Control/EB1	EB1	no	no	No effect
Control/EB1	GFP	no	no	No effect
Control/EB1	no	yes	no	Cell death, no recovery
Control/EB1	All	yes	no	Cell death extensive, no recovery
Control/EB1	no	no	yes	Rounded cells, no differentiation
Control/EB1	All	no	yes	Rounded cells, no differentiation

Table 4.1: Summary of results from all the experiments, using DsRNA and transfection agents in primary embryonic cultures. FuGENE had a negative effect on the cells. Electroporation resulted in round, undifferentiated cells in the culture.

4.3.2: Soaking of dsRNA directly

Incubation for 2 hours with 2 μ g, 4 μ g and 6 μ g dsRNA on wild-type and EB1-GFP culture preparations had no effect on the development of the cells monitored over a 2 week period. Incubation with 2 μ g dsRNA overnight at 25°C or 16°C showed no effect on wild-type and EB1-GFP primary culture preparations. For the initial 24 hours cells were observed to develop as controls, by day 3 contamination affected three quarters of the wild type slides and all of the EB1-GFP cultures. Surviving cultures continued to develop as the controls for the following 2 weeks.

Wild-type cells and Clone 8+ cells incubated with 4 μ g dsRNA and 6 μ g dsRNA *th* overnight at 25°C or 16°C contained significant areas of cell death when examined on day 3 (figure 4c). By day 5 the cultures had recovered, cell death was no longer evident and no further effects were observed (table 4.1).

Incubation with 4 μ g and 6 μ g dsRNA EB1 and GFP overnight at 25°C or 16°C appeared to have no effect on the wild-type cultures or Clone 8+ cells.

Antibody staining with anti-EB1 antibody on days 4 and 10 on wild-type

cultures soaked with 6µg dsRNA EB1, showed a positive result for EB1. EB1 appeared to be located at the ends of microtubules in all cell types examined (figure 4d). Many cultures, including the Clone 8+ cells became contaminated, surviving cultures developed as normal control cultures.

Incubation overnight at 25°C or 16°C with 4µg and 6µg dsRNA EB1, GFP and *th* on EB1 cultures examined on day 3 appeared to have no effect on the cells (table 4.1). Areas of cell death were not observed. Cultures were examined daily using fluorescence microscopy which showed the presence of EB1-GFP in all cell types examined and they appeared to develop in parallel with the controls. By day 6 no further development of these cultures was observed due to contamination.

4.3.3: FuGENE

Cells with FuGENE

By day 3 extensive cell death was observed in both wild-type and EB1-GFP cultures where cells had been treated with the transfection agent FuGENE (table 4.1). Single cells which had begun to differentiate were observed infrequently.

Cells and dsRNA and FuGENE

Extensive cell death was observed in all cultures where cells had been treated with dsRNA and the transfection agent FuGENE (table 4.1). As in the controls, single cells which had begun to differentiate were observed on the slides where the ratio of FuGENE to dsRNA 1:1 (figure 4e). Recovery of the cells was never observed in any of the cultures.

4.3.4: Electroporation

Cells and Electroporation

Electroporation resulted in cells which were undifferentiated with a round morphology, floating in the medium. Cell attachment to the coverslip was rarely observed and the cells remained undifferentiated for the two week period.

Cells and dsRNA and Electroporation

After 24 hours and for the following two weeks, cultures which had been subjected to electroporation and dsRNA were observed to be the same as the controls, undifferentiated and rounded in appearance (figure 4f). No recovery of the cultures was observed (table 4.1).

4.4: Discussion

Successful introduction of dsRNA into primary embryonic cultures remains to be resolved. Optimisation of RNA Interference in primary embryonic cultures has not been fully explored but there are several conclusions that can be drawn from the results so far.

4.4.1: Incubation and dsRNA concentration

An abnormal amount of cell death was observed in wild-type cultures incubated overnight with dsRNA *thread* (DIAP1) when compared to controls (figure 4c). As *thread* normally functions to inhibit apoptosis this result suggests that RNAi was successful and *thread* activity had been abolished in these cells (Muro et al., 2002). These cultures subsequently recovered which is

possibly an indication that the dsRNA was not dispersed sufficiently enough to cause loss of protein expression in all of the cells in the cultures. From this we can conclude that adding dsRNA directly onto cells on the coverslip should be avoided. Cells and dsRNA should be mixed together well prior to plating.

Successful introduction of dsRNA into all of the cells may also depend on the concentration of dsRNA, however as only a few molecules of dsRNA are required to cause an effect, and experiments on S2 cell lines have used as little as 2µg in a comparable number of cells (Clemens et al., 2000). The concentration of dsRNA added to the primary embryonic cultures should not necessarily be greater than the ones used in other experiments. However repeated exposure to dsRNA has been shown to have a positive affect on the success of introduction of dsRNA into cells and this would be a preferred method of action (Clemens et al., 2000).

4.4.2: Transfection agents

It has been clearly shown that transfection agents such as FuGENE and electroporation should not be used in future experiments during initiation of primary embryonic cultures. FuGENE alone appeared to have a cytotoxic effect on the cells (figure 4e), causing extensive cell death. The primary embryonic cells may be more sensitive at the time of culture initiation, there would already have been some damage caused by homogenisation and no time to recover before treatment with FuGENE. Electroporation on the other hand did not cause extensive cell death, although the products of degenerating cells were observed floating in the medium. Development of cells treated by electroporation was inhibited, cells never differentiated,

remained round in appearance (figure 4f) and were rarely observed attached to the coverslip.

The time chosen for the addition of dsRNA to the primary embryonic cultures was based on experimental evidence that primary cultures were difficult to introduce dsRNA into. Cells were more likely to take up dsRNA prior to differentiation (Baum, unpublished observation). In addition as serum and antibiotics have an impeding effect on transfection of cells culture, initiation is the time point at which these can be omitted and then added later.

Unfortunately the amount of contamination found in all of the cultures was a major drawback. It appears that addition of antibiotics should be done during initiation. If the competency of the dsRNA is affected by antibiotics before uptake by the cells perhaps repeated exposure of dsRNA to the cultures during the incubation period may solve this problem.

Only three dsRNA transcripts were examined during the optimisation process. Why choose these particular dsRNA's to initiate the optimisation of this technique?

4.4.3: EB1

Drosophila EB1 a microtubule-associated protein which localises to the plus ends of microtubules, is expressed ubiquitously during development in *Drosophila* (Elliot et al., 2005). *Drosophila* dsRNA EB1 has been shown to eliminate all the EB1 protein in an S2 cell line (Rogers et al., 2002). *Drosophila* dsRNA-EB1 was chosen for the optimisation of this technique as standard primary embryonic cultures derived from flies expressing EB1 could be assessed directly for the elimination of EB1 by fluorescence microscopy. In

addition antibodies to *DmEB1* were available which could be used in the wild-type cultures to confirm loss of EB1 in the cells.

In these experiments EB1 was observed at the ends of MTs as expected in EB1 primary cultures. Incubation of dsRNA to EB1 to these cultures during initiation did not have an effect, EB1 was still present when examined by fluorescent microscopy. Wild-type primary cultures which were soaked in dsRNA EB1, did not show any effect when examined by normal microscopy, which was to be expected as although downregulation of EB1 produces aberrant behaviour of microtubules, unfortunately it does not produce any obvious morphological abnormalities (Rogers et al., 2002). To test for possible loss of the EB1 protein these cultures were immunostained with anti-*DmEB1*. EB1 appeared to be present in all of the cell types and located at the ends of microtubules, when examined by immunofluorescence microscopy, this result was confirmed by anti α -tubulin staining which stains the microtubule network and the control slide with no dsRNA EB1 treatment. The effect of downregulation of EB1 may be difficult to assess in the initial development of primary embryonic cultures. However repeated treatment of dsRNA EB1 to established primary embryonic cultures around and during the time ecdysone is introduced may affect adult precursors and yield more interesting results (Chapter 3).

4.4.4: Thread

Drosophila thread/DIAP1 (*Drosophila* inhibitor of apoptosis), is a key regulatory protein which is known to be a cell death inhibitor, analysis of loss-of-function mutations have shown that *thread* is needed to block apoptosis very early in embryonic development (Goyal et al., 2000; Lisi et al., 2000). Introduction of dsRNA-*thread* into the cells would in theory result in

apoptosis of the cells. This could be assessed directly by fluorescence microscopy. Areas of cell death were observed in both wild-type, EB1 and the Clone 8+ cultures after incubation overnight with dsRNA-*thread*. However only isolated areas of cell death were found and the cultures subsequently recovered. This may indicate that dsRNA-*thread* was only taken up by a small number of cells during the incubation process. The distribution of dsRNA may have been inadequate or the amount of dsRNA was too little for the number of cells present.

4.4.5: dsRNA-GFP

dsRNA-GFP was used in this experiment as targeting GFP would act as a negative control against the possibility that a deleterious effect on the cells might be induced by dsRNA itself. Loss of GFP could also be directly assessed by fluorescence microscopy in EB1 cultures. Unfortunately wild type and EB1 cultures did not show any effect when incubated with dsRNA-GFP, although abnormal cell death was not observed, EB1-GFP was still present in EB1 cultures so GFP had not been suppressed.

4.4.6: Resistance to dsRNA

One possibility that cannot be overlooked is that the primary embryonic cells are resistant to dsRNA. The dsRNA used in these experiments are classed as long dsRNA's and have been used successfully in many experiments in *Drosophila* cell lines and pre-blastoderm embryos (Misquitta and Paterson, 1999; Goshima and Vale, 2003,). RNAi has been shown to be a powerful tool in *Drosophila* embryos, however injection of the embryos took place prior to cellularisation, when the cells have no membranes. At this time how dsRNA enters the cell is still an unknown. Long dsRNAs are not used in mammalian

cells as the interferon pathway is induced which results in cell death. Instead short hairpin RNA (shRNA) constructs are used in RNAi experiments (Elbashir et al., 2001a,b; Yang et al., 2001; Paddison et al., 2002, Ovcharenko et al., 2005). It is possible that introduction of long dsRNA will not work in the primary embryonic cells and it would be of interest to explore the possibility that shRNA would be more effective.

Due to time constraints, further experiments have not been undertaken but in the future further optimisation should include the following. Addition of the dsRNA to cells before plating, mixing gently but thoroughly. This should be followed by incubation of dsRNA and cells for a prolonged period.

Antibiotics should be added during initiation to prevent contamination.

Repeated exposure of the cultures to dsRNA should be assessed and shRNAs should be considered.

Figures

Figure 4a: EB1-GFP standard primary culture 7 days
 DIC image of primary embryonic culture derived from the fly line expressing EB1. Development compares with wild-type primary embryonic culture 7 days after initiation. Aggregation of nerve cells and muscle and nerve cell processes are evident.
 n, nerve cells; m, muscle; p, nerve processes
 Scale bar represents:20µm

Figure 4a: EB1-GFP standard primary culture 7 days

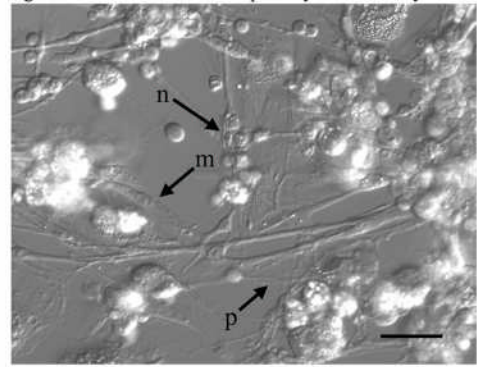


Figure 4b: EB1-GFP standard primary culture 7 days
 macrophage cell.
 Fluorescent image of a macrophage cell in EB1 primary embryonic cultures. Small constantly moving dots were observed in all cell types examined and confirmed as EB1 (arrows)
 Scale bar represents:20µm

Figure 4b: EB1-GFP standard primary culture 7 days
 macrophage cell.

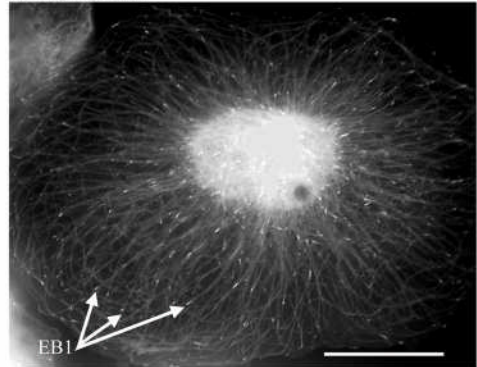


Figure 4c: Standard culture dsRNA thread, overnight incubation
 DIC image of the abnormal cell degeneration seen in areas of the wild type culture when compared to controls, 3 days after incubation with dsRNA thread. Aggregation of nerve cells and nerve processes growing away from the aggregates can be seen.
 a, nerve cell aggregation; d, degenerating cells; p, nerve processes
 Scale bar represents:20µm

Figure 4c: Standard culture dsRNA Th, overnight incubation

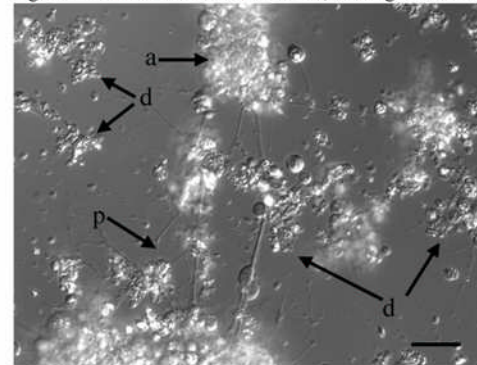


Figure 4d: Wild-type culture, anti-Dm-EB1, day 4
 Pseudo coloured fluorescent image of cells with anti-Dm-EB1 antibody staining. Wild-type cultures incubated with dsRNA EB1 overnight at 25°C when probed for anti-Dm-EB1 showed the presence of EB1 in all cell types examined.
 sm, sheet muscle; m, macrophage
 Scale bar represents:20µm

Figure 4d: Wild-type culture, anti dm-EB1, day 4

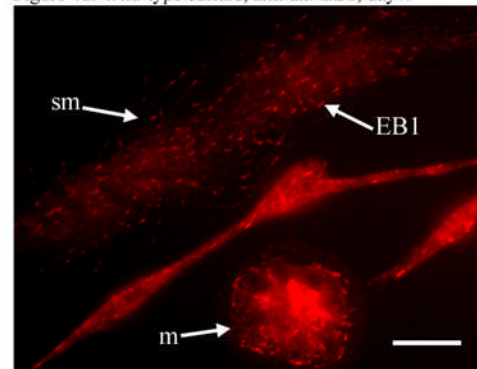


Figure 4e: Primary culture 3 days control FuGene only
DIC image of wild type primary culture and the reaction to FuGene shows the degeneration of the majority of these cells. Single cells which had begun to differentiate were seen, albeit infrequently. Aggregation of some cells was also observed but these were also undergoing degeneration.

a, aggregation of cells; c, differentiated cell; d, degenerating cells

Scale bar represents:20 μ m

Figure 4e: Primary culture 3 days, control FuGene only

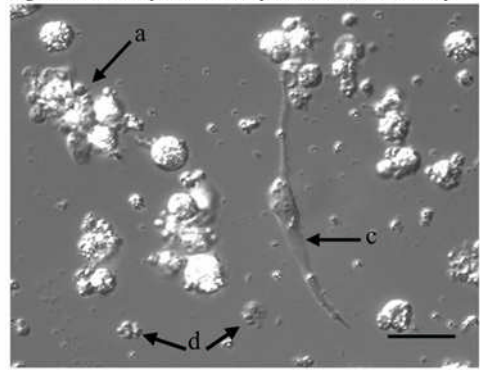
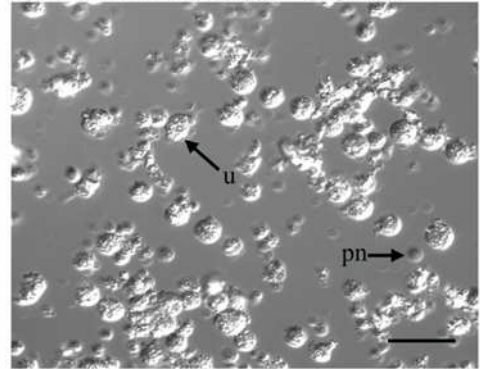


Figure 4f: Primary culture 3 days after electroporation
DIC image showing the round undifferentiated cells found after Electroporation. Most of the cells floated in the medium and cells were never seen to differentiate. Occasionally small phase dark cell of a pro-neural appearance were observed.

pn, pro-neural nerve cell; u, undifferentiated round cells.

Scale bar represents:20 μ m

Figure 4f: Primary culture 3 days Electroporation



Chapter 5

A statistical analysis of cell
adhesion in Clone 8+ cell lines

5.1: Introduction

The *Drosophila* imaginal disc cell line, CME W1, was originally derived from a single defined tissue, third instar imaginal disc epithelia, and unlike many insect cell lines is of known passage number, which is an indication of their 'in vitro' age (Currie et al., 1988; Cottam and Milner, 1997). From the original cell line, CME W1, a single cell was cloned at passage 30 and cells grown from this single cell are known as the Clone 8+ (Cl.8+) cell line. This cell line has subsequently been used for investigations in this laboratory and in others around the world (Oberdörster E et al., 1999; Kawamura et al., 1999; Oberdörster E et al., 2001; Lum et al., 2003). In this laboratory studies on the *in vitro* response to ecdysone, cell aggregation and adhesion have been undertaken, in addition they have also been used to highlight the possible changes which may take place in cell lines during long term culture (Peel and Milner, 1992; Cottam and Milner, 1997; Miller et al., 1999).

A derivative of Clone 8+, Clone 8R, was developed some years ago which is impervious to ecdysone (Peel and Milner, 1992). Recently another cell line derivative of Clone 8+ has been developed which can survive growing in medium alone, the Zero fly extract Clone 8+ cell line (ZfeClone 8+).

This Clone 8+ derivative is so named as the successful culture of many insect cell lines is dependant on additives made to standard culture medium.

Additives such as insulin and foetal bovine serum are necessary for sustained viability of the cells in culture and are available commercially. An addition of fly extract (haemolymph) which is not available commercially is required for the successful culture of the Clone 8+ cells and requires the input of a huge number of flies, which are not always available in other laboratories. The ZfeClone 8+ cells do not require fly extract in order to survive in culture,

although an increase in the amount of foetal bovine serum is required, therefore these cells represent an additional resource for researchers.

5.2: Materials and Methods

To examine the effect of ecdysone, compare the rates of growth (proliferation) and investigate the properties of adhesion, quantitatively, the following assays were undertaken on all the Clone 8+ cell lines.

5.2.1: Passage numbers (*in vitro* age)

Cell lines of low and high passage number, designated Young Clone 8+ (YCl.8+) and Old Clone 8+ (OCl.8+) respectively, Clone 8R (Cl.8R, resistant) and the Fly extract free cell line, Zfe Clone8 (ZfeCl.8+) were used.

The passage numbers were:

YCl.8+ p30 (19-21)

OCl.8+ p30 (92 -94)

Cl.8R p30 (20-21)

ZfeCl.8+ p30 (68-72)

The abbreviated form of the cell names used above will be used throughout the material and methods and results for all following chapters.

5.2.2: Growth rate and effect of ecdysone

To examine the growth rate and the effect of ecdysone on all cell lines: Cells were seeded at 3.5×10^6 per 5ml in CSM or in CSM with ecdysone

added to give a final concentration of 10 ng/ml (Peel and Milner, 1992; Cottam and Milner, 1997; Miller et al., 2000).

12 replicates were set up for each cell line with and without ecdysone, incubated at 25°C and harvested 24 hours (+ 10mins) or 5 days later.

Observations on cell morphology were recorded and cells were counted.

In order to maximise the utilisation of cell counts for an analysis on adhesion the cells were counted in the following way:

The medium and layer of suspended cells were carefully removed and counted, leaving the remaining cells attached to the substrate. These were removed and counted separately.

5.2.3: Data analysis

All analyses were carried out in Minitab V.13. Mean cell counts after 24 hours and five days without hormone were compared by one-way analysis of variance (ANOVA) with Tukey post-hoc analysis, the rate of growth and passage number was examined. Mean counts of cells after 24 hours with and without hormone were compared by two-way ANOVA. Tukey post hoc analyses were carried out to determine which data sets were significantly different from each other.

5.2.4: Cell adhesion

Based on an observation that OCI8+ cells appeared to adhere to the used substrate of YCI8+ cells, the following study was undertaken in order to examine the possibility that extracellular matrix components present on the YCI8+ used substrate had an affect on the adhesive properties of the OCI8+ cells.

YCl.8+ and OCl.8+ cells were seeded at 3.5×10^6 per 5ml onto 50mm Petri dishes which had already been used for growing YCl.8+ cells or OCl.8+ cells. 5 mls of fresh medium or a combination of conditioned medium and fresh medium was added to the cells and used substrates.

The conditioned medium (medium previously used for growing Young and Old Clone 8+ cells) was added to the cells to examine if there was an affect from factors in this medium which may have an effect on adhesion. As the addition of conditioned medium may have an adverse affect on cell viability a combination of conditioned and fresh medium was used (see table below). 12 replicates were set up for each condition and the cells were incubated at 25°C and harvested 24 hours (+ 10mins) after initiation or 5 days later. The medium and cells in suspension were carefully removed leaving the remaining attached cells which were removed and counted separately.

The cells and dishes were set up as follows:

Cell line	Dish type	CSM (fresh)		Conditioned medium (3mls) fresh medium (2mls)
YCl.8+	YCl.8+	5 mls	or	YCl.8+ conditioned medium
	YCl.8+	5 mls		OCl.8+ conditioned medium
	OCl.8+	5 mls		YCl.8+ conditioned medium
	OCl.8+	5 mls		OCl.8+ conditioned medium
OCl.8+	YCl.8+	5 mls	or	YCl.8+ conditioned medium
	YCl.8+	5 mls		OCl.8+ conditioned medium
	OCl.8+	5 mls		YCl.8+ conditioned medium
	OCl.8+	5 mls		OCl.8+ conditioned medium
YCl.8+	Unused	5 mls	or	YCl.8+ conditioned medium
YCl.8+	Unused	5 mls		OCl.8+ conditioned medium
OCl.8+	Unused	5 mls	or	YCl.8+ conditioned medium
OCl.8+	Unused	5 mls		OCl.8+ conditioned medium

5.2.5: Data analysis

The proportion of cells adhered to the substrate was established and the combined effect of used substrate, fresh substrate, fresh medium and

conditioned medium were compared using one-way and two-way analysis ANOVA. Tukey post-hoc analyses were carried out to determine which groups were significantly different from each other.

5.3: Results

Observations on the morphology, response to ecdysone and cell adhesion in Clone 8+ cell lines

5.3.1: YCl.8+ and Cl.8R cells in culture

During the first few hours the majority of low passage YCl.8+ and Cl.8R cells formed attachments to the substrate. The morphology of the majority of YCl.8+ cells and Cl.8R cells was an elongate spindle shaped type reminiscent of cultured fibroblasts. Round cells were present some of which flattened and eventually assumed a macrophage-type cell morphology with many processes (figure 5a).

After 24 hours the majority of cells had adhered to the substrate and some aggregation was beginning to become apparent (figure 5b). Confluence of single cells, with intermittent aggregations of cells, was reached by day 2. By day 3 cell migration was extensive, leaving areas of denuded substrate. By day 4 substantial aggregates had formed. Cells within the aggregates were close together and on top of one another, assuming a spherical morphology (figure 5c). Confluence of cell aggregations and single cells was reached by day 6. The characteristic pattern of aggregation normally associated with the low passage Cl.8+ cells, YCl.8+ and Cl.8R, consisted of large aggregates of phase bright cells surrounded by phase-dark single cells connecting the

aggregates (figures 5di, 5dii). It is at this stage that routine passaging of these cells takes place. Few cells were observed suspended in the medium.

5.3.2: OCl.8+ and ZfeCl.8+ cells in culture

The majority of cells in the OCl.8+ and ZfeCl.8+ cultures were of a spherical morphology. A greater number of elongate spindle shaped cells were present in the ZfeCl.8+ cell cultures compared to the OCl.8+ cell cultures.

OCl.8+ and ZfeCl.8+ cells appeared to adhere to the substrate a few hours after initiation. By 24 hours the majority of OCl.8+ and a large number of ZfeCl.8+ cells were loosely attached to the substrate or suspended in the medium (figure 5e). During the following days the medium became increasingly dense with cells. Some degree of loose aggregation of cells was observed, although many single cells were also suspended in the medium (figure 5f).

5.3.3: Morphological response to ecdysone

24 hours after the addition of ecdysone YCl.8+ cells adhered to the substrate and extended a greater number of cell processes most of which were also much longer than previously observed in cultures with no ecdysone. Many cells assumed a flattened appearance with extensive cell spreading onto the substrate, aggregations of small groups of cells were also observed (figure 5g).

The cultures appeared to be less dense and cell debris was obvious. No obvious morphological changes were apparent after day one.

OCl.8+ and ZfeCl.8+ cells which were adhered to the substrate appeared to respond morphologically to ecdysone. This was difficult to assess as the majority of cells were suspended in the medium and obscured the substrate. Single cells with a flatter appearance and much longer processes than cells

with no ecdysone were observed. The processes were often in contact with other round cells suspended in the medium (figure 5h).

Cl.8R cells did not appear to respond to ecdysone and grew as previously described YCl.8+ and Cl.8R cells without hormone.

Data analyses of growth rate (proliferation), adhesion and ecdysone response

5.3.4: Rate of growth (proliferation)

Analysis of cell counts 24 hours after initiation indicated that there were significant differences between the cell lines (ANOVA, $F=71.83$ $DF=3$ $p<0.0001$). Tukey pairwise comparison test (family error rate =0.05) indicated that this difference existed between all the cell lines. The mean number of cells indicated that YCl.8+ cells proliferate the least upon initiation, followed by Cl.8R, ZfeCl.8+ and lastly OCl.8+.

The rate of proliferation (growth) was faster in the high passage cell lines. ANOVA indicated that there were significant differences in cell proliferation after 5 days ($F=61.71$, $DF= 3$, $p<0.0001$). Tukey's pairwise comparison test indicated that the difference was between the high passage cell lines (OCl.8+ and ZfeCl.8+) and the low passage cell lines (YCl.8+ and Cl.8R). Although cell counts taken after 5 days were variable an upward trend in cell proliferation with increasing passage numbers was observed ($r^2=55.9\%$, $s=16.51$).

5.3.5: Adhesion

The proportion of cells adhered to the substrate after 24 hours was greater in the YCl.8+, Cl.8R and ZfeCl.8+ cells when compared to OCl.8+ (ANOVA, $F=17.43$, $DF=1$, $p<0.001$). Tukey's pairwise comparison indicated that the difference was between the OCl.8+ and the rest of the cell lines. There was no difference between low passage cell lines YCl.8+ and Cl.8R and the high passage cell line ZfeCl.8+.

The proportion of cells adhered to the substrate after 5 days was greater in the YCl.8+ and Cl.8R when compared to the OCl.8+ and ZfeCl.8+ cell lines (ANOVA, $F=29.87$, $DF=2$, $p<0.001$). Tukey's pairwise comparison indicated that there was no difference between the YCl.8+ and Cl.8R low passage cell lines and no difference between the high passage cell lines OCl.8+ and ZfeCl.8+.

5.3.6: Ecdysone effect

A decrease in cell numbers was found in YCl.8+, OCl.8+ and ZfeCl.8+ cultures, as a response to 10ng/ml ecdysone 24 hours after initiation.

ANOVA indicated that there was a significant difference between the cell lines after ecdysone (ANOVA, $F=128.18$, $DF=3$, $P<0.0001$). Tukey's pairwise comparison indicated that the number of cells present before and after ecdysone was significant in all cell lines except for the Cl.8R cell line which was not significant.

Cell adhesion and proliferation on used substrate and medium in YCl.8+ and OCl.8+ cells

5.3.7 Observations

The initial observations on the YCl.8+ cells that were seeded on OCl.8+ used substrate with fresh or conditioned medium were that they appeared to be comparable to the YCl.8+ cells grown on unused substrate. Observations on day one were difficult as the medium was cloudy. By day two the YCl.8+ cells had adhered to the substrate that OCl.8+ cells had been grown on previously but in a disorganised way when compared to controls (figure 5i). Cell aggregations and migration of cells appeared to be reduced. By day three the YCl.8+ cells were beginning to recover and from day five went on to grow as normal (figure 5j).

No changes were observed in high passage cells, OCl.8+ initiated on used OCl.8+ substrate with fresh or conditioned medium. The majority of cells remained suspended in the medium as previously described for OCl.8+ cells.

When OCl.8+ cells were initiated on YCl.8+ used substrate with fresh or conditioned medium observations on day one were also difficult as the medium was cloudy. By day two a greater number of OCl.8+ cells compared to the controls appeared to have adhered to the used YCl.8+ substrate. Elongate and round cells were observed and aggregations of cells were apparent (figure 5k). By day 5 the majority of cells had formed tight aggregations but appeared to be suspended in the medium with only loose attachment to the substrate. A reduced number of cells appeared to be adhered to the substrate beneath the aggregates and there were many areas of substrate where no cells were growing (figure 5m).

5.3.8: Data analyses

Controls

More YCl.8+ cells adhere to an unused substrate with fresh medium than OCl.8+ cells. After 24 hours a significantly higher proportion of YCl.8+ cells were adhered to an unused substrate and fresh medium than OCl.8+ cells (ANOVA $F=402$, $DF=1$, $p<0.0001$).

5.3.9: YCl.8+ cells and OCl.8+ substrate

The majority of YCl.8+ cells do not adhere to OCl.8+ substrate.

ANOVA indicated that after 24 hours a significantly lower proportion of YCl.8+ cells adhered to the OCl.8+ substrate with fresh or OCl.8+ conditioned medium and a lower proportion of YCl.8+ cells adhered to an unused substrate with OCl.8+ conditioned medium when compared to the control YCl.8+ cells, fresh medium and unused substrate (ANOVA $F=28.81$, $DF=2$, $p<0.0001$) (figure 5.1). By day 5 there was no significant difference between the proportion of cells adhered on OCl.8+ substrate with fresh or OCl.8+ conditioned medium.

OCl.8+ conditioned medium had a positive effect on cell proliferation in YCl.8+ cells. The total number of cells present was found to be significantly higher in the YCl.8+ cells with OCl.8+ conditioned medium compared to the control, YCl.8+ cells, fresh medium (ANOVA, $R=37.19$, $DF=2$, $p<0.005$).

By day 5 there was no significant difference in the number of YCl.8+ cells in OCl.8+ conditioned medium when compared to the YCl.8+ controls.

5.3.10: OCl.8+ cells and YCl.8+ substrate

OCl.8+ cells adhere to used YCl.8+ substrate in the first 24 hours.

A significantly higher proportion of OCl.8+ cells adhered to a fresh substrate with YCl.8+ conditioned medium when compared to the control of OCl.8+ cells fresh substrate, fresh medium (ANOVA, $R= 29.8$, $DF= 2$, $p<0.0001$) (figure 5.2). By day 5 there was no significant difference between the proportion of OCl.8+ cells adhered to the YCl.8+ substrate with fresh or YCl.8+ conditioned medium.

YCl.8+ conditioned medium had a negative effect on cell proliferation in OCl.8+ cells. The total number of OCl.8+ cells present was significantly lower when initiated on a fresh substrate with YCl.8+ conditioned medium or YCl.8+ used substrate with either fresh or conditioned medium than the control of OCl.8+ cells and fresh medium (ANOVA, $R= 21.43$, $DF= 2$, $p<0.005$). By day 5 there was no significant difference between the number of OCl.8+ cells counted when compared to the OCl.8+ controls.

Summary of the results

5.3.11: Ecdysone response

YCl.8+, OCl.8+ and ZfeCl.8+ cells responded to ecdysone morphologically. Cell division appeared to cease in YCl.8+, OCl.8+ and ZfeCl.8+ cells after ecdysone.

Cl.8R did not respond morphologically and cell division was not affected by the addition of ecdysone.

5.3.12: Rate of growth (proliferation)

As the number of passages increased there was an upward trend in the rate of proliferation.

5.3.13: Adhesion

After 24 hours fewer OCl.8+ cells had adhered to the substrate than the rest of the cell lines. There was no difference between the high passage cell lines OCl.8+ and ZfeCl.8+ adhered to the substrate after 5 days.

5.3.14: Adhesion and proliferation of YCl.8+ and OCl.8+ on used substrate with conditioned medium.

YCl.8+ cells do not adhere to OCl.8+ substrate in the initial 24 hours post initiation. OCl.8+ conditioned medium had a positive effect on cell proliferation in YCl.8+ cells.

OCl.8+ cells adhere to used YCl.8+ substrate in the initial 24 hours post initiation. YCl.8+ conditioned medium had a negative effect on cell proliferation in OCl.8+ cells.

5.4: Discussion

Four related phenomena which are integral to successful morphogenesis during *Drosophila* development are present in these cell lines; an ecdysone response, cell proliferation, cell-cell and cell-substrate adhesion. The 'normal' characteristics which the Young Clone 8+ cell line are known to exhibit,

namely response to ecdysone and cell adhesion, have changed in the cell line derivatives, Clone 8R, Old Clone 8+ and ZfeClone 8+ + cell lines.

The 'typical' response of many *Drosophila* cell lines to physiological concentrations of ecdysone *in vitro* is to undergo some degree of differentiation, cessation of cell division and formation of aggregates (Courgeon, 1972(a,b); Berger et al., 1978; Rosset, 1978; Cherbas et al., 1980).

The Young Clone 8+ cell line exhibited the 'typical' *Drosophila* cell line response to ecdysone which was as expected and has previously been shown (Peel and Milner, 1992; Cottam and Milner, 1997). The full morphological response to ecdysone on the Old Clone 8+ cells and the ZfeClone 8+ cells was undetermined. This was due to the lack of visualisation of cell attachment to the substrate. However there was a degree of morphological change observed in the cells floating in the medium. Some cells presented a flattened morphology with much longer cell processes being in evidence (figure 5h). Loosely associated aggregations of cells were also observed suspended in the medium. The statistical evidence also indicated an initial cessation of cell division in these cells after ecdysone. This suggests that the Old Clone 8+ and the ZfeClone 8+ cell lines, in common with the Young Clone 8+ cell line, do respond to the hormone.

5.4.1: Clone 8R

The Clone 8R (resistant) cell line does not respond to ecdysone in a 'typical' manner and statistical evidence supports the morphological observations that these cells are unresponsive to ecdysone. The Clone 8R cells were originally derived by subjecting cells to repeated and prolonged exposure to increasing levels of ecdysone. Studies have shown that over ten times the concentration of ecdysone which promotes the response of Young Clone 8+ was found to

have no effect on the Clone 8R cells (Peel and Milner, 1992). When *Drosophila* cell lines cultured *in vitro* no longer respond to ecdysone it is generally thought that down regulation of the ecdysone receptor (EcR) is responsible (Courgeon, 1972; Best-Belpomme and Courgeon, 1975). There are three isoforms of the EcR receptor, EcR-A, EcR-B1 and EcR-B2 and during metamorphosis of the wing disc the isoform EcR-A is predominantly expressed (Talbot et al., 1993). The apparent lack of response to ecdysone in Clone 8R cells may not mean that this is due to the loss of isoform EcR-A but may suggest that this response has been modulated by a change in the expression of the EcR-B1 and EcR-B2 isoforms.

5.4.2: ZfeClone 8+ cell line, cell proliferation and adhesion

The results from the proliferation assays have indicated that the ZfeClone 8+ and Old Clone 8+ cell lines were similar in terms of their rate of growth over a five day period. The ZfeClone 8+ cell line are of high passage, in common with the Old Clone 8+ cells. The effect of increasing passage number on the rate of proliferation has already been established in the Old Clone 8+ cells (Cottam and Milner, 1997). The data suggests therefore that the ZfeClone 8+ cell line have changed when compared to the Young Clone 8+ cells. This change may be as a result of the increasing '*in vitro*' age of the cell line.

Initially a statistical difference was observed between the ZfeClone 8+ and Old Clone 8+ in terms of their adhesion properties after 24 hours. The statistical evidence indicated that the ZfeClone 8+ cells, like the Young Clone 8+ cells were more adhesive than the Old Clone 8+ cells. However the statistical evidence indicates that there is no difference between the ZfeClone 8+ and Old Clone 8+ cell lines in terms of adhesion properties after 5 days. This suggests that after 24 hours the ZfeClone 8+ cells eventually detach from

the substrate. Therefore the ZfeClone 8+ cells differ from the Young Clone 8+ cell line in terms of cell growth and adhesion but share similarities with the Old Clone 8+ cells.

ZfeClone 8+ cells may differ from the other Clone 8+ cell lines in their nutritional uptake from the medium. No fly extract is present in the medium and the ZfeClone 8+ cells are grown in a much higher concentration of foetal bovine serum. Serum is normally required in cultured cells to promote and maintain attachment (Kawamura et al., 1999). This may account for their differential adhesive properties directly after initiation when compared to the Old Clone 8+ cells. Young Clone 8+ cells which have been cultured in medium which lack serum initially adhere to the substrate and assume a flattened appearance, but do not put out cell processes. Cell proliferation however is decreased and the cells undergo apoptosis around day four (Kawamura et al., 1999). Therefore the increased serum may also account for their decreased rate of proliferation directly after initiation when compared to the Old Clone 8+ cells.

The lack of fly extract is of unknown consequence. Insect culture medium has been designed to imitate the natural environment required to promote cell survival. Clone 8+ cells have an additional requirement for fly extract in order to maintain their 'typical' development in culture. The lack of fly extract may have affected both proliferation and adhesion capacities in the ZfeClone 8+ cells and cannot be overlooked. However the results suggest that the lack of fly extract alone is not responsible for the increase in cell proliferation observed in ZfeClone 8+ cells after 5 days in culture as the Old Clone 8+ cells are grown in the presence of fly extract.

5.4.3: Old Clone 8+ cell line compared to Young Clone 8+ cell line

There are no differences in the way that the Young Clone 8+ and Old Clone 8+ cell lines are cultured in terms of medium and additives. The only difference between these cell lines is the number of times that they have been passaged which relates to their '*in vitro* age' (Cottam and Milner, 1997).

5.4.4: Old Clone 8+ cells

The observation that a greater number of Old Clone 8+ cells appeared to adhere on Young Clone 8+ used substrate after 24 hours, has now been accompanied by statistical evidence to support this view. The proportion of Old Clone 8+ cells adhered to the used Young Clone 8+ substrate was significantly greater than the control of Old Clone 8+ cells on a fresh substrate. The Old Clone 8+ cells appear to have lost their potential to adhere directly to a substrate. However this potential was regained, albeit transiently, when grown on the substrate previously used by the Young Clone 8+ cell line. This suggests that cell adhesion may be mediated by molecules secreted by the Young Clone 8+ which are no longer expressed by the Old Clone 8+ cells. The subsequent loss of adhesion in the Old Clone 8+ cells after 24 hours may be a result of the Old Clone 8+ cells secreting excess extracellular matrix molecules such as extracellular matrix enzymes (Llano et al., 2002). These enzymes break down the extracellular matrix during wing disc morphogenesis to allow complex changes in shape and facilitate the passage of secreted signalling molecules required to communicate with other cells. An accumulation of excess extracellular matrix and a decrease in the degradation of the extracellular matrix has been found in several cell types cultured *in vitro* and is associated with prolonged serial passaging (Schnaper et al., 1996).

What was unexpected in the results was the significantly reduced proliferation and increased adhesion of the Old Clone 8+ cells in the presence of Young Clone 8+ conditioned medium on an unused substrate. These results suggest that cell adhesion and the rate of proliferation in the Old Clone 8+ cells may be mediated by molecules secreted into the medium by the Young Clone 8+ cells. These molecules may promote cell attachment and also mediate some control over proliferation and no longer be expressed by the Old Clone 8+ cells. Alternatively promotion of adhesion of the Old Clone 8+ cells alone has reduced the rate of proliferation (Pöschl et al., 2004).

5.4.5: Young Clone 8+ cells

Unexpectedly the Young Clone 8+ cells showed an increase in proliferation in the presence of Old Clone 8+ conditioned medium on an unused substrate, suggesting that there is a molecule or molecules present in the Old Clone 8+ medium which have a mitogenic effect on the Young Clone 8+ cells.

There was a significant decrease in the proportion of Young Clone 8+ cells adhered to the Old Clone 8+ substrate with fresh medium. This suggests that extracellular matrix-associated molecules, secreted by the Old Clone 8+ cells, act to inhibit the adhesion of the Young Clone 8+ cells. Adhesion of Young Clone 8+ cells was re-established 24 hours or so after initiation. One possible scenario may explain this outcome. As confluence is never reached by Old Clone 8+ cells and only a small number of Old Clone 8+ cells adhere to the substrate then there would most likely be areas of the substrate which had never been in contact with an Old Clone 8+ cell or molecules secreted by the Old Clone 8+ cells. In this scenario the Young Clone 8+ cells which adhered to these areas would undergo division, migration and remodelling of the extracellular matrix promoting adhesion. Subsequently there would be a gradual change in the micro environment which would change the adhesive

properties of previously secreted matrix by the Old Clone 8+ cells. Thus enabling the Young Clone 8+ cells to populate these areas. At this time it is not known whether the majority of Old Clone 8+ cells adhere to the substrate initially and then lose their attachment, or that only a small population of Old Clone 8+ cells adhere and the majority are only ever present as a suspended population. Selecting for Old Clone 8+ cells which show adhesive properties during initiation does not appear to increase the number of Old Clone 8+ cells which adhere to the substrate. The class of molecules which could be present in excess in the Old Clone 8+ used substrate are extracellular matrix enzymes mentioned above (Llano et al., 2002).

The characteristics displayed by the Young Clone 8+ cell line have changed in the Clone 8+ derivatives, Clone 8R and ZfeClone 8+ and the high passage Old Clone 8+ cell lines. Response to ecdysone, cell–substrate adhesion and rate of proliferation are among the characteristics that differ from cell line to cell line. In particular the observation that the high passage Clone 8+ cell lines, Old Clone 8+ and ZfeClone 8+ do not adhere to the substrate is of interest. This may be due to the loss of cell adhesion molecules or the secretion of excess of extracellular matrix material. Both have implications for cell-matrix interactions which take place during morphogenesis.

Cell line cells are by their very nature transformed. These results suggest that the high passage cell lines have undergone further transformation.

As changes in cell fate are almost always accompanied by a change in gene expression this will be addressed using microarray analysis. Potential candidates playing a role in loss of adhesion observed in the Old Clone 8+ cell line will be of particular interest.

Tables and Figures

Figure 5.1: The effect of used substrate and medium on the proportion of Young Clone 8+ cells adhered to the substrate 24 hours after initiation

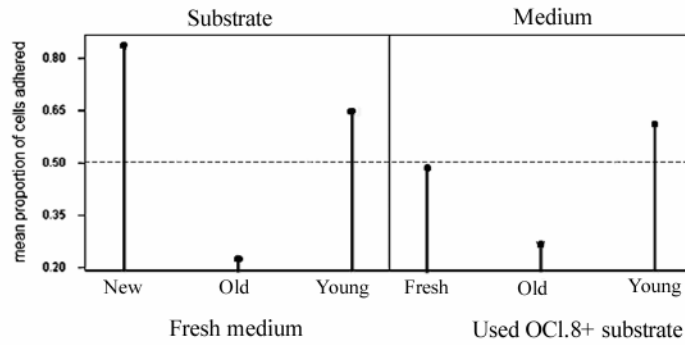


Figure 5.1: The effect of used substrate and medium on the proportion of Young Clone 8+ cells adhered to the substrate 24 hours after initiation

The mean proportion of YCl.8+ cells adhered to the O.Cl.8+ substrate has dropped from over 80% to less than 25%. More YCl.8+ cells adhered to the Old used substrate with fresh medium and Young used medium than Old used medium.

Figure 5.2: The effect of used substrate and medium on the proportion of Old Clone 8+ cells adhered to the substrate 24 hours after initiation

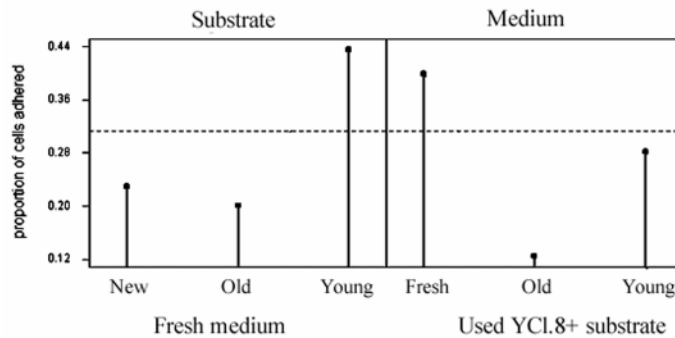


Figure 5.2: The effect of used substrate and medium on the proportion of Old Clone 8+ cells adhered to the substrate 24 hours after initiation. The mean proportion of OCl.8+ cells adhered to the Y.Cl.8+ substrate has almost doubled from less than 25% to more than 40%. More OCl.8+ cells adhered to the Young used substrate with fresh medium and Young used medium than Old used medium.

Figure 5a: YCl.8+ and Cl.8R cell morphologies 24 hours after initiation.

DIC images of Young Clone 8+ and Clone 8R cells showing elongate, round, macrophage and teardrop shaped cells which are found in these cultures 24 hours after initiation. The prospective macrophage cell types have already flattened and are putting out cell processes.

e, elongate cell type, f, flattened cell process in teardrop shaped cell, m, macrophage cell type, r, round cells.

Scale bar represents:20µm

Figure 5a: YCl.8+ and Cl.8R cells 24 hours after initiation

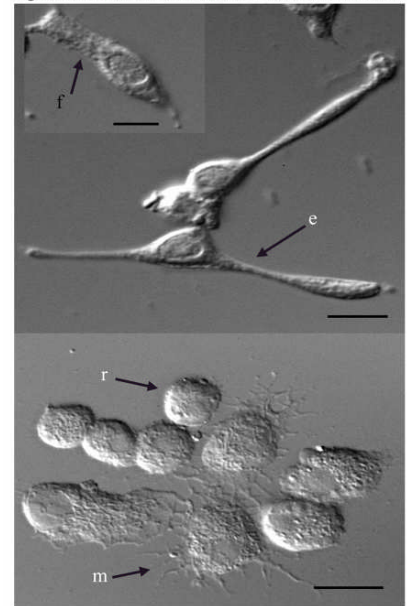


Figure 5b: Low passage Clone 8+ cells 24 hours after initiation.

Phase contrast image of low passage Clone 8+ cells 24 hours after initiation. Cells are already beginning to show signs of migration and aggregation. The elongate cells are in the majority with fewer round cells in evidence.

a, aggregate; r, round cell

Scale bar represents:50µm

Figure 5b: Low passage Clone 8+ cells 24 hours after initiation

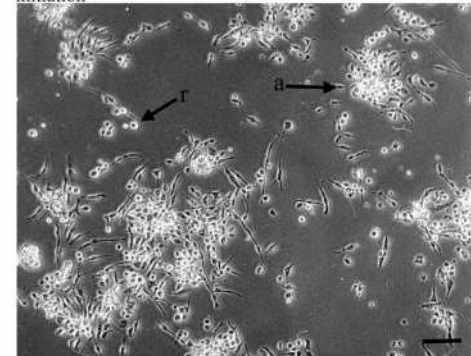


Figure 5c: Low passage Clone 8+ cells day 4 after initiation
Phase contrast image of low passage Clone 8+ cells 24 hours after initiation which shows the substantial aggregation of cells observed in these cultures. Migration of cells has left areas of denuded substrate. Cells within the aggregates are close together and on top of one another. These cells have assumed a spherical morphology.

a, aggregate

Scale bar represents:50µm

Figure 5c: Low passage Clone 8+ cells day 4 after initiation

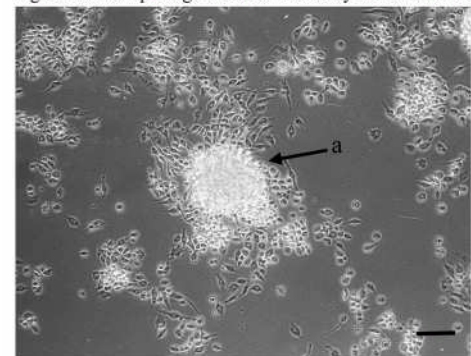


Figure 5d(i): Low passage Clone 8+ cells day 6, confluence.

Phase contrast image of low passage Clone 8+ cells showing the characteristic pattern of aggregation and association of single cells normally associated with the low passage Cl8+ cells, YCl.8+ and Cl.8R. The phase bright aggregates contain cells which are closely associated, individual cells are hard to distinguish. a, aggregates; nc, area of substrate where no cells are present.

Scale bar represents:50µm

Figure 5d(i): Low passage Clone 8+ cells day 6 confluence

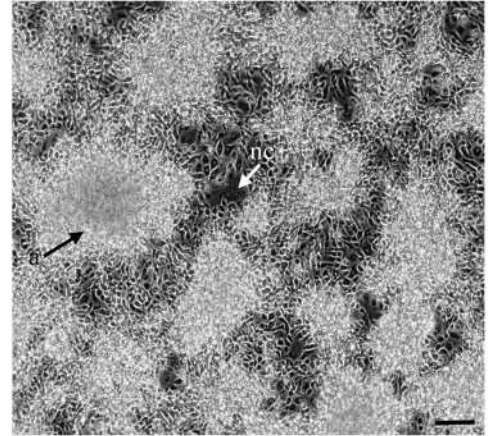


Figure 5d(ii):Aggregates connected by single cells in Low passage Clone 8+

Phase contrast image of low passage Clone 8+ cells showing elongate phase dark single cells with long processes connecting the aggregates which are phase bright, it at this stage that routine passaging of the cultures takes place.

ec, elongate cell

Scale bar represents:20µm

Figure 5d(ii): Aggregates connected by single cells in Low passage Clone 8+

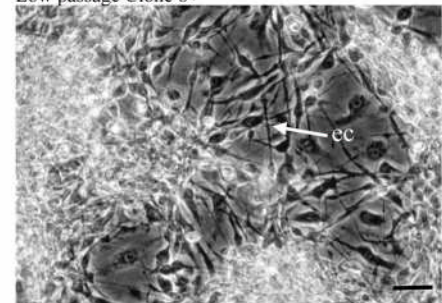


Figure 5e: High passage Clone 8+ cells 24 hours after initiation.

Phase contrast image of high passage Clone 8+ cells 24 hours after initiation which shows that the majority of cells present in these cultures were phase bright with a spherical morphology. The spherical cells were only loosely attached to the substrate and appeared loosely associated with each other. Phase dark elongate cells were also present attached to the substrate.

a, aggregate; e, elongate cells; s, spherical cells

Scale bar represents:50µm

Figure 5e: High passage cell lines Clone 8+ 24 hours after initiation.

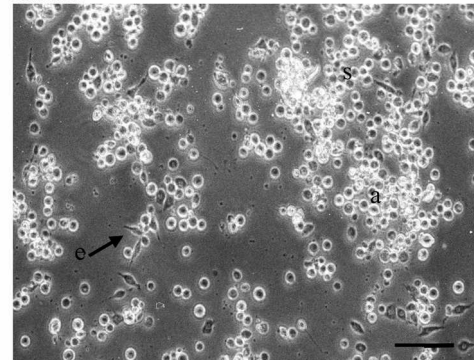


Figure 5f:High passage Clone 8+ cells 3 days after initiation

DIC image of low passage Clone 8+ cells 3 days after initiation showing the density of cells suspended in these cultures. The substrate beneath cannot be visualised due to the number of cells suspended in the medium, a number of phase bright areas in the cell aggregations can be seen.

p, phase bright cell aggregations

Scale bar represents:50µm

Figure 5f: High passage Clone 8+ cells 3 days after initiation

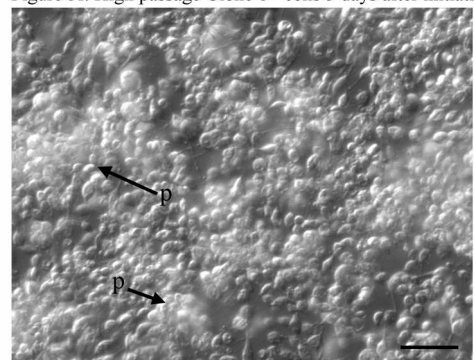


Figure 5g: Low passage Clone 8+ cells 24 hours after ecdysone

DIC image of low passage Clone 8+ cells 24 hours after ecdysone which shows the flattened appearance assumed by the cells after ecdysone. Many cell processes extending from the cells can be seen and cells have spread out onto the substrate.

cs, cell spreading; p, processes

Scale bar represents: 20µm

Figure 5g: YCl.8+ cells 24 hours after ecdysone

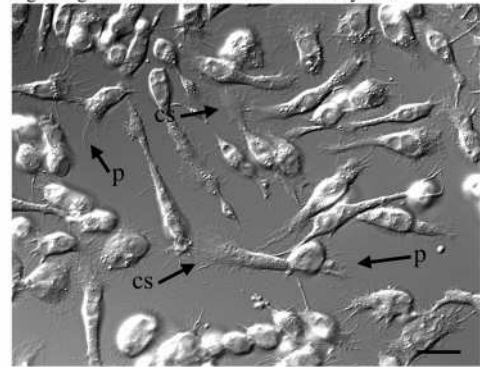


Figure 5h: High passage Clone 8+ cells 24 hours after ecdysone

DIC image of high passage Clone 8+ cells 24 hours after ecdysone showing cells suspended in the medium. Single cells with a flatter appearance and much longer processes extending into the medium can be seen. These processes appear to be associating with spherical cells.

p, processes; pc, processes which are in contact with the spherical cells

Scale bar represents: 20µm

Figure 5h: High passage Clone 8+ cells 24 hours after ecdysone

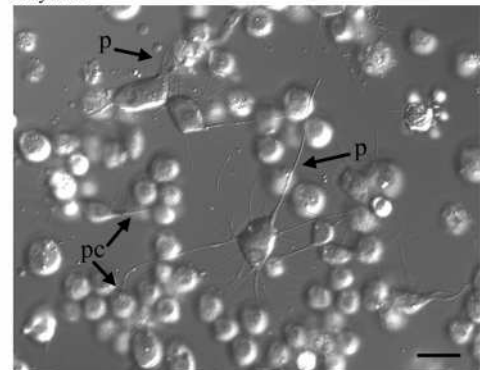


Figure 5i: Low passage YCl.8+ cells on used Old Cl.8+ substrate, day 2

Phase contrast image showing the disorganised way in which YCl.8+ cells appeared to grow when compared to the control, figure 5b. Few elongate cells were present in these cultures and cell aggregation and migration was reduced. Phase bright aggregations were only loosely attached to the substrate. Cells firmly adhered to the substrate have assumed a phase dark appearance.

a, aggregations loosely attached; c, cells firmly attached to the substrate

Scale bar represents: 50µm

Figure 5i: Low passage YCl.8+ cells on used Old Cl.8+ substrate, day 2

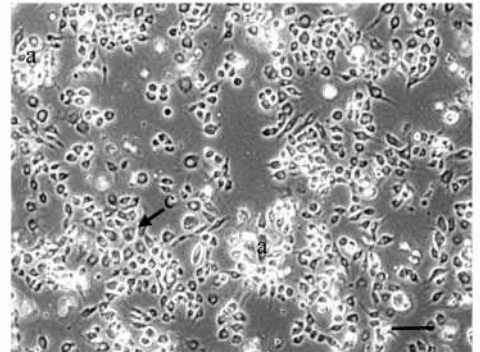


Figure 5j: Low passage YCl.8+ cells on used Old Cl.8+ substrate, day 3.

Phase contrast image of the YCl.8+ cells, cell aggregation is apparent and there are greater numbers of elongate cells present. Migration of cells is still reduced, more cells can be seen adhered to the substrate between the aggregations.

a, aggregate suspended in medium; c, phase dark cells firmly adhered to the substrate; e, elongate cell

Scale bar represents: 50µm

Figure 5j: Low passage YCl.8+ cells on used Old Cl.8+ substrate day 3

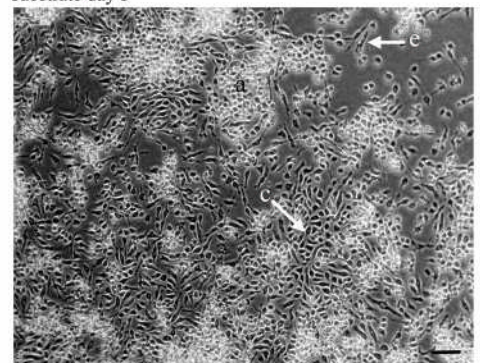


Figure 5k: Low passage Old Cl.8+ on used Young Cl.8+ substrate, day 2

Phase contrast image of OCl.8+ cells showing cell aggregations which may only be loosely attached to the substrate. Phase dark, elongate and round cells were present in these cultures.

a, aggregates; p, phase dark cells

Scale bar represents: 100µm

Figure 5k: OCl.8+ on used YCl.8+ substrate, day 2

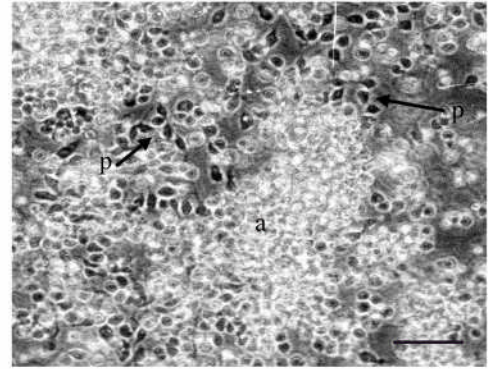


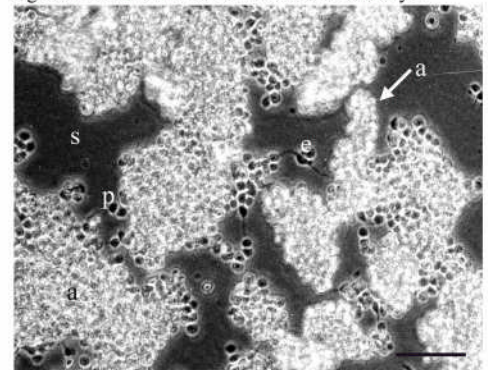
Figure 5m: Old Cl.8+ on used Young Cl.8+ substrate, day 5

Phase contrast image of the tight aggregations which had formed in these cultures which on appearance were loosely attached to the substrate. A number of phase dark cells can be seen adhered to the substrate lying beneath the aggregates and elongate cells were observed although infrequently. No cells grew in many areas of the substrate in these cultures.

a, aggregate; e, elongate cell type; p, phase dark cells; s, substrate.

Scale bar represents: 100µm

Figure 5m: OCl.8+ on used YCl.8+ substrate day 5



Chapter 6

Analysis of gene expression
data in Clone 8+ cell lines

6:1: Introduction

The parent cell line, CME W1, from which the Clone 8+ cell line was cloned, was originally derived from *Drosophila* imaginal wing disc epithelia of late third instar larvae (Currie et al., 1988). The imaginal disc of the third instar larva is a simple sac-like structure consisting of a monolayer of epithelia cells enclosing a lumen (Auerbach, 1936). The imaginal disc epithelia are surrounded by a thin outer layer, the basement membrane. This specialised layer of extracellular matrix is called the basal lamina which contains collagen IV, required for structural integrity and laminin, a glycoprotein, which acts as a ligand for integrins and an adhesion site for collagen IV (Fessler et al., 1987; Olsen et al., 1990). Adhesion between the extracellular matrix and epithelial cells is mediated principally by integrins. These transmembrane receptors also provide a physical link between the cytoskeleton and the extracellular matrix and act as signalling receptors relaying information about the substrate to the interior of the cell (Miranti and Brugge, 2002; Bökel and Brown, 2002).

The high passage epithelial derived Clone 8+ cells show changes in cell-substrate (matrix) adhesion when compared to the low passage Clone 8+ cell line (Chapter 5). Changes in cell fate during development are almost always accompanied by changes in gene expression. We have performed microarray analysis in all the Clone 8+ cells lines before and after exposure to ecdysone, in order to identify differentially expressed genes associated with cell-matrix adhesion. A comparison of all the cell lines before and after ecdysone will also generate data which will be useful for future studies on the affect of ecdysone on the Clone 8R cell line when compared to the Young Clone 8+ cell line.

6.2: Methods and Materials

6.2.1: Experimental design

For this study using 'Flychip' microarray analysis, pairwise comparisons were made on the following cell lines with and without ecdysone:

Clone 8+ cells of low passage number:

YCl.8+ p30(19) compared with Cl.8R p30(21)

Clone 8+ cells of low and high passage number:

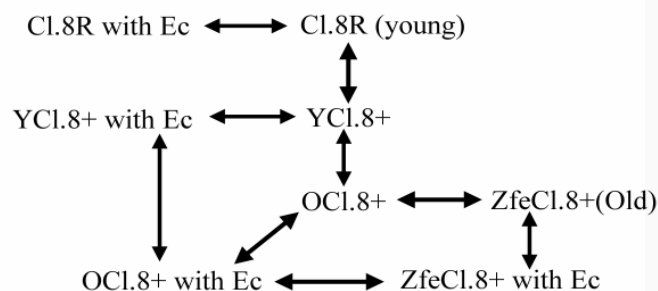
YCl.8+ p30(19) compared with OCl.8+ p30(96).

Clone 8+ cells of high passage number:

OCl.8+ p30(96) compared with ZfeCl.8+p30(74).

As our primary interest was in the differences between the YCl.8+ cells and the OCl.8+ cells, 24 hours was considered to be an appropriate time at which to harvest the cells. At this time Young Clone 8+ cells would potentially be expressing genes and proteins involved in cell attachment and the majority of Old Clone 8+ cells would no longer be attached to the substrate.

The experimental design for the microarray pairwise comparison was a loop design which compares each sample with every other sample in duplicate (dye swap). This gives the maximum comparability between each sample and reduces the variance. For this comparison the experimental design was as follows:



6.2.2: Sample preparation

A total of 25-30 μg of total RNA (2.6×10^6 cells) was required for each labelling reaction. Cells were cultured in 5cm culture dishes (Chapter 2 Materials and Methods) and seeded at 3.5×10^6 per 5ml in CSM (Complete medium) or in CSM with ecdysone added to give a final concentration of 10 ng /ml.

The cells were incubated at 25°C and harvested 24 hours (+ 10mins) later.

Cells and medium were centrifuged for 5 minutes at 1200 rpm, the supernatant removed and cells resuspended in PBS. This wash was carried out to remove any trace of medium which may interfere with the hybridisation process.

The cells were re-centrifuged at 1200rpm for 5 minutes, PBS removed and cells aliquoted into a 1.5ml RNA-ase free microfuge tube and centrifuged for 2 minutes at 1200 rpm to remove any remaining PBS. At this point all samples were placed on ice in order to prevent RNA degradation. 300 μl of TRIzol (Invitrogen) was added (TRIzol maintains the integrity of the RNA) and the cells were homogenised for 1 minute (procedure carried out in a fume hood). A further 700 μl of TRIzol added and mixed well, the samples were labelled with the project number and a unique identifier. Samples were stored for a short period at -80 °C until ready for further processing.

As it was not possible to prepare all the cells on one day methods were put in place to eliminate as much variability as possible. An equivalent number of replicates from each cell line were prepared each time. Passage numbers were kept the same throughout, the same batch of medium was used and ecdysone was made up fresh each time.

6.2.3: Microarray

A brief description of the microarray process which was carried out by the microarray facility 'Flychip' <http://www.flychip.org.uk> follows:

RNA was extracted and labelled with the fluorescent dyes CY3 (green) and CY5 (red) which are spectrally well separated. Pairwise samples were combined together (along with controls) and hybridised to 3 gene chip slides containing 5,849 non-redundant cDNA clones. A dye-swap was performed on the 3rd slide to accommodate the differential labelling efficiencies.

6.2.4: Scanning and Analysis

Microarray slides were scanned and two 16-bit Tif image files were produced for each slide. The data was normalised taking into account the dye swap and background noise (Huber et al., 2002). The relative representation of a gene in the sample was assayed by measuring the ratio of the fluorescence intensities of the 2 dyes and was presented as a ratio $Cy5/Cy3 \text{ Log [Base 2]}$. Results were recorded in Microsoft Excel spread sheets for further analysis.

For a more in depth explanation of the experimental procedure please refer to the website: <http://www.flychip.org.uk>

6.2.5: Data analysis

The raw data consisted of Ten Excel spread sheets containing over 5,000 genes in each set and were not ranked in any way. A full set of the raw and normalised data can be accessed from 'Flychip'. The normalised data sets were used for further analysis. 'Flychip' controls and slides which presented as zero in all replicates were examined and removed from the data sets.

Replicates which were rejected by 'Flychip' analysis were removed after data analysis.

Statistical analysis of the data was performed using **SAM** (Significance Analysis of Microarrays) (<http://www.stat.stanford.edu/~tibs/SAM>) Version 1 (Tusher et al., 2001). **SAM** uses multiple t-testing to analyse microarray data, the delta (difference in mean) and the False Discovery Rate (FDR), or type 1 error, can be controlled. Initially all the data was analysed using the delta dictated by **SAM** then a delta (FDR<1%) which only identified genes two fold or more significant in all replicates was used in order to reduce the number of genes (Zinke et al., 2002; Kearney et al., 2004).

A **SAM** one class response test was undertaken for all data sets.

A **SAM** two class data analysis was undertaken in order to compare the effect of ecdysone on YCl.8+ cells and Cl.8R cells. Each data set was made equivalent before the two class unpaired test was undertaken, as some transcripts did not appear in every data set.

'Flybase' (<http://flybase.bio.indiana.edu>) was searched for the genes identified by **SAM**. Summary tables were constructed and a description of the predicted gene product, role and location in the cell was listed. Genes which were identified with a two fold change in expression in the OCl.8+, Cl.8R and ZfeCl.8+ when compared to the YCl.8+ were then examined in all data sets to identify genes of particular interest.

6.3: Results

6.3.1: Individual data sets analysed by SAM

The differences in gene expression between Clone 8+ cells which were reported in the microarray analysis and analysed by **SAM** for statistical significance were described as positively or negatively significant according to **SAM** and have been reported here as an increase or upregulation and a decrease or downregulation in expression.

6.3.2: No threshold (Table 6.1).

Significance Analysis of Microarrays (**SAM**) identified a change in gene expression in over 1500 genes as increased or decreased in 8 of the pairwise comparisons of the Clone 8 cell lines (table 6.1a). There were no genes identified as being either increased or decreased in two data sets: OCl.8 + cells after ecdysone compared with YCl.8 cells after ecdysone and Cl.8R cells after ecdysone compared with Cl.8R cells. The false discovery rate (FDR) was found to be high in all the data sets indicating that one third or more of the genes identified in each data set were potentially not significant.

6.3.3: Two fold threshold (Table 6.2).

The number of genes with a change in gene expression predicted by **SAM** as significant with a threshold of two fold or more in all three replicates from pairwise comparisons from microarray data was significantly reduced. A total of 36 genes were found to be increased and 33 genes were found to be decreased in expression. For individual hybridised comparisons the

maximum number of genes identified were found in the Cl.8R cells after ecdysone when compared with YCl.8 + cells after ecdysone, 8 genes were found to be increased and 12 decreased in expression.

No difference in gene expression was found in three pairwise comparisons:

OCl.8 cells after ecdysone compared with YCl.8 + cells after ecdysone

Cl.8R cells no ecdysone compared with Cl.8R cells after ecdysone

ZfeCl.8+ cells after ecdysone compared with ZfeCl.8+ cells

The FDR was less than 1% in all analyses.

Gene expression differences between cell lines of low passage

6.3.4: Young Clone 8+ hybridised with Clone 8R (Table 6.3 a,b).

7 genes were identified as increased two fold or more in Cl.8R cells when compared with YCl.8+ cells. 2 genes were identified as decreased two fold or more in Cl.8R cells when compared to YCl.8+ cells (see tables 6.3 a,b).

6.3.5: Young Clone 8+ cells after ecdysone hybridised with Clone 8R cells after ecdysone (Table 6.4 a,b).

8 genes were identified as increased two fold or more in Cl.8R cells after ecdysone when compared to YCl.8+ cells after ecdysone. 12 genes were identified as decreased two fold or more in Cl.8R cells after ecdysone when compared to YCl.8+ cells after ecdysone. These included *ImpL2* which remained downregulated, *GstS1* which was found to be four fold lower in Cl.8R cells after ecdysone when compared to YCl.8+ cells after ecdysone and *Heat shock protein 27 (Hsp27)* which has been found to be expressed in cells in response to stress.

Gene expression differences between cell lines of low and high passage

6.3.6: Young Clone 8+ cells hybridised with Old Clone 8+ cells (Table 6.5 a,b).

Only 1 gene was identified as increased two fold or more in O.Cl8+ cells when compared to Y.Cl.8+ cells. A four fold increase was reported in gene *CG 3380* also known as *Organic anion transporting polypeptide 58Dc (Oatp58dc)*, which encodes a sodium dependent organic anion transporter. 10 genes were identified as decreased two fold or more in OCl.8+ cells when compared to YCl.8+ cells. These included *Cul-2* which encodes a nuclear ubiquitin ligase complex and *CG5384* a ubiquitin specific protease, both of these participate in protein deubiquitination.

6.3.7: Young Clone 8+ cells after ecdysone hybridised with Old Clone 8+ cells after ecdysone.

No genes were identified as increased or decreased two fold or more in OCl.8+ cells after ecdysone compared to YCl.8+ cells after ecdysone.

Gene expression differences between cell lines of high passage

6.3.8: Old Clone 8+ cells hybridised with ZfeClone 8+ cells (Table 6.6 a).

4 genes were identified as increased two fold or more in ZfeCl.8+ cells when compared to OCl.8+ cells. One of these genes *CG3273* also known as *scrambled (sced)* was significant over five fold. The remaining genes were increased two fold and included *roX1* which does not code for a protein but plays a role in

the dosage compensation reaction. No genes were found to be decreased two fold or more.

6.3.9: Old Clone 8+ cells after ecdysone hybridised with Zfe Clone 8+ cells after ecdysone (Table 6.7 a,b).

2 genes were increased two fold or more in ZfeCl.8+ after ecdysone when compared to OCl.8+ after ecdysone. *CG3074 (sced)* remained increased and *CG3273* of unknown function which was five fold higher in ZfeCl.8+ cells after ecdysone. 3 genes were found to be decreased two fold or more in ZfeCl.8+ after ecdysone when compared to OCl.8+ after ecdysone.

Gene expression differences between cell lines before and after ecdysone

6.3.10: Young Clone 8+ cells no ecdysone, hybridised with Young Clone 8+ cells after ecdysone (Table 6.8 a,b).

6 genes were identified as increased two fold or more in YCl.8+ cells after ecdysone when compared to YCl.8+ cells. *Regucalcin* was found to be nearly five fold higher in YCl.8+ after ecdysone. The remaining genes were two fold higher. 2 genes were identified as decreased two fold or more in YCl.8+ cells after ecdysone when compared to YCl.8+ cells no ecdysone.

6.3.11: Clone 8R no ecdysone hybridised with Clone 8R after ecdysone

No genes were identified as increased or decreased two fold in Cl8.R cells after ecdysone when compared to Cl.8R cells no ecdysone.

6.3.12: Old Clone 8+ no ecdysone hybridised with Old Clone 8+ after ecdysone (Table 6.9 a,b).

7 genes were identified as increased two fold or more in OCl.8+ cells after ecdysone when compared to OCl.8+ cells no ecdysone. *CG1090* was increased four fold and *regucalcin* was found to be increased three -four fold in OCl.8+ cells after ecdysone when compared to OCl.8+ cells no ecdysone. 4 genes were identified as decreased two fold or more including *Chd64* and *ERR*.

6.3.13: ZfeClone 8+ no ecdysone hybridised with ZfeClone 8+ after ecdysone

No genes were identified as increased or decreased two fold or more in ZfeCl.8+ cells after ecdysone when compared to ZfeCl.8+ cells.

6.3.14: Genes increased or decreased two fold or more in Clone 8R, Old Clone 8+ and ZfeClone 8+ cells

A comparison of the genes increased or decreased two fold or more in Clone 8R, Old Clone 8+ and ZfeClone 8+ cells when compared to Young Clone 8+ cells and their response after ecdysone was made (data not shown). A summary of the comparisons follows:

Glutactin (Glt): An increase in *Glutactin* expression was found in Cl.8R, OCl.8+ and ZfeCl.8+ cell lines when compared to YCl.8+ cell line. An increase in *Glutactin* expression was found in Young, Old and ZfeCl.8+ cells after ecdysone, no change in *Glutactin* expression was found in Cl.8R cells after ecdysone. Protein location and function: extracellular, basement membrane, calcium ion binding.

Gelsolin (Gel): An increase in the expression of *Gelsolin* was found in Cl.8R, OCl.8+ and ZfeCl.8+ cells when compared to the YCl.8+ cell line.

An increase in *Gelsolin* expression was found in YCl.8+ cells after ecdysone and a small increase in Cl.8R cells after ecdysone. No change in *Gelsolin* expression was found in OCl.8+ and ZfeCl.8+ cells after ecdysone.

Protein location and function: Cytosol and extracellular, actin filament, actin binding.

Peroxidasin (Pxn): An increase in *Peroxidasin* expression was found in Cl.8R, OCl.8+ and ZfeCl.8+ cells when compared to YCl.8+ cell line.

A increase in *Peroxidasin* expression was found in Cl.8R and OCl.8+ cells after ecdysone. No change in *Peroxidasin* expression was found in ZfeCl.8+ after ecdysone. The change in *Peroxidasin* expression in YCl.8+ after ecdysone was undetermined.

Protein location and function: extracellular matrix, peroxidase

CG10126: An increase in *CG10126* expression was found in Cl.8R, OCl.8+ and ZfeCl.8+ cells when compared to the YCl.8+ cell line. An increase in *CG10126* expression was found in YCl.8+ cells after ecdysone. A decrease in *CG10126* expression was found in OCl.8+ and ZfeCl.8+ cells after ecdysone. The change in *CG10126* expression in Cl.8R cells after ecdysone was undetermined.

Protein location and function: Calcium ion binding

CG3074: A small increase in *CG3074* expression was found in Cl.8R and OCl.8+ cells when compared to YCl.8+ cell line. An increase in *CG3074* expression was found in ZfeCl.8+ cells when compared to the OCl.8+ cell line. An increase in *CG3074* expression was found in ZfeCl.8+ cells after ecdysone and a small increase in expression in Cl.8R after ecdysone. A decrease in

CG3074 expression was found in OCl.8+ cells after ecdysone. The change in CG3074 expression in YCl.8+ cells after ecdysone was undetermined.

Protein location and function: Cytoplasm, lysosomal cysteine protease

CG3273 also known as *scrambled* (*sced*): An increase in CG3273 expression was found in Clone 8R, Old Clone 8+ and ZfeCl.8+ cells when compared to Y.Cl.8+ cell line. A decrease in CG3273 was found in the YCl.8+, OCl.8+ or ZfeCl.8 cells after ecdysone but no change in CG3273 expression was found in Cl.8R after ecdysone.

Protein location and function: actin filament re-organisation

Idgf3: An increase in *Idgf3* expression was found in Cl.8R, OCl.8+ and ZfeCl.8+ cells when compared to YCl.8+ cell line. A decrease in *Idgf3* expression was found in the Young, Old and ZfeCl.8+ cells after ecdysone. No change in *Idgf3* expression was found in Cl.8R cells after ecdysone.

Protein location and function: extracellular, imaginal disc growth factor, NOT chitinase.

Cg25C: An increase in *Cg25C* expression was found in Cl.8R, OCl.8+ and ZfeCl.8+ cells when compared to the YCl.8+ cell line. A decrease in *Cg25C* expression was found in the YCl.8+, OCl.8+ and ZfeCl.8+ cells after ecdysone.

The change in *Cg25C* expression in Cl.8R after ecdysone was ambiguous.

Protein location and function: extracellular, basement membrane, collagen type IV.

CG3380: An increase in CG3380 expression was found in OCl.8+ and ZfeCl.8+ cells and no change in Cl.8R when compared to the YCl.8+ cell line.

Ecdysone had no effect on the expression of CG3380 in Cl.8R, OCl.8+ and ZfeCl.8+ but was decreased in the YCl.8+ cells after ecdysone.

Protein location and function: cell membrane, sodium independent organic anion transporter

Regucalcin: An increase in *regucalcin* expression was found in Cl.8R and no change in OCl.8+ cells when compared to YCl.8+ cell line. A decrease in *regucalcin* expression was found in ZfeCl.8+ cells when compared to OCl.8+ cells. An increase in *regucalcin* expression was found in all cell lines after ecdysone.

Protein location and function: calcium ion binding.

CG1090: An increase in *CG1090* expression was found in Cl.8R and ZfeCl.8+ cells with no change in expression in OCl.8+ cells when compared to YCl.8+ cell line. An increase in *CG1090* expression was found in OCl.8+, ZfeCl.8+ and YCl.8+ cells after ecdysone. A decrease in *CG1090* expression was found in Cl.8R after ecdysone.

Protein location and function: calcium, potassium:sodium antiporter

roX1: An increase in *roX1* expression was found in Cl.8R and ZfeCl.8+ cells and no change in *roX1* expression in OCl.8+ cells when compared to YCl.8+ cell line. A decrease in *roX1* expression was found in OCl.8+, ZfeCl.8+ and YCl.8+ cells after ecdysone. An increase in *roX1* expression was found in Cl.8R after ecdysone.

Location and function: dosage compensation complex

6.3.15: Genes decreased in expression in Clone 8R, Old Clone 8+ and ZfeClone 8+ when compared to Young Clone 8+ cells.

Doa: A decrease in *Doa* expression was found in OCl.8+ cells and an increase in expression in Cl.8R when compared to YCl.8+ cells. An increase in *Doa*

expression was found in ZfeCl.8+ when compared to OCl.8+ cells. YCl.8+ had a decrease and OCl.8+ and ZfeCl.8+ cells had an increase in expression of *Doa* after ecdysone. There was no change in *Doa* expression in Cl.8R after ecdysone.

Protein location and function: cytoplasm, nucleus, embryonic cuticle biosynthesis

CG1105: A decrease in *CG12505* expression was found in OCl.8+ cells and an increase in Cl.8R when compared to YCl.8+ cells. An increase in *CG12505* expression was found in ZfeCl.8+ when compared to OCl.8+ cells. YCl.8+ and ZfeCl.8+ had a decrease in expression of *CG1105* after ecdysone. There was an increase in *CG12505* expression in OCl.8+ cells after ecdysone and the change in expression in Clone 8R cells after ecdysone was undetermined.

Protein location and function: Not known

CG12505: A decrease in *CG12505* expression was found in OCl.8+ cells and an increase in Cl.8R when compared to YCl.8+ cells. An increase in *CG12505* expression was found in ZfeCl.8 when compared to OCl.8+ cells.

YCl.8+, Cl.8R and ZfeCl.8+ had a decrease in expression of *CG12505* after ecdysone. There was an increase in *CG12505* expression in OCl.8+ cells after ecdysone.

Protein location and function: Not known

CG8032, *CG8223* and *CG5384*: A decrease in expression in *CG8032*, *CG8223* and *CG5384* was found in OCl.8+ cells and an increase in expression in Cl.8R when compared to YCl.8+ cells. An increase in expression of *CG5384*, *CG8032* and *CG8223* was found in ZfeCl.8+ when compared to OCl.8+ cells. All cell lines had a decrease in *CG8032*, *CG8223* and *CG5384* expression after ecdysone.

Gene product location and function: *CG5384*: ubiquitin specific protease, protein deubiquitination, *CG8032*: Not known, *CG8223*: Not known

cul-2: A decrease in *cul-2* expression was found in OCl.8+ cells and an increase in expression in Cl.8R cells when compared to YCl.8+ cells. An increase in *cul-2* expression was found in ZfeCl.8+ when compared to OCl.8+ cells.

YCl.8+ and OCl.8+ cells had a decrease in expression of *cul-2* after ecdysone.

There was no change in *cul-2* expression in Cl.8R and ZfeCl.8+ cells after ecdysone.

Protein location and function: nuclear ubiquitin ligase complex

fax: A decrease in *fax* expression was found in OCl.8+ cells and no change in Cl.8R cells when compared to YCl.8+ cells. An increase in *fax* expression was found in ZfeCl.8+ when compared to OCl.8+ cells. An increase in *fax* expression was found in YCl.8+, OCl.8+ and ZfeCl.8+ cells after ecdysone. A decrease in *fax* expression was found in Cl.8R cells after ecdysone.

Protein function: Axonogenesis

CG7224: A decrease in *CG7224* expression was found in OCl.8+ cells and no change in Cl.8R cells when compared to YCl.8+ cells. An increase in expression was found in ZfeCl.8+ when compared to OCl.8+ cells.

A decrease in *CG7224* expression was found in all cell lines after ecdysone.

Gene product location and function: Not known

Ggamma30A: A decrease in *Ggamma30A* expression was found in OCl.8+ cells and no change in Cl.8R cells when compared to YCl.8+ cells there was no data for ZfeCl.8+. A small decrease in *Ggamma30A* expression was found in YCl.8+ cells after ecdysone, a small increase in Cl.8R, an undetermined response OCl.8+ cells and no data for ZfeCl.8+ after ecdysone.

Protein location and function: cytoplasm, heterotrimeric G protein complex

CG15828: A decrease in *CG15828* expression was found in Cl.8R cells with no change in OCl.8+ or ZfeCl.8 cells when compared to YCl.8+ cells. No change in *CG15828* expression was found in Young Clone 8+ cells after ecdysone, a decrease was found in OCl.8+ and ZfeCl.8+ and a small increase in Cl.8R cells after ecdysone.

Protein location and function: Extracellular space, lipid binding

ImpL2: A decrease in *ImpL2* expression was found in Cl.8R cells and OCl.8+ cells when compared to YCl.8+ cells. An increase in *ImpL2* expression was found in ZfeCl.8+ when compared to OCl.8+ cells. A decrease in *ImpL2* expression was found in YCl.8+, Cl.8R and OCl.8+ cells after ecdysone. An increase in *ImpL2* expression was found in ZfeCl.8+ after ecdysone.

Protein location and function: extracellular, cell adhesion molecule

6.3.16: Pairwise comparison of Young Clone 8+ before and after ecdysone and Clone 8R before and after ecdysone

Out of 4,277 genes analysed, over 3,000 genes were identified as having a difference in expression in the YCl.8+ cell line after ecdysone but not in Cl.8R cells after ecdysone (data not shown). According to the comparison using **SAM** 22 genes were identified which differed more than one fold in their expression in YCl.8+ cells after ecdysone when compared Cl.8R cells after ecdysone (data not shown see appendix, table 6a,b). These genes were also identified as changing in expression in the OCl.8+ and ZfeCl.8+ cell lines after ecdysone with 2 exceptions, a hexokinase and a gene of no known function.

6.4: Discussion

Clearly there is a great deal of information that can be accessed from the microarray data. The observations that there was a difference between the cell lines, Young Clone 8+, Old Clone 8+ , Clone 8R and ZfeClone 8+ which was supported by the statistical evidence gathered in Chapter 5 is also supported by the analysis of gene expression of the microarray data by **SAM**.

6.4.1: Statistical data analysis helpful or not?

Microarray data analysed using statistical methods on cDNA microarray data sets has previously given meaningful results (Lee et al., 2000). **SAM** was initially chosen to analyse the data as it has given useful information on differences in gene expression to other laboratories (Ling Li, FCRC, personal communication). **SAM** does not make strong parametric assumptions and only order statistics are involved. However it has also been found by other researchers that although **SAM** is good at finding small numbers of significant genes it is less useful with larger array sets (Pan, 2002).

SAM initially identified many hundreds of genes as significant. Imposing a threshold of only two fold or more as significant to identify genes of interest eliminated more than 99.9% of the data (Andrews et al., 2000; Zinke et al., 2002). However the motivation for choosing a threshold was to reduce the amount of data initially presented which was overwhelming. Expansion of the data, once genes were identified as potential candidates for the loss of adhesion in the Old Clone 8+ cell line, was considered to be the right approach in this instance.

Using statistical software meant that data integral to this study was not used fully. All the data sets were required to be equivalent before data analysis could be undertaken. One data set contained only two replicates and could not be analysed using **SAM**. Two data sets contained one replicate which opposed the result in the other two replicates. As a result **SAM** indicated that ecdysone had no effect at all on the Clone 8R cells. This may be true, but the negative result found in one replicate affects the statistical analysis and significance of the other two replicates.

The conclusion arrived at after the analysis of this data, was that analysis by **SAM** is only useful if data is complete and does not show any significant deviations in any of the replicates. To reduce the number of genes, a change in the fold difference in all three replicates was employed in the analysis by **SAM**. These genes could have been identified by sorting the data in an Excel spreadsheet. However, analysis of the significant genes by **SAM** is useful in validating the microarray data in statistical terms. In addition the low False Discovery Rate (FDR) gives added confidence that the differences in gene expression revealed by the microarray experiments are in fact real differences.

Examination of the genes which were identified as increased or decreased two fold or more has revealed some interesting genes, the products of which have potential significance in the changes observed in the derivatives of the Young Clone 8+ cells. This does not imply that the gene products are significant in the cells themselves, only the possibility that there is a difference. This difference can only be determined by further experimental evidence.

6.4.2: Clone 8R

The primary interest of this study is in genes associated with cell adhesion, however a short comment on the response of Clone 8R to ecdysone is warranted. The microarray data appears to support the hypothesis that Clone 8R cells do not respond to ecdysone in the same way, with exceptions, as the other cell lines (see data). By comparing all of the cell lines and analysing the data for significant changes between Young Clone 8+ and Clone 8R after ecdysone, 22 genes were identified in which Young, Old and ZFe Clone 8+ cells had a similar change in expression after ecdysone (tables 6a 6b). This suggests that these genes were induced by the exposure of these cell lines to ecdysone. The Clone 8R cells displayed only a small change in expression of the gene or no change at all after ecdysone. Providing further support to the data gathered in chapter 5 and by previous investigators that Clone 8R cells are impervious to ecdysone (Peel and Milner, 1992). If the unresponsiveness of Clone 8R cells to ecdysone is due to down-regulation of the ecdysone receptor, this would have to be verified by further experimental evidence. There are 3 isoforms of the EcR receptor which are expressed at different times and to different degrees during development of the imaginal discs (Talbot et al., 1993). It would be interesting to establish which of these EcR receptors the Clone 8+ cell lines are expressing *in vitro*. Perhaps the Clone 8R cell line is expressing all 3 receptors which act antagonistically and results in modulation of the cells response to ecdysone. A microarray analysis at different time points with all of the cell lines would be useful in future and genes could be identified which are induced by ecdysone in a stage specific manner in the Clone 8+ cell lines.

Interpreting the biological significance of the genes of interest identified by **SAM** is difficult without further experimental evidence, however some

discussion will be given on particular genes that have been identified and are of particular interest.

6.4.3: ZfeClone 8+ cells

The gene *CG3074* which encodes the protein cathepsin B was only significantly expressed, with an increase in expression, in the fly extract free cell line ZfeClone 8+. Cathepsin B is a lysosomal cysteine protease, studies in *Drosophila* have found that the concentration and activity of cathepsin B increased with age in homogenates from whole flies (Shi et al., 1994). Cathepsin B has also been associated with the breakdown of yolk granules in *Drosophila* embryos (Medina et al., 1988). A more detailed analysis on the role of cathepsin B has been made in analysis of mammalian cells. Cathepsin B expression has been found to be increased at both the mRNA and protein levels in a wide variety of mammalian tumours (Sloane et al., 1994). Normally the enzyme is contained within lysosomes, but in malignant tumour cells the enzyme is secreted and becomes associated with the cell surface where it is proposed to degrade extracellular matrix proteins (Frosch et al., 1999; Sameni et al., 2000).

The finding that *cathepsin B* is not expressed in Old Clone 8+ cells when compared to Young Clone 8+ cells suggests that the lack of fly extract in the medium may be responsible for the upregulation of the protein cathepsin B in ZfeClone 8+ cells. The secretion of cathepsin B by the ZfeClone 8+ cells would explain the loss of adhesion of these cells, after 24 hours of culture, which we observed in chapter 5. The addition of a much higher level of serum may initially promote cell adhesion but the secretion of cathepsin B may lead to degradation of the extracellular matrix and the ZfeClone 8+ cells would detach from the substrate. This data is potentially very interesting and further

in vitro studies to analyse the ZfeClone 8+ medium after several days growth of the cells may shed some light on the action of cathepsin B on the extracellular matrix.

6.4.4: Old Clone 8+ cells

Potentially the genes *cul-2* and *CG5384* which are decreased in the Old Clone 8+ cells and encode proteins associated with ubiquitination are the most interesting. Ubiquitination is an extremely important cellular process and many of the roles ubiquitin plays in cellular processes come from studies in yeast (*S.cerevisiae*) (Wu et al., 1999; Filippov et al., 2000; Amerik et al., 2000). Roles for ubiquitin include removal of damaged proteins, modulation of levels of critical regulatory proteins and down-regulation of plasma membrane proteins (Koepp et al., 1999; Hicke, 1999). Monoubiquitination triggers endocytosis of cell-surface proteins such as membrane receptors (Hicke, 1999). Reduced activity of cell-surface proteins by their removal from their active site is one way in which a cell may return to a basal state. It has been found that cells which are unable to internalize activated receptors for epidermal growth factor (EGF) adopt the phenotypes of transformed cells (Vieira et al., 1996).

Ubiquitin is linked to a target protein by a series of reactions. This involves a complex of 2 enzymes, E1, E2 and a protein ligase, E3. Once the protein is tagged it is recognised by the proteasome where it is degraded (Wu et al., 1999; Hinke, 1999). *Drosophila* *cul-2* is a member of the family of cullins, which encode ubiquitin-protein ligases (E3). Relatively little is known about the *Drosophila* *cul-2* protein. In mammalian cells mutation of *cul-2* has been found to lead to some kidney tumours (Kaelin and Mather, 1998). Evidence suggests that members of the cullins family participate in regulation of the cell cycle,

DNA replication and the DNA damage response (Higa et al., 2006). Filippov et al (2000) found that the *Drosophila* *cul-1* protein was preferentially expressed in actively dividing tissue, although *cul-1* transcripts were also found in quiescent cells. They also found that after irradiating cells there was a two fold increase of *cul-1* gene transcription in cells undergoing apoptosis. They propose that the elevation of *cul-1* expression in irradiated cells suggests that *cul-1* is required for exit from the cell cycle to apoptosis. Evidence which supports the proposal that *cul-1* participation is required for proper execution of the cell cycle comes from *C.elegans* and yeast. In *C.elegans* *cul-1* mutants display excessive cell division in tissues, resulting in hyperplasia, and mutation of the yeast orthologue, *cdc53*, developmental arrest (Kipreos et al., 1996; Filippov et al., 2000).

The gene *CG5384* encodes a ubiquitin specific protease involved in deubiquitination. Deubiquitinating enzymes are proteins that cleave ubiquitin-protein bonds. By deubiquitinating a tagged protein, ubiquitin is released then recycled and the intracellular pool of free ubiquitin is maintained. In yeast it has been proposed that the ubiquitin which is released by the deubiquitinating enzyme is in the form of chains or linked to remnants of degraded proteins, freeing the ubiquitin or breaking the chains up may prevent the ubiquitin from clogging the proteasome (Papa and Hochstrasser, 1993; Amerik et al., 1997). Although the role of deubiquitinating enzymes are largely unknown, *Drosophila* deubiquitination by the Fat facets protein, a regulator of photoreceptor differentiation during eye development, has been found to activate endocytosis. *Drosophila* Fat facets is thought to be singular in deubiquitinating a specific substrate and thereby preventing its proteolysis (Huang et al.,1995, Chen and Fisher, 2000).

Clearly downregulation of these genes and the proteins, cul-2 and Cg5384, would have important consequences in Old Clone 8+ cells and could explain the excessive proliferation observed. This may be due to disruption of the cell cycle by loss of cul-2. Loss of the deubiquitinating enzyme CG5384 may lead to reduced levels of ubiquitin. This in turn could result in a cell which is expressing cell surface proteins which should be downregulated. The regulation of the level of receptors present on the cell membrane is vital to the control of cell signalling and is critical in control of cell growth. In addition the lack of cell-matrix adhesion may be due to upregulation of a protein not normally expressed at such high levels.

An increase in *Idgf3* expression was found in Clone 8R, Old Clone 8+ and ZfeClone 8+ cells when compared to Young Clone 8+ cell line. Imaginal Disc Growth Factors (Idgf) have previously been isolated from Young Clone 8+ conditioned medium. They are not related to known growth factors but are related to the chitinases (Kawamura et al., 1999). Young Clone 8+ cells were stimulated to grow in the presence of these Imaginal Disc Growth Factors and cell survival was promoted (Kawamura et al., 1999). Cell adhesion, however was not affected even when the cells were subjected to very high levels of the proteins suggesting that *Idgf3* is a potential cause of the increased rate of proliferation observed in Old Clone 8+ cells but is not related to the loss of adhesion.

An increase in *Peroxidasin* expression was found in Clone 8R, Old Clone 8+ and ZfeClone 8+ cells when compared to Young Clone 8+ cell line.

The protein product of *Peroxidasin* is primarily synthesised by *Drosophila* haemocytes (Nelson et al., 1994). Peroxidasin was found co-localised with the extracellular matrix components collagen IV and laminin once the basement membranes had been completed which suggests that secreted peroxidasin

plays a role in extracellular matrix consolidation. Peroxidase is a potential candidate for the loss of adhesion observed in the Old Clone 8+ cells.

An increase in *Collagen IV (Cg25C)* expression was found in Clone 8R, Old Clone 8+ and ZfeClone 8+ cells when compared to the Young Clone 8+ cell line. *Cg25C* encodes the protein collagen IV, an important extracellular matrix protein required to maintain the structural integrity of *Drosophila* basement membranes. Collagen IV is 'prominently' associated with the wing disc basement membrane before evagination (Murray et al., 1995). Like peroxidase, collagen IV is also secreted by haemocytes although evidence suggests that epithelial cells also secrete collagen IV (Mirre et al., 1988; Murray et al., 1995). Collagen IV is a prospective candidate for the loss of adhesion observed in the Old Clone 8+ cells. Unfortunately the change in *collagen IV* expression in Clone 8R after ecdysone was ambiguous and therefore this gene is precluded from further studies.

The gene *glutactin* which encodes a calcium ion binding, extracellular matrix protein is of the most interest. *Glutactin* is increased in all three cell lines, Old Clone 8+, ZfeClone 8+ and Clone 8R. *Drosophila* glutactin is expressed in basement membranes of imaginal discs and surrounds embryonic internal organs which are enclosed by basement membranes. The role of glutactin and interaction in the extracellular matrix are unknown although it has been found to colocalise with laminin (Olsen et al., 1990).

Levi et al (1991) state that the sole presence of a protein is not sufficient to assess its functionality. This can also be said for a gene. As stated above the loss of cell-matrix adhesion may be due to upregulation of a protein not normally expressed at such high levels. Is the identification of *glutactin* as a significant gene reflected in the expression of the protein glutactin? In other

words is the protein glutactin actually expressed in the Clone 8+ cells? If it is in what way does glutactin interact with the cytoskeleton?

In order to validate the microarray data, and to investigate whether the upregulation of *glutactin* has a role in the loss of adhesion in the Old Clone 8+ cells, further experiments using the Clone 8+ cell lines and antibody staining of the Clone 8+ cell lines with *Drosophila* anti-glutactin antibody was carried out (Chapter 7).

Tables

Table 6.1: The number of genes identified by **SAM** with significant expression in each pairwise comparison on Clone 8+ cell lines

Cell Line	SAM Significant genes	SAM Significant genes	FDR
Pairwise Comparison	Increased	Decreased	%
YCl.8+ vs YCl.8+ +E	1746	3363	45%
YCl.8+ vs OCl.8+	2219	2927	45%
YCl.8+ vs Cl.8R	2754	2408	63%
YCl.8+ +E vs OCl.8+ +E	0	0	N/A
YCl.8+ +E vs Cl.8R +E	1800	2283	45%
OCl.8+ vs OCl.8+ +E	2194	2735	52%
OCl.8+ vs ZfeCl.8+	2258	2464	33%
OCl.8+ +E vs ZfeCl.8+ +E	2005	2870	33%
Cl.8R vs Cl.8R +E	0	0	N/A
ZfeCl.8+ vs ZfeCl.8+ +E	2564	2437	51%

Table 6.1: The number of genes revealed by **SAM**, with a significant change in expression from the microarray data of pairwise hybridisations between the Clone 8+ cell lines before and after ecdysone. The expression of over 1500 genes in each set were found to be significantly increased or decreased with the exception of 2 raw data sets. YCl.8 + after ecdysone vs OCl.8 after ecdysone, where data was only available in two replicates. Cl8.R vs Cl.8R after ecdysone where no genes were found to be significant. The data is listed in accordance with the 'Flychip' Excel normalised data files.

FDR=False discovery rate

vs =hybridised with.

+E = after ecdysone

Table 6.2: Number of genes identified by **SAM** increased two fold or more

Cell Line	SAM	SAM	FDR
	Significant genes	Significant genes	
Pairwise Comparison	Increased	Decreased	%
YCl.8+ vs YCl.8+ +E	6	2	<1%
YCl.8+ vs OCl.8+	1	10	<1%
YCl.8+ vs Cl.8R	7	2	<1%
YCl.8 + +E vs OCl.8 +E	0	0	N/A
YCl.8 + E vs Cl.8R +E	8	12	<1%
OCl.8+ vs OCl.8 + E	7	4	<1%
OCl.8+ vs ZfeCl.8+	4	0	<1%
OCl.8+ +E vs ZfeCl.8+ +E	2	3	<1%
Cl.8R vs Cl.8R +E	0	0	N/A
ZfeCl.8+ vs ZfeCl.8+ +E	0	0	N/A

Table 6.2: The number of genes revealed by **SAM** as expressed with a threshold of two fold or more in the Clone 8+ cell line hybridisations. No genes were found to be significant in 3 pairwise hybridisations. The data is listed in accordance with the 'Flychip' excel data files.

FDR=False discovery rate

vs =hybridised with.

+E= after ecdysone.

Table 6.3a: Genes increased two fold or more in Cl.8R cells

Gene	Gene product: location and role
<i>CG10126</i>	Calcium ion binding
<i>CG1090</i>	Calcium, potassium:sodium antiporter
<i>Cg25C</i>	Basement membrane, collagen type IV,
<i>Gel</i>	Actin filament, cytosol, extracellular
<i>Idgf3</i>	Extracellular, imaginal disc growth factor ,
<i>Pxn</i>	Extracellular matrix, peroxidase
<i>regucalcin</i>	Calcium ion binding

Table 6.3a: Genes increased two fold or more in Cl.8R cells

Genes identified by analysis with **SAM** with an increased expression in Clone 8R cells when compared to Young Clone 8+ cells are listed. 7 genes were identified which were increased two fold or more.

Table 6.3b: Genes decreased two fold or more in Cl.8R cells

Gene	Gene product: location and role
<i>CG15828</i>	Extracellular space, lipid binding
<i>Imp-L2</i>	Extracellular, cell adhesion molecule

Table 6.3b: Genes decreased two fold or more in Cl.8R cells

Genes identified by analysis with **SAM** with a decreased expression in Clone 8R cells when compared to Young Clone 8+ cells are listed. 2 genes were identified which were decreased two fold or more.

Table 6.4a: Genes increased two fold or more in Cl.8R cells after ecdysone

Gene	Gene product: location and role
<i>Cg25C</i>	Basement membrane, collagen type IV,
<i>CG9089</i>	Not known
<i>Chd64</i>	Actin binding
<i>Chit</i>	Extracellular, chitinase
<i>ERR</i>	Ligand dependent nuclear receptor
<i>Idgf2</i>	Extracellular, imaginal disc growth factor, NOT chitinase
<i>Inos</i>	Inositol3phosphate synthase
<i>Pxn</i>	Extracellular matrix, peroxidase

Table 6.4a: Genes increased two fold or more in Cl.8R cells after ecdysone. Genes identified by analysis with **SAM** which were increased in Clone 8R cells after ecdysone when compared to Young Clone 8+ cells after ecdysone are listed. 8 genes were identified which were increased two fold or more.

Table 6.4b: Genes decreased two fold or more in Cl.8R cells after ecdysone

Gene	Gene product: location and role
<i>CG14749</i>	poly(A)+ mRNA nucleus export
<i>fax</i>	Axonogenesis
<i>GstS1</i>	Cellular component unknown, Glutathione peroxidase
<i>Hsp27</i>	Heat shock protein, AGE
<i>Impl2</i>	Extracellular, cell adhesion molecule
<i>poe</i>	Calmodulin binding AGE
<i>regucalcin</i>	Calcium ion binding
<i>CG31363</i>	Not known
<i>CG5854</i>	Not known
<i>CG6234</i>	Not known
<i>CG9213</i>	Not known
<i>CG7874</i>	Not known

Table 6.4b Genes decreased two fold or more in Cl.8R cells.

Genes identified by analysis with **SAM** which were decreased in Clone 8R cells after ecdysone when compared to Young Clone 8+ cells after ecdysone are listed. 7 genes of known function were identified which were decreased two fold, 5 genes were of unknown function.

Table 6.5a: Genes increased two fold or more in Old Cl.8+ cells

Gene	Gene product: location and role
CG3380	Sodium independent organic anion transporter

Table 6.5a: Genes increased two fold or more in OCl.8+ cells

Genes identified by analysis with **SAM** increased in expression in Old Clone 8+ cells when compared to Young Clone 8+ cells are listed. 1 gene was identified which was increased two fold or more.

Table 6.5b: Genes decreased two fold or more in Old Cl.8+ cells

Gene	Gene product: location and role
CG5384	Ubiquitinspecific protease, protein deubiquitination
cul-2	Nuclear ubiquitin ligase complex
Doa	Cytoplasm, nucleus, protein kinase, protein amino acid phosphorylation
fax	Axonogenesis
Ggamma30A	Cytoplasm, GTPase, Gprotein coupled receptor protein signalling pathway
CG1105	Not known
CG12505	Not known
CG7224	Not known
CG8032	Not known
CG8223	Not known

Table 6.5b: Genes decreased two fold or more in OCl.8+ cells

Genes identified by analysis with **SAM** which were decreased in Old Clone 8+ cells when compared to Young Clone 8+ cells are listed. 10 genes were identified which were decreased two fold or more. 5 genes were reported as unknown: *CG1105*, *CG12505*, *CG7224*, *CG8032* and *CG8223*.

Genes are listed alphabetically.

Table 6.6a: Genes increased two fold or more in ZfeCl.8+ cells

Gene	Gene product: location and role
CG3074	Cathepsin B
CG3273	Actin filament reorganisation (aka scrambled (<i>sced</i>))
Glt	Basement membrane, calcium ion binding
roX1	Dosage compensation complex

Table 6.6a: Genes increased two fold or more in ZfeCl.8+ cells

Genes identified by analysis with **SAM** increased in expression in ZfeClone 8+ cells when compared to Old Clone 8+ cells are listed. 4 genes were identified which were increased two fold or more. The gene CG3273 is also known as *scrambled (sced)*.

Genes are listed alphabetically.

Table 6.7a: Genes increased two fold or more in ZfeCl.8+ cells after ecdysone

Gene	Gene product: location and role
CG3074	Cathepsin B
CG3273	Not known

Table 6.7a: Genes increased two fold or more in ZfeCl.8+ cells after ecdysone
 Genes identified by analysis with **SAM** with an increase in expression in ZfeClone8 cells after ecdysone when compared to Old Clone 8+ cells after ecdysone are listed. 2 genes were identified which were increased two fold or more.

Table 6.7b: Genes decreased two fold or more in ZfeCl.8+ cells after ecdysone

Gene	Gene product: location and role
CG31305	Not known
CG7777	Water transporter
regucalcin	Calcium ion binding

Table 6.7b: Genes decreased two fold or more in ZfeCl.8+ cells after ecdysone
 Genes identified by analysis with **SAM** with a decreased expression in ZfeClone8 cells after ecdysone when compared to Old Clone 8+ cells after ecdysone are listed. 3 genes were identified which were decreased two fold or more.

Genes are listed alphabetically.

Table 6.8a: Genes increased two fold or more in YCl.8+ cells after ecdysone

Gene	Gene product: location and role
<i>CG14749</i>	poly(A)+ mRNA nucleus export
<i>CG31305</i>	Not known
<i>CG9213</i>	Not known
<i>fax</i>	Axonogenesis
<i>GstS1</i>	Cellular component unknown, glutathione peroxidase
<i>regucalcin</i>	Calcium ion binding

Table 6.8a: Genes increased two fold or more in YCl.8+ cells after ecdysone

Genes identified by analysis with **SAM** with an increased expression in Young Clone 8+ cells after ecdysone when compared to Young Clone 8+ cells no ecdysone are listed. 6 genes were identified which were increased two fold or more after ecdysone.

Table 6.8b: Genes decreased two fold or more in YCl.8+ cells after ecdysone

Gene	Gene product: location and role
<i>Chd64</i>	Actin binding
<i>ERR</i>	Ligand dependent nuclear receptor

Table 6.8b: Genes decreased two fold or more in YCl.8+ cells after ecdysone

Genes identified by analysis with **SAM** with a decreased expression in Young Clone 8+ cells after ecdysone when compared to Young Clone 8+ cells no ecdysone are listed. 2 genes were identified which were decreased two fold or more after ecdysone.

Genes are listed alphabetically.

Table 6.9a: Genes increased two fold or more in OCI.8+ cells after ecdysone

Gene	Gene product: location and role
CG1090	Calcium, potassium:sodium antiporter
CG9213	Not known
fat-spondin	Extracellular, cytoskeleton organisation
fax	Axonogenesis
GstS1	Cellular component unknown, glutathione peroxidase
Inos	Inositol3phosphate synthase
regucalcin	Calcium ion binding

Table 6.9a: Genes increased two fold or more in OCI.8+ cells after ecdysone

Genes identified by analysis with **SAM** in the Old Clone 8+ cells after ecdysone when compared to Old Clone 8+ cells no ecdysone, are listed. 7 genes were identified which were increased two fold or more after ecdysone.

Table 6.9b: Genes decreased two fold or more in OCI.8+ cells after ecdysone

Gene	Gene product: location and role
CG10527	Farnesoic acid Omethyltransferase
CG9089	Not known
Chd64	Actin binding
ERR	Ligand dependent nuclear receptor

Table 6.9b: Genes decreased two fold or more in OCI.8+ cells after ecdysone

Genes identified by analysis with **SAM** with a decreased expression in Old Clone 8+ cells after ecdysone when compared to Old Clone 8+ cells no ecdysone are listed. 4 genes were identified which were decreased two fold or more after ecdysone.

Genes are listed alphabetically.

Chapter 7

Glutactin Expression in Clone 8+ cells

7.1: Introduction

The *Drosophila* protein Glutactin is an acetylcholinesterase-like adhesion molecule (AChE), which has been described as a nonenzyme protein due to the lack of an essential serine catalytic region (Olsen et al., 1990; Grisaru et al., 1999). Evidence suggests that *glutactin* is a single copy gene located on 29D with no homologues being revealed. Other members of this catalytically inactive family are the proteins gliotactin and neurotactin. Gliotactin is expressed in neural and epithelial tissues. Neurotactin is expressed transiently in *Drosophila* embryonic and larval tissue, namely the third instar larval wing disc, but is not expressed in the adult (Barthalay et al., 1990). *Drosophila* gliotactin and neurotactin are both transmembrane glycoproteins, glutactin is the only member of this family to be secreted (Olsen et al., 1990).

Glutactin was originally isolated from *Drosophila* Kc cell culture medium. Immunofluorescence staining of sections of *Drosophila* embryos with anti-glutactin antibody colocalized glutactin with laminin at sites where basement membranes had been demonstrated by electron microscopy (Olson et al., 1990). The basement membranes which envelop the imaginal discs also showed distinct outlines of glutactin. Glutactin has been characterised and was identified as containing a large AChE-like extracellular domain, the overproduction of AChE in several tumour types has been associated with cell proliferation and/or invasive migration capacities (Grisaru et al., 1999).

Microarray analysis identified the gene *glutactin* with an increased expression in Old Clone 8+, Clone 8R and ZfeClone 8+ when compared to the Young Clone 8+ cell line. Glutactin is an extracellular matrix protein, secretion and

deposition of an excess extracellular matrix product such as glutactin may have an adverse affect on attachment of Old Clone 8+ cells to the substrate. The aim of this chapter therefore is to establish that the protein glutactin is expressed in the various Clone 8+ cell lines, to discover if there any major differences between the cell lines, and examine glutactin interaction with the cytoskeleton.

7.2: Materials and Methods

To examine the presence of the *Drosophila* protein Glutactin in Clone 8+ cells anti-*Dm*-glutactin antibody was kindly provided by John Fessler.

Anti- α -tubulin antibody which decorates the microtubule cytoskeleton and phalloidin, which stains for the f-actin cytoskeleton were also employed in order to assess the association of glutactin with the cytoskeleton.

7.2.1: Immunohistochemistry

Sterile coverslips were placed in Petri dishes and Clone 8+ cells were seeded at 3.5×10^6 per 5ml in CSM or in CSM with ecdysone added to give a final concentration of 10ng/ml and incubated at 25°C. After 24 hours the medium was removed and the cells were rinsed carefully with PBS. As the majority of OCl.8+ cells and ZfeCl.8+ cells were suspended in the medium, rinsing with PBS was not always carried out and the medium was removed as carefully as possible.

7.2.2: Glutactin and f-actin

Staining for filamentous actin was performed with phalloidin conjugated to a red-fluorescent dye, Alexa Fluor 568 phalloidin (Molecular probes). In order to preserve the actin filaments, cells were fixed with 4% paraformaldehyde for

20 minutes (this procedure was carried out in a fume hood) followed by gentle rinsing in PBS four x five minutes. 0.1% Glycine in PBS was added to the cells for 5 minutes in order to quench any aldehyde fluorescence. Cells were rinsed in PBS three x 5 minutes and incubated with 0.1% Triton-X in PBS for 1 minute to permeabilise the cells. This was followed by rinsing in PBS three x 5 minutes. The cells were then incubated for 1 hour 20 minutes at room temperature with phalloidin, then rinsed gently 4 x 5 minutes in PBS. This was followed by incubation for 2 hours at 25°C with primary antibody, rabbit anti-*Dm*-Glutactin used at 1:1500 diluted in PBS. Cells were rinsed gently 4 x 5 minutes in PBS followed by incubation with secondary antibody anti-rabbit IgG conjugated with fluorescein 1:500 for 2 hrs at 25°C, after which cells were rinsed gently 4 x 5 minutes in PBS.

In some preparations cells were also incubated for 2 hours at 25°C with monoclonal mouse anti- α -tubulin (Sigma T9026) diluted 1:1000 in PBS. Cells were rinsed with gentle agitation 4 x 5 minutes in PBS and incubated with secondary antibody anti-mouse IgG conjugated with fluorescein, Texas red or AMCA, 1:250 for 2 hrs at 25°C.

7.2.3: α -tubulin and Glutactin

Cells were fixed in ice-cold methanol, 0°C, for 4 minutes and rinsed gently in PBS three x 5 minutes. They were then incubated for 2 hours at 25°C with primary antibody rabbit anti-*Dm*-glutactin, used at 1:1500 diluted in PBS, followed by rinsing with gentle agitation 4 x 5 minutes in PBS. Incubation of the cells with secondary antibody anti-rabbit IgG conjugated with fluorescein or Texas red 1:500 was carried out for 2 hrs at 25°C. Following this cells were rinsed with agitation 4 x 5 minutes in PBS and incubated for 2 hours at 25°C

with monoclonal mouse anti- α -tubulin antibody diluted 1:1000 in PBS. Cells were rinsed with gentle agitation 4 x 5 minutes in PBS and incubated with secondary antibody anti-mouse IgG conjugated fluorescein or Texas red 1:250 for 2 hrs at 25°C. Finally the cells were rinsed with gentle agitation for at least 4 x 5 minutes in PBS.

Controls: Cells were fixed only to monitor autofluorescence

Cells were incubated with secondary antibodies to assess non-specific binding of the secondary Anti-actin antibody to confirm the presence of f-actin.

Nuclear DNA was stained by incubation with 0.125 μ g/ml DAPI solution for 10 minutes at room temperature, followed by rinsing in PBS, with gentle agitation, 4 x 5 minutes.

Cells were kept covered at all times and the procedures were carried out in a darkened room. Primary and secondary antibody preparations were centrifuged for 20 seconds and the supernatant was used. To confirm the presence of glutactin in the wing disc, third instar larvae were dissected and anti-*Dm*-glutactin antibody was used to stain the disc tissue (figure 7.1, pg 105).

7.2.4: Microscopy

Coverslips were mounted in Vectamount (Vectashield) and left overnight in the refrigerator and viewed the next day. Immunofluorescence microscopy was carried out and the images were contrast enhanced using Openlab (v2.1.5). In an aid to examine areas of colocalisation, images were sharpened using Adobe Photoshop (v5.5). The letters l and o were not used to label the images.

To confirm the presence of glutactin in the wing disc, third instar larvae were dissected and anti-*Dm*-glutactin antibody was used to stain the disc tissue (figure 7.1).

Figure 7.1: Wild-type third instar imaginal wing disc

A DIC image showing an imaginal disc dissected from a late third instar larva shortly after culture initiation. The process of evagination has begun and the disc is beginning to curl upwards. The folds of the disc proper which forms the adult appendage can be seen. Dissected larval tissue is also present.

d, imaginal disc; f, folds; l, larval tissue
Scale bar represents:200 μ m

Figure 7.1: Wild-type late 3rd instar imaginal wing disc

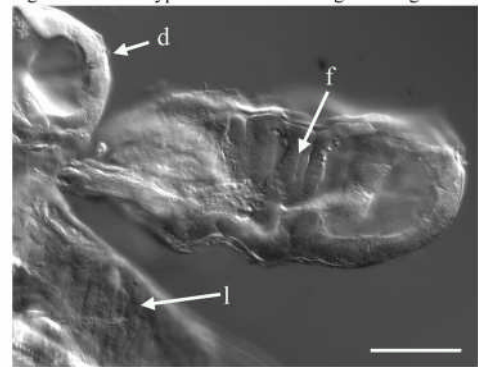
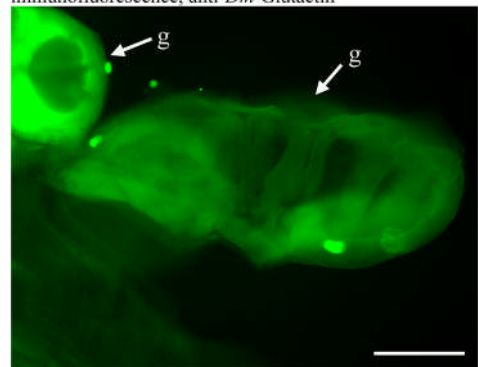


Figure 7.2: 3rd instar wing imaginal disc, anti-*Dm*-Glutactin

Immunofluorescence image showing the imaginal disc in figure 7.1 after antibody staining with the protein anti-*Dm*-Glutactin. Glutactin surrounds the whole wing disc and appears like an amorphous layer in some areas. Another imaginal disc is present which has also been positively stained. The larval tissue which can be seen in figure 7.1 has not stained for glutactin.

g, glutactin
Scale bar represents:200 μ m

Figure 7.2: Late 3rd instar wing imaginal disc, immunofluorescence, anti-*Dm*-Glutactin



7.3: Results

The presence of the protein, *Drosophila* glutactin, was detected in all Clone 8+ cell lines, but not in all cells probed with anti-*Drosophila*-glutactin antibody.

7.3.1: 24 hours after culture initiation

24 hours after culture initiation glutactin was detected in the cytoplasm of single YCl.8+, Cl.8R and ZfeCl.8+ cells which had formed an attachment to the substrate revealing a punctate expression within all cells (figure 7a(i)).

Visualisation of the glutactin by immunofluorescence microscopy indicated that glutactin was expressed mainly in the uppermost region of the cell as opposed to the lower region attached to the substrate. Small vesicles of secreted glutactin were visualised, the immunofluorescence detected was brighter in these vesicles (figure 7a(i)). Long and short processes were observed emanating from cells in contact with the substrate. There appeared to be a thinner layer of cell membrane or secreted extracellular matrix associated with some cells and the substrate (figure 7a(ii)). Secreted glutactin vesicles were detected along cell processes and close to areas where the cells had aggregated and in association with the thin layers of putative extracellular matrix (figures 7b, 7c(i,ii)). Secreted glutactin was also detected on the apical cell surface in the majority of YCl.8+ and Cl.8R cells (figure 7d(i,ii,iii)).

7.3.2: The cytoskeleton

At 24 hours after culture initiation anti- α -tubulin antibody which decorates the microtubule cytoskeleton and phalloidin which detects f-actin for the actin

cytoskeleton were both detected in the cytoplasm of all Clone 8+ cells. α -tubulin was detected underlying the membrane of cells which had formed an attachment to the substrate. An amorphous layer of glutactin was also detected surrounding some cells. α -tubulin did not colocalise with glutactin although close association was observed (figure 7e(i,ii,)). f-actin was detected close to the nucleus at the uppermost part of Clone 8+ cells and colocalisation of f-actin with glutactin was detected (image overlay of glutactin and f-actin expression produced orange and/or yellow immunofluorescence in areas where glutactin and f-actin were colocalised) (figure 7f(i,ii,)).

Glutactin was detected in the cytoplasm and as a secreted molecule in a small number of ZfeCl.8+ cells which had formed an attachment to the substrate as in the YCl.8+ and Cl.8R cells described above (figure 7a(i)). Cells of this type were not observed in OCl.8+ preparations. Large membrane bound vesicles were observed closely associated to the cell membrane in the majority of ZfeCl.8+ cells attached to the substrate. Glutactin and f-actin were detected in association with these large vesicles (figures 7g (i,ii,iii)). Cells of this type were not observed in OCl.8+ preparations. Large vesicles which stained for glutactin and f-actin were also detected at the basolateral region of cells attached to the substrate (these were also present in the YCl.8+ and Cl.8R cells attached to the substrate but not shown). No secreted vesicles of glutactin were observed.

α -tubulin was prominent in all rounded cells which had been fixed whilst undergoing mitosis and a greater proportion of cells were observed undergoing cell division in the OCl.8+ and ZfeCl.8+ preparations (figure 7h). Glutactin was detected in the cytoplasm and surrounding YCl.8+ and Cl.8R cells. Colocalisation with f-actin was observed in the cytoplasm (figure 7i).

Glutactin was detected in the cytoplasm of OCl.8+ and ZfeCl.8+ round cells which had been suspended in the medium (no attachments to the substrate were observed in these cells). The intensity of the glutactin was variable, some cells contained an abundance of cytoplasmic glutactin whereas glutactin was not detected at all in some cells (figure 7j(i,ii)). α -tubulin was detected just beneath the plasma membrane of these round cells and did not colocalise with glutactin.

Four distinct OCl.8+ rounded cell types were associated with glutactin and f-actin expression. Firstly cells in which glutactin was located throughout the cytoplasm and f-actin was located just beneath the plasma membrane, colocalisation was observed (figure 7j(i)). In others, glutactin was located at one pole of the cell and f-actin was located at the other and colocalisation was observed in the mid region (data not shown). In cells where glutactin was located throughout the cytoplasm no f-actin was observed (figure 7j(i)). Finally cells were found where f-actin was located throughout the cytoplasm, but no glutactin was observed (figure 7j(ii)).

7.3.3: Filopodia and cell aggregates

Glutactin was evident between cell-cell contacts of all round cell aggregates. DIC microscopy revealed that these cells were connected by processes (figures 7k(i,ii)). In the Cl.8R cells longer, thicker processes (filopodia) were present. These processes stained intensely with the anti-glutactin antibody. The processes appeared to emanate from single cells, were conspicuous at cell-cell contacts, and connected groups of cells (figures 7m(i,ii)). After 24 hours large aggregates of cells attached to the substrate were only found in the YCl.8+ and Cl.8R cell preparations (figures 7n(i,ii)). Glutactin enveloped the cells and was present as an amorphous deposit. Glutactin colocalised with f-actin around

the cell membrane (figure 7n(ii)). Aggregates were also connected by processes which stained for f-actin (figure 7p).

7.3.4: Day 5 after culture initiation

By day five after culture initiation, YCl.8+ and Cl.8R cells had formed the aggregates of cells normally associated with YCl.8+ at this time (Chapter 5). Examination of the cells by DIC microscopy revealed processes underlying layers, on the tops and between cells. Cytoplasmic and secreted glutactin was detected in cells and along cell processes (figures 7q(ii)). Glutactin was colocalised with f-actin along cell processes (figures 7q(iii)). Many cells appeared to be pentagonal in shape when visualised with f-actin (figure 7r(i)). An abundance of glutactin vesicles were observed secreted from Cl.8R covering the tops of cells (figures 7r(ii)).

After five days glutactin was detected completely surrounding the ZfeCl.8+ suspended cells (figure 7s(i,ii)). Colocalisation of glutactin with f-actin and α -tubulin was not observed. High background staining of glutactin was observed due to fixation of residual medium. OCl.8+ cell aggregates were not found in cell preparations.

7.3.5: After ecdysone treatment

After ecdysone treatment glutactin and f-actin were detected in small membrane vesicles which were present in the extracellular space, fixed to the coverslip, in YCl.8+ fixed preparations (figure 7t(i)). Membrane bound vesicles of up to 2 μ m in diameter were also observed in close association with the YCl.8+ cells where glutactin was detected (figures 7t(ii,iii,iv)). The vesicles appeared to be in close association with cells via processes and at times were

attached to the cell membrane by stalk-like protruberances or fine cytoplasmic threads which appeared to be budding off (figure 7tiii).

There were no apparent changes in the expression of glutactin in the Cl.8R cells.

After ecdysone treatment glutactin was detected in a large number of membrane bound vesicles in ZfeCl.8+ cells. Vesicles were detected within the cell cytoplasm and as secreted vesicles in close association with the cell membrane (figure 7u(i)). Staining for f-actin and glutactin showed colocalisation in these vesicles. Further examination showed that the vesicles were still bound to the cell membrane (figure 7u(ii,iii,iv)). No vesicles were observed in the extracellular space fixed to the coverslip.

In OCl.8+ round cells one large area of glutactin was detected in the cell cytoplasm. Many of the OCl.8+ cells appeared to be damaged (figure 7v(i)). The extruded contents of the OCl.8+ cell cytoplasm stained intensely for glutactin and f-actin. Small vesicles of glutactin were surrounded by the f-actin and glutactin (figure 7v(ii)).

7.4: Discussion

The analysis of microarray data using **SAM** (Significant Analysis Microarrays) comparing the differential gene expression of the cell line Young Clone 8+ and three derivatives Old Clone 8+, ZfeClone 8+ and Clone 8R identified the *Drosophila* gene *Glutactin* as being increased two fold or more in ZfeClone 8+ cells when compared to Old Clone 8+ cells. *Glutactin* was also identified in Old Clone 8+ cells and Clone 8R cells as increased when compared to Young Clone 8+ cells.

The results of the immunofluorescence staining of the Clone 8+ cell lines with anti-*Dm*-glutactin antibody shows several things. The protein glutactin was present in all the Clone 8+ cell lines before and after ecdysone addition. Glutactin colocalised with f-actin but not with α -tubulin. Long cell processes (filopodia) connecting aggregates of cells appeared to emanate from single cells (figure 7m). These filopodia stained for f-actin and glutactin especially between cell-cell contacts (figure 7q). Singular vesicles of glutactin were associated with these processes and membrane bound vesicles of glutactin and f-actin were also observed (figure 7p(i)). Membrane bound vesicles of glutactin and f-actin were associated with ZfeClone 8+ cells before ecdysone treatment and in ZfeClone 8+ and Young Clone 8+ cells after ecdysone (figures 7g(iii), 7u, 7t). What does the expression of the protein glutactin in Clone 8+ cell line cells suggest and how does that relate to imaginal discs?

7.4.1: Young Clone 8+ cell line

The basal lamina or basement membrane which surrounds the imaginal disc epithelia during embryogenesis and larval development is composed of specialised extracellular matrix. The basement membrane extracellular matrix components are secreted by the imaginal disc epithelial cells and associated haemocytes, while circulating haemocytes are associated with the secretion of basal lamina, collagen IV and peroxidase (Murray et al., 1995; Brabant et al., 1996). *In vivo* epithelial cells are highly polarized and have distinct apical and basolateral plasma membrane domains. These domains are characterized by different sets of trans-membrane proteins and associated cortical proteins (Bilder and Perrimon, 2000; Bilder et al., 2000; Harris and Peifer, 2005).

At the time, developmentally, that the Clone 8+ cell line was derived, the disc is composed of two epithelial layers which perform different roles during

morphogenesis to form the wing. The epithelial layers lie juxtaposed and the respective disc epithelia have apical-basal polarity. At this point the basal surface of the cells is outermost, supported by the basal lamina and facing the haemocoel. The apical surface of the wing epithelium faces the disc lumen.

It has previously been asserted that the Clone 8+ cell line lacks any sign of apical-basal polarity (Miller et al, 2000). However, I would argue that there may be a form of polarity present. In Clone 8+ cells the basal surface could possibly be represented by the membrane that is bathed in the medium (as the basal surface *in vivo* faces the haemocoel) and the apical surface by the membrane and extracellular matrix which is attached to the substrate. Adhesion of the cells to the substrate imposes a non-uniform environment on the cells to which they respond by developing differences between their two surfaces in terms of cellular structure and protein localisation. Glutactin was secreted from the uppermost (apical region) of the Clone 8+ cells, facing the culture medium, and although secreted vesicles were observed close to the substrate, the majority of glutactin remained located to the top of the cell (the apical region) (figure 7d(iii)). Maintenance of the secreted glutactin to the outer membrane of the cell would probably be mediated by laminin and integrins. Glutactin has been found to colocalise with laminin which is a ligand for integrins, mediators of cell-matrix adhesion *in vivo* (Olsen et al., 1990).

Collagen IV and peroxidase secretion is accredited to the associated haemocyte population. I propose that glutactin is secreted from the basal membrane of imaginal disc epithelial cells *in vivo* (which corresponds to the upper portion of Clone 8 cells *in vitro*) and not haemocytes. Glutactin was in fact secreted from the upper region of the cell in all Clone 8+ cell lines *in vitro* which represents the basal region of cells *in vivo*. Glutactin in association with

other extracellular matrix components such as laminin and collagen IV form the basal lamina. This layer is represented in Young Clone 8+ cells by the amorphous layer of extracellular matrix detected covering single cells and aggregates (figure 7n(ii)). As glutactin is prevalent in areas where basement membranes are found and may be a relatively inert molecule, as evidenced by the lack of an essential serine catalytic region (Olsen et al., 1990), glutactin may be predominant in the outward facing layers of extracellular matrix in imaginal discs, thus acting as a barrier, affording epithelial cells protection from the larval haemolymph. This role would be essential during metamorphosis when degeneration of the larval cells leads to the expulsion of potentially degradative enzymes.

Interestingly attachment of unpolarized canine kidney cells (MDCK) cells to a substrate has been found to induce polarization of apical marker proteins to the free surface (Vega-Selas et al., 1988; Boulan and Nelson, 1989). In the case of the Clone 8+ cells induction of both apical and basal associated proteins to the surface may occur. Therefore there may be aspects of the apical-basal polarity observed *in vivo* in wing disc epithelial cells which are not faithfully reproduced *in vitro* in the Young Clone 8+ cells. Cell polarity could be investigated in the Young Clone 8+ cells in future experiments.

7.4.2: The cytoskeleton

Glutactin was found to colocalise with f-actin at the apical region of the Clone 8+ cells but did not appear to associate with microtubules. This suggests that glutactin is transported to the apical plasma membrane and secreted there via the actin cytoskeleton. The microtubule cytoskeleton may also play a role in glutactin transport which has yet to be elucidated. The role of actin and microtubule cytoskeleton in secretion of glutactin could be examined in future

experiments using cytoskeletal disrupting agents such as cytochalasin, colchicine and nocodazole.

7.4.3: Filopodia

Filopodia were identified and appeared to traverse the cells between points of cell-cell contacts (figure 7k(i)). Filopodia are long cell extensions that contain actin filaments and play a role in a range of cell processes during *Drosophila* development. These include long range cell-cell communication, border cell migration during oogenesis, dorsal closure in embryos and imaginal thorax closure (Joussineau et al., 2003; Rørth, 2002; Jacinto et al., 2000; Martin-Blanco et al., 2000). Basal filopodia have also been identified in whole mount studies on the wing disc epithelium and a putative role proposed in relation to changes in cell shape during larval and pupal development (Eaton et al., 1995). The filopodia observed in the Clone 8+ cells stained intensely for glutactin (figure 7q(ii)). Membrane bound vesicles which contained both glutactin and f- actin were observed along these processes (figure 7t(ii)) perhaps suggesting that these vesicles were being directed to specific sites on the filopodia where glutactin and possibly actin is required. *In vivo* this would ensure that the dynamic filopodia would be covered in basal extracellular matrix affording protection from the larval haemolymph during development. A membrane bound vesicle would protect the glutactin from binding with other extracellular matrix proteins until it is required. Alternatively actin may be required in the propulsion of the vesicles to these sites. An interesting hypothesis for future experimentation is that the membrane vesicles which contain glutactin are also a mechanism for dispatching signalling molecules to specific sites (see Chapter 8).

7.4.4: After ecdysone

The microarray data suggests that glutactin was upregulated in the Young Clone 8+ cells after ecdysone. The presence of glutactin in the secreted vesicles in the surrounding extracellular space seems puzzling (figure 7t(i)). Why would a cell upregulate a protein and then partition it in vesicles? *In vivo* single, isolated, cells would not be present and we have to consider what changes are taking place during metamorphosis. During eversion of the *Drosophila* wing disc which occurs during metamorphosis in response to ecdysone, there is movement of the epithelial layers. The basement membrane breaks down and there is cell rearrangement, with the basal epithelium moving inwardly. Cell rearrangements would be accompanied by changes in cell-matrix adhesion. Extra glutactin may be required in order to afford flexibility of the basal lamina. The vesicles observed in the Clone 8+ cells after ecdysone may be transported to areas where extra glutactin is required. This would ensure the integrity of the extracellular matrix surrounding the disc during morphogenesis of the adult appendage and continuous protection from the degradative enzymes released in the haemolymph by the larval cells during metamorphosis.

Glutactin may also play a role post eversion. The extracellular matrix molecule, collagen IV, gradually diminishes and is not found in the wing margin after eversion (Murray et al., 1995). Evidence suggests that the circulating haemocytes are responsible for removing collagen IV (Nardi and Miklasz, 1989). Laminin however is found at the wing margin basement membrane after eversion. Glutactin which colocalises with laminin has been found throughout the embryo, staining the basement membrane of all internal organs (Olson et al., 1990). Glutactin may also play a role in the adult fly, as it may be present in the wing, possibly at the wing margin, after eversion. The

glutactin vesicles which were observed in the Young Clone 8+ after ecdysone are possibly awaiting relocation and placement at sites of requirement.

7.4.5: How do the cell line derivatives Clone 8R, Old Clone 8+ and ZfeClone 8+ differ from Young Clone 8+?

Although quantitative analysis was not carried out, visual observations indicated that the Clone 8R cell line cells appeared to express more cytoplasmic and secreted glutactin twenty-four hours and also five days after initiation when compared to the Young Clone 8+ cells. Although the reason for the upregulation of the gene *glutactin* in Clone 8R cannot be explained without further analysis, it is possible that regulatory control of protein production has been lost. Saturation of glutactin's binding partner would explain the apparent excess of secreted molecules. Changes in the Clone 8R cells after ecdysone compared to the Young Clone 8+ are evident from the data so far (Chapters 5 and 6). No change in the expression of glutactin was found after ecdysone in the microarray data analysis and this appeared to be the case based on observations. Glutactin was sequestered into vesicles after ecdysone in Young Clone 8+, these vesicles were never observed in the Clone 8R cells after ecdysone and treated cells continued to develop in the same way as untreated Clone 8R cells.

The hypothesis that the Old Clone 8+ cells were secreting excess glutactin which caused a lack of adhesion is false. Glutactin secretion was rarely observed in Old Clone 8+ cells. The role of glutactin in *Drosophila* wing disc epithelial cells may be to dictate the boundary between the developing wing disc and the larval haemolymph and facilitate the changes which take place in cell-matrix adhesion during imaginal disc morphogenesis. It is possible that loss of glutactin from the basal lamina prevents the Old Clone 8+ cells from

adhering to each other. Loss of cell-cell adhesion also leads to detachment of cells from the extracellular matrix and an increase in cell proliferation.

Observations on Old Clone 8+ cells (Chapter 5) indicate that although these cells associated at times they only appeared to be loosely associated and cells were mostly rounded in appearance.

Examination of the Old Clone 8+ and ZfeClone 8+ cells which were suspended in the medium revealed the presence of an abundance of glutactin in the cell cytoplasm five days after culture initiation. Glutactin enveloped some groups of elongate ZfeClone 8+ cells (figure 7s(ii)) and was secreted from some but not all Old Clone 8+ cells. F-actin was detected at various locations within the cell cytoplasm and colocalised with glutactin in some cells but not in other cells. Cell division was increased. From the description above it would appear that many different cell phenotypes are present in these cultures. Senescent cells are also known to acquire multiple phenotypic changes which can result in loss of adhesion and increased proliferation (Parrinello et al., 2005).

In many ZfeClone 8+ cells adhered to the substrate, substantial foci where glutactin and f-actin colocalised were observed. These foci were associated with membrane bound vesicles, which probably fulfill the same role as the ones observed in the Young Clone 8+ and Clone 8R which were found along filopodia. As the vesicles were still attached to the actin cytoskeleton in ZfeClone 8+ cells, this suggests that exocytosis had been disrupted (figures 7g(iii) 7u(iv)). A role for actin in endocytosis has previously been shown where treatment of cells with cytochalasin increased the number of vesicles which failed to pinch off from the apical surface back into the cells cytoplasm (Gottlieb et al., 1994). Disruption of the actin cytoskeleton during exocytosis of the glutactin and glutactin-actin vesicles may be responsible for lack of detachment of the vesicles from the apical surface of the ZfeClone 8+ cells.

In the Old Clone 8+ cells cytoplasmic glutactin did not colocalise with f-actin and secreted glutactin vesicles were rarely observed. This suggests that transportation of glutactin molecules via f-actin to the apical plasma membrane has been disrupted. Regulation of glutactin production most likely occurs via the integrins in their role as signalling receptors (Bökel and Brown, 2002). There is evidence that interactions between integrins and their ligands can regulate transcription (Giancotti and Ruoslahti, 1999; Miranti and Brugge, 2002). If the amount of glutactin required by the extracellular matrix is regulated by integrins then loss of glutactin interaction with the extracellular matrix and integrins could result in the increased transcription of the *glutactin* gene.

Transportation of vesicles to the plasma membrane and successful exocytosis require accessory proteins in the cytoplasm and at the apical membrane. Loss of these functions and disruption of the cytoskeleton may be associated with loss of cell polarity. Loss of cell polarity is also associated with an increase in cell proliferation and a loss of cell adhesion (Woods et al., 1997). Comparing the microarray data from the adhesive cell line Clone 8R with the Old Clone 8+ and ZfeClone 8+ may reveal other genes implicated in loss of cell polarity and cell adhesion. Further analysis of the microarray data is warranted and potential genes will be discussed in the following chapter.

Figures

Figure 7a(i): Y Cl.8+ cells 24 hours after initiation immunofluorescence, glutactin (green)

Immunofluorescent image showing the presence of glutactin located throughout the cell cytoplasm of single cells which presented a speckled appearance. The secreted vesicles were small, ovoid or rod shaped and had a brighter expression than the cytoplasmic glutactin.

cv, cytoplasmic glutactin vesicle; p, process; sv, secreted glutactin vesicle.

Figure 7a(i): YCl.8+ single cells 24 hours after initiation, immunofluorescence, glutactin (green)

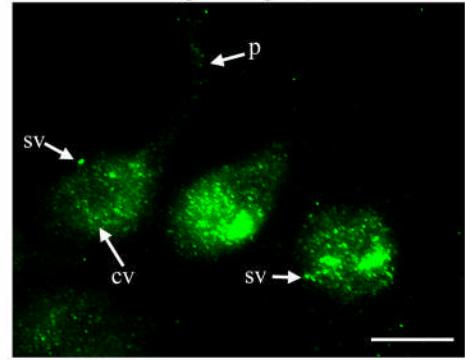


Figure 7a(ii): YCl.8+, 24 hours after initiation no ecdysone.

DIC image of the single Young Clone 8+ cells in cell cultures 24 hours after initiation. Long processes and shorter cell extensions are in evidence. There are vesicles associated with the round cell in this image. Areas where the cells appeared to have spread onto the substrate is flattened cell membrane (fm) or putative extracellular matrix.

e, extensions; fm flattened cell membrane ; p, process; v, vesicle of unknown origin.

Scale bar represents:10µm

Figure 7a(ii): YCl.8+ single cells, 24 hours after initiation no ecdysone.

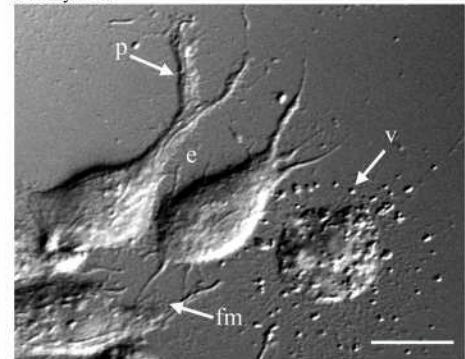


Figure 7b(i): Young Clone 8+, 24 hours after initiation, elongate cells

DIC image of Young Clone 8+ elongate cells, focused above the plane of coverslip. In this image the aggregation of cell bodies with long processes can be seen.

f, focal contact; n, nucleus; p, process; v; vesicle.

Scale bar represents:10µm

Figure 7b(i): YCl.8+ cells 24 hours after initiation, elongate cells

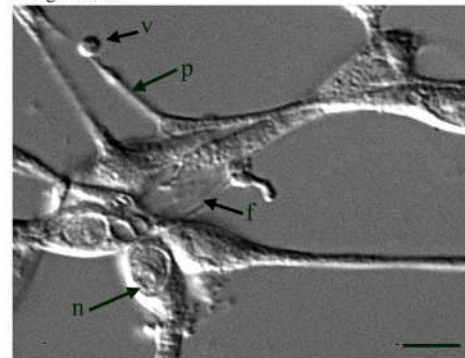


Figure 7b(ii): Immunofluorescence, glutactin green, DAPI blue

This immunofluorescent image of figure 7b(i) shows the secreted glutactin (pseudo green) closely associated with the long cell processes and surrounding the cell bodies. The nuclei have been stained with DAPI, and the cells were stained with anti-actin antibody (pseudo red).

sv, secreted glutactin vesicle

Scale bar represents:10µm

Figure 7b(ii): Immunofluorescence, glutactin (green), DAPI (blue)

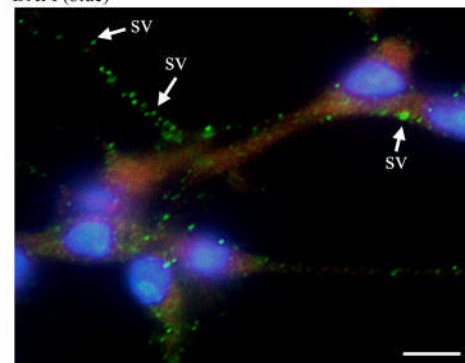


Figure 7c(i): Cl.8R cells 24 hours after initiation, no ecdysone

DIC image of Clone 8R cells 24 hours after initiation. In this image the Cell-matrix contact can be seen with the focal contact or putative extracellular matrix visible. fc, focal contact; n, nucleus p, process; v, vesicle
Scale bar represents:10µm

Figure 7c(i): Cl.8R cells 24 hours after initiation, no ecdysone

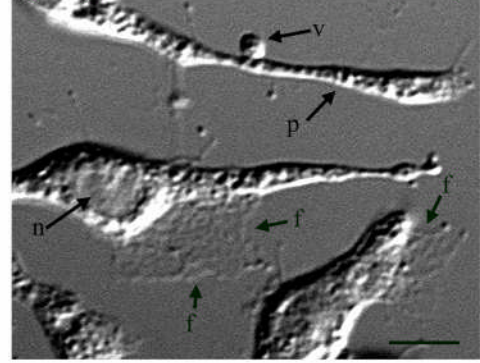


Figure 7c(ii): Immunofluorescence overlay, glutactin (green)

Immunofluorescence overlay showing glutactin secreted as a rod shaped vesicle and associating with the focal contact. In this image glutactin is also associated with a membrane bound vesicle along one of the cell processes. sv, secreted glutactin vesicle
Scale bar represents:10µm

Figure 7c(ii): Immunofluorescence overlay, glutactin (green)

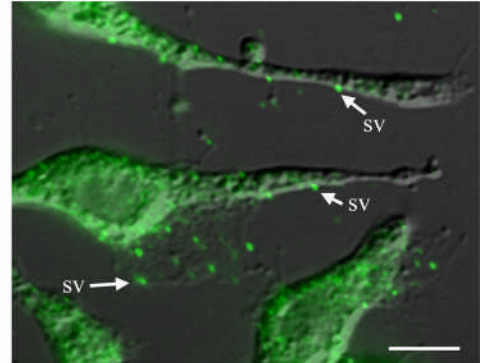


Figure 7d(i): YCl.8+ cells 24 hours after initiation

DIC image focused above the substrate to visualise the uppermost region of Young Clone 8+ cells. In this image vesicles were observed which were in close association at the uppermost membrane of the cell.
c, cell; v, vesicle
Scale bar represents:5µm

Figure 7d(i): YCl.8+ cells 24 hrs after initiation.

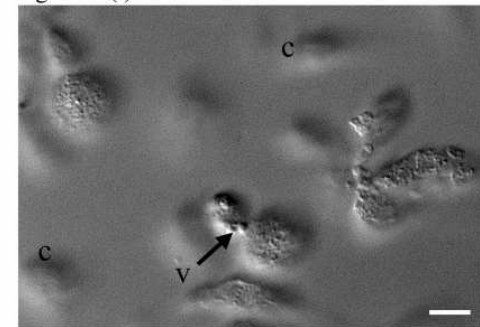


Figure 7d(ii): YCl.8+ cells DIC immunofluorescence overlay

This image shows the location of the secreted glutactin on the cell surface of the Young Clone 8+ cells.

g, glutactin
Scale bar represents:5µm

Figure 7d(ii):DIC immunofluorescence overlay, glutactin (green)

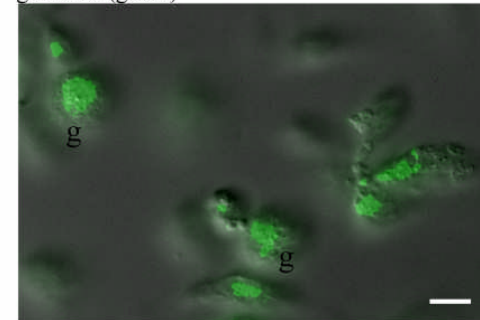


Figure 7d(iii): Immunofluorescence, glutactin green

Immunofluorescence showing glutactin which was secreted from the uppermost region of YCl.8+ and Cl.8R cells.

g, glutactin
Scale bar represents:5µm

Figure 7d(iii): Immunofluorescence, glutactin

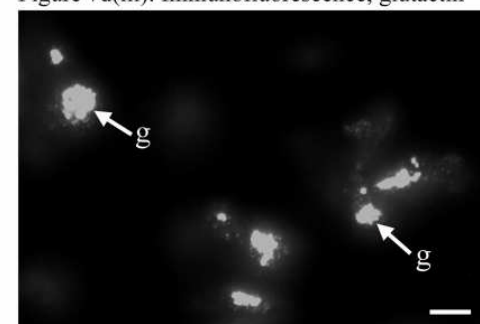


Figure 7e(i): Cl8R cells 24 hours after initiation.
 Immunofluorescence, glutactin (green).
 This immunofluorescent image shows the abundance of glutactin which was detected using anti-*Dm*-glutactin antibody in Cl8R cells
 sv, secreted glutactin
 Scale bar represents:10 μ m

Figure 7e(i): Cl8R cells 24 hours after initiation
 Immunofluorescence glutactin (green)

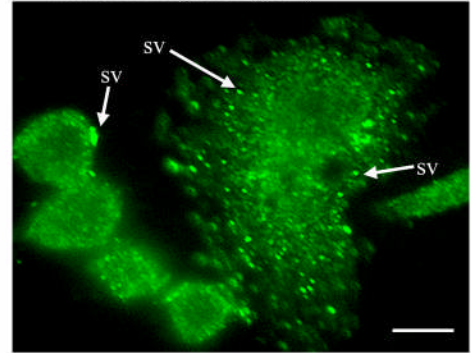


Figure 7e(ii): Cl8R cells 24 hours after initiation.
 Immunofluorescence α -tubulin (blue)
 An immunofluorescent image showing the microtubule cytoskeleton detected using anti α -tubulin in Cl8R cells.
 c, cytoskeleton
 Scale bar represents:10 μ m

Figure 7e(ii): Cl8R cells 24 hours after initiation
 Immunofluorescence α -tubulin (blue)

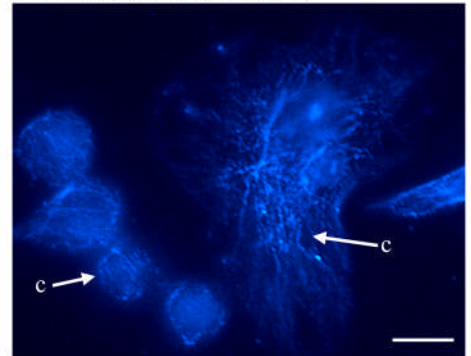


Figure 7e(iii): Cl8R cells 24 hours after initiation, no ecdysone
 DIC image of the flattened cell and round cells in figures 7e(i,ii). There appears to be an area of thin cell membrane (focal contact) surrounding the cell. The round cells have extended small processes.
 f, focal contact; n, nucleus; p, process
 Scale bar represents:10 μ m

Figure 7e(iii): Cl8R cells 24 hrs after initiation no ecdysone

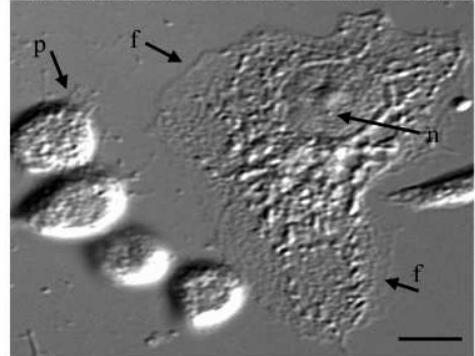


Figure 7e(iv): Cl8R cells 24 hours after initiation.
 Immunofluorescence α -tubulin (blue) glutactin (green)
 An overlay image of figures 7e(i,ii) showing glutactin and α -tubulin immunofluorescence. Colocalisation of glutactin and α -tubulin was not observed in these cells.
 In this image the amorphous extracellular matrix which has been stained with anti-*Dm*-glutactin antibody can clearly be seen between the round cells.
 g, glutactin; v, vesicles
 Scale bar represents:10 μ m

Figure 7e(iv): Cl8R cells 24 hours after initiation
 Immunofluorescence α -tubulin (blue) Glutactin (green)

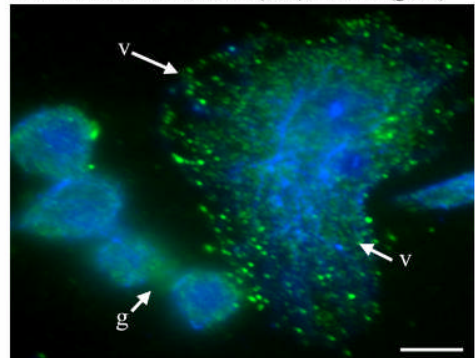


Figure 7f(i): Cl.8R 24 hours after initiation, immunofluorescence, glutactin (green), f-actin (red), α -tubulin (blue)

These Cl.8R cells were stained for glutactin, f-actin (phalloidin) and α -tubulin.

The f-actin was located in a discrete area at the uppermost region of the cell surrounding the nucleus. Cytoplasmic glutactin and f-actin colocalised as seen in the small round cell. The overlay of glutactin and f-actin immunofluorescent images produced areas of yellow and orange.

n, nucleus; m, microtubule cytoskeleton; s, secreted glutactin vesicle
Scale bar represents:5 μ m

Figure 7f(i): Cl.8R 24 hours after initiation, immunofluorescence, glutactin (green), f-actin (red), α -tubulin (blue)

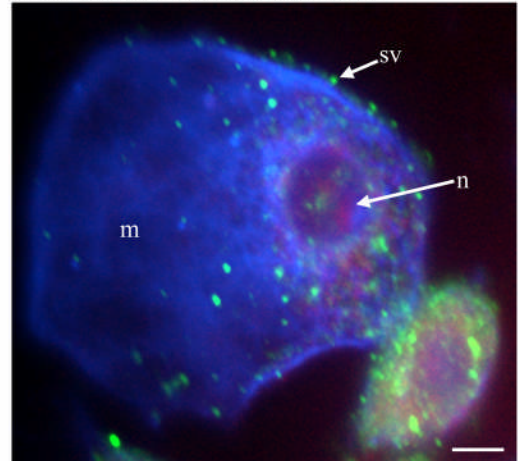


Figure 7f(ii): Immunofluorescence glutactin (green) f-actin (red)

Region of interest where the cytoplasmic glutactin and f-actin colocalised at the uppermost region of the cell close to the nucleus (overlay orange).

c, colocalisation; sg, secreted glutactin vesicle
Scale bar represents:5 μ m

Figure 7f(ii): Immunofluorescence glutactin (green) f-actin (red)

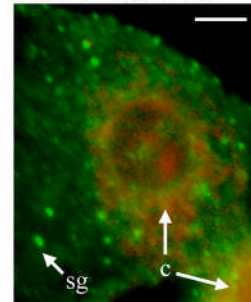


Figure 7g(i): ZfeCl.8 cells 24 hrs after initiation
 DIC image taken of the ZfeCl.8+ cells showing the vesicles which were closely associated with these cells. The vesicles are present at the uppermost region of the cells
 v, vesicles
 Scale bar represents:5µm

Figure 7g(i): ZfeCl.8 cells 24 hrs after initiation

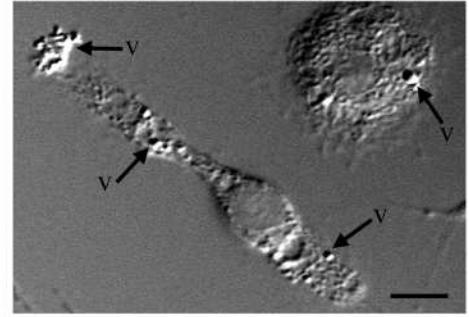


Figure 7g(ii): Immunofluorescence, glutactin
 Immunofluorescence of the ZfeCl.8+ showing glutactin staining. Glutactin was primarily located in discrete foci. Cytoplasmic glutactin appeared to be reduced in these cells when compared to the YCl.8+ and Cl.8R cells and no secreted glutactin was observed.
 g, glutactin
 Scale bar represents:5µm

Figure 7g(ii): Immunofluorescence, glutactin

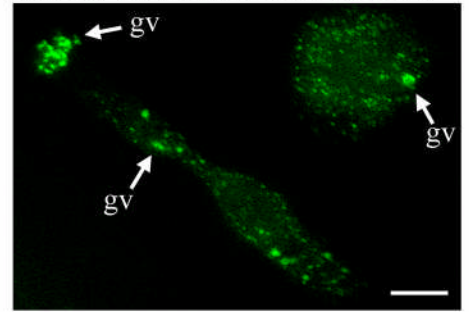


Figure 7g(iii):Immunofluorescence, glutactin (green), f-actin (red), DAPI (blue)
 Immunofluorescence of the ZfeCl.8 showing glutactin and f-actin staining. Glutactin and f-actin were colocalised in the foci. Colocalisation was incomplete as shown by the yellow and orange produced by the overlay of glutactin and f-actin staining. Areas of green, (glutactin) and red, (f-actin) were also present in the foci, shown in the close up, where glutactin was detected at one pole and f-actin at the other.
 a, f-actin; c, colocalisation; g, glutactin
 Scale bar represents:5µm

Figure 7g(iii):Immunofluorescence, glutactin (green), f-actin (red), DAPI (blue)

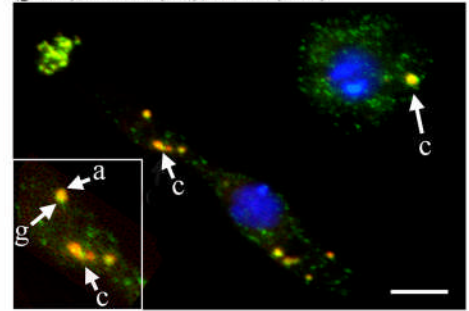


Figure 7h: Old Clone 8+ 24 hours after initiation, dividing cells, Immunofluorescence: glutactin (green), α-tubulin (red), DAPI (blue). α-tubulin was prominent in all round cells which had been fixed whilst undergoing mitosis. This image shows the number of cells undergoing cell division in one OCl.8+ and ZfeCl.8+ preparation. The midbody, mb, contains microtubules, (α-tubulin, red), and is present just prior to cleavage. DIC image of the cells undergoing cleavage shows the mid-body.
 g, glutactin; mb, midbody.
 Scale bar represents:10µm

Figure 7h: OCl.8+ 24 hours after initiation, dividing cells. Immunofluorescence: glutactin (green), α-tubulin (red), DAPI (blue).

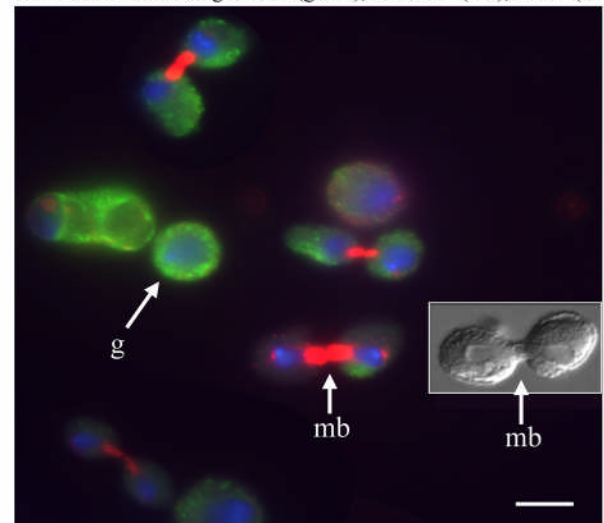


Figure 7i: Cl.8R 24 hours after initiation.

Immunofluorescence round cells, glutactin (green), f- actin (red), DAPI (blue)

Immunofluorescence overlay of glutactin (green), f-actin (red), DAPI (blue) of YCl8+ and Cl.8R cells which was taken above the plane of the substrate. Glutactin and f-actin were located at the uppermost region of these cells and f-actin was located close to the nucleus. Colocalisation of glutactin with f-actin was detected in the cytoplasm, (yellow).

c, colocalisation; g, glutactin; n, nucleus

Scale bar represents:5µm

Figure 7i: Cl.8R 24 hours after initiation
Immunofluorescence round cells, glutactin (green)
f-actin (red), DAPI (blue)

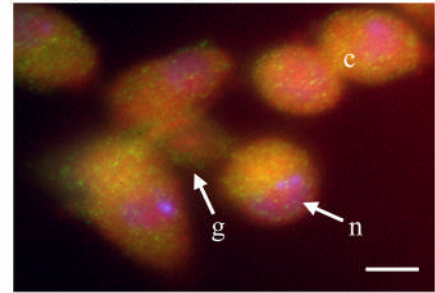


Figure 7j(i): OCl.8+ round cells, immunofluorescence glutactin (green), f-actin (red)

Immunofluorescence overlay of glutactin (green) and f-actin (red) expression in OCl.8+ round cells showing the distribution of glutactin in these cells. An abundance of cytoplasmic glutactin can be seen in some cells, f-actin was not detected in the cell cytoplasm in this image. F-actin was detected just beneath the plasma membrane and in processes which connected cells. Colocalisation of glutactin and f-actin can be seen at the plasma membrane (overlay, yellow). Secretion of glutactin vesicles can also be seen in this preparation.

a, f-actin; g, glutactin; v, vesicles

Scale bar represents:10µm

Figure 7j(i): OCl.8+ round cells,
Immunofluorescence glutactin (green),f-actin (red)

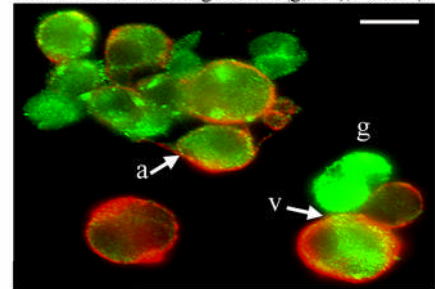


Figure 7j(ii): OCl.8+ round cells; Immunofluorescence, glutactin (green), f-actin (red)

Immunofluorescence overlay of glutactin (green) and f-actin (red) in OCl.8+ round cells showing the distribution of cytoplasmic f-actin in some cells. The presence of glutactin was not detected in all OCl.8+ round cells. In this image the cells are connected by what appear to be strands of f-actin (s). Glutactin is only present in one cell where it shows colocalisation with f-actin at the plasma membrane and secretion of vesicles.

a, f-actin; g, glutactin; s, strand

Scale bar represents:10µm

Figure 7j(ii): OCl.8+ round cells,
Immunofluorescence, glutactin (green), f-actin (red)

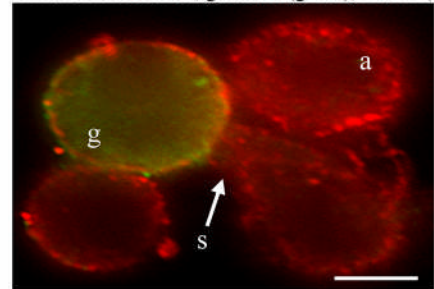


Figure 7k(i): OCI.8+, 24 hours, no ecdysone, cell processes

DIC of OCI.8+ cells which were connected by processes, (p). The processes can be seen between the cell-cell contacts and connecting groups of cells. The origin of the processes from either one cell or several cells cannot be determined.

p, processes

Scale bar represents:5µm

Figure 7k(i): OCI.8+, 24 hours, no ecdysone, cell processes

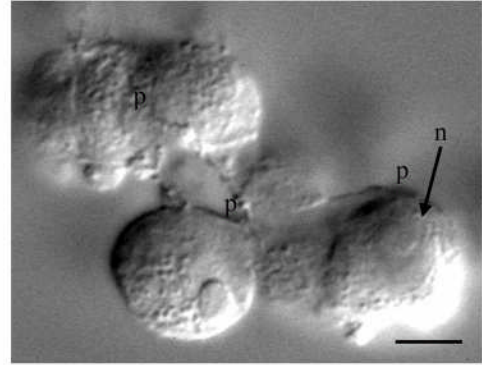


Figure 7k(ii): Immunofluorescence, glutactin (green), DAPI (blue)

Immunofluorescence overlay of glutactin (green) and DAPI (blue) the OCI.8+ cells which were connected by processes which stained for glutactin. Cytoplasmic glutactin is also evident in these cells. Visualisation of the cells by immunofluorescence was obscured by an amorphous layer which was possibly due to residue medium.

g, glutactin

Scale bar represents:5µm

Figure 7k(ii): Immunofluorescence, glutactin (green), DAPI (blue)

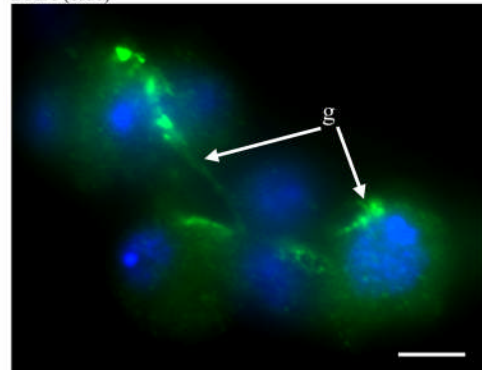


Figure 7m(i): Cl.8R 24 hours after initiation, long processes

DIC image showing the long, thick processes (filopodia) found in the Cl.8R cells. The processes were present at the uppermost region of these cells and appeared to emanate from single cells (c). In this image several processes converge to run through cell-cell points of contact, connecting the groups of cells.

c, cell; p, process

Scale bar represents:5µm

Figure 7m(i): Cl.8R 24 hours after initiation, long processes

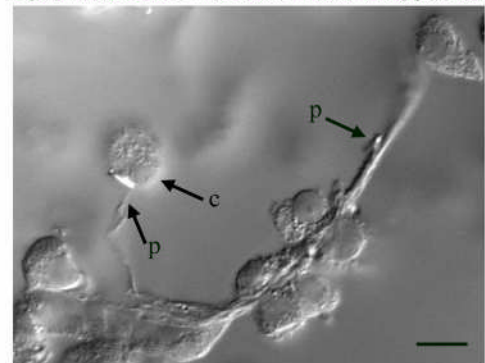


Figure 7m(ii): Immunofluorescence, glutactin (green), DAPI (blue)

Immunofluorescence overlay glutactin (green), DAPI (blue) of the cell processes in figure 7m(i). The processes stained intensely with the anti-glutactin antibody.

g, glutactin; p, process; v, secreted glutactin vesicles

Scale bar represents:5µm

Figure 7m(ii): Immunofluorescence, glutactin (green), DAPI (blue)

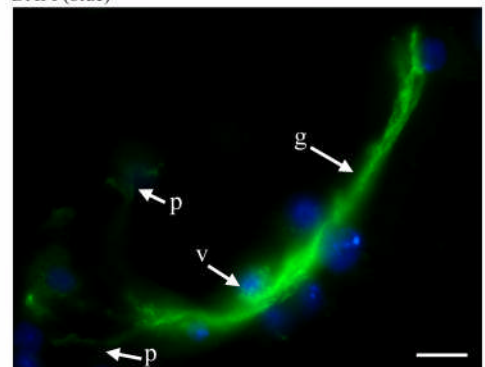


Figure 7n(i): YCl.8+ 24 hours, cell aggregation.
 DIC image of an aggregation of YCl.8+ cells. The cell appear to be surrounded by an extracellular matrix which surrounds and connects the cells
 ecm, extracellular matrix; n, nucleus
 Scale bar represents:10µm

Figure 7n(i) : YCl.8+ 24 hours after initiation, aggregation

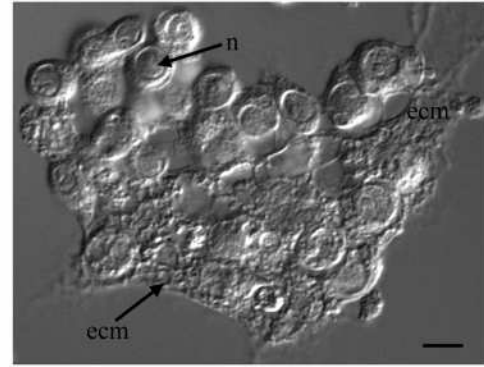


Figure 7n(i): Immunofluorescence, glutactin (green), f-actin(red)
 Immunofluorescence overlay glutactin (green) f-actin (red) of the YCl.8+ cells in figure 7n. Glutactin covered the YCl.8+ cells and was present as an amorphous deposit. In all the YCl.8+ cells glutactin colocalised with f-actin in the cytoplasm and around the cell membrane (yellow).
 Scale bar represents:10µm

Figure 7n(ii): Immunofluorescence, glutactin (green), f-actin (red)

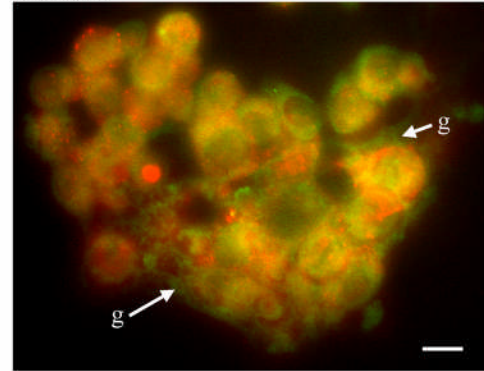


Figure 7p: YCl.8+ 24 hours after initiation, no ecdysone, long processes, glutactin (green)f-actin (red) DAPI (blue)
 Immunofluorescence overlay of an aggregate of YCl.8+ cells showing processes which connect cells to one another and which stained for f-actin. The image is taken just above the plane of the substrate and just below the cells uppermost region. Glutactin vesicles are evident and colocalisation of f-actin and glutactin in a large vesicle in the centre of this image (vc) can be seen.
 p, processes; vc, colocalisation of f-actin and glutactin; sv, secreted glutactin vesicle
 Scale bar represents:20µm

Figure 7p(i): YCl.8+ 24hours after initiation, no ecdysone, overlay long processes, glutactin (green) f-actin (red) DAPI (blue)

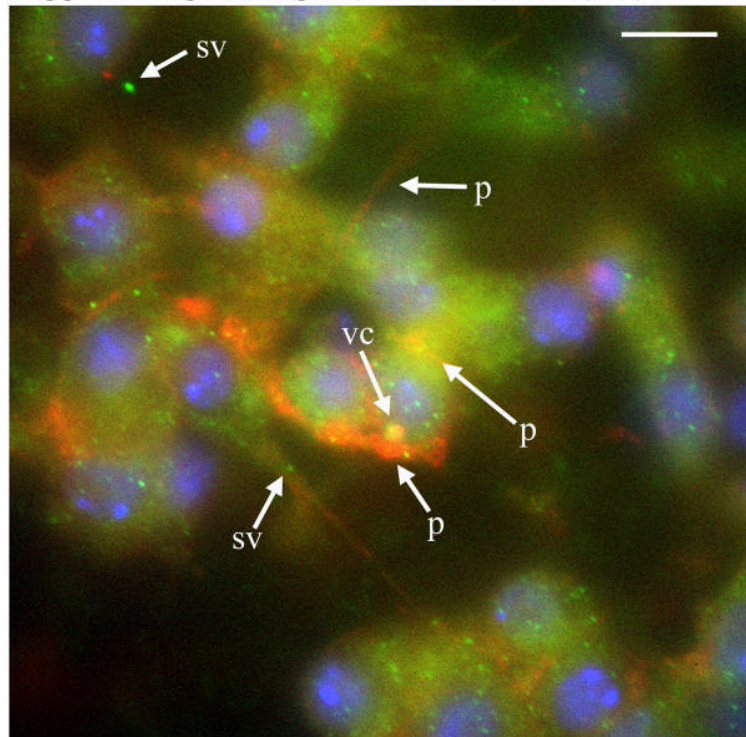


Figure 7q(i): YCl.8+ cells 5 days after initiation
 This DIC image shows the long processes which are found along the tops and between YCl.8+ cells. These processes were not present throughout the aggregates but in isolated areas.

p, process
 Scale bar represents 10µm

Figure 7q(i): YCl.8+ cells 5 days after initiation

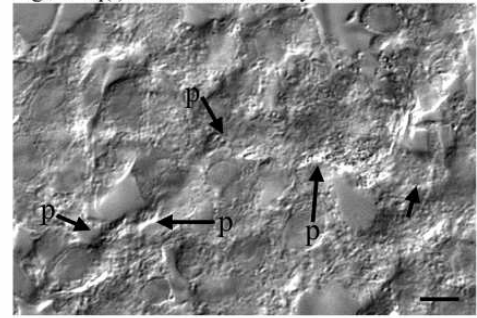


Figure 7q(ii): DIC and Immunofluorescence overlay glutactin (green)

This DIC and immunofluorescent overlay image of figure 7q(i) shows the localisation of glutactin particularly surrounding the processes. Cytoplasmic and secreted glutactin were also evident in these YCl.8+ cells

g, glutactin; p, process
 Scale bar represents 10µm

Figure 7q(ii): DIC-Immunofluorescence overlay glutactin (green)

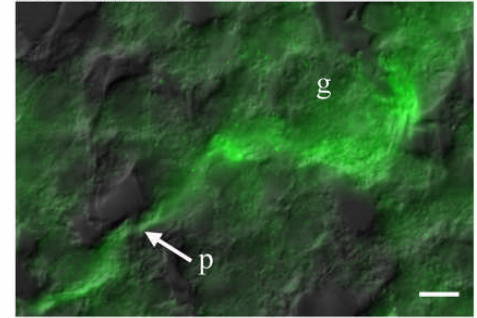


Figure 7q(iii): Immunofluorescence, glutactin (green), f-actin (red), DAPI, (blue)

Immunofluorescent overlay image of the YCl.8+ cells from figure 7q(i) showing the expression of glutactin, f-actin, and nuclear DAPI. The glutactin and f-actin colocalise along the process or processes (yellow).

p, process; a, f-actin
 Scale bar represents:10µm

Figure 7q(iii): Immunofluorescence, glutactin (green), f-actin (red), DAPI, (blue)

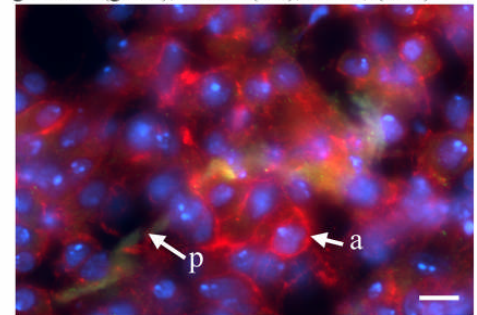


Figure 7r(i) : Cl.8R 5 days, no ecdysone
 Immunofluorescence glutactin (green), f-actin (red), DAPI, (blue)

Immunofluorescent image of Cl.8R cells 5 days after initiation. Secretion of glutactin appeared to be in excess when compared to the YCl.8+ cells at the same stage. The majority of these cells appear to be pentagonal in morphology when visualised with f-actin.

a, f-actin, g, glutactin
 Scale bar represents:10µm

Figure 7r(i) : Cl.8R 5 days, no ecdysone Immunofluorescence glutactin (green), f-actin (red), DAPI (blue)

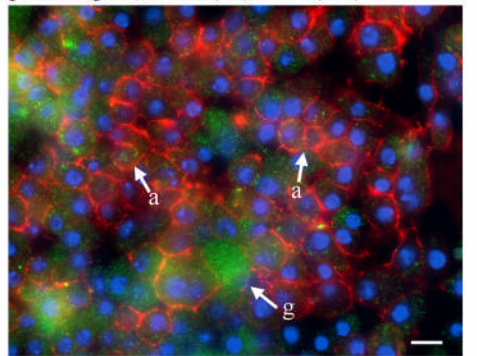


Figure 7r(ii) : Immunofluorescence glutactin, (green) f-actin, (red) DAPI (blue) This close up image of figure 7r(i) shows the secretion of glutactin vesicles in the Cl8R cells which are beginning to cover the top of a single cell. v, glutactin vesicles.

Scale bar represents:5µm

Figure 7r(ii): Immunofluorescence, glutactin (green) f-actin (red), DAPI (blue)

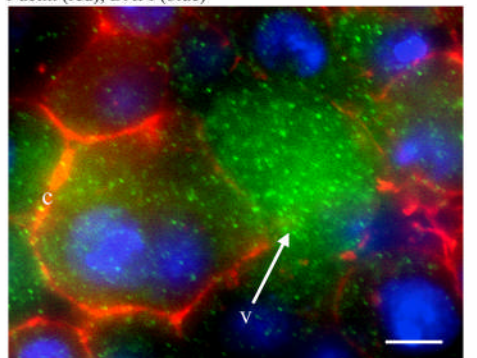


Figure 7s(i): ZfeClone8+ 5 days, suspended cells, no ecdysone

DIC image showing an aggregate of ZfeClone8+ cells which had been suspended in the medium. The majority of cells have an elongate morphology with few round cells in evidence. Processes can also be seen which connect the cells and the cells appear to be covered with extracellular material.

ecm, extracellular matrix, p, process

Scale bar represents:10µm

Figure 7s(i): ZfeCl.8 5 days, suspended cells, no ecdysone

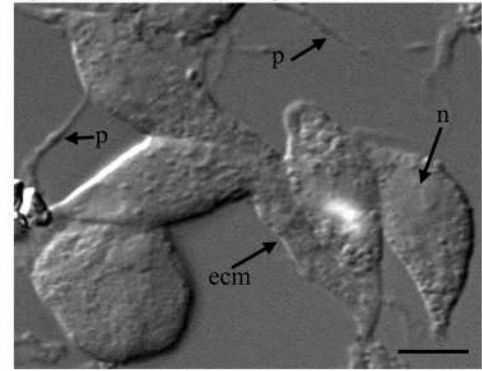


Figure 7s(ii): Immunofluorescence, glutactin (green), f-actin (red), α -tubulin (blue).

The immunofluorescence image overlay of the cells in figure 7s(i) shows glutactin completely surrounding the ZfeCl.8+ cells. Colocalisation of glutactin with f-actin or α -tubulin cannot be seen. The f-actin appears to be located in the cell cytoplasm where it colocalises with α -tubulin. α -tubulin was detected in some cell processes. High background staining of glutactin can also be seen which is probably due to fixation of residue medium.

α , α -tubulin, b, background, c, colocalisation (α -tubulin and f-actin)

g, glutactin

Scale bar represents:10µm

Figure 7s(ii): Immunofluorescence, glutactin (green), f-actin (red), α -tubulin (blue)

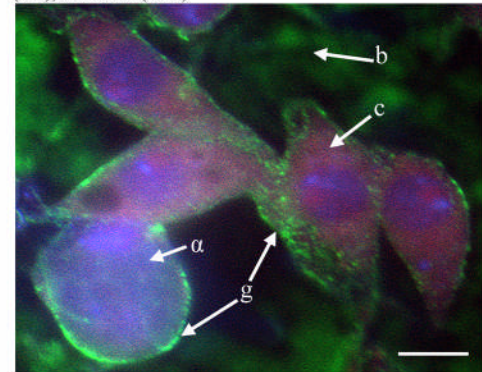


Figure 7t(i): YCl.8+ 24 hours after ecdysone

This DIC image shows membrane bound vesicles which were present in the extracellular space and fixed to the coverslip in YCl.8+ preparations. Membrane bound vesicles can also be seen in close association with the YCl.8+ cells.

v, vesicles

Scale bar represents:10µm

Figure 7t(i): YCl.8+ 24 hours after ecdysone

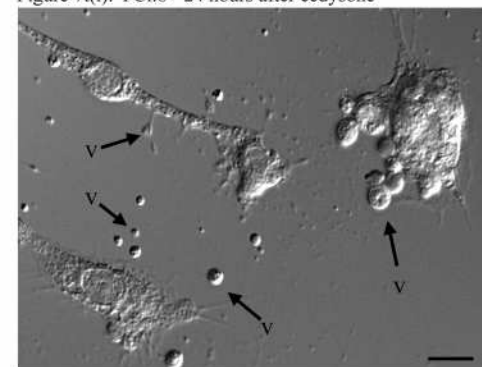


Figure 7t(ii): YCl.8+ 24 hours after ecdysone, DIC and Immunofluorescence, glutactin (green), f-actin (red)

A close up of the cells in figure 7t(i) both the DIC image and the immunofluorescence show a vesicle which appears to be on a cytoplasmic stalk. The vesicle stains for glutactin and f-actin where colocalisation is observed (yellow). Secreted glutactin can also be seen in the background.

c, colocalisation; s, stalk; v, vesicles

Scale bar represents:5µm

Figure 7t(ii): YCl.8+ 24 hours after ecdysone, DIC and Immunofluorescence, glutactin (green), f-actin (red)

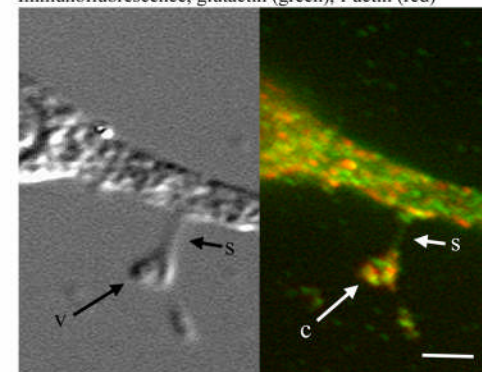


Figure 7t(iii): DIC and Immunofluorescence overlay, glutactin (green), f-actin (red), DAPI (blue)

These DIC and immunofluorescence images show the membrane bound vesicles located in the extracellular space surrounding the YCl.8+ cells. Glutactin and f-actin can be detected in these vesicles, and colocalisation is evident. In this preparation one vesicle appeared to be on a cytoplasmic stalk (v).

c, colocalisation; v, vesicle; s, stalk

Scale bar represents:5µm

Figure 7t(iii): DIC & Immunofluorescence overlay, glutactin (green), f-actin (red), DAPI (blue)

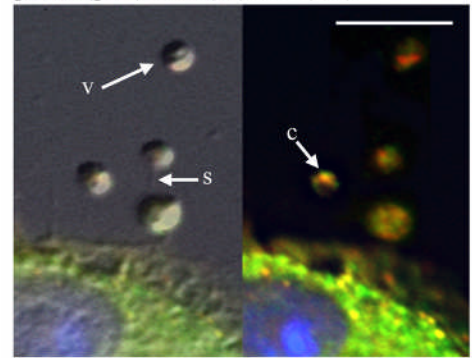


Figure 7t(iv): DIC, Immunofluorescence, glutactin (green), f-actin (red), DAPI (blue)

These DIC and Immunofluorescent images show the larger membrane bound vesicles which were closely associated with the YCl.8+ cells. Membrane bound vesicles which mainly stained for glutactin, (green) can be seen along the processes which stained for glutactin and f-actin (yellow).

g, glutactin, p, process, v, vesicle

Scale bar represents:5µm

Figure 7t(iv): DIC, Immunofluorescence, glutactin (green), f-actin (red), DAPI (blue)

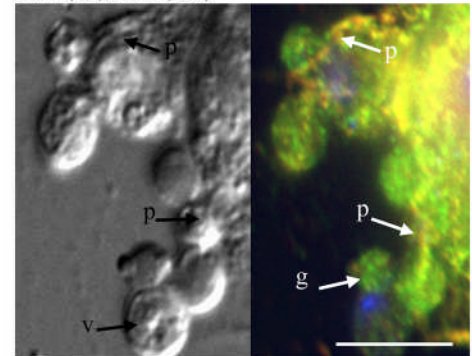


Figure 7u(i): ZfeCl.8+ cells 24 hours after ecdysone
DIC image showing the vesicles which were detected within the cell cytoplasm and as secreted vesicles in close association with the cell membrane in ZfeCl.8+ cells. Two of the cells in this image appear binucleate. The image has been taken just above the plane of the substrate. A small vesicle appears to be in the extracellular space (arrow, v).

n, nucleus; v, vesicle

Scale bar represents:10µm

Figure 7u(i): ZfeCl.8 cells 24 hours after ecdysone

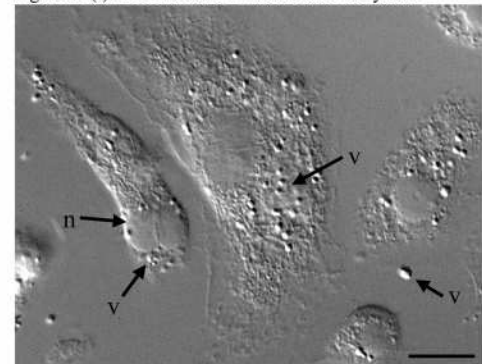


Figure 7u (ii): Immunofluorescence, overlay, glutactin (green), f-actin (red), DAPI (blue)

Immunofluorescent image of the cells in figure 7u(i) which shows the colocalisation of f-actin and glutactin in the vesicles (yellow). Some vesicles stained exclusively for glutactin (green) or f-actin (red). Many vesicles appear to be associated with the actin cytoskeleton.

a, f-actin; v, vesicles

Scale bar represents:10µm

Figure 7u (ii): Immunofluorescence, overlay, glutactin (green), f-actin (red), DAPI (blue)

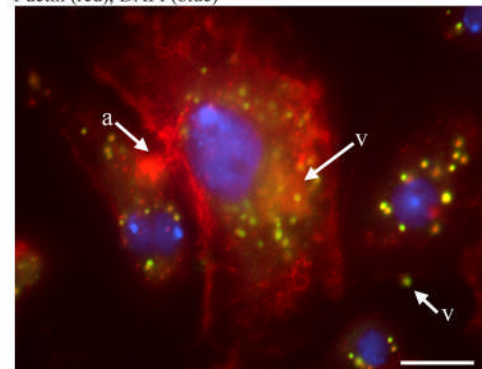


Figure 7u (iii): ZfeCl.8+ cells after ecdysone, Vesicle
 DIC close up of the vesicle in figure 7u(ii) which appears to be fixed to the coverslip in this preparation of ZfeCl.8+ cells.

v, vesicle

Scale bar represents:5µm

Figure 7u (iii): ZfeCl.8 cells after ecdysone, Vesicle

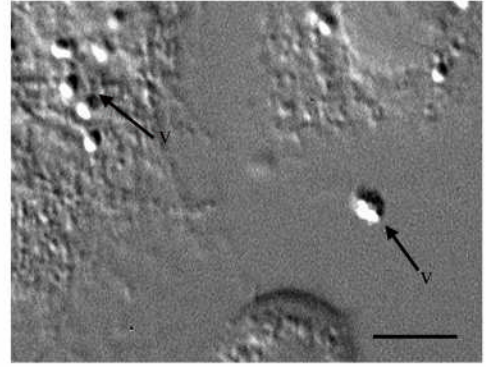


Figure 7u (iv): Immunofluorescence, vesicle, glutactin (green) f-actin (red), DAPI (blue)

This immunofluorescent overlay of the DIC image in figure 7u(iii) shows that f-actin and glutactin were detected in the vesicle and appears to be in close associated with the cell membrane.

a, f-actin; v, vesicle

Scale bar represents:5µm

Figure 7u (iv): Immunofluorescence, vesicle, glutactin (green) f-actin (red), DAPI (blue)

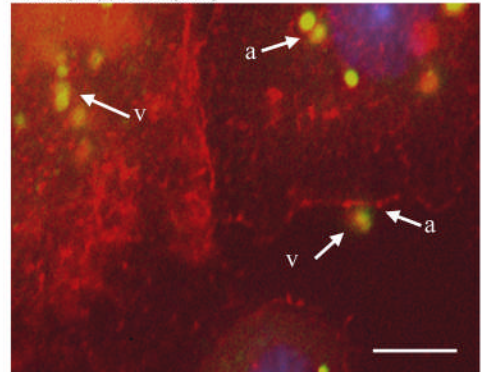


Figure 7v(i): OCI.8+ 24 hours after ecdysone

DIC image showing a OCI.8+ rounded cell after ecdysone. In all the fixed preparations these cells had sustained damaged. The contents of the OCI.8+ cells were extruded onto the substrate.

c, cytoplasm; n, nucleus

Scale bar represents:5µm

Figure 7v(i): OCI.8+ 24 hours after ecdysone

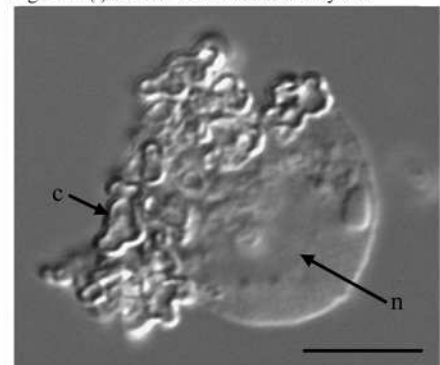


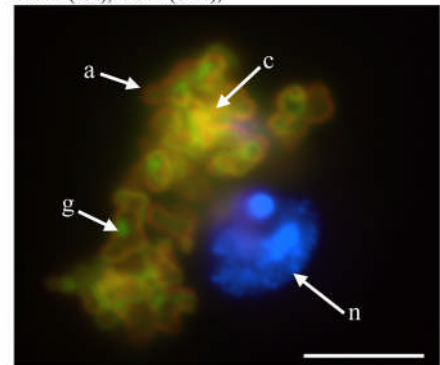
Figure 7v(ii): Immunofluorescence, glutactin (green) f-actin (red) DAPI (blue)

Immunofluorescence image overlay of figure 7v(i) showing the expression of glutactin and f-actin in the damaged OCI.8+ cells. The cytoplasmic contents stained intensely for both glutactin and f-actin. Colocalisation is evident (yellow) and areas of glutactin were present surrounded by glutactin and f-actin.

a, f-actin, c, colocalisation, g, glutactin, n, nucleus

Scale bar represents:5µm

Figure 7v(ii): Immunofluorescence, glutactin (green), f-actin (red), DAPI (blue),



Chapter 8

Cell polarity in Clone 8+ cell lines

8.1: Introduction

Successful morphogenesis is dependant on the generation and maintenance of polarised cells and tissue. Epithelial cells are polarised along an apical-basal axis in simple monolayered epithelium such as the wing disc (Drubin and Nelson, 1996). Successful polarisation of an epithelial cell depends on the placement and maintenance of proteins to the appropriate location within these domains. In addition the association of the cytoskeleton with the cell membrane is integral in maintaining cell polarity. Genes associated with apical membrane identity in *Drosophila* epithelial cells have been identified and include *Discs Lost (Dl)* and *crumbs* (Bhat et al., 1999; Tepass et al., 1990). In *Drosophila* embryos the protein scribble acts to confine apical membrane determinants (Bilder and Perrimon, 2000). Loss of scribble results in small round cells that detach from each other and lose contact with the underlying layer (Bilder and Perrimon, 2000).

The plasma membrane around the cell is separated into two distinct domains, an apical domain and a baso-lateral domain. Septate and zonula adherens junctions are located at sites of cell-cell contact on the baso-lateral membrane (Müller, 2000). In *Drosophila* epithelial cells the zonula adherens is located nearer the apical membrane and the septate junction is located closer to the lateral plasma membrane. The zonula adherens consists of transmembrane cadherins and associated proteins, such as armadillo and Drac1, which function to anchor the actin cytoskeleton (Pai et al., 1996). Neuroglian, which is a component of the septate junctions, is involved in the apicolateral distribution of the plasma membrane proteins neurexin IV and contactin (Faivre-Sarrailh et al., 2004). The protein Discs-large is associated with the septate junctions where it is required for restricting the Baz/Par3–Par6–aPKC

complex to the apical membrane domain (Bryant et al., 1993; Bilder and Perrimon, 2000; Rolls et al., 2003). Mutations in *Discs-large (Dlg)* lead to a loss of apico-basal polarity and the formation of septate junctions is compromised (Woods et al., 1996). The association of the cytoskeleton with the basal membrane and extracellular matrix is mediated by integrins via focal adhesion complexes (Brown et al., 2000). Vinculin, found at cell-cell and cell-matrix complexes induces actin polymerisation by recruiting the Arp2/3 complex (DeMali et al., 2002). Mutations in the *Arp 2/3* genes cause defects in the cortical actin cytoskeleton (Hudson and Cooley, 2002).

Antibody staining of ZfeClone 8+ cells with anti-*Drosophila* -glutactin antibody revealed the majority of these cells did not secrete glutactin. Membrane vesicles appeared to be attached to the actin cytoskeleton. Old Clone 8+ and ZfeClone 8+ round cells suspended in medium did not appear to secrete glutactin and the location of actin within the cell was variable. These results suggest that vesicular transport, exocytosis and the cytoskeleton have been perturbed. It is proposed that a loss of cell polarity may have occurred, affecting cell adhesion and proliferation in the Old Clone 8+ and ZfeClone 8+ cells. Therefore the aim of this chapter is further analysis of the microarray data in order to elucidate candidate genes which affect cell polarity and adhesion.

8.2: Materials and Methods

In order to identify potential genes of significance and to include data which was not analysed statistically by the software **SAM** (Significant Analysis of Microarrays) further analysis of the microarray data was undertaken. The relative increase or decrease in gene expression observed in two or more

replicates was taken as an indication of the significance of a gene (Butler et al., 2003). Small increases or decreases in the expression of a protein may have a significant effect on a cell. The relative representation of a gene in the sample presented as a ratio reported as at least 0.5 increased or decreased in the normalised data was used in order to reduce the amount of data to be searched for genes of interest. Expansion of the search and further analysis of the data would be undertaken later. All microarray data files were sorted according to changes in gene expression in an Excel spreadsheet. Genes of significance were removed into separate Excel data files, leaving the original data unchanged.

8.2.1: Genes of interest

The FlyBase data base (<http://flybase.bio.indiana>) was searched for genes of interest relating to cell adhesion, the cytoskeleton, wing disc development and age. Over 1,000 genes were identified and compared to the Clone 8+ cells in order to identify potential differences in the OCl.8+, ZfeCl.8+ and Cl.8R cells when compared to the YCl.8+ cells.

Tables of the genes of interest were constructed with the predicted gene product role and location for each Clone 8+ cell line as in chapter 6. Tables comparing genes of interest were then constructed and the original microarray data was used to examine differential gene expression. In this way genes of interest which were upregulated or downregulated in the OCl.8+ and ZfeCl.8+ cells could be compared with the Cl.8R cells where loss of adhesion was not observed. In the following results section differential gene expression analysed in the Excel spread sheets has been reported as upregulation or downregulation (Beckstead et al., 2005). This does not necessarily mean that the proteins encoded by the genes have been expressed by the Clone 8+ cells.

8.3: Results

8.3.1: Young Clone 8+ hybridised with Old Clone 8+ (table 8.1a,1b).

362 genes were identified as upregulated in OCl.8+ cells compared to YCl.8+ cells. 53 genes of interest were identified as upregulated, 15 of which were upregulated 1.5 fold or more. 285 genes were identified as downregulated in OCl.8+ cells compared to YCl.8+ cells. 24 genes of interest were identified as downregulated only 2 were identified as being downregulated 1.5 fold or more. Genes identified included *dispatched (disp)* which encodes a membrane protein involved with exocytosis, the protein dispatched is expressed in the *Drosophila* wing disc.

8.3.2: Old Clone 8+ cells hybridised with ZfeClone 8+ cells (table 8.2a,2b).

103 genes were identified as upregulated in ZfeCl.8+ cells when compared to OCl.8+ cells. 31 genes of interest were identified, 9 were upregulated 1.5-fold or more. Genes identified included *Ank2* which encodes for a cytoskeletal anchoring protein located in the plasma membrane. 199 genes were identified as downregulated in ZfeCl.8+ cells when compared to OCl.8+ cells. 18 genes of interest were identified, 9 of these were downregulated 1.5-fold or more. Genes of interest included *Frizzled (fz)* a planar polarity gene which encodes a receptor molecule and has a role in epithelial cell polarity.

8.3.3: Young Clone 8+ hybridised with Clone 8R (table 8.3a,3b).

A total of 115 genes were identified as upregulated in Cl.8R cells when compared to YCl.8+ cells. 27 genes of interest were identified, 10 of these

genes were upregulated 1.5 fold and more including *scab* (*scb*) which encodes a calcium dependant cell adhesion receptor associated with focal adhesion. 123 genes were identified as downregulated in Cl.8R cells when compared to YCl.8+ cells. 21 genes of interest were identified, 8 of these were downregulated 1.5 fold or more.

8.3.4: Young Clone 8+ hybridised with Young Clone 8+ after ecdysone (data not shown see appendix, table 8.4a,4b).

117 genes were identified as upregulated in YCl.8+ cells after ecdysone when compared to YCl.8+ cells no ecdysone. 29 genes of interest were identified, 6 were upregulated 1.5-fold or more. 468 genes were identified as downregulated in YCl.8+ cells after ecdysone when compared to YCl.8+ cells no ecdysone. 34 genes of interest were identified, 5 were downregulated 1.5 - fold or more.

8.3.5: Old Clone 8+ hybridised with Old Clone 8+ after ecdysone (data not shown see appendix, table 8.5a,5b).

126 genes were identified as upregulated in OCl.8+ after ecdysone when compared to OCl.8+cells no ecdysone. 46 genes of interest were identified, 13 of which were upregulated 1.5-fold or more. 180 genes were identified as downregulated in OCl.8+ after ecdysone when compared to OCl.8+ cells no ecdysone. 17 genes of interest were identified with 3 genes downregulated more than 1.5-fold.

8.3.6: ZfeClone 8+ hybridised with ZfeClone 8+ after ecdysone (data not shown see appendix, table 8.6a,6b).

352 genes were identified as upregulated in ZfeCl.8+ cells after ecdysone when compared to ZfeCl.8+ cells no ecdysone. 55 genes of interest were identified, 17 of which were upregulated 1.5-fold or more. 306 genes were identified as downregulated in ZfeCl.8+ cells after ecdysone when compared to ZfeCl.8+ cells no ecdysone. 26 genes of interest were identified, 5 genes were downregulated greater than 1.5-fold.

8.3.7: Clone 8R hybridised with Clone 8R after ecdysone (data not shown see appendix, table 8.7a,7b).

351 genes were identified as upregulated in Cl.8R cells after ecdysone when compared to Cl.8R cells no ecdysone. 39 genes of interest were identified, 13 were upregulated 1.5-fold or more. 67 genes were identified as downregulated in Cl.8R cells after ecdysone when compared to Cl.8R cells no ecdysone. 7 genes of interest were identified, no genes were downregulated greater than 1.5-fold.

8.3.8: Young Clone 8+cells after ecdysone hybridised with Old Clone 8+ cells after ecdysone (data not shown see appendix, table 8.8a,8b).

603 genes were identified as upregulated in OCl.8+ cells after ecdysone when compared to YCl.8+ after ecdysone. 78 genes of interest were identified as upregulated in OCl.8+ cells after ecdysone when compared to YCl.8+ cells after ecdysone, 41 of which were upregulated 1.5-fold or more. 211 genes were identified as downregulated in OCl.8+ cells after ecdysone when

compared to YCl.8+ cells after ecdysone. 25 genes of interest were identified, 9 of which were downregulated 1.5-fold or more.

8.3.9: Old Clone 8+ after ecdysone hybridised with ZfeClone 8+ after ecdysone (data not shown see appendix, table 8.9a,9b).

168 genes were identified as upregulated in ZfeCl.8+ cells after ecdysone when compared to OCl.8+ cells after ecdysone. 28 genes of interest were identified, 5 were upregulated 1.5-fold or more. 351 genes were identified as downregulated in ZfeCl.8+ cells after ecdysone when compared to OCl.8+ cells after ecdysone. 45 genes of interest were identified, 11 were downregulated 1.5-fold or more.

8.3.10: Young Clone 8+ after ecdysone hybridised with Clone 8R after ecdysone (data not shown see appendix, table 8.10a,10b).

133 genes were identified as upregulated in Cl.8R cells after ecdysone when compared to YCl.8+ cells after ecdysone. 26 genes of interest were identified, 12 of which were upregulated 1.5-fold or more. 179 genes were identified as downregulated in Cl.8R cells after ecdysone when compared to YCl.8+ cells after ecdysone. 32 genes of interest were identified, 14 were upregulated 1.5-fold or more.

Comparison of the genes of interest in Old Clone 8+, ZfeClone 8+ and Clone 8R cells

8.3.11: Decreased expression in Old Clone 8+ cells (table 8.11a,11b)

32 genes of interest were identified as downregulated in OCl.8+ cells when

compared to YCl.8+ cells. *CG14991*, *CG6805* and *fz* were downregulated in OCl.8+ cells and ZfeCl.8+ cells and upregulated in Cl.8R cells when compared to YCl.8+ cells. *Chit2* and *disp* were downregulated in ZfeCl.8+ cells when compared to OCl.8+ cells with no change in expression found in Cl.8R cells when compared to YCl.8+ cells. 8 genes which were downregulated in OCl.8+ cells had an unknown outcome in ZfeCl.8+ or Cl.8R cells (table 8.11b).

8.3.12: No change in expression in Old Clone 8+ when compared to Young Clone 8+ cells (table 8.12).

14 genes of interest were identified which had no change in gene expression in the OCl.8+ cells when compared to YCl.8+ cells. 3 of these genes *CG7635*, *Chit* and *Idgf2* were also identified as having no change in ZfeCl.8+ cells when compared to the OCl.8+ cells. 7 genes were upregulated and 4 genes were downregulated in ZfeCl.8+ cells when compared to the OCl.8+ cells. 3 genes were differentially expressed in all 3 cell lines, *Idgf1*, *mask* and *phl*. 1 gene, *Trxr-1*, was upregulated in ZfeCl.8+ with no change in expression in OCl.8+ or Cl.8R.

8.3.13: Positive change in expression in Old Clone 8+ cells when compared to Young Clone 8+ cells (tables 8.13a,b,c).

28 genes of interest were identified which were upregulated in all the cell lines, OCl.8+, ZfeCl.8+ and Cl.8R when compared to YCl.8+ cells (table 8.13a). 20 genes of interest were identified which were upregulated in the OCl.8+ and differentially expressed in ZfeCl.8+ and Cl.8R cells when compared to YCl.8+ cells (table 8.13b). 6 genes were upregulated in OCl.8+ and downregulated in ZfeCl.8+ and Cl.8R cells. 3 genes were upregulated in OCl.8+ and ZfeCl.8+ cells, with no change in expression in Cl.8R. 2 genes were upregulated in

OCl.8+ with no change in the Cl.8R cells or the ZfeCl.8+ when compared to the OCl.8+ cells. 30 genes of interest were identified where the microarray data was ambiguous or not available in all three cell lines (see appendix table 8.13c).

8.4: Discussion

In Chapter 7 it was proposed that the Old Clone 8+ and ZfeClone 8+ cells had lost cell polarity. The establishment of epithelial polarity relies on the placement of proteins required to assemble adhesion complexes at the appropriate location around the cell membrane. Adhesion complexes are made up of proteins which interact with each other linking the cytoskeleton to the extracellular matrix and maintaining cell-cell adhesion. As so many genes were differentially expressed in the Clone 8+ cell lines searching the microarray data for individual genes and examining their expression would have been like looking for the proverbial needle in a haystack. By identifying genes of interest which are associated with cell adhesion and imposing a threshold of a ratio reported as at least 0.5 increased or decreased in two or more replicates, further analysis of the microarray data has revealed genes which are potential candidates for the loss of adhesion in Old Clone 8+ cells.

The genes of most interest are those which are differentially expressed in the Old Clone 8+, ZfeClone 8+ cells and Clone 8R cells. 6 genes were upregulated in the Old Clone 8+ cell line *CG6933*, *Hsp23*, *Hsp26*, *Hsp27*, *poe*, and *Su(var)205* and downregulated in the ZfeClone 8+ cells and Clone 8R cells (table 8.13b). 5 genes were upregulated in both the Old Clone 8+ and the ZfeClone 8+ cell line. However as it is more difficult to interpret the affect that the upregulation of a gene and protein would have on the cells this discussion

will concentrate on the downregulation of genes in the Old Clone 8+ cells. The genes of most interest therefore are those which are downregulated in the Old Clone 8+ and ZfeClone 8+ cells and upregulated or have no change in expression in the Clone 8R cells (table 8.11a). Five genes have been identified which have these characteristics. *CG14991*, *CG6805* and *frizzled* were all downregulated in Old Clone 8+ and ZfeClone 8+ and upregulated in Clone 8R when compared to Young Clone 8+ cells. *Chitinase 2* and *dispatched (disp)* were downregulated in Old Clone 8+ cells and ZfeClone 8+ cells with no change in expression in Clone 8R cells. As there is little data on *Chitinase 2* and *CG6805* only *CG14991*, *frizzled* and *dispatched* will be discussed further.

8.4.1: Genes downregulated in the Old Clone 8+ cells

Frizzled (Fz) is a planar polarity gene. Planar polarity specifies polarity orthogonal to the apical basal axis in wing disc epithelium. The protein frizzled acts through the Frizzled/Dishevelled (dsh) Planar Cell Polarity (PCP) pathway controlling cell polarity decisions (McEwen and Peifer, 2000; Jenny et al., 2005). As a planar polarity protein frizzled is required in order to specify the correct orientation and placement of wing hairs (trichomes) and thoracic bristles (Choi and Benzer, 1994; Shulman et al., 1998). Loss of planar polarity genes in the wing can cause misorientation of trichomes, or multiple multiple trichomes to form in a single cell (Fanto and McNeill, 2004).

During the establishment of planar polarity, frizzled is distributed around the circumference of the wing cell membrane, located at the distal edge of the cell (Fanto and McNeill, 2004). Proteins associated with planar polarity are also recruited to the apical membrane and assembly of these proteins relies on frizzled, dishevelled and an association with the transmembrane protein strabismus (Bastock et al., 2003; Fanto and McNeill, 2004). In the absence of

strabismus, dishevelled and prickle are mislocalised within the cell. Once polarity becomes established frizzled relocates to the distal edge of the cell (Strutt, 2001). Strabismus relocates to the adherens junctions and recently cell adhesion molecules such as flamingo, dachsous and fat have also been implicated in planar cell polarity. This has led to the proposal that planar polarity is linked to cell adhesion (Saburi and McNeill, 2004). Frizzled is required in order to maintain planar polarity and facilitate cell adhesion. If the Clone 8+ cells have maintained polarity *in vitro* then the apical membrane is attached to the substrate. Downregulation of frizzled in Old Clone 8+ cells may affect cytoskeletal organisation at the apical membrane and cell-cell adhesion on the basal-lateral membrane. Localisation of cytoskeletal proteins by frizzled may be required in order to promote attachment of the cell membrane to the apical extracellular matrix.

In the wing disc the apical membrane forms a specialized surface and faces the lumen. Cells that make up the ventral side of the disc adhere to the dorsal side via integrins probably mediated by luminal extracellular matrix (Bökel et al., 2004). *Drosophila* proteins Papillote (Pot) and piopio (Pio) are membrane proteins required for wing disc epithelial cell adhesion to the apical extracellular matrix (Bökel et al., 2004). Mutations in *pot* and *pio* lead to the apical extracellular matrix detaching from the apical membrane (Bökel et al., 2004). Interestingly *pio* (CG3541) is required for the formation of microtubule transalar arrays and is downregulated in Old Clone 8+, ZfeClone 8+ and Clone 8R cells. Alternatively the Clone 8+ cells may not have maintained apical-basal polarity in which case loss of apical extracellular matrix would affect exocytosis and placement of vesicle trafficking proteins at the membrane associated with the cell surface in Clone 8+ cells.

The protein dispatched (disp) is required exclusively for the morphogen, Hedgehog (Hh). Dispatched releases the cholesterol-tethered form of Hedgehog from internal and surface membranes of Hedgehog producing cells (Burke et al., 1999). Many morphogens including Hedgehog and Wingless associate tightly with the cell membrane. One mechanism of morphogen dispersal throughout the epithelia of the imaginal discs is via argosomes. Argosomes appear to be membrane bound vesicles which are derived from basolateral membranes and travel throughout wing disc epithelium (Greco et al., 2001). The authors showed that Wingless colocalised with argosomes and suggest that both Wingless and Hedgehog use argosomes as a mechanism of dispersal. The membrane bound vesicles observed in the Clone 8+ cells could be argosomes. If diffusion of Hedgehog is via argosomes then loss of dispatched may result in membrane bound vesicles remaining at the cell membrane as observed in the ZfeClone 8+. Argosomes are also associated with the basolateral surface of cells which supports the hypothesis that the parent line Young Clone 8+ cells have maintained cell polarity.

Both Hedgehog and frizzled are associated with Wingless, in the canonical pathway. Wingless is the *Drosophila* homologue of vertebrate Wnt (Wnt). Wnt genes in association with β -catenin play a role in oncogenesis in mammalian tissues (Nusse et al., 1984 cited in Hinck et al., 1994). Wingless a secreted protein can be induced in response to Hedgehog signalling. Loss of Hedgehog signalling from Old Clone 8+ and ZfeClone 8+ cells may mean that Wingless would not be induced. However a cholesterol free variant of Hedgehog exists which does not require dispatched and this may compensate for the loss of the cholesterol tethered Hedgehog. Once Wingless is induced it binds to the trans-membrane receptor, frizzled. Frizzled acts through dishevelled to antagonize the activity of Shaggy, a component of the armadillo degradation complex. This results in the stabilization of cytoplasmic armadillo (Blitzer and

Nusse, 2006). Armadillo the *Drosophila* homologue of vertebrate β -catenin, responds in two ways to Wingless signalling. Armadillo assembles in complexes at the adherens junction, binding to DE-cadherin and associating with the actin cytoskeleton thereby maintaining cell-cell adhesion (Oda et al., 1994; Cox et al., 1996). Armadillo also translocates to the nucleus where it interacts with the transcription factor pangolin, which belongs to the Lef1 family of transcription factors, and initiates transcription of Wingless targeted genes (Hinck et al., 1994; Blitzler and Nusse, 2006). In the absence of Wingless, armadillo is degraded, therefore gene transcription via pangolin would be disrupted. This may explain the differential gene expression between Old Clone 8+ and Young Clone 8+. Armadillo is also associated with adherens junctions and DE-cadherin, cell-cell contact would also be disrupted. Disruption of cell-cell contact between vertebrate β -catenin and cadherins is associated with an increase in the invasive capacity of cells and tumour progression (Navarro et al., 1991).

The gene *CG14991* which is now known as *Fermitin 1* encodes the protein FIT1. FIT1 has only been identified recently and unfortunately there is no data on where or how it interacts in the cell. However, FIT1 has been identified as a pleckstrin-like molecule sharing homology with unc-112, found in *C. elegans* and *Drosophila* talin (Rogalskia et al., 2000; Brown et al., 2002). In *C. elegans* unc-112 colocalizes with integrins at cell-matrix adhesion complexes and is required to attach the cytoskeleton to the basal cell membrane (Williams and Waterston, 1994; Rogalskia et al., 2000). Rogalskia et al (2000) suggest that the absence of unc-112 may block association of integrins with other proteins leading to failure of muscle attachment.

Drosophila talin also plays an important role as a link between integrins and the cytoskeleton. Loss of talin is associated with lack of formation of focal

adhesions and stress fibres in embryonic stem cells leading to reduced adhesion (Priddle et al., 1998). Talin is particularly associated with focal adhesions on the basal surface of wing disc epithelia (Brown et al., 2002). Integrins are still able to bind to the extracellular matrix in talin deficient flies, but clustering of integrins is affected along with disruption of the cytoskeleton (Brown et al., 2000). *In vivo*, talin activates PIPK1gamma, which produces the enzyme PIP2 (Blitzer and Nusse, 2006). PIP2 is required in order to facilitate the formation of focal adhesion complexes. The interaction of talin with PIPK1gamma requires growth factor signalling. Talin does not associate with PIPK1gamma in cells which are cultured in medium deprived of growth factors (Blitzer and Nusse, 2006)

At present the location of FIT1 is unknown. FIT1, like talin, may be located at the basal membrane *in vivo* and, like talin, be associated with focal adhesions with a requirement for growth factors. If polarity of the Clone 8+ cells has been lost, loss of FIT1 may affect cell-matrix adhesion via the cytoskeletal-integrin protein complex. Alternatively FIT1 may be required at the adherens junctions, loss of FIT1 would the result in loss of cell-cell adhesion which in turn would lead to cell detachment. It is possible that FIT1 is required in order for exocytosis and placement of vesicle trafficking proteins to take place at the basal membrane or baso-lateral membrane. If polarity of the Clone 8+ cells has not been maintained the basal membrane is attached to the substrate. Loss of FIT1 could affect cell-substrate or cell-cell adhesion in Old Clone 8+ and ZfeClone 8+ cells. The expression of FIT1 could be examined in the Young Clone 8+ cells using anti-FIT1 antibody and compared with the expression in the Old Clone 8+ and ZfeClone 8+ cells. If FIT1 has a requirement for growth factors then a lack of growth factor activity may explain the loss of adhesion in a population of ZfeClone 8+ cells. Fly extract, which is absent from ZfeClone 8+ medium, may contain growth factor associated molecules or

precursors required for growth factor production. The extra serum added to ZfeClone 8+ cells in culture may promote attachment for a period of time, the affected cells eventually detaching. Adding fly extract back to ZfeClone 8+ cells appears to promote attachment for a short while (this would have to be verified by statistical analysis) but many cells were still observed suspended in the medium.

Downregulation of both frizzled and FIT1 may affect placement of proteins required for exocytosis at the cell membrane. Cell adhesion may be affected via the cytoskeleton and integrins, loss of extracellular matrix proteins or loss of cell-cell adhesion. Further experimental evidence would have to be obtained in order to validate the microarray analysis.

8.4.2: How do the Old Clone 8+ cells differ from ZfeClone 8+?

cul-2 a ubiquitin associated gene has already been discussed in Chapter 6 (table 8.11a). The protein Brain Tumor (*brat*) is a transcriptional regulator implicated in the control of differentiation and growth (Sonoda and Wharton, 2001). Recessive *brat* alleles result in metastasis of transplanted imaginal discs (Woodhouse et al., 1998). Reduced expression of *brat* may contribute to the increase in cell proliferation in Old Clone 8+ cells. *Darkener of apricot (Doa)* encodes a putative serine/threonine protein kinase thought to be required for cell viability (Yun et al., 1994). *Doa* is required at various stages of development, Morris et al (2003) suggest that *Doa* plays a role in cell cycle regulation and propose that *Doa* may act 'globally' in regulating chromosome behaviour. The decreased expression of *cul-2*, *brat* and *Doa* suggests that the Old Clone 8+ cells have undergone further changes which supports the observation in Chapter 7 that the Old Clone 8+ and ZfeClone 8+ appear to be of mixed phenotypes.

Changes in adhesion, proliferation and gene expression in the Old Clone 8+ and ZfeClone 8+ are similar. How they differ in gene expression may hold clues on how the lack of fly extract and increased serum has affected the ZfeClone 8+ cells. However the focus of this study is to compare Old Clone 8+ and Young Clone 8+ cells. Further discussion in regard to the Old Clone 8+ cell line may also apply to the ZfeClone 8+ cell line but that would have to be verified through future experiments.

In chapter 5 the accumulation of secreted extracellular matrix components was suggested to be one possible reason why the Old Clone 8+ cells lost the capacity to adhere to the substrate. Although this may still be the case a population of Old Clone 8+ cells also proliferates more rapidly than Young Clone 8+ cells. Cells which undergo anchorage independent cell growth and migratory behaviour are a characteristic of tumour cell lines (Bates et al., 2000; Santini et al., 2000).

8.4.3: Age difference

The differences in adhesion, proliferation and gene expression in the Old Clone 8+ and Young Clone 8+ cells promotes the questions, are these change related? Or have multiple unrelated changes occurred in the Old Clone 8+ cells?

One difference between the low passage Young Clone 8+ cells and high passage Old Clone 8+ cells which has not been addressed so far is age. There is evidence to support a hypothesis that a population of Old Clone 8+ cells have undergone cellular senescence. Aging mechanisms in *Drosophila* have mainly concentrated on the life span of the whole organism (Grotewiel et al., 2005). Much of the work on cellular aging has been done on cultured

mammalian cells and there are parallels about what is known and how it might relate to the Old Clone 8+ cell line.

In the 1960's Hayflick noted that normal cells appeared aged when they exhausted their replicative potential in culture (Hayflick and Moorehead, 1961; cited in Parrinello et al., 2005, Hayflick, 1965, cited in Campisi, 2001). This phenomenon is now known as cellular senescence. It is not known whether transformed cell lines have a finite lifespan, in this study Young Clone 8+ would have undergone in the region of 150 population doublings and Old Clone 8+ over 400 population doublings. Cultured fibroblasts may senesce after 5 or 50 doublings (Parrinello et al., 2005). Telomere shortening or an accumulation of DNA damage induces normal mammalian cells to undergo senescence arrest (Robles and Adami, 1998). The changes in gene expression in Old Clone 8+ when compared to the Young Clone 8+ cells may be due to telomere shortening or an accumulation of DNA damage.

Mammalian fibroblasts that undergo senescence secrete high levels of extracellular matrix metalloproteinases (Mmp's) and epithelial growth factors which change the microenvironment (Krtolica and Campisi, 2002). *Drosophila* has two Mmp genes, *Mmp1* and *Mmp2*. Page-McCaw et al (2003) suggested that detachment of cells from the larval cuticle during development requires Mmp1. The secretion of excess Mmps by a population of senescent Old Clone 8+ cells would alter the microenvironment leading to cell detachment from the substrate. The Old Clone 8+ cells in suspension may contain senescent and non-senescent cells. The presence of excess Mmp's would also account for the loss of adhesion seen by the Young Clone 8+ on used Old Clone 8+ substrate (Chapter 5).

The expression of *timp* (tissue inhibitor of metalloproteases) is required to inhibit the effects of the Mmp's. Deletion of *Drosophila timp* gives an inflated-wing phenotype, indicating loss of the extracellular matrix which holds the two surfaces of the wing blade together (Godenschwege et al., 2000). As the protein timp is a secreted molecule and present in the extracellular matrix, expression of this protein by the Young Clone 8+ may explain the initial adherence of a greater number of Old Clone 8+ cells to the Young used substrate. Unfortunately there is no microarray data to support a positive change in gene expression for the *Mmp* genes in Old Clone 8+. The *timp* gene however is downregulated in both the Old Clone 8+ and ZfeClone 8+ cells. An increase in secretion of epithelial growth factors in senescent cells would account for the excess proliferation of Old Clone 8+ cells and also the Young Clone 8+ cells in Old Clone 8+ conditioned medium.

Heat Shock Promoters are also thought to play a role in cell senescence (Campisi, 2001). Heat Shock Promoters (Hsp) are expressed when cells are under stress and their role is thought to be protective, facilitating the disposal of damaged proteins. Williams et al (2003) propose that heat shock promoters may also overly stimulate signalling pathways involved in proliferation. Three Heat Shock Promoters (Hsp) genes were upregulated in the Old Clone 8+ cells.

Mammalian cells entering senescence normally undergo permanent cell cycle arrest although some cells persist in a damaged form (Melk, 2003). However inactivation of p53 in some replicatively senescent mammalian cells has been shown to reverse the senescent growth arrest (Gire and Wynford-Thomas, 1998; Beausejour et al., 2003). p53 is downregulated in the Old Clone 8+ cell line with no change in the other cell lines when compared to Young Clone 8+. This suggests that if a population of senescent cells is present in the Old Clone

8+ cultures, these cells may be able to replicate and maintain a senescent population.

In mammalian cells loss of cell-substrate contact has been found to trigger a special type of programmed cell death as a result of loss of cell–matrix interactions, this is called anoikis (Frisch and Francis, 1994; Frisch and Screaton, 2001; Stupack and Cheresch, 2002; Douma et al., 2004). The acquisition of anoikis resistance is regarded as a crucial step in the metastatic transformation of a tumour (Yawata et al., 1998; Windham et al., 2002). In addition senescent human fibroblasts can promote the proliferation and tumourigenic conversion of epithelial cells bearing potentially oncogenic mutations (Krtolica et al., 2001). It is possible that a population of Old Clone 8+ cell suspended in the medium may have acquired a resistance to anoikis. In addition the Clone 8+ cells are already transformed and may have oncogenic mutations. Signals from senescent cell may promote proliferation and conversion of the nonsenescent cells into malignant cells.

From the evidence presented it is possible that a population of the high passage Old Clone 8+ cell line have undergone cellular senescence. It is most likely that these changes have occurred gradually in this Clone 8+ cell line. It has been noted that Clone 8+ cell lines appear to change in adherence from p(30)30, 180 doublings. Evidence for this gradual change also comes from the differential gene expression which is observed between the Old Clone 8+ and the ZfeClone 8+ cell lines. The ZfeClone 8+ cell line is of a younger '*in vitro*' age. However as the ZfeClone 8+ cell line differ from the Old Clone 8+ cells in their nutritional input this may have had an additional impact on these cells. Further experimental analysis would have to be undertaken to ascertain whether changes take place gradually in the Clone 8+ cell lines as they age.

The question of cell polarity in the Clone 8+ cells could be addressed using electron microscopy to identify the positions of septate and adherens junctions and an examination of the basal and apical membranes. Antibody staining of septate and adherens junctions with proteins associated with these junctions could also be used along with confocal microscopy.

Changes in gene expression which have taken place in the Old Clone 8+ cell compared to the Young Clone 8+ cell are very interesting in relation to cellular senescence. How molecular signals from other cells or the substrate are then transduced from the cell surface into a cell affecting genetic control of proliferation and cell death is of interest (Orford et al., 1999; Yan et al., 1995). All of the genes differentially expressed in Old Clone 8+ discussed in Chapters 6 and 8 may be implicated in cell senescence, particularly *cul-2*, *frizzled*, *wingless* and *Doa*.

As only a subset of genes of interest have been identified in the Clone 8+ cells, in the future further analysis of the data may be instructive. One way in which this could be addressed in the future is by undertaking microarray analysis using the whole of the *Drosophila* genome which is now available. Samples could be taken from different passage (age) ranges and at different times, starting from as close to initiation as possible.

Markers for cellular senescence are also available which could be used to identify senescent cells (Dimri et al., 2000; Ben-Porath and Weinberg, 2004). Comparing telomere lengths in Clone 8+ cells could also be accomplished using Q-fish, a quantitative fluorescent *in situ* hybridisation technique (Satyanarayana et al., 2006).

In the future the Clone 8+ cell line may be instructive on dissecting out cell signalling pathways, cell adhesion, polarity and aging.

Tables

Table 8.1a : Genes of Interest upregulated in OCI.8+ cells

Gene	Gene product: Location and function
<i>Abl</i>	Adherens junction, nonmembrane spanning protein tyrosine kinase
<i>Act57B</i>	Actin filament, cytoskeleton
<i>ago</i>	Ubiquitin protein ligase, regulation of mitosis
<i>bt</i>	Cytoplasm, myosin light chain kinase, phosphorylation
<i>CG16974</i>	Not known
<i>Cg25C</i>	Basement membrane, collagen type IV
<i>CG3210</i>	Microtubule associated complex
<i>CG32245</i>	Not known
<i>CG6509</i>	Not known
<i>CG6933</i>	Structural constituent of peritrophic membrane
<i>chic</i>	Actin binding, actin polymerization and/or depolymerization
<i>ck</i>	Myosin ATPase, Myosin, nonmuscle myosin, actin binding
<i>Cyp1</i>	Cytoplasm, transcription elongation factor complex b, protein folding
<i>did</i>	Not known
<i>dlg1</i>	Plasma membrane, cytoskeleton, proliferation, epithelial morphogenesis
<i>dp</i>	Extracellular matrix
<i>Dr</i>	Nucleus, specific RNA polymerase II transcription factor
<i>en</i>	Nucleus, specific RNA polymerase II transcription factor, regulator
<i>eya</i>	Nucleus, hydrolase, transcription, eyeantennal disc metamorphosis
<i>Fim</i>	Actin binding
<i>flw</i>	Protein serine/threonine phosphatase, cell adhesion
<i>for</i>	cGMPdependent protein kinase, phosphorylation
<i>Gel</i>	Cytosol, extracellular, actin filament, actin binding
<i>Grip84</i>	Gammatubulin small complex, microtubule nucleation
<i>heix</i>	Integral to membrane
<i>Hsp23</i>	Actin binding, heat shock protein
<i>Hsp26</i>	Heat shock protein
<i>Hsp27</i>	Heat shock protein
<i>klar</i>	Microtubule associated complex, dynein ATPase, m/t based movement
<i>klg</i>	Not known
<i>Klp61F</i>	Cytoplasm, microtubule associated complex, mitotic spindle
<i>Lnk</i>	Not known
<i>lola</i>	Nucleus, RNA polymerase II transcription factor, axonogenesis
<i>lolal</i>	Nucleus, specific RNA polymerase II transcription factor
<i>N</i>	Integral to membrane, receptor, transcriptional activator, adhesion

Table 8.1a: Genes of Interest upregulated in OCl.8+ cells continued

Gene	Gene product: Location and function
<i>Oda</i>	Ornithine decarboxylase inhibitor, cell differentiation
<i>osa</i>	Nucleus, DNA binding
<i>Pbprp2</i>	Extracellular, phenylalkylamine binding
<i>pnut</i>	Apical plasma membrane, actin & microtubule binding, cytokinesis
<i>poe</i>	Calmodulin binding
<i>Pxn</i>	Extracellular matrix, peroxidase
<i>Rbf</i>	Nucleus, DNA binding, negative regulation of cell proliferation
<i>RhoGAP68F</i>	Rho GTPase activator
<i>RhoL</i>	Rho small monomeric GTPase
<i>SCAR</i>	Cytoskeletal regulator, actin binding
<i>scb</i>	Focal adhesion, laminin receptor, Cell-cell & cell-matrix adhesion
<i>sqd</i>	Ribonucleoprotein complex, nucleus, chromatin, nuclear speck,
<i>Su(dx)</i>	Ubiquitin protein ligase, N receptor signaling pathway, ubiquitin cycle
<i>Su(var)205</i>	Nucleus, establishment of chromatin silencing
<i>tomosyn</i>	Synaptic vesicle, syntaxin1 binding, neurotransmitter secretion
<i>Tor</i>	Phosphatidylinositol 3 kinase, +ve regulation cell growth
<i>trol</i>	Basement membrane, extracellular matrix
<i>Tsp96F</i>	Integral to membrane

Table 8.1a: Genes of Interest upregulated in OCl.8+ cells

53 genes of interest were identified as upregulated in the OCl.8+ cells when compared to the YCl.8+ cells. 15 genes which were upregulated 1.5 fold or more are indicated in red type.

The genes have been listed alphabetically.

Table 8.1b: Genes of Interest downregulated in OCI.8+ cells

Gene	Gene product: Location and function
<i>blot</i>	Integral to membrane, n-transmitter transporter, epithelial morphogenesis
<i>brat</i>	rRNA metabolism
<i>CG14991</i>	Not known
<i>CG7298</i>	Structural constituent of peritrophic membrane
<i>cul-2</i>	Nuclear ubiquitin ligase complex
<i>disp</i>	Membrane, exocytosis
<i>dm</i>	Nucleus, transcription factor, +ve regulation of cell growth, cell cycle
<i>DNasell</i>	Deoxyribonuclease II
<i>Doa</i>	Cytoplasm, nucleus, protein kinase, embryonic cuticle biosynthesis
<i>E(z)</i>	Nucleus, -ve regulation of transcription by homeotic gene (Polycomb)
<i>EcR</i>	Nucleus, ecdysteroid hormone receptor, RNA p I transcription factor
<i>Egfr</i>	Plasma membrane, EGFreceptor, antiapoptosis
<i>Impl2</i>	Extracellular, cell adhesion molecule
<i>kal-1</i>	Extracellular matrix
<i>Klp3A</i>	Cytoplasm, plus end directed kinesin ATPase, microtubule binding
<i>lqf</i>	Neurotransmitter secretion, synaptic vesicle endocytosis
<i>mts</i>	Protein phosphatase type 2A complex, microtubule/chromatin interaction
<i>mus304</i>	Cytoplasm, DNA damage checkpoint, DNA repair
<i>ninaA</i>	Cytoplasmic, integral to plasma membrane, 'de novo' protein folding
<i>Nrt</i>	Basolateral plasma membrane, integral to membrane
<i>Prm</i>	Striated muscle thick filament
<i>Pvf1</i>	Cytoplasm, extracellular, receptor binding
<i>Tak1</i>	MAP protein kinase, apoptosis, defense response, JNK cascade
<i>toy</i>	Nucleus, specific RNA polymerase II transcription factor

n-transmitter=neurotransmitter

Table 8.1b: Genes of Interest downregulated in OCI.8+ cells

24 genes of interest were identified as downregulated in the OCI.8+ cells when compared to the YCI.8+ cells. Only 2 genes were downregulated 1.5 fold or more, indicated in red type.

The genes have been listed alphabetically.

Table 8.2a: Genes of Interest upregulated in ZfeCl.8 cells

Gene	Gene product: Location and function
<i>Abl</i>	Adherens junction, nonmembrane spanning protein tyrosine kinase
<i>Ank2</i>	Plasma membrane, cytoskeletal protein, cytoskeletal anchoring
<i>bt</i>	Cytoplasm, structural constituent of cytoskeleton, phosphorylation
<i>CG12042</i>	Dynactin complex, microtubulebased movement
<i>CG2789</i>	Benzodiazepine receptor
<i>CG9279</i>	Dynactin complex, microtubule based movement
<i>crc</i>	Nucleus, transcription factor
<i>cul-2</i>	Nuclear ubiquitin ligase complex
<i>disco</i>	Nucleus, transcription factor
<i>Dr</i>	Nucleus, specific RNA polymerase II transcription factor
<i>Eip55E</i>	Sulphur amino acid metabolism
<i>eya</i>	Nucleus, hydrolase, transcription, eyeantennal disc metamorphosis
<i>fat-spondin</i>	Extracellular
<i>Flo-2</i>	Flotillin complex, structural molecule, cell adhesion
<i>gl</i>	Nucleus, specific RNA polymerase II transcription factor
<i>Glt</i>	Basement membrane, calcium ion binding
<i>Impl2</i>	Extracellular, cell adhesion molecule
<i>klg</i>	Not known
<i>mask</i>	Structural constituent of cytoskeleton, cell growth/maintenance, proliferation
<i>osa</i>	Nucleus, DNA binding
<i>Pbprp2</i>	extracellular, phenylalkylamine binding
<i>phl</i>	Cytoplasm, NOT plasma membrane, protein kinase, RAS signal transduction
<i>Pxn</i>	extracellular matrix, peroxidase
<i>Rbf</i>	Nucleus, DNA binding, negative regulation of cell proliferation & cell cycle
<i>rho</i>	Golgi apparatus, positive regulation of EGF receptor signalling pathway
<i>SK</i>	Calcium activated potassium channel
<i>Toll-7</i>	Integral to membrane, transmembrane receptor, signal transduction
<i>tomosyn</i>	Synaptic vesicle, syntaxin1 binding, neurotransmitter secretion
<i>Trxr-1</i>	Cytoplasm, glutathione reductase (NADPH)

Table 8.2a: Genes of Interest upregulated in ZfeCl.8 cells

31 genes of interest were identified as upregulated in the ZfeCl.8 cells when compared to the OCl.8+ cells. 9 genes which were upregulated 1.5 fold or more are indicated in red type.

Table 8.2b: Genes of Interest downregulated in ZfeCl.8 cells

Gene	Gene product: Location and function
<i>Ank</i>	Plasma membrane, spectrosome, cytoskeletal anchoring
<i>bun</i>	Cytoplasm, nucleus, RNA polymerase II transcription factor, cell fate
<i>cdc2</i>	Nucleus, cyclindependent protein kinase, regulation of cell cycle
<i>CG6805</i>	Inositol trisphosphate phosphatase, dephosphorylation
<i>CG7800</i>	Not known
<i>Cht2</i>	Chitinase, cuticle chitin catabolism
<i>flw</i>	Protein serine/threonine phosphatase, cell adhesion
<i>fz</i>	Integral to membrane, receptor, Wnt protein binding, epithelial cell polarity
<i>Gug</i>	Cytoplasm, nucleus, transcription co-repressor, leg morphogenesis
<i>HLHmbeta</i>	Nucleus, DNA binding, transcriptional repressor, N receptor signalling p/way
<i>Hsp23</i>	Actin binding, heat shock protein
<i>Hsp27</i>	Heat shock protein
<i>ImpL1</i>	Extracellular
<i>Jra</i>	Cytoplasm, nucleus, RNA polymerase II transcription factor, JNK cascade
<i>mnd</i>	Amino acid transporter
<i>Rca1</i>	Not known
<i>sno</i>	Nucleus, N receptor signaling pathway, positive regulation of transcription
<i>Syx1A</i>	Integral to membrane, SNAP receptor, cuticle biosynthesis, exocytosis

Table 8.2b: Genes of Interest downregulated in ZfeCl.8+ cells

18 genes of interest were identified as downregulated in the ZfeCl.8+ cells when compared to the OCl.8+ cells. 9 genes were downregulated 1.5 fold or more, indicated in red type.

Table 8.3a: Genes of Interest upregulated in Cl.8R cells

Gene	Gene product: Location and function
<i>Abl</i>	Adherens junction, nonmembrane spanning protein tyrosine kinase
<i>Act57B</i>	Actin filament, cytoskeleton
<i>ap</i>	Nucleoplasm and nucleus. Transcription factor, zinc ion binding
<i>bt</i>	Cytoplasm, structural constituent of cytoskeleton, phosphorylation
<i>CG16974</i>	Not known
<i>Cg25C</i>	Basement membrane, collagen type IV
<i>CG32245</i>	Not known
<i>CG7635</i>	Not known
<i>chic</i>	Actin binding, actin polymerization and/or depolymerization
<i>Chit</i>	Extracellular, chitinase, cuticle chitin catabolism
<i>Eip55E</i>	Sulphur amino acid metabolism
<i>Gel</i>	Cytosol, extracellular, actin filament, actin binding
<i>Gl1</i>	Basement membrane, calcium ion binding
<i>Idgf1</i>	Extracellular, imaginal disc growth factor, NOT chitinase
<i>Idgf2</i>	Extracellular, imaginal disc growth factor, NOT chitinase
<i>Idgf3</i>	Extracellular, imaginal disc growth factor, NOT chitinase
<i>ldh</i>	Isocitrate dehydrogenase (NADP+)
<i>klg</i>	Not known
<i>osa</i>	Nucleus, DNA binding
<i>Pbprp2</i>	extracellular, phenylalkylamine binding
<i>Ppn</i>	Basement membrane, extracellular matrix
<i>Pxn</i>	extracellular matrix, peroxidase
<i>Rbf</i>	Nucleus, DNA binding, negative regulation of cell proliferation, cell cycle
<i>scb</i>	Focal adhesion, integrin complex, cell adhesion receptor
<i>Thor</i>	Eukaryotic initiation factor 4E binding, defense response
<i>tomosyn</i>	Synaptic vesicle, syntaxin1 binding, neurotransmitter secretion
<i>trol</i>	Basement membrane, extracellular matrix

Table 8.3a: Genes of Interest upregulated in Cl.8R cells

27 genes of interest were identified as upregulated in the Cl.8R cells when compared to the YCl.8+ cells. 10 genes which were upregulated 1.5 fold or more are indicated in red type.

The genes have been listed alphabetically.

Table 8.3b: Genes of Interest downregulated in Cl.8R cells

Gene	Gene product: Location and function
<i>blot</i>	Integral to membrane, neurotransmitter transport
<i>cdc2</i>	Nucleus, cyclindependent protein kinase, regulation of cell cycle
<i>CG3960</i>	Cytoskeleton, actin binding
<i>CG6933</i>	Structural constituent of peritrophic membrane
<i>dp</i>	Extracellular matrix
<i>dpld</i>	Not known
<i>Egfr</i>	Integral to plasma membrane, EGF-receptor, cell fate determination
<i>GstS1</i>	Cellular component unknown, glutathione peroxidase and transferase
<i>Hsp23</i>	Actin binding, heat shock protein
<i>Hsp26</i>	Heat shock protein
<i>Hsp27</i>	Heat shock protein
<i>ImpL1</i>	Extracellular
<i>ImpL2</i>	Extracellular, cell adhesion molecule
<i>lolal</i>	Nucleus, specific RNA polymerase II transcription factor
<i>mbt</i>	Receptor signalling protein serine/threonine kinase, phosphorylation
<i>mts</i>	Phosphatase type 2A complex, mitosis, spindle assembly
<i>phl</i>	Cytoplasm, extrinsic to plasma membrane, signal transduction
<i>poe</i>	Calmodulin binding
<i>r</i>	Cytoplasm, carbamoyltransferase, pyrimidine base biosynthesis
<i>Rapgap1</i>	RAS GTPase activator
<i>Su(var)205</i>	Nucleus, chromatin binding and establishment of chromatin silencing

Table 8.3b: Genes of Interest downregulated in Cl.8R cells

21 genes of interest were identified as downregulated in the Cl.8R cells when compared to the YCl.8+ cells. 8 genes were downregulated 1.5 fold or more, indicated in red type.

The genes have been listed alphabetically.

Comparison of Genes of Interest downregulated in OCl.8+ cells

Table 8.11a: Gene comparison, downregulated genes in OCl.8+ cells compared to ZfeCl.8+ and Cl.8R

Gene	OCl.8+	ZfeCl.8	Cl.8R
<i>CG14991</i>	d	d	u
<i>CG6805</i>	d	d	u
<i>fz</i>	d	d	u
<i>Cht2</i>	d	d	nc
<i>disp</i>	d	d	nc
<i>brat</i>	d	u	u
<i>cul-2</i>	d	u	nc
<i>Doa</i>	d	u	nc
<i>Ank2</i>	d	u	d
<i>ImpL2</i>	d	u	d
<i>Rapgap1</i>	d	u	d
<i>Ank</i>	d	d	d
<i>blot</i>	d	d	d
<i>dm</i>	d	d	d
<i>E(z)</i>	d	d	d
<i>Egfr</i>	d	d	d
<i>ImpL1</i>	d	d	d
<i>Klp3A</i>	d	d	d
<i>mbt</i>	d	d	d
<i>mts</i>	d	d	d
<i>Nrt</i>	d	d	d
<i>Tak1</i>	d	d	d
<i>Jra</i>	d	d	d
<i>Pvf1</i>	d	d	d

Table 8.11a: Gene comparison, downregulated gene expression in OCl.8+ cells compared to ZfeCl.8+ and Cl.8R

32 genes of interest were identified as downregulated in OCl.8+ cells when compared to YCl.8+ cells. 24 genes of known expression in ZfeCl.8+ and Cl.8R are listed in this table. 5 genes, *CG14991*, *CG6805*, *fz*, *Cht2* and *disp* were downregulated in OCl.8+ cells and ZfeCl.8+ cells and upregulated or with no

change in expression in Cl.8R (highlighted in yellow). 3 genes were downregulated in OCl.8+ cells only (highlighted in grey). amb, ambiguous; d, downregulated; ds, small negative change; nc, no change; u, upregulated; us, small positive change; N/D, no data

Table 8.11b: Downregulated genes in OCl.8+ unknown outcome in ZfeCl.8+ or Cl.8R

Gene	OCl.8+	ZfeCl.8	Cl.8R
<i>kal-1</i>	d	N/D	nc
<i>ninaA</i>	d	N/D	nc
<i>Prm</i>	d	N/D	nc
<i>DNasell</i>	d	amb	d
<i>lqf</i>	d	nc	amb
<i>toy</i>	d	ds	amb
<i>CG7800</i>	d	d	amb
<i>CG12042</i>	d	u	amb

Table 8.11b: Gene comparison, downregulated gene expression in OCl.8+ cells, unknown outcome in ZfeCl.8+ or Cl.8R

8 genes which were downregulated in Old Clone 8+ cells had an unknown outcome in either ZfeCl.8+ or Cl.8R cells

amb, ambiguous; d, downregulated; ds, small negative change; nc, no change; u, upregulated; us, small positive change; N/D, no data

Table 8.12: No change in gene expression in OCI.8+ cells when compared to YCI.8+ cells

Gene	OCI.8+	ZfeCI.8	CI.8R
<i>Idgf1</i>	nc	d	u
<i>bun</i>	nc	d	amb
<i>Gug</i>	nc	d	amb
<i>cdc2</i>	nc	d	d
<i>CG7635</i>	nc	nc	u
<i>Chit</i>	nc	nc	u
<i>Idgf2</i>	nc	nc	u
<i>Eip55E</i>	nc	u	u
<i>fat-spondin</i>	nc	u	u
<i>gl</i>	nc	u	u
<i>CG2789</i>	nc	u	u
<i>Trxr-1</i>	nc	u	nc
<i>mask</i>	nc	u	d
<i>phl</i>	nc	u	d

Table 8.12: No change in gene expression in OCI.8+ cells when compared to YCI.8+ cells.

14 genes of interest had no change in expression in the OCI.8+ cells when compared to YCI.8+ cells. 3 genes *CG7635*, *Chit* and *Idgf2* were identified as having no change in ZfeCI.8+ cells. 4 genes were differentially expressed in all 3 cell lines, *Idgf1*, *mask* and *phl*, (highlighted in yellow). One gene, *Trxr-1*, (highlighted in grey) was upregulated only in ZfeCI.8+ with no change in expression in OCI.8+ or CI.8R cells.

amb, ambiguous; d, downregulated; ds, small negative change; nc, no change; u, upregulated; us, small positive change; N/D, no data

Table 8.13a: Genes upregulated in OCI.8+, ZfeCl.8+ and Cl.8R cells compared to YCl.8+

Gene	OCI.8+	ZfeCl.8+	Cl.8R
<i>Abl</i>	u	u	u
<i>Act57B</i>	u	u	u
<i>ago</i>	u	u	u
<i>CG16974</i>	u	u	u
<i>CG3210</i>	u	u	u
<i>chic</i>	u	u	u
<i>did</i>	u	u	u
<i>disco</i>	u	u	u
<i>Dr</i>	u	u	u
<i>en</i>	u	u	u
<i>eya</i>	u	u	u
<i>Flo-2</i>	u	u	u
<i>Gel</i>	u	u	u
<i>GlT</i>	u	u	u
<i>heix</i>	u	u	u
<i>klg</i>	u	u	u
<i>Lnk</i>	u	u	u
<i>N</i>	u	u	u
<i>osa</i>	u	u	u
<i>Pbprp2</i>	u	u	u
<i>Pxn</i>	u	u	u
<i>Rbf</i>	u	u	u
<i>SK</i>	u	u	u
<i>tomosyn</i>	u	u	u
<i>ck</i>	u	us	u
<i>Cg25C</i>	u	nc	u
<i>Fim</i>	u	nc	u
<i>trol</i>	u	nc	u

Table 8.13a: Genes upregulated in OCI.8+, ZfeCl.8+ and Cl8R cells compared to YCl.8+

28 genes of interest were identified which had a positive change in expression in all the cell lines, OCI.8+, ZfeCl.8+ and Cl.8R, when compared to the YCl.8+ cell line.

amb, ambiguous; d, downregulated; ds, small negative change; nc, no change; u, upregulated; us, small positive change; N/D, no data

Table 8.13b: Genes upregulated in OCl.8+ cells when compared to YCl.8+ cells

Gene	OCl.8+	ZfeCl.8	Cl.8R
CG6933	u	d	d
Hsp23	u	d	d
Hsp26	u	d	d
Hsp27	u	d	d
poe	u	d	d
Su(var)205	u	d	d
GstS1	u	nc	d
dp	u	nc	d
CG6509	u	u	nc
crc	u	u	nc
SCAR	u	u	nc
Klp61F	u	nc	nc
RhoGAP68F	u	nc	nc
Ppn	u	nc	u
ldh	u	nc	u
scb	u	d	u
ldgf3	u	d	u
Oda	u	d	u
flw	u	d	nc
Syx1A	us	d	nc

Table 8.13b: Genes upregulated in OCl.8+ cells when compared to YCl.8+ cells

20 genes of interest were identified which had a positive change in expression in OCl.8+ and differentially expressed in ZfeCl.8+ and Cl.8R.

6 genes were upregulated in OCl.8+ and downregulated in ZfeCl.8+ and Cl.8R cells (highlighted in yellow). 2 genes were upregulated in OCl.8+, *Klp61F* and *RhoGAP68F* and no change in the ZfeCl.8+ cells or Cl.8R (highlighted in blue)

3 genes, *CG6509*, *crc*, and *SCAR* (highlighted in grey) were also upregulated in the ZfeCl.8+ with no change in Cl.8R.

amb, ambiguous; d, downregulated; ds, small negative change; nc, no change; u, upregulated; us, small positive change; N/D, no data

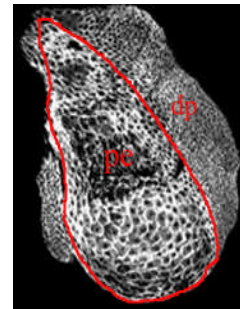
Chapter 9

Peripodial Epithelium

9.1: Introduction

During morphogenesis coordinated changes in individual cell shapes contribute towards the movement of whole sheets of epithelial tissue. Local contraction of the cytoskeleton, particularly the actin cytoskeleton, underpins these movements (Condic et al., 1991). The peripodial epithelium is a thin monolayer of squamous and cuboidal epithelial cells underlying the columnar epithelium of the disc (figure 9.1).

In vitro studies have shown that contraction of the peripodial epithelium during the process of evagination reduces the surface area of the peripodial epithelium during eye-antennal disc morphogenesis (Milner et al., 1984). In leg and wing discs



evagination only proceeds in the presence of an intact peripodial epithelium. Removal of the peripodial epithelium disrupts eversion and the process of elongation, leading to the

Figure 9.1: Third instar wing disc. The peripodial epithelium is bounded by a red outline. Adapted from McClure and Schubiger, 2005.

conclusions that the peripodial epithelium expands to accommodate elongation and contracts, leading to the eversion of appendages (Milner et al., 1984). Gibson and Schubiger (2001) have suggested that cytoskeletal reorganisation drives the contraction of the peripodial epithelium. As imaginal disc eversion is cytocholasin-sensitive the contraction of the peripodial epithelium is likely to be driven by the actin cytoskeleton (Martin-Blanco et al., 2000). How contraction of the peripodial membrane during evagination is mediated and the role of actin will be examined using *in vitro* tissue culture of *Drosophila* imaginal discs.

9.2: Materials and Methods

The use of *Drosophila* transgenic flies expressing actin-*lacZ*/GFP using the GAL4 enhancer detection technique was employed to visualise actin expression in the peripodial epithelium (Brand and Perrimon, 1993).

Direct visualisation of the actin cytoskeleton in live imaginal discs using immunofluorescence microscopy was carried out using the transgenic fly strain actin-GFP. The transgenic fly strain actin-*lacZ* was used to visualise the actin cytoskeleton in fixed imaginal disc tissue. *LacZ* encodes beta-galactosidase which is transcribed in a pattern reflecting actin expression. The pattern of actin expression was visualised by staining the discs for beta-galactosidase which is reported as a blue stain. In addition the use of transgenic flies expressing GFP which outlines the cell membrane in peripodial epithelia was utilised, the discs from these flies and wild-type flies were also fixed and stained for f-actin.

9.2.1: Fly stocks

Fly strains expressing GFP in living cells derived from a GAL4 enhancer detection technique (Brand and Perrimon 1993) were as follows:

The 6990 fly line, expressing *GawB* } *C855a* was crossed with *UAS-mCD8:GFP.L* } *LL5*. Gal4 is expressed in leg disc peripodial epithelium outlining the cell membrane.

The 6773 fly line expressing *GAL4* } *Gug* [*AGir*]/*TM6B, Tb*[1] was also crossed with *UAS-mCD8:GFP.L* } *LL5*. Gal4 is expressed in wing disc peripodial epithelium outlining the cell membrane. In each cross virgins were collected from both fly strains, crossed and the imaginal discs were dissected from the resulting F1 late third instar larvae (Chapter 2).

9.2.2: Dissection

Imaginal discs from late third instar larvae of wild type flies, actin-*lacZ* and actin-GFP transgenic flies were dissected (Chapter 2). The individual discs were suspended in cavity slides in medium only or in medium with 100ng/ml ecdysone. Immediately after dissection the discs were incubated overnight at 16°C.

9.2.3: Microscopy

After incubation, discs dissected from transgenic flies expressing actin-GFP were examined continuously and imaged using immunofluorescence microscopy. Imaginal discs from wild-type and transgenic flies actin-*lacZ* and CD8-GFP were imaged and fixed at intervals. Images were taken of the peripodial epithelium before fixation to ensure there was no damage sustained by the fixation procedure.

9.2.4: Histochemical staining

To reveal the expression of actin in the peripodial epithelium of flies actin-*lacZ*. Visualisation of β -galactosidase was performed using the chromogenic substrate X-gal (5-bromo-4-chloro-3-indolyl- β -D-galctopyranoside) (O'Kane and Gehring, 1987).

Discs were fixed in 1% glutaraldehyde in PBS for 4 minutes. The fixative was removed and the discs were rinsed several times with PBS.

8% X-gal solution was added to Fe/Na P staining buffer to give 0.2% solution of X-gal (see appendix). Discs were incubated with 0.2% X-gal staining

solution at 37°C until the development of a blue stain was observed. This was in order to visualise the peripodial epithelium only and not the disc proper. The X-gal solution was removed immediately by repeated rinsing with PBS. Individual discs were suspended in glycerol in cavity slides. Controls: Wild type imaginal discs with and without ecdysone were used as controls in order to monitor the endogenous expression of *lacZ*.

9.2.5: Immunohistochemistry

Wild-type and CD8-GFP imaginal discs were stained for filamentous actin (f-actin). In order to preserve the peripodial epithelium and f-actin, imaginal discs were fixed in 4% paraformaldehyde for 4 minutes. This was followed by several washes with PBS. Discs were incubated with phalloidin conjugated to a red-fluorescent dye, Alexa Fluor 568, for 15-20 minutes, followed by several washes with PBS. Individual discs were then suspended in Vectamount in cavity slides.

Controls: In this experiment wild-type discs with and without ecdysone were fixed to monitor autofluorescence.

Nuclear DNA was stained by incubation with 0.125µg/ml DAPI solution for 10 minutes at room temperature, followed by extensive rinsing in PBS. At no time were imaginal discs allowed to dry out. A total of 300 wild type, 80 actin-GFP, 220 actin-*lacZ* and 60 CD8-GFP discs were examined.

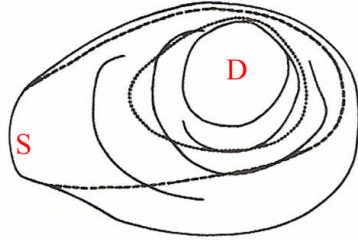
9.2.6: Peripodial epithelium

In order to appreciate the extent of the squamous peripodial epithelium in late third instar imaginal discs figures 9.2 and 9.3 (pg 218) show the peripodial epithelium before and during evagination in the leg and wing disc.

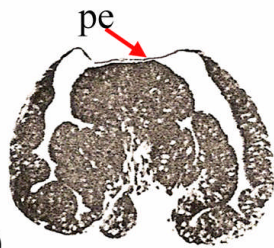
Peripodial Epithelium (figures 9.2 and 9.3)

Figure 9.2: Leg disc

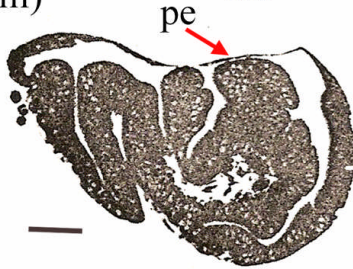
9.2(i)



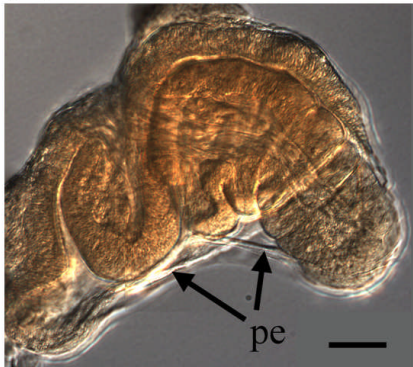
9.2(ii)



9.2(iii)



9.2(iv)



9.2(v)

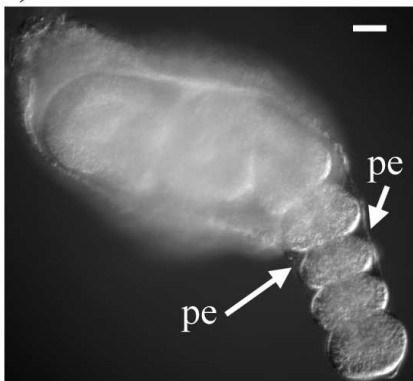
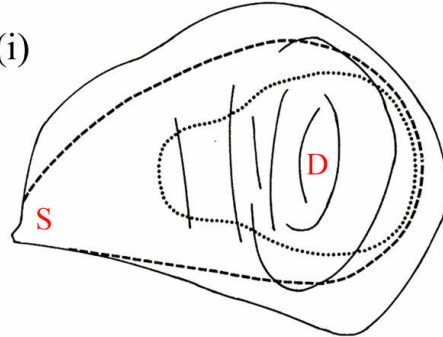
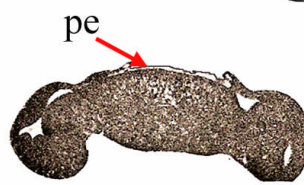


Figure 9.3: Wing disc

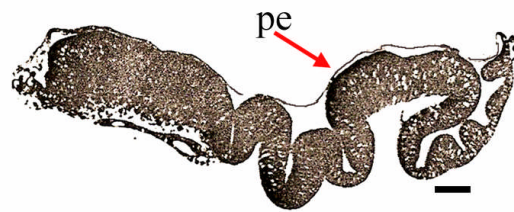
9.3(i)



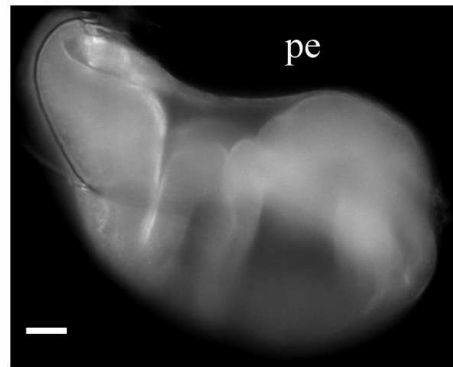
9.3(ii)



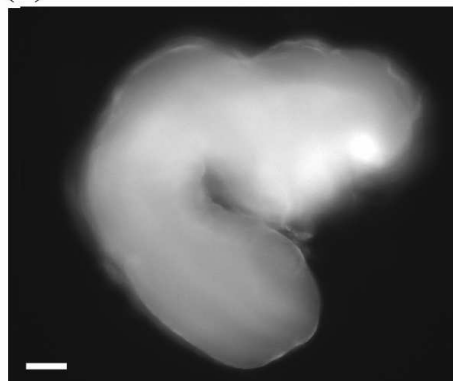
9.3(iii)



9.3(iv)



9.3(v)



At the end of the third instar larval period peripodial cells are approximately 20-30 μm diameter and 5 μm in depth, the disc proper cells are 5-6 μm diameter. The peripodial epithelium is confined to an oval shape which overlies the disc proper and extends towards the region where the stalk is attached to the epidermis. Thinner squamous epithelium is contained within the inner dotted line and slightly thicker tissue is bounded by the outer dashed line (stalk region, s, distal enlargen, d). Figures 9.2(ii) and 9.3(ii) are longitudinal sections and 9.2(iii) and 9.3(iii) are transverse sections through the leg and wing disc respectively (pe, peripodial epithelium). During the early stages of evagination the peripodial epithelium undergoes considerable stretching. The distal segments of the developing appendage elongate within the confines of the peripodial epithelium (figures 9.2(iv), 9.3(iv)). As elongation proceeds the stalk opens and the appendage emerges through the stalk mediated by contraction of the peripodial epithelium (figure 9.3(v)). In some instances the appendage may rupture the peripodial epithelium before evagination is completed (figure 9.2(v)) (adapted from Milner et al., 1983; Milner et al, 1984; Milner and Muir, 1987).

Scale bar represents:50 μm

9.3: Results

9.3.1: Wild-type flies

The process of evagination was completed in imaginal discs in the presence or absence of ecdysone. 114 wild-type imaginal discs evaginated prior to examination. Of the remaining discs, 152 went onto develop further after incubation overnight at 16°C and 111 completed evagination. The remaining discs degenerated or development was arrested.

9.3.2: Transgenic fly strain actin-GFP

17 imaginal discs had evaginated prior to examination and 11 proceeded with further development after incubation but did not complete evagination. 52 discs arrested immediately after dissection. Immunofluorescence of the peripodial epithelium and the expression of actin showed that actin was present throughout the discs. The majority of discs from transgenic flies expressing actin-GFP had sustained some damage from the dissection especially around the proximal region close to where the stalk originates (figures 9a, 9b). Peripodial cells around the stalk region appear to be elongated, as outlined by actin. Actin also appears to be concentrated in discrete areas. The immunofluorescence of actin-GFP was diffuse due to the presence of excess mounting medium and visualisation was generally poor. A lack of depth of focus and the orientation of many discs during the process of evagination also prevented visualisation of the peripodial epithelium.

9.3.3: Transgenic fly strain *actin-lacZ*

Prior to examination evagination was completed in 72 discs. 35 discs proceeded with development after incubation, 8 of these discs completed evagination. Actin was detected in the cell membrane, outlining the cells of the peripodial epithelium in all discs (figures 9c, 9d, 9e). Actin expression was particularly concentrated in the proximal region of the disc close to the stalk represented by the dense blue staining. A stripe of actin expression which extended from the proximal towards the distal end of the disc towards the tip of the appendage was observed in the wing disc indicating possible contractile or cell shape changes in these areas (figure 9c). Haemocytes or aepithelial cells loosely attached to the basal lamina were also observed.

Closer examination of the stalk region in wing and leg discs revealed a putative lumen (figures 9f, 9g). Cells appeared to be orientated around the lumen. Actin was detected outlining peripodial cells, many of which had undergone a change in morphology. A number of squamous peripodial cells had assumed an elongated diamond shape, many cells appeared rounder (figures 9f, 9g). Cuboidal peripodial cells at the margin between the peripodial epithelium and disc proper were of an elongate morphology (figure 9f). In the control slides wild-type flies showed no evidence of *actin-lacZ* activity

9.3.4: Wild-type flies stained for f-actin

Preservation of the peripodial epithelium was accomplished and no detriment to the integrity of the epithelium was found after fixation. This was verified by examination of images taken before and after the procedure. F-actin was detected throughout the imaginal discs (figure 9h(i)). Examination of a wing

disc revealed f-actin which was more intense in a region close to the stalk. Individual cell boundaries could not be visualised. Phase contrast microscopy revealed the presence of large cells which were of peripodial or stalk origin (figure 9h(ii)). High background staining of phalloidin and residual phalloidin and DAPI prevented visualisation of the peripodial epithelium in the majority of slides examined.

9.3.5: Transgenic fly strains CD8-GFP

CD8-GFP was not expressed solely in wing or leg disc peripodial epithelium. Examination of the imaginal wing and leg discs before fixation revealed that CD8-GFP was expressed either throughout the discs or in isolated areas within the disc. Additional staining of the discs with phalloidin revealed an area close to the stalk region in the wing discs which stained more intensely for f-actin (figure 9i). Colocalisation of the CD8-GFP (green) and f-actin (red) was observed in this region which produced a bright yellow area. Due to the lack of depth of focus the outlines of individual disc cells were not in evidence in any preparations examined.

9.4 Discussion

Visualisation of actin as reported by *lacZ* is potentially very interesting. Actin was detected in the peripodial epithelium during evagination and was expressed around the cell membrane. A hole or putative lumen was observed associated with intense staining around the stalk region (figure 9f). Examination of the stalk area in all actin-*lacZ* discs revealed that the peripodial cells stained intensely for actin. Actin outlined the cell shape indicating that actin was active in these areas.

There are two possible explanations for the presence of a lumen and actin expression in the area close to the stalk. Closure of the observed hole or lumen which was observed during elongation, would result in contraction of the peripodial epithelium during eversion. Contraction of the peripodial epithelium during evagination may be mediated by a collection of cells which express actin facilitating cell shape changes. In other morphogenetic processes such as dorsal closure, which results in the closure of a hole, the formation of an actin rich cable is present which facilitates the movement of a whole sheet of cells (Kiehart et al., 2000). In some peripodial cells actin appeared to be accumulated at one edge of the cell (figure 9f). In a similar way therefore the peripodial cells surrounding the lumen may form an actin rich cable at their leading edge facilitating the movement of peripodial epithelium.

Another possibility is that the actin-*lacZ* discs have sustained damage around the stalk region due to dissection. In the majority of dissections the imaginal discs were removed at the base of the stalk, leaving no stalk attached to the disc. The pattern of actin expression may be due to the role of actin in the wound healing process. Similar to dorsal closure, wound healing in *Drosophila* necessitates the movement of epithelium and accumulation of actin at one edge of cells (the leading edge) along the tissue margin (Wood et al., 2003, Martin and Pankhurst, 2004).

The elongated cell shapes observed surrounding the lumen during this study share similarities with wound healing images in zebra fish embryo's and *Drosophila* larvae (Martin and Pankhurst, 2004; Galko and Krasnow, 2004) (figure 9.2). Recent studies on wound healing in imaginal discs have shown that cell migration does not occur during this process. However the formation of an actin rich cable mediates the contraction of peripodial cells (Bosch et al., 2005).

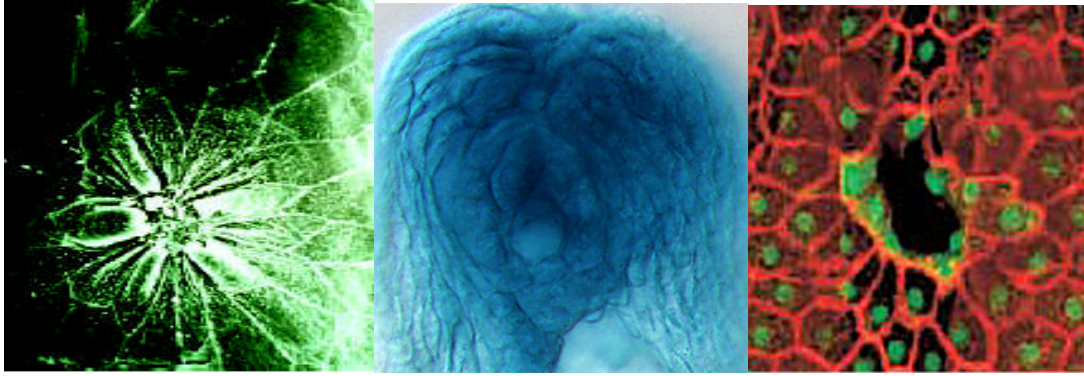


Figure 9.4: Wound healing in zebra fish embryo, left (Martin and Pankhurst, 2004) and *Drosophila* larvae, after 8 hours, on the right (Galko and Krasnow, 2004) compared to the leg disc of *Drosophila*, actin-*lacZ* centre.

Bryant and Fraser (1988) showed that fusion of *Drosophila* imaginal discs after wounding took twenty-four hours to perform. This would result in wound healing taking place during evagination and the actin expression detected by actin-*lacZ* around the stalk region is possibly a result of wounding.

The remaining results were disappointing. Visualisation of discs was poor due to the excess of mountant which was required to suspend the discs. Discs from transgenic flies were particularly sensitive to dissection and all discs from the transgenic fly line actin-GFP showed some damage (figure 9a). The majority of discs dissected from transgenic flies, actin-*lacZ* arrested during the early stages of evagination or did not proceed with evagination after initiation. Several issues can be addressed in order to improve visualisation, conserve the integrity of the disc and promote successful evagination in future experiments.

Imaginal discs were suspended in cavity slides due to their large size and the need to be unrestrained in order to accommodate the dynamic process of evagination. Construction of a cavity slide from glass coverslips should replace the traditional cavity slide. This reduced amount of mountant required will improve visualisation of the peripodial epithelium. Even though

discs were rinsed extensively, high background staining of the imaginal discs was observed. Residual staining fluid was also transported with the disc to the cavity slide, this means that in future prolonged and extensive rinsing of the discs should be carried out. Visualisation of the disc before actual completion of the cavity slide should also be carried out.

Examination of imaginal discs after a prolonged incubation at 16°C did not appear to perturb the development of wild-type discs. *In vivo* the imaginal discs transform into the adult structures in around twelve hours and evagination is completed in approximately six hours (Agnès et al., 1999). *In vitro* the process of evagination has also been shown to be completed in around six hours (Milner et al., 1987). Discs were examined after prolonged incubation as the process of evagination is slowed down allowing time to examine the discs individually. However the majority of discs dissected from transgenic flies arrested during incubation. In order to eliminate any abnormalities which may occur due to prolonged incubation at a lower temperature examination of the discs should take place immediately after dissection.

A number of discs dissected from transgenic flies did not respond to ecdysone. Imaginal discs were selected from third instar larvae which had reached the 'wandering stage'. The 'wandering stage' is a behavioural response triggered by changing ecdysone levels when the larvae move into prepupal development and enter pupariation (Fristrom and Fristrom, 1993). *In vivo* the metamorphic response to ecdysone is a pre-requisite to successful evagination. Damage incurred by discs dissected from actin-GFP transgenic flies may have affected the discs' response to ecdysone. In many cases the disc epithelium was damaged around the region of potential interest, the stalk. In order to prevent damage to discs in the region of the stalk, associated stalk

tissue and larval ectoderm should also be dissected.

As dorsal closure in *Drosophila* has been compared to the wound healing and actin is employed during both processes to facilitate changes in cell shape it would seem likely that the intense actin expression visualised close to the stalk region is being employed during changes in cell shape. Although data generated from the actin-*lacZ* discs has been the most informative in these studies, large numbers of fixed imaginal discs would be required in order to construct a comprehensive time course.

Real-time imaging of actin expression in the peripodial epithelium during the process of evagination would be the most informative and results from these experiments have prompted the following work. Transgenic flies moesin-GFP have been used successfully for studies on wound healing and dorsal closure in *Drosophila* (Bloor and Kiehart, 2001; Dutta et al, 2002). The fluorescent pattern observed in moesin-GFP flies is similar to the pattern produced by staining actin with fluorescent phalloidin (Edwards et al., 1997). Therefore for further exploration of morphogenesis in *Drosophila* imaginal wing discs using transgenic flies, moesin-GFP, will be examined.

Figures

Figure 9a: Leg disc transgenic fly line actin-GFP
 This DIC image shows the typical kind of damage incurred by discs from the transgenic flies actin-GFP during dissection. The damage is mainly situated in the proximal region of the disc at the stalk region.
 sr, stalk region; pe, peripodial epithelium; dp, disc proper
 Scale bar represents:50µm

Figure 9a: Leg disc, transgenic fly line actin-GFP

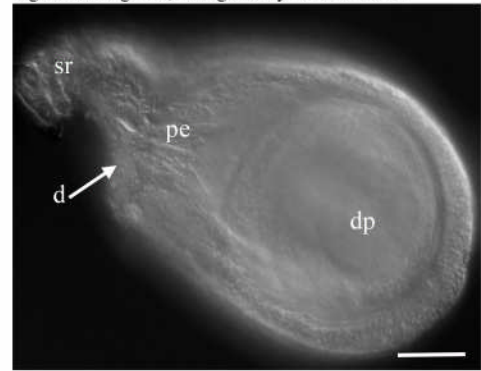


Figure 9b: Leg disc, actin-GFP
 Fluorescent image of the above leg disc showing that actin is highly expressed in tissue where damage has been done (d). Cells around the stalk region appear to be elongated, as outlined by actin. Actin also appears to be accumulated in discrete areas.
 d, damaged peripodial epithelium; s, stalk region; dp, disc proper.
 Scale bar represents:100µm

Figure 9b: Leg disc actin-GFP

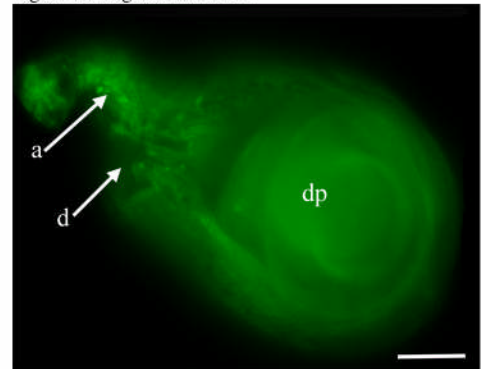


Figure 9c: Wing disc actin-*lacZ*
 Brightfield image showing the expression of actin in a wing disc during evagination using the reporter, *lacZ*. Actin expression was detected throughout the peripodial epithelium. In this image the expression of actin is particularly intense at the proximal region of the disc close to the stalk region. A stripe of actin extends from the proximal towards the distal end of the disc towards the tip of the appendage indicating possible contractile or cell shape changes in these areas. Haemocytes or adepithelial cells are loosely associated with the basal lamina.
 a, actin expression; pe, peripodial epithelium; c, haemocytes or adepithelial cells
 Scale bar represents:100µm

Figure 9c: Wing disc, actin-*lacZ*

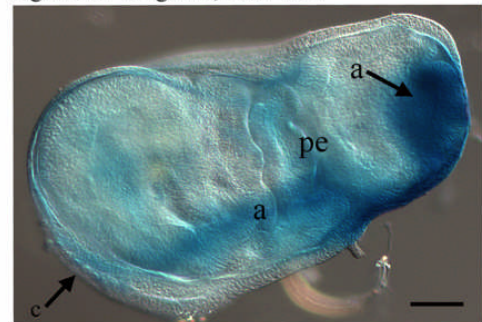


Figure 9d: Leg disc, actin-*lacZ*

Actin expression was detected throughout the peripodial epithelium in leg discs. In this brightfield image actin as reported by *lac-Z* was particularly intense around the region which would be situated close to the stalk.

pe, peripodial epithelium; s, stalk region

Scale bar represents: 100µm

Figure 9d: Leg disc, actin-*lacZ*

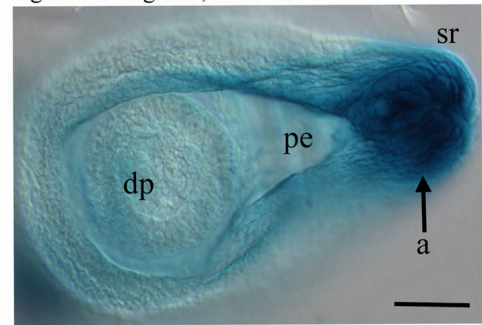


Figure 9e: Paired leg disc, actin-*lacZ*

The process of evagination is nearly completed in this bright field image of the paired leg discs. Actin expression can be seen throughout the peripodial epithelium in paired leg discs. Actin expression is particularly intense in a continuous region situated in the stalk region.

a, actin expression; pe, peripodial epithelium; s, stalk region.

Scale bar represents:50µm

Figure 9e: Paired leg disc actin-*lacZ*

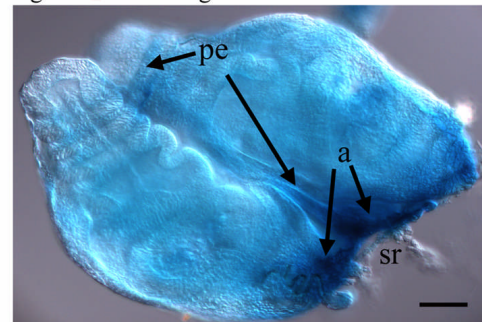


Figure 9f: Leg disc actin-*lacZ*, stalk region

Brightfield image showing the shape of the peripodial cells revealed by the expression of actin outlining the cell during the process of evagination. A putative lumen can also be seen which is represented by the area where no cells seem to be located. Cells surrounding the lumen are of mixed morphology, round, elongate and wedged shaped cells are present.

e, elongate cell; l, putative lumen; r, round cell; w, wedged shaped cells

Scale bar represents:50µm

Figure 9f: Leg disc actin-*lacZ*, stalk region

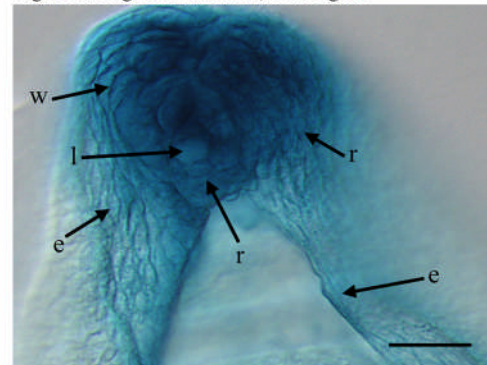


Figure 9g: Wing disc actin-*lac-Z*, stalk region

This brightfield image shows actin expression in the stalk region which stained intensely for actin. There appears to be a lumen (l) although this is difficult to visualise. The putative lumen is surrounded by peripodial cells, the outline of which is not obvious, but a range of morphologies appear to be present.

a, actin expression; l, lumen; t, trachea (larval)

Scale bar represents:50µm

Figure 9g: Wing disc actin-*lacZ*, stalk region

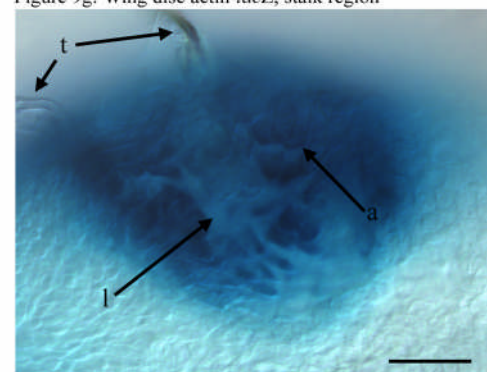


Figure 9h(i): Wild-type leg disc, immunofluorescence f-actin expression
 Immunofluorescence image showing that f-actin is detected throughout the wing disc. In a region close to the stalk a group of cells in the peripodial epithelium have stained more intensely for f-actin. Individual cell boundaries cannot be visualised.
 dp, disc proper; pe, peripodial epithelium; s, stalk
 Scale bar represents:50µm

Figure 9h(i): Wild-type leg disc, immunofluorescence f-actin expression

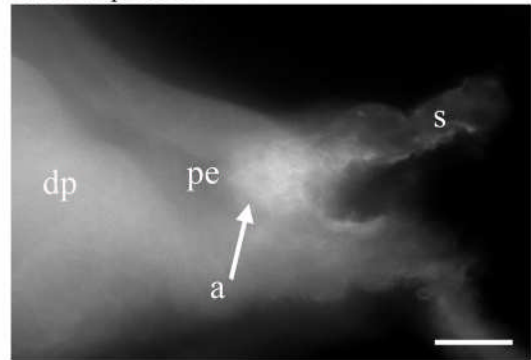


Figure 9h(ii): Leg disc, stalk region, peripodial cells
 Phase contrast image of the immunofluorescent image above showing large cells situated close to and along the stalk. These are peripodial cells or possibly stalk cells.
 dp, disc proper; pe, peripodial epithelium; s, stalk
 Scale bar represents:50µm

Figure 9h(ii): Leg disc, stalk region, peripodial cells

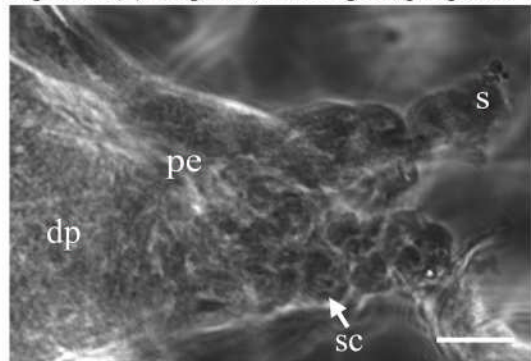
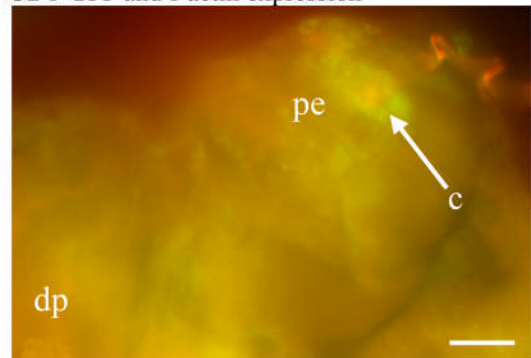


Figure 9i: Wing disc, immunofluorescence CD8-GFP and f-actin expression This immunofluorescent image of a wing disc reveals an area close to the stalk region which appeared to be more intensely stained for f-actin and CD8-GFP (figure 9i). Colocalisation of the CD8-GFP (green) and f-actin (red) was observed in this region which produced a bright yellow area. Individual cells can not be visualised.
 c, colocalisation; dp, disc proper; pe, peripodial epithelium;
 Scale bar represents:100µm

Figure 9i: Wing disc, immunofluorescence CD8-GFP and f-actin expression



Chapter 10

The Actin Ring

10.1: Introduction

During embryogenesis in *Drosophila* whole sheets of epithelium move during dorsal closure (Kiehart et al., 2000, Bloor and Kiehart, 2002, Jacinto et al., 2002). Dorsal closure is required at the end of germ band retraction when a hole is left, leaving the dorsal amnioserosa of the embryo exposed (figure 10.1). A combination of cell shape changes in the amnioserosa and lateral epithelium contribute to the closure of this hole. Movement of the lateral epithelium is mediated by the polarisation of the leading edge cells and the accumulation of filamentous actin at the apical edge. The concentration of f-actin at this 'free edge' extends the circumference of the epithelial margin and is described as an 'actin cable' (Jacinto et al., 2002). Contraction of the 'actin cable' leads to constriction and elongation of cells which then act like a 'purse-string'. The action of the actin cable in conjunction with filopodia 'zip' the opposing epithelial surfaces together (Wood et al., 2002).

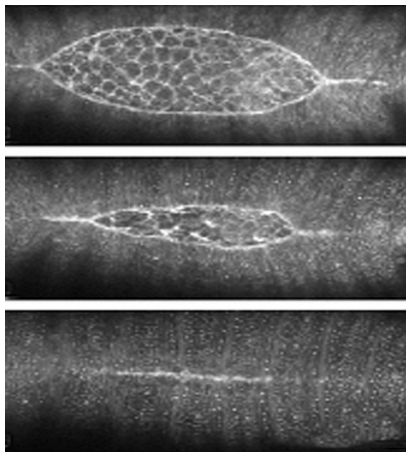


Figure 10.1: Dorsal closure during *Drosophila* embryogenesis: The top image shows the large hole which is left exposing the amnioserosa in the embryo after germ band retraction. The amnioserosa is gradually covered by the movement of the lateral epidermis from either side of the embryo coming together. This is accomplished by actin, cell elongation of the leading edge cells, filopodia and a 'zipping up' process (Kiehart et al., 2000).

The process of wound healing in *Drosophila* larvae proceeds in a similar way. An actin 'cable' assembles within minutes of wounding and cells surrounding the edge of the wound constrict and elongate. The closure of the wound is then mediated by the actin cable and filopodia (Wood et al., 2002).

The dynamic processes of dorsal closure and wound healing in *Drosophila* have been studied using transgenic flies expressing moesin-GFP (Bloor and Kiehart, 2001; Kiehart et al., 2002; Wood et al., 2002). Moesin is the *Drosophila* homologue of the moesin, ezrin and radixin group of vertebrate proteins which function as membrane-cytoskeleton linkers (Edwards et al., 1994; Brooke and Fehon, 1996). Moesin binds tightly to cortical actin which forms most of the cellular f-actin. Therefore moesin-GFP acts to identify the activation of actin and outlines the cell shape (Dutta et al., 2002).

Using actin-*lacZ* transgenic flies, a region around the stalk area in fixed imaginal disc tissue has been identified where cells stained intensely for actin expression. This has prompted the possibility that contraction of peripodial epithelium is potentially mediated by a lumen associated with actin rich ring of cells or that the discs have been damaged during the dissection and the process of wound healing has been identified. Using moesin-GFP flies and improved culture initiation techniques real-time imaging of the process of evagination will be undertaken.

10.2: Materials and Methods

In order to identify a lumen associated with peripodial epithelial contraction, wing discs dissected from transgenic flies expressing moesin-GFP were used to illuminate the actin cytoskeleton. Transgenic flies which express the moesin-GFP construct were kindly provided by Paul Martin.

10.2.1: Imaginal Disc Dissection

Imaginal wing discs and associated stalk tissue were dissected from third instar larvae of transgenic flies expressing moesin-GFP. Wing discs were

placed in medium only or in medium with 100ng/ml ecdysone and suspended on cavity slides made from glass coverslips using two glass coverslips as spacers. All discs were examined immediately after initiation.

10.2.2: Microscopy and image analysis

Analysis of peripodial cell shape changes during evagination was undertaken using Adobe Photoshop V5. Sequential images from the microscopic examination of the discs were layered into a photoshop file and where possible the outline of cells drawn. Cell diameters were measured, the diameter of the cell was defined as the distance between the lateral cell boundaries of the cell.

There is no figure 10l or 10o

10.3: Results

10.3.1: Actin expression moesin-GFP wing discs

General observations

Live imaging of wing discs dissected from the transgenic fly line moesin-GFP revealed the presence of actin expressed throughout the wing disc. As the process of evagination progressed intense actin expression was observed outlining peripodial cells in the proximal region of the disc, close to the stalk. Due to the constant changes in wing disc orientation during the process of evagination observations and images have been combined from a series of images taken from 2 wing discs in particular. One disc was visualised close to the onset of elongation (figure 10a) a second disc was observed where elongation had progressed further (figure 10b). The presence of a lumen surrounded by peripodial cells expressing actin was observed in 7 wing discs

out of 18 culture preparations. The peripodial epithelium could not be visualised in the remaining 11 discs due to the orientation of the discs during evagination. We will now consider morphogenesis in two individual discs.

10.3.2: Wing disc one

Observations from imaginal wing discs immediately after culture initiation showed the presence of a lumen surrounded by peripodial cells situated close to the stalk (figure 10c(i)). The orientation of the wings discs prevented a direct view of the lumen which was situated towards the right hand side of the wing disc. Actin expression remained particularly intense throughout contraction and elongation of the disc proper in peripodial cells situated at the proximal end of the disc and surrounding the lumen in the stalk region. The outline of the peripodial cells was evident and they appeared to be orientated towards the lumen (figure 10c(i)). Actin expression was also intense in a line of peripodial cells which extended towards the distal region of the disc towards to presumptive wing blade (figure 10c (i)).

During the initial stages of elongation the wing discs underwent small morphogenetic movements. The proximal and distal ends began to curl upwards and towards one another and the folded columnar epithelium of the disc proper began to expand (figures 10c(ii,iii)). This was accompanied by circumferential constriction of the proximal region of the wing disc. At the same time the area covered by the peripodial epithelium at the proximal region contracted.

During contraction of the peripodial epithelium the lumen was observed to change shape, becoming more elongate in appearance. The lumen did not close and was present throughout this period of elongation. At this point a

change in disc orientation prevented further visualisation of the lumen (figure 10d). Visualisation of the wing disc from the side showed that the peripodial epithelium appeared to be thicker at the stalk region where areas of intense actin expression were observed, although individual cells were hard to distinguish. As evagination proceeded the peripodial epithelium covering the median section of the disc proper appeared to be stretched and thinner as the wing blade began to unfold (figures 10e,f). The process of elongation of the wing disc within the confines of the peripodial epithelium proceeded until near completion (figure 10g). At this point the peripodial epithelium was still in evidence although the cells surrounding the margin of the wing blade may have been the result of peripodial epithelium degeneration.

10.3.3: Cell morphology and size analysis

Closer examination of the peripodial cells surrounding the lumen and along the margin between the peripodial epithelium and disc proper revealed that a variety of cell shapes and sizes were present in the stalk region (figures 10h(i,ii,iii)). A number of cells had undergone a change from a squamous to more elongate or diamond shaped morphology. Rounder and smaller squamous cells were also present. Measurements of the peripodial cells during this period showed that a majority of large cells were present at the onset of observation (figure 10h(iv)). The average diameter of the peripodial cells was between 20-30 μ m (figure 10h(iv) red outline). As evagination proceeded the average cell diameter situated in the stalk region was 10-20 μ m (figure 10h(iv) green outline). Prior to a change in disc orientation the majority of cells measured between 5-15 μ m in diameter (figure 10(iv) blue outline). The shape and size of the lumen also changed, becoming more elongate as evagination proceeded in the wing disc (figures 10h(i,ii,iii)).

10.3.4: Wing disc two

The observations made on this wing disc began when a change in disc orientation made it possible to observe the stalk region which was approximately 2 hours after initiation. An area which appeared to be an opening to a putative lumen was observed, which was situated in the stalk region of the disc (figure 10i). Peripodial cells were orientated around the lumen where the expression of actin outlining the cells immediately adjacent to the lumen was particularly intense (figures 10i). Closer examination of peripodial cells in the immediate area surrounding the lumen revealed that cells were oblong (trapezoidal) and wedged shaped in appearance (figure 10i(i)). The lumen and cells next to the lumen appeared to be below the plane of the peripodial epithelium. Actin expression was particularly intense in some cells adjacent to the lumen, at times an accumulation of actin was observed in cells (figure 10i(i),10j). The configuration of the lumen and actin expression outlining cells changed very quickly (figures 10i(i),10j,10k). Peripodial cells appeared three or four cell rows away from the lumen (figure 10j). These cells appeared to be under tension as they were elongate in morphology. There also appeared to be the formation of a groove which ran along from the tip of the lumen to the dorsal side of the disc (figure 10j). Minutes later the expression of actin in cells close to the lumen formed an actin ring (figure 10k). Cells within the boundary of the actin ring and adjacent to the lumen were also expressing actin although it was difficult to visualise the changes in cell shape. As these changes in actin expression were taking place, changes in the disc proper occurred. The space between the furrows expanded and the wing blade curled further forward (figures 10j,10k).

Visualisation of the wing discs in phase contrast microscopy revealed an area of peripodial cells present in the stalk region which appeared to be raised and which corresponded to the immunofluorescence of peripodial cells expressing actin most intensely (figure 10m(i,ii,iii)). A small dark line was observed in the peripodial tissue which corresponded to the lumen visualised by immunofluorescence microscopy (figure 10m(ii)).

Reorientation of the wing disc revealed that a thickened area of peripodial tissue was situated at the stalk region (figure 10n). Measurements of the depth of peripodial tissue at this point indicated that the peripodial tissue was approximately 30µm (figure 10n(i)). Actin expression in the wing disc was evident in areas of the thickened tissue. Peripodial cells which had formed a thickened strand of epithelium emanated from the region of the stalk extending towards the distal region of the disc ((figures 10p(i,ii) 10q(i,ii)). Individual cells could not be visualised but actin expression was intense along the strand and at the stalk region.

As elongation progressed measurement of the depth of peripodial tissue at the stalk region point indicated that the tissue was approximately 40µm (figure 10q(ii)). The strands of peripodial cells emanating from the stalk region stretched to accommodate morphogenesis in the disc proper. Becoming taut as the disc proper expanded and twisted, contracting as the disc proper contracted (figures 10q (i,ii,iii)). A change in disc orientation at this point prevented further observations.

10.3.5: Cell morphology and size analysis

During the process of evagination the arrangement of peripodial cells surrounding the lumen also changed. Images taken shortly after observations

began until the time evagination ceased showed the extent of elongation of the wing disc (figures 10r(i,ii)). Actin expression in cells extended towards the stalk (figure 10r(iii)). A mixture of cell morphologies was observed although the larger cells appeared to be of regular and compressed hexagonal morphology, trapezoidal and rounder cells were also apparent. Outlining the shape of the peripodial cell, where possible, showed that the cell diameters varied in the stalk region. At the onset the average diameter of the peripodial cells was found to be 15-25 μ m (figure 10r(iv) red outline). As elongation progressed a larger number of smaller cells were present in the stalk region, the average cell diameter was 10-15 μ m (figure 10r(iv) green outline).

10.4: Discussion

10.4.1: The lumen

Real-time imaging of the peripodial epithelium during evagination of wing discs, in the transgenic fly line *moesin-GFP*, identified a hole or putative lumen present in the stalk region of the imaginal wing discs (figure 10a). Peripodial cells which changed shape and size during evagination were orientated towards the lumen. Actin expression was particularly intense in peripodial cell situated in the stalk region and an 'actin ring' was visualised (figure 10j). These results concur with the results from the previous chapter using transgenic flies *actin-lacZ*. As no apparent damage appeared to be incurred by the wing discs the lumen is not associated with the wound healing process. The implication is that the lumen is a real phenomenon. The presence of the lumen found at the stalk during evagination in association with peripodial cell shape changes could indicate a role for the lumen during evagination. Movement of sheets of epithelial cells are associated with holes and closure of, as in dorsal closure and wound healing (Kiehart et al., 2000,

Bloor and Kiehart 2002, Jacinto et al., 2002; Wood et al., 2002). Therefore the lumen potentially plays an active role in the contraction of the peripodial epithelium during elongation and eversion.

The role of the peripodial epithelium during evagination has been regarded as acting mainly to contract during eversion and so aiding the adult appendage out to the external surface. However the results suggest that contraction of the peripodial epithelium also takes place during the initial stages of elongation. During the early stages of evagination contraction of the peripodial epithelium at the proximal or stalk region may be required in order to facilitate the constriction and reorganisation of columnar cells in the disc proper. Peripodial cells have been shown to form microtubule-based translumenal extensions during the mid-third instar stage which traverse acellular space (Gibson and Schubiger, 2000). Contact via the peripodial extensions to the disc proper is required for furrow progression in the eye disc. In many discs these extensions terminate on the surface of developing columnar epithelia of the disc proper. In the wing disc direct contact between the peripodial cells and the disc proper is required in order for bristle and trichome development to proceed (Gibson and Schubiger, 2000). It is possible that signalling from the peripodial epithelium may also be required in order for the disc proper cells to proceed with elongation. Therefore it may be important that during evagination directed movement of the wing disc peripodial cells ensures they are in close or direct contact with the cells of the disc proper at the appropriate time and place.

Previous studies on elongation *in vitro* have indicated that there is an increase in peripodial epithelium surface area during elongation (Milner et al., 1984). The thickness of the epithelium is greatly reduced, with little or no cytoplasm observed between the cell membranes. Peripodial cells at the distal region

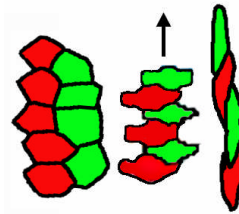
appeared to remain squamous and little change was observed in their shape or size. A reduction in peripodial cell size around the stalk area would result in cell re-arrangement and a subsequent reduction in the total surface area of peripodial epithelium. Stretching of the peripodial cells at the distal end of the epithelium by the elongating appendage would result in the dramatic decrease of epithelial thickness found. In addition the contraction of peripodial cells at the proximal region during this point of elongation may be required in order to maintain stability of this region in the disc proper whilst the distal end changes shape.

During both dorsal closure and wound healing the holes or wounds require that a hole is closed. The movement of epithelia is mediated by a row of actin rich cells, the 'actin cable' which acts like a purse string pulling tissue together. During eversion, contraction of the peripodial epithelium may be mediated by the closure of the lumen at the stalk region, thereby facilitating the movement of the appendage towards the region of the stalk where eversion takes place. As the lumen appeared to be quite small the net movement of peripodial epithelium would also be quite small. However only a small contraction may be required as recent evidence suggests that the stalk cells become highly mobile and move out to form an extended area through which the appendage everts. This does not require extensive contraction of the peripodial epithelium (Pastor-Pareja et al., 2004).

Actin expression in the cuboidal outer peripodial cells which formed the margin was particularly intense during the initial stages of elongation. These peripodial cells elongated to form thickened strands of cells (figure 10q). The thickened strands of cells emanated from the region of the stalk where the lumen was situated. During elongation of the disc proper the thickened

strands appeared taut and then slackened off to accommodate the changes in morphology of the disc proper. The transformation of cuboidal or squamous cells to elongate thickened strands is possibly an example of convergent extension; during convergent extension, a tissue narrows along one axis while extending along a perpendicular axis (Keller, 1986) (figure 10.2). Convergent extension usually involves cell intercalation, the rearrangement of the cells then forming longer, narrower tissue (Condic et al., 1991, Keller et al., 1991).

Figure 10.2: Convergent extension in the peripodial epithelium:
A proposed model of cell intercalation of the peripodial cells in order to form thickened strands observed during evagination.



During development convergent extension plays an important role during gastrulation, germ band extension and evagination on the disc proper in *Drosophila* (Fristrom, 1976; Kam et al., 1991; Irvine and Wieschaus, 1994). Convergent extension also plays a role during embryogenesis in *Xenopus laevis* and sea urchins and dorsal hypodermis formation in *C. elegans* (Ettensohn, 1985; Keller et al., 1991; Williams-Masson et al., 1997). During development convergent extension is most often associated with major alteration of the body plan which occurs during embryogenesis; from spherical balls of cells to longer narrower body forms. Convergent extension also plays a role in formation of large tissues and organs such as the tracheal system and gut (Lengyel and Iwaki, 2002 cited by Lecuit, 2005). However 'convergent extension' has been found in *C. elegans* whereby intercalation of two adjacent rows of cells lead to the formation of single cell chains (Heid et al., 1998). This is reminiscent of the description of the thickened strands of peripodial cells, although how many cell rows intercalate, if any, is unknown. Changes in cell shape contribute to convergent extension, this may account for the intense actin expression observed in these cells during elongation.

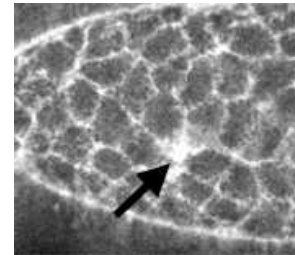
Intercalation of the cuboidal peripodial cells to form epithelial strands would give added strength and elasticity to the epithelium when stretched by the elongating wing blade. The strands may also prevent the premature rupture of the peripodial epithelium by the elongating appendage. Protection of the developing appendage would be required during metamorphosis as larval cells breakdown and release harmful digestive enzymes. Interestingly the non-canonical PCP signalling pathway (planar cell polarity pathway as discussed in previous chapters) is required for convergent extension movements in vertebrates (Park and Moon, 2002, Munoz et al., 2006). It has been proposed that modification of the invertebrate PCP pathway, with extra signalling molecules, has occurred in vertebrate systems (Wallingford, 2004).

Filopodia and lamellipodia are associated with wound healing and dorsal closure (Jacinto et al., 2000, 2002). Filopodia and lamellipodia were not in evidence in these studies. Closer examination of cells may be required than was possible at this time, to reveal whether these were present. However during re-epithelialisation after wounding mouse embryos lamellipodia were not observed extending from the leading edge cells when compared to the adult (McClusky and Martin, 1995).

During dorsal closure individual cells of the amnioserosa are observed dropping out of the plane of the epithelial surface pulling adjoining cells over themselves as they do so (Kiehart et al., 2000). Has the number of peripodial cells visible in the epithelium also decreased? In the wing disc approximately 400 peripodial cells are present at the end of the third instar larval stage. Although it was not possible to count the cells at this time, if cells had dropped out of the surface of the epithelium their presence should have been apparent. No extraneous peripodial cells were observed on the surface of the epithelium but a number of cells identified as potentially aepithelial or

haemocytes were observed around the margin of the disc (figure 10a). However the accumulation of actin observed in some peripodial cells during elongation (figure 10j) is similar to images of the amnioserosa cells which drop out of the plane during dorsal closure (Kiehart et al., 2000) (figure 10.3).

Figure 10.3: The accumulation of actin at the apical end of the cell (arrow) results in the cell dropping out of the plane of the amnioserosa (Kiehart et al., 2000).



Peripodial cells may gradually drop out of the plane beneath the epithelium and pull other peripodial cells over themselves; this would contribute to a reduced area of peripodial epithelium required for evagination (Milner et al., 1983). An accumulation of cells at the stalk region would also account for the thickened peripodial tissue which was observed at the stalk region in the wing discs (figure 10p).

Contraction of the peripodial epithelium at the lumen more closely resembles descriptions of the amnioserosa and not the lateral epithelium during dorsal closure. Like the peripodial epithelium, the amnioserosa is composed of squamous cells surrounded by the lateral epidermis of the retracted germ band. During dorsal closure as the lateral epithelium comes together the more central amnioserosal cells undergo cell-shape changes. The cells constrict apically which results in the bulk of their cytoplasm being pushed into the interior of the embryo (Kiehart et al., 2000; Hutson et al., 2003). There is an alternate and intriguing possibility that the disc proper is forcing the contraction of the peripodial epithelium. During elongation the disc proper cells from each side of the peripodial epithelium come together at the

proximal region and this may force shape changes in the peripodial cells. Pushing peripodial cell cytoplasm into the region between the epithelia layers would also result in thickened peripodial tissue which was observed close to the lumen. In addition removal of the amnioserosa inhibits zipping and closure of the embryo fails, similarly removal of the peripodial epithelium results in loss of eversion of the adult appendage (Hutson et al., 2003; Milner et al., 1984).

The formation of an actin ring which mediates contraction of the peripodial epithelium is fundamentally different from the actin rings associated with wound healing and dorsal closure. The lumen did not appear to close at any time although it did appear to get smaller. One possible scenario is that the cells of the peripodial epithelium may change shape and move out of the plane at times but are reinstated when required. In addition the actin ring or actomyosin cable was not present throughout elongation of the wing disc. Studies suggest that during dorsal closure the actomyosin cable may act to restrain epithelial cells at the leading edge so that movement of the epithelial cells occurs in a uniform manner (Bloor and Kiehart., 2002; Jacinto et al., 2002). As the appearance of the actin ring in the wing disc was accompanied by the curling forward of the wing blade this suggests that at times whole rows of peripodial cells are required to advance. It would be interesting to see if the actin ring was indeed transient or present throughout evagination but not visualised in these studies.

An interesting hypothesis is that the lumen has arisen due to invagination of peripodial epithelium. As in dorsal closure and wound healing, epithelial invaginations involve changes in cell shape (reviewed in Ettensohn, 1985; Leptin and Grunewald, 1990). Invagination of peripodial cells during evagination would contribute to peripodial epithelium contraction.

During gastrulation in *Drosophila* and epiboly in zebra fish embryos invagination of tissue also requires changes in cell shape (Leptin, 1999; Oda and Tsukita, 2000; Cheng et al., 2004; Köppen et al., 2006). The process of invagination includes apical constriction to produce wedge shaped cells, a shallow groove stage associated with cell elongation followed by cell shortening and inward movement of the cells.

10.4.2: What evidence is there to support the hypothesis that peripodial cells invaginate?

At the end of the third instar larval stage, prior to metamorphosis, the peripodial epithelium is made up of large squamous and cuboidal cells measuring 20-30 μm in diameter. In this study measurement of peripodial cells during the initial stages of elongation in the wing disc indicated that peripodial cells in the stalk region had already undergone changes in morphology from squamous to elongate and a reduction in cell size. As elongation proceeded cells in the region of the stalk became smaller measuring approximately 10 μm diameter although smaller cells of 5 μm were present. This suggests that the process of columnarisation has occurred in some peripodial cells and that these cells could measure up to 20 μm in the long axis. The thicker tissue observed at the stalk region (figure 10 q(ii)) measured up to a depth of 40 μm towards the end of elongation. This suggests that there are two or more layers of peripodial cells located in this region. As cells do not divide in the peripodial epithelium during evagination the most likely explanation is that during evagination peripodial cells have invaginated.

In 1985 Ettensohn proposed that if epithelium cells become broader at one apex than another, this could produce an invagination he also states that

placodes of tissue are associated with these invaginations. During elongation the peripodial cells surrounding the lumen may have become wedge or flask shaped. The raised tissue observed by phase microscopy could be a placode (figure 10m). However further investigations will be required in order to identify the origin of the lumen and if peripodial cells change shape and invaginated as proposed.

Actin and nonmuscle myosin are implicated in cell shape changes associated with dorsal closure, wound healing and invagination of epithelial cells (Young et al., 1992; Kiehart et al., 2000; Köppen et al., 2006). The actin cytoskeleton plays a role in cell shape changes in the columnar disc proper cells (Condic et al., 1991). The adult leg telescopes out along the proximodistal axis and constricts along its circumference. These morphogenetic movements are driven by changes in cell shape (Gates and Thummel, 2000). Cells observed surrounding the lumen in the peripodial epithelium expressed actin throughout the process of elongation. This probably means that cell shape changes in the peripodial epithelium, like other cell shape changing processes such as dorsal closure, are mediated via actin.

Although a time series of images during the process of evagination was made where possible, continuity was poor due to loss of focus during which time the disc orientation changed, making it impossible to follow individual cells. Further studies on the contraction of the peripodial epithelium using live imaging techniques such as confocal microscopy will be useful. The lumen may not have been present throughout wing disc evagination. As the final fate of the lumen during eversion was not visualised and it is possible that the lumen remains open throughout eversion of the adult appendage, it would be interesting to discover if the lumen found in the stalk area was alone responsible for the peripodial contraction. Although a single lumen was

visualised in the wing disc peripodial epithelium, multiple lumens may arise during evagination of discs, such as the eye discs which undergo more complex morphogenetic movements.

Although changes in cell shape appear to be mediated around the peripodial actin ring it would be difficult to test whether the actin ring in the stalk area is responsible for contraction. Repeated ablation of cells in the amnioserosa during dorsal closure showed that actin is rapidly recruited to the margins of the wound and dorsal closure still proceeds (Kiehart et al., 2000). Gibson and Schubiger (2000) genetically ablated the peripodial epithelium using a peripodial specific Gal4 driver combined with a UAS Ricin transgene. Surgical or genetic ablation of tissue in the stalk area may only result in a newly formed lumen. Genetic ablation would also require a Gal4 driver that was specific for peripodial cells situated in the stalk region of the peripodial epithelium.

Studies made on the disc proper and changes in cell shape are thought to be mediated by the apical contractile belt which is composed of actin and nonmuscle myosin II and is attached to the inner surface of the cell at intercellular adherens junctions. The molecular motor protein nonmuscle myosin II drives the contraction of the actin cytoskeleton (Bloor and Kiehart, 2002). Mutations in genes which encode subunits of nonmuscle myosin II result in loss of cell intercalation and defects in dorsal closure and leg elongation (Bertet et al., 2004; Bloor and Kiehart, 2002). To examine whether nonmuscle myosin II was present in the peripodial epithelium, antibody anti-*Dm*-nonmuscle myosin II was used (kindly provided by Dan Kiehart). However despite repeated attempts, antibody anti-*Dm*-nonmuscle myosin II staining was not successful. This may have been partly due to the age of antibody, which was 10 years old (personal communication D. Kiehart). The

use of cytoskeletal disrupting drugs such as cytochalasin and nocodazole was also considered but these drugs would also affect the columnar disc proper cells.

Migration of whole sheets or individual cells is essential during morphogenesis. Many genes and proteins expressed during dorsal closure, gastrulation and germ band retraction could be expressed during epithelial cell movement and shape change in the peripodial epithelium. However one of the constraints of using mutant fly strains to examine imaginal disc morphogenesis is the failure of the embryo to proceed past embryogenesis. Cdc42 is a small GTP-ase which regulates filopodia assembly in fibroblasts and dorsal closure; mutants undergo developmental arrest before larval stages (Genova et al., 2000). Armadillo mutants disrupt gastrulation (Cox et al., 1996). *Drosophila* RhoA plays a role in dorsal closure, inactivation of RhoA leads to loss of cell-cell adhesion and is associated with loss of cell polarity and e-cadherin (Bloor and Kiehart, 2002). Decapentaplegic (Dpp) is secreted in the eye disc peripodial cells during development of the columnar epithelium (Cho et al., 2000). Dpp also plays a major role in defining the location and fate of the leading edge cells during dorsal closure (Jacinto et al., 2002). Comparison of genes and proteins such as *puckered* and *canoe* required for cell shape changes expressed during early morphogenetic processes such as dorsal closure may be difficult (Glise and Noselli, 1997; Agnes et al., 1999; Pastor-Pareja et al., 2004; Jacinto et al., 2002).

Live imaging of imaginal discs derived from transgenic flies using a peripodial specific Gal4 driver would be an instructive way in which to identify if the peripodial cells are the only cells involved in contraction and the lumen (this was attempted but was unsuccessful). The protein *puc* is expressed in leading edge cells in dorsal closure, imaginal discs derived from

puc-lacZ reveal groups of cells which stain for *puc*. These have been identified as stalk cells and peripodial cells (Usui and Simpson, 2000). Using *puc*-GFP transgenic flies it may be possible to identify a role for *puc* in peripodial cells during elongation of the disc proper and/or follow the fate of peripodial and stalk cells. Transgenic flies (*Dmcd-GFP*) have also been generated by Oda and Tsukita (2000) which visualise the adherens junctions. Visualisation of the adherens junctions may be useful in identifying how cell-cell interactions change during elongation in the imaginal disc.

In the future investigations could be undertaken in how control of cell-cell and cell-matrix adhesion is mediated during peripodial epithelium contraction. Contraction of the peripodial epithelium which involves changes in cell shape and cell re-arrangement will be accompanied by changes in cell-cell and cell-matrix adhesion. It is possible that the peripodial cells located close to the lumen may differ in terms of their adhesion properties, when compared to the peripodial cells located at the distal region of the disc. Studies already undertaken on the organisation of septate junctions in imaginal discs has lead to the proposal that there is dynamic re-arrangement of the septate junctions during cell re-arrangement (Fristrom, 1982). The above possibilities could be examined using electron microscopy. Imaginal discs are also known to secrete proteases when exposed to ecdysone. This may be in order to loosen the cell-matrix contact in order to facilitate movement of the peripodial cells during elongation (Pino-Heiss and Schubiger, 1989).

In the past studies have generally focused on the disc proper cells during *Drosophila* imaginal disc morphogenesis and it has been shown that the peripodial cells changed from squamous to columnar during this time (Fristrom and Fristrom, 1973). It appears that, similar to dorsal closure,

wound healing and gastrulation, actin and most likely nonmuscle myosin II, are responsible for the cell shape changes observed in the peripodial cells. A potential mechanism behind the cell shape change and contraction had not previously been identified. From the evidence presented above it seems likely that the formation of the lumen co-ordinates cell shape changes and contraction of the peripodial epithelium, thereby facilitating morphogenesis of the disc proper.

Although this study has concentrated on *Drosophila*, Nardi et al (1987) also found that during wing disc evagination in the Lepidopteran *Manduca sexta* the cuboidal peripodial cells became columnar. They proposed that cell shape changes could be a general mechanism for epithelial morphogenesis. It would be interesting to explore whether a lumen was also present in the peripodial epithelium of Lepidopteran *Manduca sexta*. Imaginal disc morphogenesis in all holometabolous insects may be dependent on active cell migration and invagination of peripodial epithelial cells, thereby contributing to the successful formation of the adult integument.

Figures

Figure 10a: Wing disc one, moesin-GFP.

Fluorescent image showing actin expression in the wing disc during the initial stages of elongation. A putative lumen was observed in the region of the stalk area (l). The lumen was surrounded by peripodial cells and the expression of actin outlining the cells immediately adjacent to the opening was particularly intense. Cells of ad epithelial or haemocyte origin can also be seen along the outer edge of the disc.

c, cells of ad epithelial or haemocyte origin; dp, disc proper; l, lumen; pe, peripodial epithelium; s, stalk; sr, stalk region

Scale bar represents:100µm

Figure 10a: Wing disc one moesin-GFP

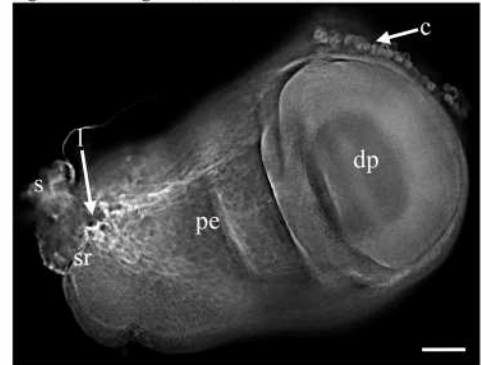


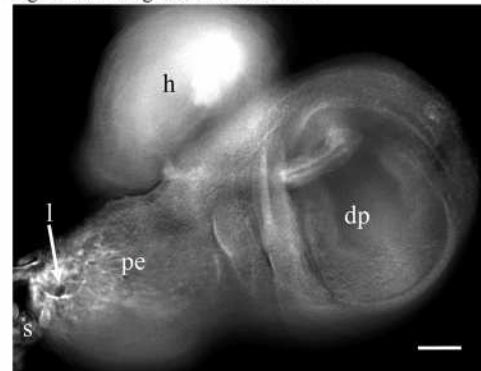
Figure 10b: Wing disc two, moesin-GFP

Visualisation of actin expression present in the wing disc during later stages of elongation. A lumen can be seen in the proximal region close to the stalk surrounded by peripodial cells. Cell shapes have been outlined by actin expression and an actin ring has formed in cells situated 2-3 cells distant from the lumen.

dp, disc proper; h, haltere; l, lumen; pe, peripodial epithelium; s, stalk

Scale bar represents:100µm

Figure 10b: Wing disc two moesin-GFP



Figures 10c(i,ii): Wing disc one moesin-GFP
 10c(i) immediately after initiation (ii) 2 hours
 after dissection

Immunofluorescent images visualising actin expression in the wing discs. The orientation of the wing discs prevented a direct view of the lumen in this disc which was situated towards the right hand side. Expression of actin can be seen outlining peripodial cells close to the lumen which initially appears to be round in shape. The peripodial cells also appear to be orientated towards the lumen. Intense actin expression can be seen in a line of peripodial cells which extend from the proximal region close to the lumen towards the distal end of the prospective wing blade. In figure (10c(ii)) the disc appears shorter as it has begun to curl upwards.

c, putative haemocytes or ad epithelial cells; l, lumen; pe, peripodial epithelium; s, stalk
 Scale bar represents:100µm

Figure 10c(iii): 2 hours 55 minutes after initiation.

Although the wing disc appears to be smaller lengthways and widthways, the proximal and distal ends have begun to curl upwards towards one another and the folded columnar epithelium of the disc proper is beginning to expand. The lumen has also changed shape becoming more elongate. The area of peripodial epithelium situated in the stalk region, where actin expression was particularly intense in 10c(i), appears to have contracted in this disc as elongation has proceeded.

c, putative haemocytes or ad epithelial cells; l, lumen; pe, peripodial epithelium; s, stalk.
 Scale bar represents:100µm

Figures 10c(i,ii): Wing disc one, moesin-GFP
 (i) Immediately after dissection (ii) 2 hours after dissection

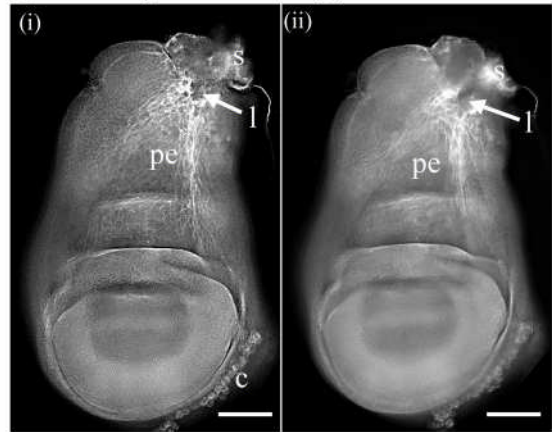
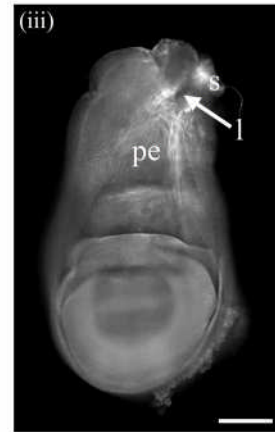


Figure 10c(iii): 2 hours 55 minutes after initiation.



A series of immunofluorescence images follows showing the elongation of the wing disc, 3 hours after culture initiation 10d, to the point at which evagination halted 10g, 5½ hours after initiation.

Figure 10d: Wing disc one, moesin-GFP, orientation change during elongation.

Immunofluorescent image showing the morphogenetic movement of the wing disc as elongation proceeds. The proximal and distal ends of the disc have curled upwards towards one another and the folded columnar epithelium of the disc proper has expanded.

s, stalk region; pe, peripodial epithelium; wb; wing blade
Scale bar represents:100µm

Figure 10d: Wing disc one moesin-GFP, disc orientation change during elongation

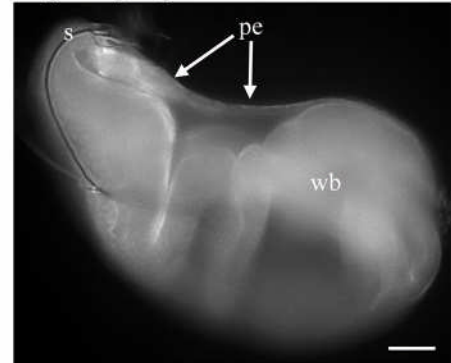


Figure 10e: Moesin-GFP elongation of wing disc

Fluorescent image of the wing disc showing further changes in as elongation proceeds. The stalk region can no longer be visualised, the peripodial epithelium is stretched during further movement and elongation of the developing appendage. The folded columnar epithelium of the disc proper is unfolding (u).

pe, peripodial epithelium; u, unfolding; wb; wing blade
Scale bar represents:100µm

Figure 10e: Moesin-GFP wing disc elongation

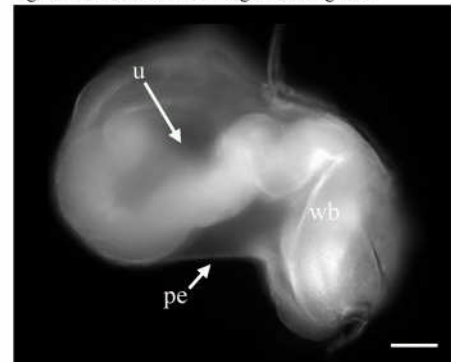


Figure 10f: Wing disc one, moesin-GFP

This fluorescent image shows further unfolding and elongation of the wing blade. The stalk region still cannot be visualised, the peripodial epithelium has stretched further to accommodate the elongating appendage.

pe, peripodial epithelium; wb, wing blade
Scale bar represents:100µm

Figure 10f: Wing disc one, moesin-GFP

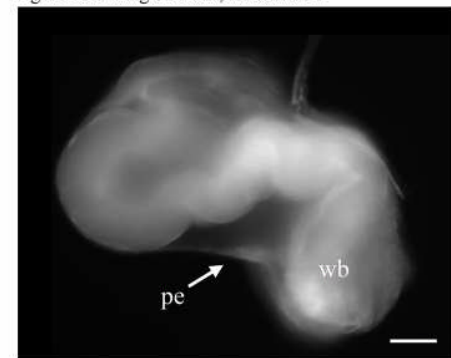


Figure 10g: Wing disc, elongation near completion

Fluorescent image showing the wing disc which was nearing completion of the process of elongation within the confines of the peripodial epithelium. The peripodial epithelium is still in evidence although cells which can be seen surrounding the margin of the wing blade may be an indication that the peripodial epithelium has been ruptured.

c, cells; pe, peripodial epithelium; wb, wing blade
Scale bar represents:100µm

Figure 10g: Wing disc, elongation near completion

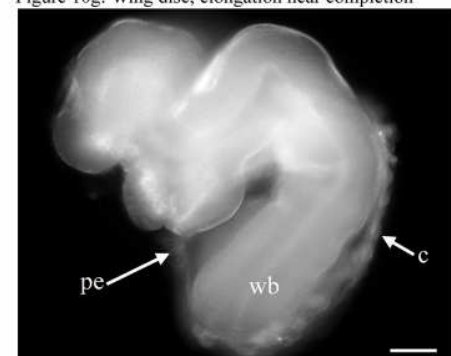
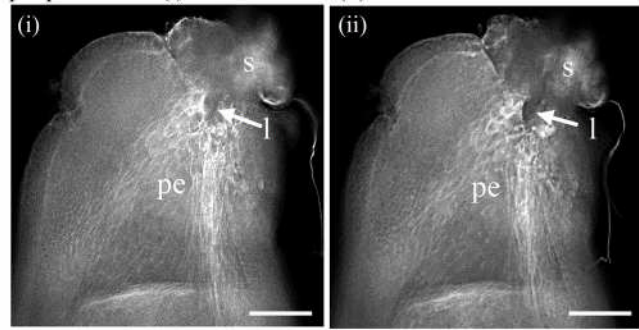


Figure 10h(i,ii): Image analysis, stalk region, lumen and peripodial cells
 10h(i) Immediately after initiation

In this close up image of the stalk region, actin expression can be seen outlining peripodial cells close to the lumen. The lumen is round in shape. Peripodial cells appear to be orientated towards the lumen and a line of peripodial margin cells which extend from the stalk region towards the distal end of the prospective wing blade show intense actin expression. l, lumen; m, margin cells; pe, peripodial epithelium; s, stalk

Scale bar represents: 100µm

Figure 10h(i,ii): Fluorescence, stalk region, lumen and peripodial cells (i) After initiation (ii) 2 hours after initiation.



10h(ii) 2 hours after initiation

This image taken two hours after 10h(i) shows that the peripodial cells are still orientated towards the lumen but the intensity of actin expression in cells has changed. The lumen also appears to be more elongated and although actin expression can still be observed in the peripodial margin cells which extend from the proximal region close to the lumen it does not appear to be so intense. l, lumen; pe, peripodial epithelium; s, stalk

Scale bar represents: 100µm

Figure 10h(iii): 2 hours 55 minutes after initiation

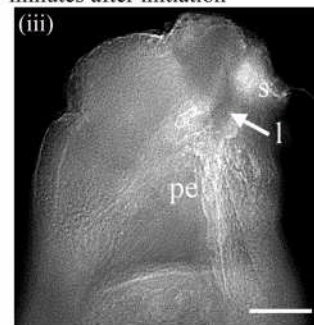


Figure 10h(iv): Peripodial cell outlines

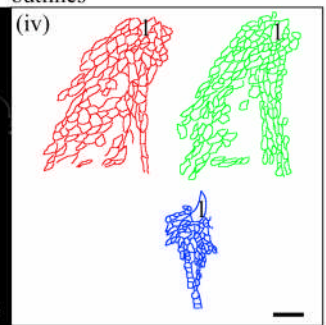


Figure 10h(iii): 2 hours 55 minutes after initiation

In this fluorescent image, actin activity appears to be more intense close to the stalk region and absent from cells on the left hand side of the stalk region. Further elongation of the lumen can be seen which now appears to be a diamond shape. l, lumen; pe, peripodial epithelium; s, stalk

Scale bar represents: 100µm

Figure 10h(iv): Peripodial cell outlines

The outlines of the peripodial cells were traced in Adobe photoshop. A smaller number of large cells appear to be present in the stalk region immediately after culture initiation. The average diameter of the peripodial cells is 20-30µm (red outline). As evagination proceeded the average cell diameter situated in the stalk region was 10-20µm (green outline). Prior to a change in disc orientation a larger number of small cells were present, the cells measure between 5-15µm in diameter (blue outline). The area of cells expressing actin appears to be reduced.

l, lumen

Scale bar represents:100µm

Figure 10i: Wing disc two moesin-GFP, 2 hours 32 minutes after culture initiation

This fluorescent image shows the presence of a lumen in the stalk region of the wing disc during elongation. Although actin is expressed throughout the disc, actin can be seen outlining individual cells in the stalk region surrounding the lumen.

a, actin; dp, disc proper, h, haltere; pe, peripodial epithelium; s, stalk

Scale bar represents:100µm

Figure 10i: Wing disc two moesin-GFP, 2 hours 32 minutes after culture initiation

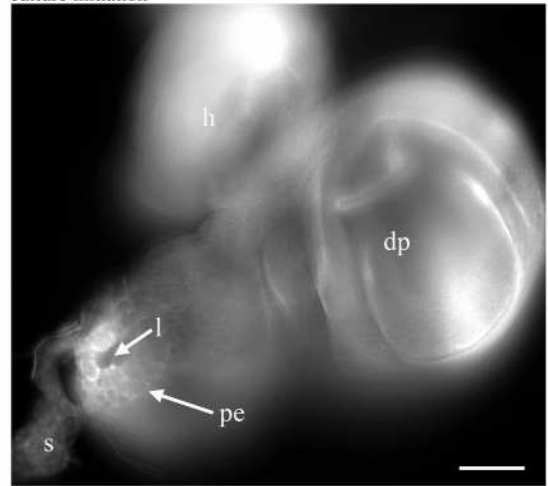


Figure 10i(i): Lumen, actin expression

Fluorescent image showing the stalk region from the image above, 2 hours 32 minutes after culture initiation.

Actin can be seen outlining the cells surrounding the lumen. Wedge shaped, elongate and teardrop shaped peripodial cells are apparent. Actin expression is particularly intense along the edges of some cells. The lumen appears to be situated below the plane of the epithelium.

a, actin; pe, peripodial epithelium; s, stalk; w, wedged shape cell

Scale bar represents:100µm

Figure 10i(i): Lumen, actin expression

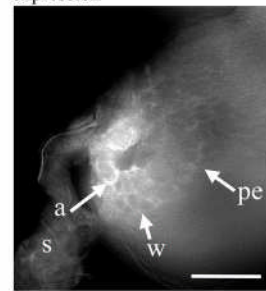


Figure 10j: Wing disc two, moesin-GFP, 2 hours 33 minutes after culture initiation

Fluorescent image showing a close up of the stalk region taken one minute after the previous image figure 10(i). Actin can be seen outlining the cells surrounding the lumen which is changing shape, becoming slightly rounder. There appears to be a groove (g) which runs from the tip of the lumen towards the dorsal side of the disc. The expression of actin has changed in cells closest to the lumen and an accumulation of actin can be seen in some cells. To the right of the lumen cells of the peripodial epithelium(pe) have now become outlined by actin and they have taken on an elongate morphology.
a, actin; g, groove; pe, peripodial epithelium; f, furrow
Scale bar represents:100µm

Figure 10j: Wing disc two moesin-GFP, 2 hours 33 minutes after culture initiation

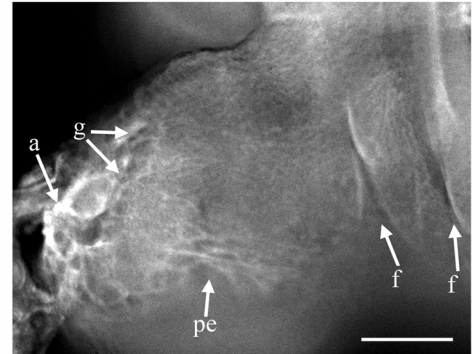


Figure 10k: Actin ring, 2 hours 45 minutes after culture initiation

Fluorescent image showing a close up of the stalk region taken minutes after the previous image figure10(j). Actin expression has changed in the cells surrounding the lumen these cells have changed shape becoming rounder. From this angle the lumen also appears to be smaller. The putative groove also appears less obvious (g). The expression of actin has changed in cells closest to the lumen and a ring of actin is apparent which does not encircle the lumen, but surrounds the far edge of the row of cells adjacent to the lumen. The lumen and surrounding cells appear to be slightly below the plane of the epithelium. Movement of the disc proper can also be seen, the space between the furrows (f) has expanded.
a, actin; f, furrow; pe, peripodial epithelium; s, stalk
Scale bar represents:100µm

Figure 10k: Actin ring, 2 hours 45 minutes after culture initiation

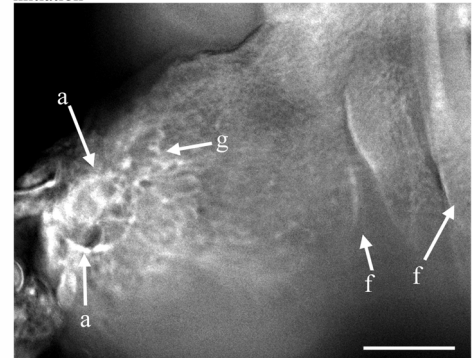


Figure 10m(i): Wing disc two stalk region

This phase contrast image shows where an area of peripodial tissue present in the region close to the stalk appears to be raised.

dp, disc proper; h, haltere; t, raised tissue s, stalk
Scale bar represents:100µm

Figure 10m(i): Wing disc two, stalk region

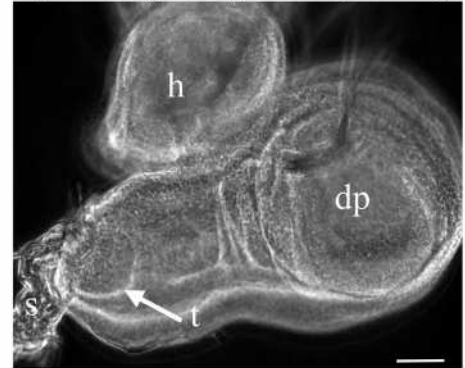


Figure 10m(ii): Raised tissue stalk region

Close up of the area present in the stalk region in figure 10m(i) which appears to be raised (arrows). It is possible that there is a depression in the epithelium which gives the surrounding tissue an elevated appearance. There also appears to be a small dark line (l) which may be the opening of the lumen.

l,lumen; r, raised tissue
Scale bar represents:100µm

Figure 10m(ii): Raised tissue stalk region

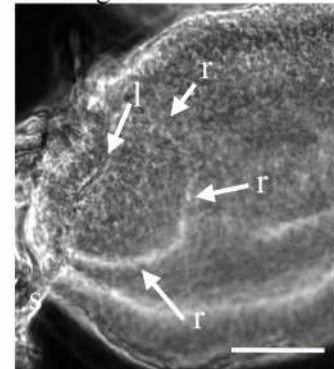


Figure 10m(iii): Moesin-GFP raised tissue

This fluorescent image shows the corresponding area in the stalk region which appears to be raised. Intense actin expression of the area can be seen surrounding the lumen. The area which is circled is where the putative opening to the lumen was observed in phase contrast.

l, lumen
Scale bar represents:100µm

Figure 10m(iii): Moesin-GFP raised tissue

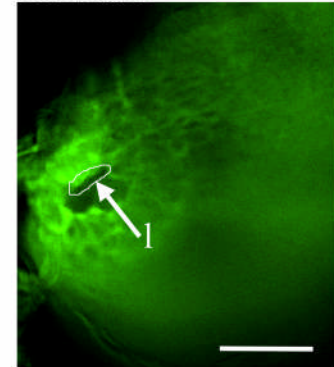


Figure 10n: Wing disc two, moesin-GFP, thickened peripodial epithelium

In this fluorescent image reorientation of the wing disc has revealed that a thickened area of peripodial tissue is situated at the stalk region (figure 10c). Measurements of the depth of peripodial tissue at this point indicates that the peripodial tissue is approximately 30µm.

Scale bar represents: 50µm

f, folded disc proper epithelium pe, peripodial epithelium; wb, wing blade

Figure 10n: Wing disc two, moesin-GFP, thickened peripodial epithelium

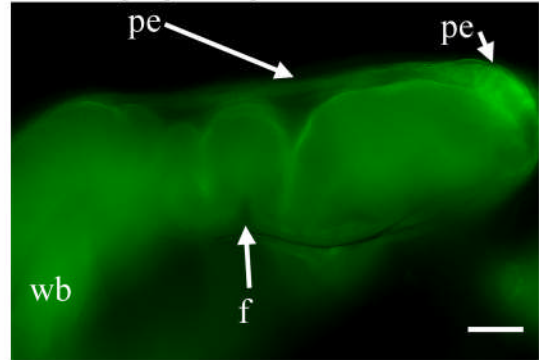


Figure 10p(i): Wing disc two elongation

This fluorescent image shows the strands of peripodial epithelium extending from the stalk region as the disc proceeds with morphogenesis. Actin expression is particularly intense in this region.

e, elongating disc proper epithelium; pe, peripodial epithelium; wb, wing blade

Scale bar represents: 50µm

Figure 10p(i): Wing disc two, elongation

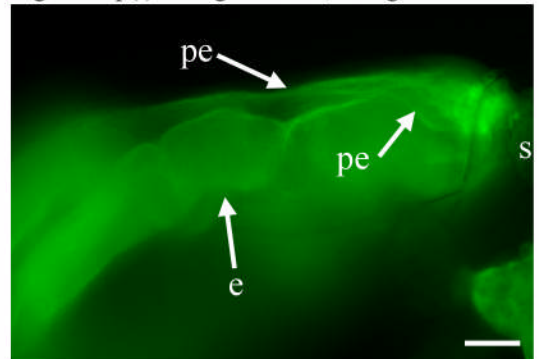


Figure 10p(ii) : Close up of stalk region during elongation

This fluorescent image shows the extent of the thickened strands of epithelial tissue. Although individual cell outlines are not obvious, actin expression is intense along this row of cells. A long piece of trachea can be seen lying across the region of interest, the stalk region.

a, actin; pe, peripodial epithelium; t, trachea; s, stalk.

Scale bar represents: 20µm

Figure 10p(ii): Close up of stalk region during elongation

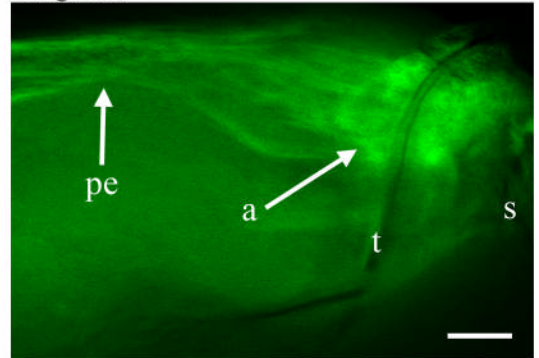


Figure 10q(i): Wing disc two, stretched peripodial epithelium during elongation of disc proper
 DIC image of the wing disc revealing the thickened strands of peripodial tissue emanating from the stalk region. The disc proper is undergoing morphogenetic movements and the peripodial strands appear to be pulled taut at this point.

pe, peripodial epithelium; wb, wing blade
 Scale bar represents: 100µm

Figure 10q(i): Wing disc two, stretched peripodial epithelium during elongation of disc proper

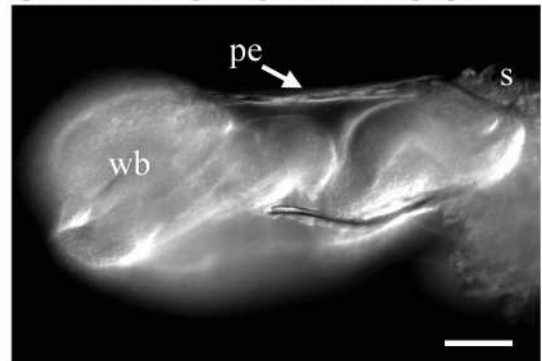


Figure 10q(ii): Moesin-GFP, stalk region
 Fluorescent image taken a few minutes after image 10q(i). The thickened area of peripodial tissue situated at the stalk region measurement a depth of approximately 40µm. Actin expression is most intense at the region where the thickened tissue is situated.

pe, peripodial epithelium; s, stalk; wb, wing blade
 Scale bar represents: 100µm

Figure 10q(ii): Moesin-GFP, stalk region

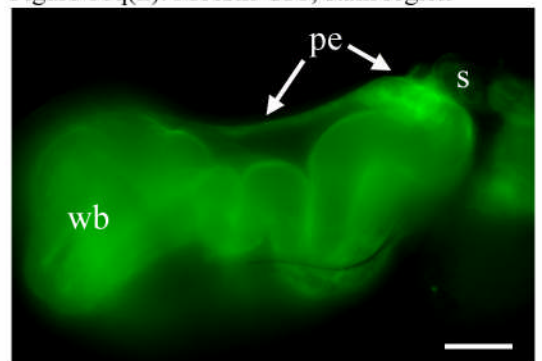
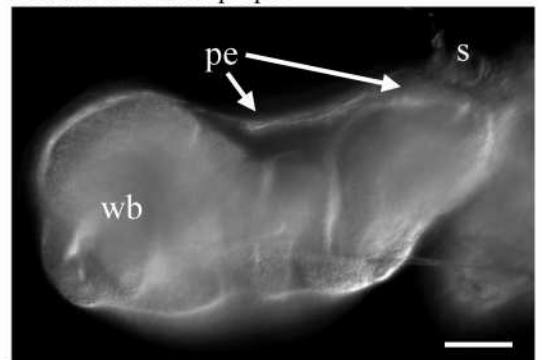


Figure 10q(iii): Peripodial epithelium during contraction of disc proper
 DIC image taken just few minutes after image 10q(ii) showing the contraction of the disc proper, this was accompanied by the relaxation of the thickened peripodial strand or strands.

pe, peripodial epithelium; s, stalk; wb, wing blade
 Scale bar represents: 100µm

Figure 10q(iii): Peripodial epithelium during contraction of disc proper



Figures 10r(i,ii): Wing disc two, cell shape changes around the stalk region during elongation

These fluorescent images of the wing disc during elongation were taken shortly after culture initiation 10r(i) and 1 hour later 10r(ii) to show the extent of elongation of the wing disc in relation to the change in cell morphology and size. The outline of the peripodial cells situated around the lumen is shown.

h, haltere; pe, peripodial cells; s, stalk; wb, wing blade

Scale bar represents:100µm

Figures 10r(i,ii): Wing disc two, cell shape changes around the stalk region during elongation

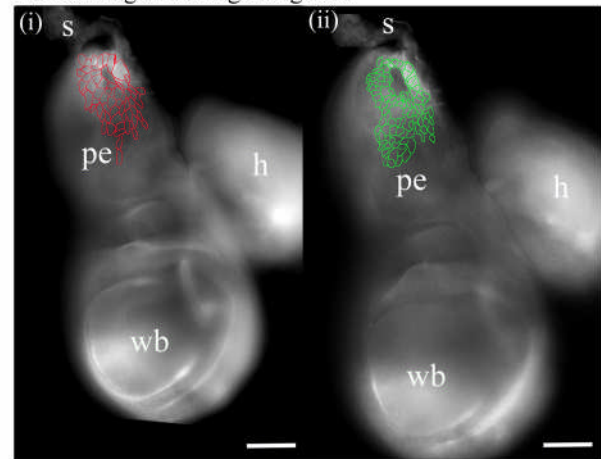


Figure 10r(iii): Stalk region fluorescence

This image shows that peripodial cells expressing actin extend to the proximal area of the disc, close to the stalk.

a, actin; pe, peripodial epithelium

Scale bar represents:100µm

Figure 10r(iii): Stalk region fluorescence Figure 10r(iv): Peripodial cell shape changes

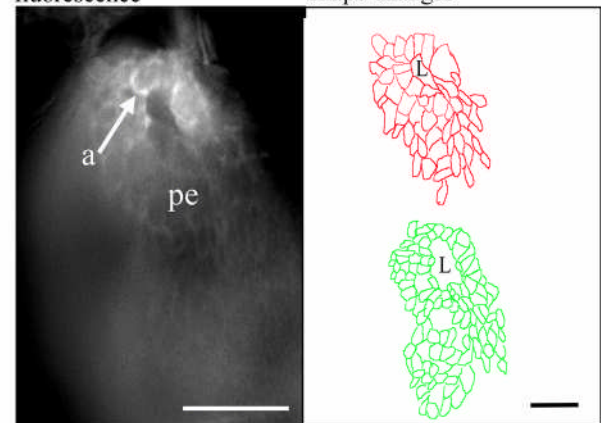


Figure 10r(iv): Peripodial cell shape changes

Outlining the shape of the peripodial cell, where possible, showed that the cell sizes and morphologies varied in the stalk region. The average diameter of the peripodial cells is 15µm or more (figure 10d red).

As elongation progressed a larger number of smaller cells were present in the stalk region, the average cell diameter was 15µm or less (figure 10d green).

Scale bar represents: 50µm

Summary

Summary

The study of morphogenesis in *Drosophila* cells and tissue in three *in vitro* culture systems has proved to be rewarding. Genes have been identified which are associated with cell adhesion and loss of cell polarity which may have implications in the aging process and cellular senescence. The identification of a lumen in the imaginal wing disc cultures is of particular interest.

The aim of the study on *Drosophila* primary embryonic cultures was to assess the possibility that this *in vitro* culture system could be used to examine the effect of the moulting hormone ecdysone on larval and imaginal precursor cells. If these cells responded to ecdysone in a way which could be directly compared to events which take place during metamorphosis *in vivo* then the primary embryonic cultures could be used as an *in vitro* model system. Using the primary embryonic tissue culture technique, transgenic fly lines expressing GFP were useful as an aid to visualise and identify specific cell types. The degeneration, proliferation and subsequent differentiation of *Drosophila* cells and tissue *in vitro* did share similarities with the stage-specific response found *in vivo* to ecdysone. However the precise timing of these changes which took place during metamorphosis '*in vitro*' was impossible to pinpoint. This was mainly due to the breakdown of fat body cells and the apparent breakdown of all the larval cell types such as muscle. However there may be other proteins present in the medium as a result of cell degeneration in response to ecdysone, proteins such as glutactin, which was observed in membrane bound vesicles after ecdysone during the studies on Clone 8+. Interestingly, membrane bound vesicles were also observed in the primary embryonic cultures. Vesicles were observed traversing the processes between

nerve aggregates (figure 3w) and in association with imaginal muscle cells (figure 3g).

Further characterisation of glutactin could be carried out using the primary embryonic cells. As epithelial cell types are observed in these cultures it may be possible to explore whether glutactin is expressed in these cells or other cells, such as the nerve cells. If nerve cells express glutactin this could be explored using the early cultures which were predominantly nerve. When ecdysone is added to these cultures degeneration of the nerve is not obscured by the breakdown of fat body, it would be interesting to see whether glutactin was involved in this process, although this may be difficult as glutactin is a secreted molecule.

The variability in morphogenesis that was observed between all culture preparations is one that would be impossible to address. Although studies undertaken in *Drosophila* primary embryonic cultures were largely unsuccessful, these primary cultures will be an extremely useful resource for the development of new cell lines. Undifferentiated cell types which arise towards the latter stages of development of these cultures have been cultured from primary embryonic cultures previously. This was attempted during the course of this study and the cloned cells grew successfully in culture for several weeks before dying. The primary embryonic cultures should be utilised in the future as it would be especially beneficial to derive a continuous nerve cell line and a cell line which expresses GFP. For this study cell line derivation was not pursued as it is a time consuming process requiring huge numbers of culture preparations.

It was possible to identify several cell types in primary culture, suggesting that this system would be useful for the technique of RNA interference. The

effect of RNA Interference (RNAi) on a defined cell type would be of interest to many researchers - cell lines do not contain cells of defined cell type. Although optimisation of this technique was not accomplished during the course of this study the use of shRNAs which are used in mammalian tissue culture studies on RNAi may prove to be successful. It would be interesting to see if loss of glutactin expression leads to loss of adhesion in the Young Clone 8+ cells which could be explored using the RNAi technique.

In the second part of this study high passage cell lines derived from Young Clone 8+ cell line were found to have changed in relation to their adhesion and proliferation properties. The observations that the Old Clone 8+ cell line appeared to be less adherent than the parent line was substantiated by the statistical analysis carried out in Chapter 5. It was proposed that in the Old Clone 8+ cell line the loss of adherence to the substrate was due to the loss of cell adhesion molecules or the secretion of excess of extracellular matrix material. Analysis of the microarray data revealed potential genes which were differentially expressed and which would possibly account for loss of adhesion such as extracellular matrix associated protein *collagen IV* and *peroxidase*. However the gene *glutactin* was chosen as there was the possibility that this protein acted as a de-adhesion molecule, as it had previously been found enveloping the internal organs of the embryo and imaginal disc cells *in vitro* (Olson et al., 1990).

Glutactin was expressed in all cell lines but contrary to expectations antibody staining revealed that glutactin was not secreted from Old Clone 8+ cells (Chapter 7). Many additional experiments were undertaken when it appeared that perhaps the anti-*Dm*-glutactin antibody was not working in the Old Clone 8+ cell line cells. Glutactin was however secreted from the uppermost region of the Young Clone 8+ cell which lead to the proposal that glutactin

was secreted from wing disc epithelial cells and not haemocytes. If glutactin was secreted from haemocytes then it would appear that the whole Clone 8+ cell population was composed from haemocytes. This seems unlikely and unfortunately a preliminary search for genes which are expressed in the wing discs is equivocal. The microarray data shows that transcripts which are enriched in the body wall (*regucalcin*) and associated with haemocytes (collagen IV) are both present in the Clone 8+ cells (Butler et al., 2003). Further analysis of the Young Clone 8+ cells is required, as a cell line which has maintained epithelial characteristics will be of great interest to researchers studying epithelial morphogenesis 'in vitro'.

The protein glutactin colocalised with actin in the Young Clone 8+ cells and it was observed that loss of secretion of glutactin in the high passage cells was accompanied by loss of colocalisation of actin with glutactin in the Old Clone 8+. In addition vesicles were observed attached to the membrane of ZfeClone 8+ suggesting that the high passage cell line Old Clone 8+ and possibly the ZfeClone 8+ had lost cell polarity. It was concluded that glutactin was not responsible for loss of adhesion in the Old Clone 8+ cells. Although it cannot be discounted entirely as it is likely that the integrity of the extracellular matrix surrounding the cells depends on all of the components being present.

Further analysis of the microarray data appeared to support the proposal that cell polarity had been affected. The gene *frizzled*, a planar polarity gene, was identified as being down regulated in Old Clone 8+ cells. It was hypothesized that the downregulation of the receptor *frizzled* affected proteins associated with cell-cell adhesion such as armadillo and cadherins. It will be difficult to dissect out what came first in the Old Clone 8+ cell line, loss of cell polarity which has possibly lead to loss of cell-cell or cell-matrix adhesion or downregulation of genes such as *cul-2* and *timp* (tissue inhibitor of

metalloproteases). However as *frizzled* and *disp* were downregulated in both high passage cell lines and *cul-2* and *CG5384* which are both associated with ubiquitination only appeared to be downregulated in the Old Clone 8+ cells this suggests that polarity was affected first, with loss of *frizzled* occurring in both cell lines and other changes in gene expression have taken place later, such as downregulation of *cul-2* in the Old Clone 8+ cell line and upregulation of *cathepsin B* in the ZfeClone 8+ cell line. The most interesting question then is how or why does loss of *frizzled* occur in the Clone 8+ cell lines? In the future further analysis of the microarray data could lead to some very interesting studies on downregulation of the protein *frizzled* in the Clone 8+ cell lines.

The irregularities observed in the expression of actin and glutactin in the Old Clone 8+ cells also suggested that these cells were of mixed phenotypes and it was established that the microarray data would also support the hypothesis that the Old Clone 8+ cell line was composed of cells undergoing cellular senescence. If *cul-2*, like *cul-1*, is required for exit from the cell cycle to enable apoptosis *cul-2* may be involved in anoikis resistance where cells which detach from the substrate do not undergo cell death. At the moment very little is known about ubiquitination, *cul-2* and *CG5384* may be implicated in cellular senescence and the Clone 8+ cell lines could be used for studies on ubiquitins. The changes which take place during aging in Clone 8+ cell lines could be used to study neurodegenerative disease processes in mammals.

Clearly there is a lot of information in the microarray data which has not been examined. Unfortunately the microarray data was incomplete and many genes of interest which may be of importance were not represented. However in future experiments on the Clone 8+ cell lines it would be more instructive if one cell sample was hybridised to one gene chip, it would have been

particularly useful in this analysis to have microarray data of the parent cell line Young Clone 8+ only and all the genes in the *Drosophila* genome assayed. Although that would involve the generation of a huge amount of data it would be more useful in dissecting out genetic pathways and possible associations of proteins could be examined *in vitro* and *in vivo*.

Many of the *Drosophila* cell lines used in laboratories today have been sub-cultured almost continuously from that time and as such they are many 'in vitro' years old. It has been shown in this study on the Clone 8+ cell lines that the properties such as adhesion and gene expression of a cell line have changed with the increasing number of passages which also relates to their *in vitro* age. This supports the evidence that cell lines change as they age previously presented by Cottam and Milner (1997). As many as 60% of genes implicated in mammalian disease processes share homology with *Drosophila* genes and many studies are undertaken using *Drosophila* cell lines to study mammalian disease processes. The finding in this study may have serious implications in the results that are produced from those studies. During the normal course of sub-culturing mammalian cells the passage number is always recorded, it would be recommended therefore that this practice be made throughout the *Drosophila* community.

One of the most interesting findings came towards the end of the study on morphogenesis in *Drosophila* imaginal discs after many imaginal discs had been dissected and examined (Chapter 9). This was the discovery of a putative lumen in fixed tissue of the peripodial epithelium in the actin-*lacZ* fly line. The identification of a putative lumen in peripodial epithelium situated close to the stalk region lead to the proposal that this may be due to wound healing. This assumption was based on the fact that many of the actin-GFP transgenic flies incurred an inordinate amount of damage from the dissection

when compared to the wild-type imaginal discs. An alternative explanation which would account for the presence of a lumen was that this hole closed during evagination, in a process similar to dorsal closure, and thereby contributed to the contraction of the peripodial epithelium during eversion. These proposals lead to the use of the fly line moesin-GFP which had previously been used to study the role of actin in dorsal closure. Using moesin-GFP and real time imaging, the lumen was visualised in conjunction with changes in shape of cells which surrounded the lumen. These contractions and changes in cell shape were also associated with the morphogenesis of the disc proper and the change in expression of actin. It was proposed that the lumen did not close during evagination and that invagination of the epithelial tissue was a possible mechanism by which the peripodial epithelium contracted. The evidence for this was the presence of a large amount of peripodial tissue which was observed at the region of the stalk in association with the lumen. It was concluded that actin was responsible for cell shape changes and the lumen situated in the stalk region of the imaginal wing disc mediated contraction of the peripodial epithelium during elongation.

There are many genes which are associated with processes such as dorsal closure and gastrulation, which involve changes in cell shape and movement of cells during morphogenesis and many or all of these may be involved in peripodial contraction during elongation. Although antibody staining of the lumen area with *Drosophila* anti-nonmuscle myosin II failed, it is more than likely that this protein in association with actin is implicated in the contraction of the peripodial epithelium.

In *Drosophila* the Jun-N-terminal Kinase (JNK) signalling pathway is required for epithelial cell shape changes in the embryo and processes such as dorsal

closure. Signalling pathways have not been discussed in this study however it is proposed that the JNK signalling pathway is implicated in contraction of the peripodial epithelium. The JNK signalling pathway has been studied in the imaginal wing discs using *puckered* (*puc*) which encodes a protein that negatively regulates the JNK signalling pathway during dorsal closure (Glise and Noselli, 1997; Martin-Blanco et al., 1998). The protein *puc* is specifically expressed in leading edge cells of the lateral epithelium during dorsal closure. The expression of *puc-lacZ* has been examined in the third instar imaginal wing discs where it was found in the peripodial epithelium, specifically around the stalk region (Agnes et al., 1999). The authors suggested that *puc* and the JNK signalling pathway were required in a 'specific subset of peripodial cells'. It is more than likely that 'the specific subset of peripodial cells' which were identified in their experiments are cells which are associated with the edge cells surrounding the lumen. A fly line expressing *puc-GFP* would be useful in future studies on contraction of the peripodial epithelium during elongation. In addition the role of glutactin in cells surrounding the lumen could also provide interesting data on changes in cell-matrix adhesion. Cell-matrix adhesion complexes will be remodelled to accommodate the changes in cell shape and movement of the epithelium during the contraction of the peripodial epithelium during elongation.

Future studies

Genes of interest in the Clone 8R and ZfeClone 8+ cell lines were not investigated during this study, but there is potentially some very interesting data.

Many genes were differentially expressed in the Young Clone 8+ cell line after exposure to ecdysone, to which the Clone 8R or showed little or no response. However one gene in particular which may be of interest is *regucalcin*. *Regucalcin* was upregulated two fold or more in Clone 8R cells when compared to the Young Clone 8+ cell line before ecdysone. *Regucalcin* encodes a protein which is involved with binding calcium ions (Ca^{2+}) and plays a role in the maintenance of intracellular Ca^{2+} homeostasis. In the past it has been hypothesised that ecdysone exerts its effects on puffing in the polytene chromosomes by altering intracellular cation concentrations (Kroeger et al., 1977 cited in Andres and Thummel, 1995). Ca^{2+} binding proteins have been shown to regulate transcription factors and steroid hormone receptors in mammalian cells (Tsurusaki and Yamaguchi, 2004 cited in Nakagawa and Yamaguchi, 2005). Upregulation of the gene *regucalcin* in the Clone 8R cells may play a role in regulating ecdysone receptors in these cells. Interestingly overexpression of *regucalcin* has also been found to have a suppressive effect on cell proliferation (Misawa et al., 2002, cited in Nakagawa and Yamaguchi, 2005). *Regucalcin* was upregulated in all Clone 8+ cell lines after ecdysone and statistical analysis (Chapter 5) indicated that addition of ecdysone resulted in the cessation of cell division in all cell lines, with the exception of Clone 8R. The microarray analysis on the Clone 8+ cell lines could be used in future studies to elucidate genes implicated in the ecdysone response.

The finding that *cathepsin B*, which was upregulated in ZfeClone 8+ and encodes a protein which may degrade extracellular matrix proteins, is interesting and the suggestion that the lack of fly extract in the medium may be responsible for this could be explored further. However this observation may be more complex than that. Younger cells (cells with low passage numbers) have been found to be more sensitive to the changes of fly extract in the medium, to the extent where it has not been possible to obtain a fly extract

free cell culture at low passage numbers. This suggests that changes in gene expression may have already taken place which have affected adhesion in the ZfeClone 8+ cells, such as loss of *frizzled*, which makes them more amenable to lack of fly extract. If this is the case this suggests that *cathepsin B* is not responsible for the loss of adhesion as was suggested in chapter 6. However the expression of the protein cathepsin B in ZfeClone 8+ cell lines would be of interest.

Using three *in vitro* tissue culture systems I have been able to study processes which are integral to successful morphogenesis of an organism. These were, a morphological response to hormone, cell adhesion, cell shape change and the subsequent rearrangement of these cells to form an adult appendage. In *Drosophila* during metamorphosis all these processes are mediated by the changing levels of ecdysone. Ecdysone was also used in these studies to observe the response of these *Drosophila* cells and tissues *in vitro*.

During metamorphosis in response to changing levels of ecdysone, tissue of the late third instar larva begins to degenerate. The destruction of the majority of larval cells is followed by proliferation and differentiation of adult precursors. This response to ecdysone was also observed in the primary embryonic cultures, the degeneration of larval cells was apparent and adult muscle was observed. *In vivo* the adult precursors of the integument, imaginal discs, respond to ecdysone by beginning to undergo the process of morphogenesis. These changes in cell shape and elongation of the disc proper are mediated in part by the actin cytoskeleton. Imaginal discs dissected from late third instar larvae also responded to ecdysone and the process of evagination was observed. This study went on to show that the movement of the disc proper was associated with a lumen in the peripodial epithelium which has not been previously identified. The changes in cell shape of the

peripodial epithelium were also mediated by the actin cytoskeleton. In order for cell shape changes to occur the wing disc epithelial cells must become polarised. Loss of the polarity in the imaginal disc epithelium would lead to loss of cell shape changes and loss of cell-cell and cell-matrix adhesion, and morphogenesis would not occur in these discs. The effect of downregulation of genes which are important for adhesion in wing disc epithelial cells were identified in the Clone 8+ cell line. Analysis of the Old Clone 8+ cells revealed that genes associated with polarity and the extracellular matrix such as *frizzled* and *glutactin* were important in maintaining cell-cell and cell-matrix adhesion in imaginal wing disc epithelial cells. The loss of extracellular matrix during metamorphosis may also mean that the developing appendage would be exposed to the larval environment during morphogenesis. Degeneration of larval cells may lead to harmful enzymes present in the haemolymph which would damage the developing appendage. These enzymes may have been present in the primary cultures when the products of the larval fat body, muscle and nerve degenerated. As a result of these findings it can be concluded that events which take place in cells and tissue *in vitro* recapitulate events which take place during development *in vivo* and that *Drosophila* cells in culture continue to be a useful tool in order to study morphogenesis.

References

References

Abrams JM, White K, Fessler LI and Steller H. 1993. Programmed cell death during *Drosophila* embryogenesis. *Development* 117:29-43.

Adams MD, Celniker SE, Holt RA, Evans CA, Gocayne JD, Amanatides PG, Scherer SE, Li PW, Hoskins RA, Galle RF et al., 2000. The genome sequence of *Drosophila melanogaster*. *Science* 287:2185–2195

Adams JC and Watt FM. 1991. Expression of 1, 3, 4 and 5 integrins by human epidermal keratinocytes and non-differentiating keratinocytes. *J Cell Biol.* 115: 829–841.

Adams JC and Watt FM. 1993. Regulation of development and differentiation by the extracellular matrix. *Development* 117:1183-1198.

Agnes F, Suzanne M and Noselli S. 1999. The *Drosophila* JNK pathway controls the morphogenesis of imaginal discs during metamorphosis. *Development* 126:5453–5462

Amerik AY, Swaminathan S, Krantz B A, Wilkinson KD and Hochstrasser M. 1997. *In vivo* disassembly of free polyubiquitin chains by yeast Ubp14 modulates rates of protein degradation by the proteasome. *EMBO J.* 16:4826-4838

Andrews J, Bouffard GG, Cheadle C, Lu J, Becker KG and Oliver B. 2000. Gene discovery using computational and microarray analysis of transcription in the *Drosophila melanogaster* testis. *Genome Res.* 10:2030-2043.

Arbeitman MN, White D, Furlong EM, Imam F, Johnson E, Null BH, Baker BS, Krasnow MA, Scott MP and Davis RW. 2002. Gene expression during the life cycle of *Drosophila melanogaster*. *Science* 297:2270-2275.

Armknecht S, Boutros M, Kiger A, Nybakken K, Mathey-Prevot B and Perrimon N. 2005. High-throughput RNA interference screens in *Drosophila* tissue culture cells. *Methods Enzymol.* 392:55-73.

Auerbach C. 1936. The development of the legs, wings and halteres in wild type and some mutant strains of *Drosophila melanogaster*. *Trans. R. Soc. Edinb.* 58:114–119.

Awasaki T and Ito K. 2004. Engulfing Action of Glial Cells Is Required for Programmed Axon Pruning during *Drosophila* Metamorphosis. *Current Biology* 14:668-677

Baeg GH, Selva EM, Goodman RM, Dasgupta R, Perrimon N. 2004. The Wingless morphogen gradient is established by the cooperative action of Frizzled and Heparan Sulfate Proteoglycan receptors. *Dev. Biol.* 276:89-100.

- Baeg GH, Zhou R, Perrimon N. 2005. Genome-wide RNAi analysis of JAK/STAT signaling components in *Drosophila*. *Genes Dev.* 19:1861-1870.
- Baehrecke EH and Thummel CS. 1995. The *Drosophila* E93 gene from the 93F early puff displays stage- and tissue-specific regulation by 20-hydroxyecdysone. *Dev. Biol.* 17:85-97.
- Barthalay Y, Hipeau-Jacquotte R, de la Escalera S, Jimenez F and Piovant M. 1990. *Drosophila* neurotactin mediates heterophilic cell adhesion. *EMBO J.* 9: 3603-3609.
- Bastock R, Strutt H and Strutt D. 2003. Strabismus is asymmetrically localised and binds to Prickle and Dishevelled during *Drosophila* planar polarity patterning. *Development* 130:3007-3014.
- Bate M. 1990. The embryonic development of larval muscles in *Drosophila* *Development* 110:791-794
- Bate M and Martinez Arias A. 1991. The embryonic origin of imaginal discs in *Drosophila*. *Development* 112:755-761
- Bates RC, Edwards NS, Yates JD. Spheroids and cell survival. 2000. *Crit Rev Oncol Hematol.* 36:61-74.
- Baum B and Perrimon N. 2001. Spatial control of the actin cytoskeleton in *Drosophila* epithelial cells. *Nature Cell Biol.* 3:883-890.
- Beausejour CM, Krtolica A, Galimi F, Nanta M, Lowe SW, Yaswen P and Campisi J. 2003. Reversal of human cellular senescence: roles of the p53 and p16 pathways. *EMBO J.* 22:4212-4222.
- Beckstead RB, Lam G, Thummel CS. 2005. The genomic response to 20-hydroxyecdysone at the onset of *Drosophila* metamorphosis. *GenomeBiol.* 6: 120-138.
- Begg M and Cruickshank WJ. 1963. A partial analysis of *Drosophila* larval haemolymph. *Proc. r. Soc. Edinb. B. Biol.* 68:215-236.
- Ben-Porath I and Weinberg RA. 2004. When cells get stressed: an integrative view of cellular senescence *J. Clin. Invest.* 113:8-13
- Berger E, Ringler R, Alahiotis S and Frank M. 1978. Ecdysone-induced changes in morphology and protein synthesis in *Drosophila* cell cultures. *Dev. Biol.* 62:498-511.
- Bernstein E, Caudy AA, Hammond SM and Hannon GJ. 2001a. Role for a bidentate ribonuclease in the initiation step of RNA interference. *Nature* 409: 363-366
- Bernstein E, Denli AM and Hannon GJ. 2001b. The rest is silence. *RNA* 7: 1509-1521

- Bertet C, Sulak L and Lecuit T. 2004. Myosin-dependent junction remodelling controls planar cell intercalation and axis elongation. *Nature* 429:667-671.
- Best-Belpomme M, Courgeon AM. 1980. A critical period of ecdysterone action on sensitive clones of *Drosophila* cultured *in vitro*: the maturation of the cells. *Europ. J. Biochem.* 112:185-191.
- Best-Belpomme M, Courgeon AM, Echalié G. 1980. Development of a model for the study of ecdysteroid action: *Drosophila melanogaster* cells established *in vitro*. *Hoffman Progress in Ecdysone Research* 1980:379-392.
- Bhat M, Izaddoost S, Lu Y, Cho K, Choi K and Bellen H. 1999. Discs Lost, a Novel Multi-PDZ Domain Protein, Establishes and Maintains Epithelial Polarity. *Cell* 115:765-766
- Bilder D and Perrimon N. 2000. Localization of apical epithelial determinants by the basolateral PDZ protein Scribble. *Nature* 403:676-680
- Bilder D, Li M and Perrimon N. 2000. Cooperative regulation of cell polarity and growth by *Drosophila* tumor suppressors. *Science* 289:113-116.
- Bilder D and Perrimon N. 2000. Localization of apical epithelial determinants by the basolateral PDZ protein Scribble. *Nature* 403:676-680.
- Blitzer J T and Nusse R. 2006. A critical role for endocytosis in Wnt signaling. *BMC Cell Biol.*6:7-28.
- Bloor J W and Kiehart D P. 2001. zipper Nonmuscle myosin- II functions downstream of PS2 integrin in *Drosophila* myogenesis and is necessary for myofibril formation. *Dev. Biol.* 239:215–228.
- Bloor JW and Kiehart DP. 2002. *Drosophila* RhoA regulates the cytoskeleton and cell–cell adhesion. *Development* 129:3173–3183
- Bökel C, Prokop A and Brown NH. 2005. Papillote and Piopio: *Drosophila* ZP-domain proteins required for cell adhesion to the apical extracellular matrix and microtubule organization. *J. Cell Sci.*118:633-642.
- Bosch M, Serras F, Martin-Blanco E and Baguna J. 2005. JNK signaling pathway required for wound healing in regenerating *Drosophila* wing imaginal discs. *Dev. Biol.* 280:73-86.
- Boutros M, Kiger AA, Armknecht S, Kerr K, Hild M, Koch B, Haas SA, Paro R and Perrimon N; Heidelberg Fly Array Consortium. 2004. Genome-wide RNAi analysis of growth and viability in *Drosophila* cells. *Science* 303:832-5.

- Brabant MC, Fristrom D, Bunch TA, Brower DL. 1996. Distinct spatial and temporal functions for PS integrins during *Drosophila* wing morphogenesis. *Development* 122:3307-3317.
- Brand AH and Perrimon N. 1993. Targeting gene expression as a mean of altering cell fates and generating dominant phenotypes. *Development* 118:401-415.
- Broadie K, Skaer H and Bate CM. 1992. Whole embryo culture of *Drosophila*: development of embryonic tissues *in vitro*. *Roux Arch. dev. Biol.* 201:364-375.
- Brower DL. 1987. Ultrabithorax gene expression in *Drosophila* imaginal discs and larval nervous system. *Development* 101: 83-92.
- Brower DL, Piovant M, Salatino R, Brailey J and Hendrix MJ. 1987. Identification of a specialized extracellular matrix component in *Drosophila* imaginal discs. *Dev. Biol.* 119:373-381.
- Brown HLD, Cherbas L, Cherbas P and Truman J W. 2006. Use of time-lapse imaging and dominant negative receptors to dissect the steroid receptor control of neuronal remodeling in *Drosophila*. *Development* 133:275-285.
- Brown NH, Gregory SL and Martin-Bermudo M D. 2000. Integrins as mediators of morphogenesis in *Drosophila*. *Dev. Biol.* 223:1-16
- Brown NH, Gregory SL, Rickoll WL, Fessler LI, Prout M, White RAH and Fristrom JW. 2002. Talin is essential for integrin function in *Drosophila*. *Dev. Cell* 3:569-579.
- Bryant P J Fraser S E. 1988. Wound healing, cell communication, and DNA synthesis during imaginal disc regeneration in *Drosophila*. *Dev Biol* 127:197-208.
- Bryant PJ. 1993. Towards the cellular functions of tumour suppressors. *Trends Cell Biol.* 3:31-35.
- Bryant PJ, Watson KL, Justice RW, Woods DF. 1993. Tumor suppressor genes encoding proteins required for cell interactions and signal transduction in *Drosophila*. Ingham, Brown, Martinez Arias, 1993, Signals, polarity and adhesion in development:239-249.
- Burke R, Nellen D, Bellotto M, Hafen E, Senti KA, Dickson BJ and Basler K. 1999. Dispatched, a novel sterol-sensing domain protein dedicated to the release of cholesterol-modified hedgehog from signalling cells. *Cell* 99:803-815.
- Butler MJ, Jacobsen TL, Cain DM, Jarman MG, Hubank M, Whittle JR, Phillips R and Simcox A. 2003. Discovery of genes with highly restricted expression patterns in the *Drosophila* wing disc using DNA oligonucleotide microarrays. *Development* 130:659-670.

- Campisi J. 2001. From cells to organisms: can we learn about aging from cells in culture? *Experimental Gerontology, Slowly Aging Organisms* 36:607-618
- Chen X, Overstreet E, Wood SA and Fischer JA. 2000. On the conservation of function of the *Drosophila* Fat facets deubiquitinating enzyme and Fam, its mouse homolog. *Dev. Genes Evol.* 210:603-610.
- Chen X and Fischer JA. 2000. *In Vivo* Structure/Function Analysis of the *Drosophila* fat facets Deubiquitinating Enzyme. *Gene Genetics* 156:1829-1836
- Cheng JC, Miller AL and Webb SE. 2004. Organization and function of microfilaments during late epiboly in zebrafish embryos. *Developmental Dynamics* 231:313-323
- Cherbas L, Cherbas P, Savakis C, Demetri G, Cymborowska-Manteuffel M, Rebers J and Williams CM. 1979. Studies on the action of ecdysteroid hormones on a *Drosophila* cell line. *Abstr. 5th Int. Conf. Invert. Tissue Culture* 4:27.
- Cherbas L, Cherbas P, Savakis C, Demetri G, Manteuffel-Cymorowska M, Yonge CD and Williams CM. 1980. Studies of ecdysteroid action on a *Drosophila* cell line. *Invertebrate Systems In Vitro*, Eds: Kurstak, E. Maramorosch K and Dubendorfer A. Elsevier North Holland 19 217-252
- Cho KO, Chern J, Izaddoost S and Choi K W. 2000. Novel signalling from the peripodial membrane is essential for eye disc patterning in *Drosophila*. *Cell* 103:331-342
- Choi KW and Benzer S. 1993. Retinal glia migrate along photoreceptor axons in *Drosophila* eye. *C.S.H. Development* 2:24
- Clemens JC, Worby CA, Simonson-Leff N, Muda M, Maehama T, Hemmings BA, Dixon JE. 2000. Use of double-stranded RNA interference in *Drosophila* cell lines to dissect signal transduction pathways. *Proc. Natl. Acad. Sci. USA* 97:6499-6503.
- Condic M, Fristrom J and Fristrom J. 1991. Apical cell shape changes during *Drosophila* leg disc elongation: a novel morphogenetic mechanism. *Development* 111:23-33
- Cottam DM and Milner MJ. 1997. Effect of age on the growth and response of a *Drosophila* cell line to moulting hormone. *Tissue and Cell* 29:727-732.
- Cottam DM and Milner MJ. 1997. The effects of several ecdysteroids and ecdysteroid agonists on two *Drosophila* imaginal disc cell lines. *Cell. Molec. Life Sci.* 53:600-603.
- Cottam DM and Milner MJ. 1998. The effect of juvenile hormone on the response of the *Drosophila* imaginal disc cell line Cl 8 + to moulting hormone. *J. Insect Physiol.* 44:1137-1144.

- Cottam DM, Tucker JB, Rogers-Bald MM, Mackie JB, Macintyre J, Scarborough JA, Ohkura H and Milner MJ. 2006. Non-centrosomal microtubule-organising centres in cold-treated cultured *Drosophila* cells. *Cell Motility Cytoskel.* 63:88-100.
- Courgeon AM. 1972. Action of insect hormones at the cellular level. Morphological changes of a diploid cell line of *Drosophila melanogaster* treated with ecdysone and several analogues *in vitro*. *Exp. Cell Res.* 74:327-336.
- Courgeon AM. 1972. Effects of α and β ecdysone on *in vitro* cell multiplication in *Drosophila melanogaster*. *Nature New Biol.* 238:250-251.
- Courgeon AM. 1975. Action of insect hormones at the cellular level. *Exp. Cell Res.* 94:283-291.
- Cox RT, Kirkpatrick C and Peifer M. 1996. Armadillo Is Required for Adherens Junction Assembly, Cell Polarity, and Morphogenesis during *Drosophila* Embryogenesis. *The Journal of Cell Biology* 134:133-148.
- Currie DA, Milner MJ and Evans CW. 1988. The growth and differentiation *in vitro* of leg and wing imaginal disc cells from *Drosophila melanogaster*. *Development* 102:4:805-814
- De Joussineau C, Soule J, Martin M, Anguille C, Montcourrier P, Alexandre D. 2003. Delta-promoted filopodia mediate long-range lateral inhibition in *Drosophila*. *Nature* 426:555-559.
- DeMali KA, Barlow CA and Burridge K. 2002. Recruitment of the Arp2/3 complex to vinculin: coupling membrane protrusion to matrix adhesion. *The Journal of Cell Biology* 159:881-891
- Dimri R, Sharabi Y and Shoham J. 2000. Specific Inhibition of Glucocorticoid-Induced Thymocyte Apoptosis by Substance P1. *The Journal of Immunology* 164:2479-2486.
- Dinan L, Spindler-Barth M and Spindler KD. 1990. Insect cell lines as tools for studying ecdysteroid action. *Invert. Reprod. Dev.* 18:43-53.
- Douma S, Van Laar T, Zevenhoven J, Meuwissen R, Van Garderen E and Peeper DS. 2004. Suppression of anoikis and induction of metastasis by the neurotrophic receptor TrkB. *Nature* 430:973-4
- Drubin DG Nelson WJ. 1996. Origins of cell polarity. *Review Cell.* 84:335-44.
- Dübendorfer A and Shields G. 1972. Proliferation *in vitro* and *in vivo* of a cell line originally derived from imaginal disc cells. *D. I. S.*49:43.
- Dübendorfer A, Shields G and Sang JH. 1974. Pattern formation by embryonic *Drosophila melanogaster* imaginal cells cultured *in vitro*. *Heredity* 33:138-139

- Dübendorfer A, Shields G and Sang JH. 1975. Development and differentiation *in vitro* of *Drosophila* imaginal disc cells from dissociated early embryos. Journal Experimental Morphology 33:487-498.
- Dübendorfer A. 1976. Metamorphosis Of Imaginal Disc Tissue Grown *In Vitro* From Dissociated Embryos Of *Drosophila*. reprinted from Invertebrate tissue culture, Applications in Medicine, Biology and Agriculture. Eds: Kurstak, Maramorosch 10:151-159.
- Dübendorfer A, Blumer A, Deak. I.I. 1978. Differentiation *in vitro* of larval and adult muscles from embryonic cells of *Drosophila*. Roux Arch. dev. Biol. 184:233-249.
- Dübendorfer A and Eichenberger-Glinz S. 1980. Development and metamorphosis of larval and adult tissues of *Drosophila in vitro*. Kurstak, Maramorosch, Dübendorfer 1980:169-185.
- Dübendorfer A. 1982. Ecdysteroid conversion in primary cultures of developing embryonic cells of *Drosophila melanogaster*. Biol. Cell 45:187.
- Dübendorfer A and Eichenberger-Glinz S. 1985. *In vitro* metamorphosis of insect cells and tissues: development and function of fat body cells in embryonic cell cultures of *Drosophila*. Eds: Balls, Bownes :145-161.
- Dutta D, Bloor JW, Ruiz-Gomez M, VijayRaghavan K and Kiehart D P. 2002. Real-time imaging of morphogenetic movements in *Drosophila* using Gal4-UAS-driven expression of GFP fused to the actin-binding domain of moesin. Genesis 34:146 -151
- Dutkowski AB, Oberlander H and Leach CE. 1977. Ultrastructure of cuticle deposited in *Plodia interpunctella* wing discs after various β -ecdysone treatments *in vitro*. Wilhelm Roux's Archives 183:155-164
- Eaton S, Auvinen P, Luo L, Jan YN, Simons K. 1995. CDC42 and Rac1 control different actin-dependent processes in the *Drosophila* wing disc epithelium. J. Cell Biol. 131:151-164.
- Echalier G, Ohanessian A, Brun G. 1965. Cultures 'primaires' de cellules embryonnaires de *Drosophila melanogaster*. Insecte, Diptere. C. r. hebd. Seanc. Acad. Sci., Paris 261:3211--3213.
- Echalier G. 1976. *In vitro* established lines of *Drosophila* cells and applications in physiological genetics. Eds. Kurstak, Maramorosch 1976:131-150.
- Echalier G. 1980. Necessity of radically new insect cell culture methods. eds:Kurstak, Maramorosch, Dübendorfer, 1980:589-592.
- Echalier G, Ohanessian A and Brun G. 1965. Cultures 'primaires' de cellules embryonnaires de *Drosophila melonagaster*. C.R. hebd. Seanc. Acadamie Science, Paris, 261:3211-3213,

- Echeverri CJ and Perrimon N. 2006. High-throughput RNAi screening in cultured cells: a user's guide. *Nature Reviews Genetics* 7:384-96
- Edwards KA and Kiehart DP. 1996. *Drosophila* nonmuscle myosin II has multiple essential roles in imaginal disc and egg chamber morphogenesis. *Development* 122:1499-1511
- Edwards K, Demsky AM, Montague RA, Weymouth N and Kiehart DP. 1997. GFP-moesin illuminates actin cytoskeleton dynamics in living tissue and demonstrates cell shape changes during morphogenesis in *Drosophila*. *Dev. Biol.* 191:103-117.
- Eide PE. 1975. Establishment of a Cell Line from Long term primary Embryonic House Fly cell Cultures. *Journal Insect Physiology* 20:1431-1438.
- Elliott SL, Cullen CF, Wrobel N, Kernan MJ and Ohkura H. 2005. EB1 Is Essential during *Drosophila* Development and Plays a Crucial Role in the Integrity of Chordotonal Mechanosensory Organs. *Molecular Biology of the Cell* 16:891-901
- Elbashir SM, Harborth J, Lendeckel W, Yalcin A, Weber K and Tuschl T. 2001. Duplexes of 21-nucleotide RNAs mediate RNA interference in cultured mammalian cells. *Nature* 411:494-498.
- Elbashir SM, Lendeckel W and Tuschl T. 2001. RNA interference is mediated by 21- and 22-nucleotide RNAs. *Genes Dev.* 15:188-200.
- Elbashir SM, Martinez J, Patkaniowska A, Lendeckel W and Tuschl T. 2001. Functional anatomy of siRNAs for mediating efficient RNAi in *Drosophila melanogaster* embryo lysate. *EMBO J.* 20:6877-6888.
- Ettensohn CA. 1985. Mechanisms of Epithelial Invagination. *The Quarterly Review of Biology* 60:289-307.
- Ettensohn CA. 1985. Gastrulation in the sea urchin embryo is accompanied by the rearrangement of invaginating epithelial cells. *Dev. Biol.* 112:383- 390
- Fahrbach SE and Truman JW. 1989. Autoradiographic identification of ecdysteroid-binding cells in the nervous system of the moth *Manduca sexta* *Journal of Neurobiology* 20:681-702
- Faivre-Sarrailh C, Banerjee S, Li J, Hortsch M, Laval M and Bhat MA. 2004. *Drosophila* contactin a homolog of vertebrate contactin, is required for septate junction organization and paracellular barrier function. *Development* 131:4931-4942.
- Fanto M and McNeill H. 2004. Planar polarity from flies to vertebrates. *J. Cell Sci.* 117:527-533.

Fessler L, Fogerty F, Nelson R and Fessler J. 1994. An integrin ligand, Tiggrin, and a cross-linker of extracellular matrix, peroxidasin, are made by phagocytic hemocytes in *Drosophila* embryos. *A. Dros. Res. Conf.* 35:24.

Fessler LI, Campbell AG, Duncan KG and Fessler JH. 1987. *Drosophila* laminin: characterization and localization. *J. Cell Biol.* 105:2383-2391.

Filippov V, Filippova M, Sehnal F and Gill SS. 2000. Temporal and spatial expression of the cell-cycle regulator cul-1 in *Drosophila* and its stimulation by radiation-induced apoptosis. *J. exp. Biol.* 203:2747-2756.

Fire A, Xu S, Montgomery MK, Kostas SA, Driver SE and Mello CC. 1998 Potent and specific genetic interference by double-stranded RNA in *Caenorhabditis elegans*. *Nature* 391:806–811.

Frisch SM and Francis H. 1994. Disruption of epithelial cell-matrix interactions induces apoptosis. *J. Cell Biol.* 124:619-626.

Frisch SM and Sreaton RA. 2001. Anoikis mechanisms. *Curr. Opin. Cell Biol.* 13:555-562.

Fristrom JW, Logan R and Murphy C. 1973. The synthetic and minimal culture requirements for evagination of imaginal discs of *Drosophila melanogaster in vitro*. *Devl Biol.* 33:441-456

Fristrom DK . 1982. Septate Junctions in Imaginal Disks of *Drosophila*: A Model for the Redistribution of Septa during Cell Rearrangement. *The Journal of Cell Biology* 94:77-87

Fristrom DK and Rickoll WL. 1982. The morphogenesis of imaginal discs of *Drosophila*. *King, Akai*, 982:247-277.

Fristrom DK and Liebrich W. 1986. The hormonal coordination of cuticulin deposition and morphogenesis in *Drosophila* imaginal discs *in vivo* and *in vitro*. *Dev. Biol.* 114:1-11.

Fristrom D and Fristrom JW. 1993. The metamorphic development of the adult epidermis. In: Bate M and Martínez-Arias A. 1993. *The Development of Drosophila melanogaster*, Cold Spring Harbor Laboratory Press, New York, pp. 843–897.

Fristrom DK, Wilcox ME and Fristrom J. 1993. The distribution of PS integrins, laminin A and F-actin during key stages in *Drosophila* wing development. *Development* 117:509-523.

Fristrom DK, Gotwals P, Eaton S, Kornberg TB, Sturtevant MA, Bier E and Fristrom JW. 1994. blistered: a gene required for vein/intervein formation in wings of *Drosophila*. *Development* 120:2661-2671.

- Frosch BA, Berquin I, Emmert-Buck MR and Moin KBF. 1999. Molecular regulation, membrane association and secretion of tumor cathepsin B. *APMIS*, 107:28-37
- Galko MJ and Krasnow MA. 2004. Cellular and Genetic Analysis of Wound Healing in *Drosophila* Larvae 2:1114-1126
- Gates J and Thummel CS. 2000. A screen for ecdysone-regulated genes required for the morphogenesis of adult appendages during metamorphosis. *A. Dros. Res. Conf.* 41:569
- Gendre N, Luer K, Friche S, Grillenzoni N, Ramaekers A, Technau GM and Stocker RF. 2004. Integration of complex larval chemosensory organs into the adult nervous system of *Drosophila*. *Development* 131:83-92.
- Genova JL, Jong S, Camp JT and Fehon RG. 2000. Functional analysis of Cdc42 in actin filament assembly, epithelial morphogenesis, and cell signalling during *Drosophila* development. *Dev Biol* 221:181-194.
- Giancotti FG and Ruoslahti E. 1999. Review. Integrin signaling. *Science* 285:1028-32.
- Gibson MC and Schubiger G. 2000. Peripodial cells regulate proliferation and patterning of *Drosophila* imaginal discs. *Cell* 103:343 -350
- Gibson MC and Schubiger G. 2001. *Drosophila* peripodial cells, more than meets the eye? *BioEssays* 23:691-697.
- Gibson MC and Schubiger G. 2001. Peripodial membrane cells regulate imaginal disc development in *Drosophila*. *Dev. Biol.* 235:183.
- Gibson MC, Lehman DA. and Schubiger G. 2002. Luminal transmission of decapentaplegic in *Drosophila* imaginal discs. *Dev. Cell* 3, 451-460.
- Gibson MC and Perrimon N. 2004. DPP signaling via TKV drives epithelial morphogenesis during wing disc development. *A. Dros. Res. Conf.* 45:536B.
- Gibson MC and Perrimon N. 2005. Extrusion and death of DPP/BMP-compromised epithelial cells in the developing *Drosophila* wing. *Science* 307:1785 -1789.
- Gire V and Wynford-Thomas D. 1998 Origin and progression of thyroid epithelial tumors: molecular and cellular mechanisms. *Arch Anat Cytol Pathol* 46:11-8.
- Glise B and Noselli S. 1997. Coupling of Jun amino-terminal kinase and Decapentaplegic signalling pathways in *Drosophila* morphogenesis. *Genes Dev* 11:1738-1747

- Glise B, Jacinto A, Parsons LM and Ingham PW. 1999. A screen to identify new components of the Hedgehog and Decapentaplegic signalling pathways in *Drosophila*. *Europ. Dros. Res. Conf.* 16:49.
- Godenschwege TA, Pohar N, Buchner S and Buchner E. 2000. Inflated wings, tissue autolysis and early death in tissue inhibitor of metalloproteinases mutants of *Drosophila*. *Europ. J. Cell Biol.* 79:495-501.
- Goshima G and Vale RD. 2003. The roles of microtubule-based motor proteins in mitosis: comprehensive RNAi analysis in the *Drosophila* S2 cell line. *J. Cell Biol.* 162:1003-1016.
- Gottlieb E, Haffner R, von Rüden T, Wagner EF and Oren M. 1994. Down-regulation of wild-type p53 activity interferes with apoptosis of IL-3-dependent haematopoietic cells following IL-3 withdrawal. *EMBO J.* 13:1368-1374
- Grace TDC. 1954. Culture of insect tissues. *Nature* 173:187-188.
- Grace TDC. 1962. Establishment of four strains of cells from insect tissues grown *in vitro*. *Nature* 195:788-789
- Grace TDC. 1966. Establishment of a Line of Mosquito (*Aedes aegypti* L.) Cells Grown *In Vitro*. *Nature* 211:366 - 367
- Greco V, Hannus M and Eaton S. 2001. Argosomes. A potential vehicle for the spread of morphogens through epithelia. *Cell* 106:633-645.
- Grisaru D, Sternfeld M, Eldor A and Glick D. 1999. Structural roles of acetylcholinesterase variants in biology and pathology. Soreq H. *Eur J Biochem.* 264:672-86.
- Grotewiel MS, Martin I, Bhandari P and Cook-Wiens E. 2005. Functional senescence in *Drosophila melanogaster*. *Ageing Res. Revs* 4:372-397.
- Guertin D, Guntur K, Bell G, Thoreen C, and Sabatini D. 2006. Functional Genomics Identifies TOR-Regulated Genes that Control Growth and Division. *Current Biology* 16:958-970.
- Harris TJ and Peifer M. 2005. The positioning and segregation of apical cues during epithelial polarity establishment in *Drosophila*. *J. Cell Biol.* 170:813-823.
- Hayflick L and Moorhead PS. 1961. The serial cultivation of human diploid cell strains. *Exp Cell Res* 25:585-621
- Heid CA, Stevens J, Livak KJ and Williams PM. 1996. Real time quantitative PCR. *Genome Res.* 6:986-994

- Hicke L. 1999. Gettin' down with ubiquitin: turning off cell-surface receptors, transporters and channels. *Trends in Cell Biol.* 9:107-112.
- Higa LA, Yang X, Zheng J, Banks D, Wu M, Ghosh P, Sun H and Zhang H. 2006. Involvement of CUL4 ubiquitin E3 ligases in regulating CDK inhibitors Dacapo/p27Kip1 and cyclin E degradation. *Cell Cycle* 5:71-77.
- Hinck LW, Nelson J and Papkoff J. 1994. Wnt-1 Modulates Cell-Cell Adhesion in Mammalian Cells by Stabilizing β -Catenin Binding to the Cell Adhesion Protein Cadherin. *The Journal of Cell Biology* Volume 124:729-741
- Hogness DS, Talbot WS, Bender MT and Koelle M. 1992. Ecdysone receptors and genetic regulatory hierarchies determining the developmental response of *Drosophila* tissues to ecdysone. *Abstr. Ecdysone Wkshp* 10:45.
- Huang Y, Baker RT and Fischer-Vize JA. 1995. Control of cell fate by a deubiquitinating enzyme encoded by the fat facets gene. *Science* 270:1828-1831.
- Huber W, von Heydebreck A, Sultmann H, Poustka A and Vingron M. 2002. Variance stabilization applied to microarray data calibration and to the quantification of differential expression. *Bioinformatics* 18:96-104
- Hudson AM and Cooley L. 2002. A subset of dynamic actin rearrangements in *Drosophila* requires the Arp2/3 complex. *J. Cell Biol.* 156:677-687.
- Hutson MS, Tokutake Y, Chang MS, Bloor JW, Venakides S, Kiehart DP and Edwards G. S. 2003. Forces for morphogenesis investigated with laser microsurgery and quantitative modeling. *Science* 300:145-149
- Irvine KD and Wieschaus E. 1994. Cell intercalation during *Drosophila* germband extension and its regulation by pair-rule segmentation genes. *Development* 120:827-841
- Ito K and Hotta Y. 1992. Proliferation pattern of postembryonic neuroblasts in the brain of *Drosophila melanogaster*. *Dev. Biol.* 149:134-148.
- Jacinto A, Wood W, Woolner S, Hiley C, Turner L, Wilson C, Martinez-Arias A and Martin P. 2002. Dynamic Analysis of Actin Cable Function during *Drosophila* Dorsal Closure. *Current Biology* 12:1245-1250
- Jacinto A, Wood W, Balayo T, Turmaine M, Martinez-Arias A and Martin P. 2000. Dynamic actin-based epithelial adhesion and cell matching during *Drosophila* dorsal closure. *Curr. Biol.* 10:1420-1426
- Jacinto A, Wood W, Woolner S, Hiley C, Turner L, Wilson C, Martinez Arias A and Martin P. 2002. Dynamic analysis of actin cable function during *Drosophila* dorsal closure. *Curr. Biol.* 12:1245-1250.

- Jacinto A, Woolner S, Martin P. 2002. Dynamic analysis of dorsal closure in *Drosophila*. From genetics to cell biology. *Dev. Cell* 3:9-19.
- Jacobs JR and Stevens JK. 1986. Changes in the organization of the neuritic cytoskeleton during nerve growth factor-activated differentiation of PC12 cells: a serial electron microscopic study of the development and control of neurite shape. *The Journal of Cell Biology* 103:895-906.
- Jan YN and Jan LY. 2003. The Peripheral Nervous System. In: *The Development of Drosophila melanogaster* 20:1207-1244
- Jan YN and Yan LY. 2004. The control of dendrite development. *Neuron* 40 2: 229-242.
- Jenny A, Reynolds-Kenneally J, Das G, Burnett M and Mlodzik M. 2005. Diego and Prickle regulate Frizzled planar cell polarity signalling by competing for Dishevelled binding. *Nature Cell Biol.* 7 :691-697.
- Jiang C, Baehrecke EH and Thummel C.S. 1997. Steroid regulation of program cell death during *Drosophila* metamorphosis. *Dev. Biol.* 186:253.
- Jiang C, Lamblin AFJ, Steller H and Thummel CS. 2000. A steroid-triggered transcriptional hierarchy controls salivary gland cell death during *Drosophila* metamorphosis. *Molec. Cell* 5:445-455.
- Kaltschmidt JA, Davidson CM, Brown NH and Brand AH. 2000. Rotation and asymmetry of the mitotic spindle direct asymmetric cell division in the developing central nervous system. *Nature Cell Biol.* 2:7-12.
- Kaltschmidt JA, Lawrence N, Morel V, Balayo T, Fernandez BG, Pelissier A, Jacinto A and Martinez Arias A. 2002. Planar polarity and actin dynamics in the epidermis of *Drosophila*. *Nature Cell Biol.* 4:937-944.
- Kam ZV, Minden JS, Agard DA, Sedat JW and Leptin M. 1991. *Drosophila* gastrulation: analysis of cell shape changes in living embryos by three-dimensional fluorescence microscopy. *Development* 112:365-370
- Kawamura K, Shibata T, Saget O, Peel D and Bryant PJ. 1999. A new family of growth factors produced by the fat body and active on *Drosophila* imaginal disc cells. *Development* 126:211-219.
- Kearney JB, Wheeler SR, Estes P, Parente B and Crews ST. 2004. Gene expression profiling of the developing *Drosophila* CNS midline cells. *Dev. Biol.* 275:473-492.
- Kee Y, Muñoz W, Lyon N and Huibregtse JM. 2006. The Deubiquitinating Enzyme Ubp2 Modulates Rsp5-dependent Lys63-linked Polyubiquitin Conjugates in *Saccharomyces cerevisiae*. *J. Biol. Chem* 281:36724-36731

- Keller R E.1986. The cellular basis of amphibian gastrulation. In *Developmental Biology: A Comprehensive Synthesis. The Cellular Basis of Morphogenesis.* ed. L. Browder 2:241-327.
- Keller R E. 1991. Early embryonic development of *Xenopus laevis*. *Methods in Cell Research Xenopus laevis: Practical Uses in Cell and Molecular Biology.* ed. B. Kay and B. Peng 36:61-113.
- Keller R, Davidson L, Edlund A, Elul T, Ezin M, Shook D and Skoglund P. 1991. Mechanisms of Convergence and Extension by Cell Intercalation *Philosophical Transactions: Biological Sciences* 355:471–490
- Kiehart DP, Galbraith C G, Edwards K A, Rickoll W L and Montague R A 2000. Multiple Forces Contribute to Cell Sheet Morphogenesis for Dorsal Closure in *Drosophila*. *The Journal of Cell Biology* 149:471–490
- Kiger JA Jr, Natzle JE and Green MM. 2001. Hemocytes are essential for wing maturation in *Drosophila melanogaster*. *Proc Natl Acad Sci U S A.* 98:10190–10195
- Kiger A, Baum B, Jones S, Jones M, Coulson A, Echeverri C and Perrimon N. 2003. A functional genomic analysis of cell morphology using RNA interference. *J. Biol.* 2:4-27.
- Kiger JA Jr, Natzle JE, Kimbrell DA, Paddy MR, Kleinhesselink K and Green MM. 2007. Related Tissue remodelling during maturation of the *Drosophila* wing. *Dev Biol.* 301:178-91.
- Kipreos ET, Lander LE, Wing JP, He WW and Hedgecock EM. 1996. *cul-1* is required for cell cycle exit in *C. elegans* and identifies a novel gene family. *Cell* 85:829–839.
- Koelle M, Talbot WS, Segraves WA, Bender MT, Cherbas P and Hogness DS. 1991. The *Drosophila* EcR gene encodes an ecdysone receptor, a new member of the steroid receptor superfamily. *Cell* 67:59-77.
- Koepp 1999. How the cyclin became a cyclin: regulated proteolysis in the cell cycle. *Cell* 97:431-434.
- Kopec S.1924. Studies on the influence of inaction on the development and the duration of life in insects. *Biol. Bull., Wood's Hole* 46:1-21.
- Köppen M, Fernández BG, Carvalho L, Jacinto A and Heisenberg CP. 2006. Coordinated cell-shape changes control epithelial movement in zebrafish and *Drosophila* *Development* 133:2671-2681
- Kozlova T and Thummel CS. 2000. Steroid regulation of postembryonic development and reproduction in *Drosophila*. *Trends Endocrinol. Metab.* 11:276-280.

Kozlova T and Thummel CS. 2002. Spatial patterns of ecdysteroid receptor activation during the onset of *Drosophila* metamorphosis. *Development* 129:1739-1750.

Kozlova T and Thummel C.S. 2003. Essential roles for ecdysone signaling during *Drosophila* mid-embryonic development. *Science* 301:1911-1914.

Krtolica A, Parrinello S, Lockett S, Desprez PY and Campisi J. 2001. Senescent fibroblasts promote epithelial cell growth and tumorigenesis: a link between cancer and aging. *Proc Natl Acad Sci U S A*. 98:12072-7

Krtolica A and Campisi J. 2002. Cancer and aging: a model for the cancer promoting effects of the aging stroma. *Int. J. Biochem. Cell Biol.* 34:1401-1414

Kurtti TJ and Brooks M.A. 1976. The Dissociation Of Insect Embryos For Cell Culture. *In Vitro* 12:2

Kurtti TJ and Brooks MA. 1976. Preparation of Mycetocytes for Culture *In Vitro*. *Journal of Invertebrate Pathology* 27:209-214

Landureau JC and Jollès 1969. Etude des exigences d'insectes souch Epa Acides amines *Experimental Cell Research* 54:391-398

Lecuit T. 2005. Adhesion Remodeling underlying tissue morphogenesis *Review Trends in Cell Biology* 15:505-507

Lee T, Lee A and Luo L. 1999. Development of the *Drosophila* mushroom bodies: sequential generation of three distinct types of neurons from a neuroblast. *Development* 126:4065-4076.

Lee T, Lee A and Luo, L. 1999. Function of RhoA in the development of mushroom body revealed by mosaic analysis with a repressible cell marker. *A. Dros. Res. Conf.* 40:494A.

Lee CY, Cooksey BAK and Baehrecke EH. 2002. Steroid regulation of midgut cell death during *Drosophila* development. *Dev. Biol.* 250:101-111.

Lengyel JA and Iwaki DD. 2002. It takes guts: the *Drosophila* hindgut as a model system for organogenesis. *Dev. Biol.* 243:1-19

Leptin M. and Grunewald B. 1990. Cell shape changes during gastrulation in *Drosophila*. *Development* 110:73-84.

Levi MS, Borne RF & Williamson JS. 2001 A review of cancer chemopreventive agents. *Current Medical Chemistry* 8:1349-1362.

Li TR and White KP. 2003. Tissue-specific gene expression and ecdysone-regulated genomic networks in *Drosophila*. *Dev. Cell* 5:59-72.

- Lin DM and Goodman CS. 1994. Ectopic and increased expression of Fasciclin II alters motoneuron growth cone guidance. *Neuron* 13:507-523.
- Lisi S, Mazzon I and White K. 2000. Diverse domains of THREAD/DIAP1 are required to inhibit apoptosis induced by REAPER and HID in *Drosophila*. *Genetics* 154:669-678.
- Llano E, Adam G, Pendas A.M, Quesada V, Sanchez L.M, Santamaria I, Noselli S and Lopez-Otin C. 2002. Structural and enzymatic characterization of *Drosophila* Dm2-MMP, a membrane-bound matrix metalloproteinase with tissue-specific expression. *J. Biol. Chem.* 277 :23321-23329.
- Lum L, Yao S, Mozer B, Rovescalli A, Von Kessler D, Nirenberg M and Beachy PA. 2003. Identification of Hedgehog pathway components by RNAi in *Drosophila* cultured cells. *Science* 299:2039-45
- Lynn DE and Oberlander H. 1981. The effect of cytoskeletal disrupting agents on the morphological response of a cloned *Manduca sexta* cell line to 20-hydroxy-ecdysone. *Journal Development Genes and Evolution* 190:150-155
- Lynn D and Hung ACF. 1991. Development of Continuous Cell Lines from the Egg Parasitoids *Trichogramma confusum* and *T. exiguum*. *Archives of Insect Biochemistry and Physiology* 18:99-104.
- Lynn DE. 1996. Development and characterization of insect cell lines. *Cytotechnology* 20:3-11.
- Lynn DE, Oberlander H and Porcheron P. 1998. Tissues and Cells in Culture. *Microscopic Anatomy of Invertebrates* 11:1119-1141
- Lynn DE. 2001. Novel techniques to establish new insect cell lines. *In Vitro Cell. Dev. Biol. Animal* 37:319-321.
- Marks EP. 1970. The Action of Hormones in Insect cell and Organ Cultures. *General and Comparative Endocrinology* 15:289-302
- Marks EP, Balke J and Klosterman H. 1984. Evidence for Chitin Synthesis in an Insect Cell line. *Archives of Insect Biochemistry and Physiology* 1:225-230
- Marks EP and Ward GB. 1987. Cell culture Techniques for Studying Insect Cuticle *Archives of Insect Biochemistry and Physiology* 6:217-225
- Martin D, Zusman S, Li X, Williams EL, Khare N, DaRocha S, Chiquet-Ehrismann R, Baumgartner S. 1999. wing blister, a new *Drosophila* laminin alpha chain required for cell adhesion and migration during embryonic and imaginal development. *J. Cell Biol.* 145:191-201.

- Martin P and Parkhurst SM. 2004. Parallels between tissue repair and embryo morphogenesis. *Development* 131:3021 -3034
- Martín-Blanco E, Gampel A, Ring J, Virdee K, Kirov N, Tolkovsky A.M. and Martínez-Arias A. 1998. puckered encodes a phosphatase that mediates a feedback loop regulating JNK activity during dorsal closure in *Drosophila*. *Genes Dev.*12:557–570.
- McCartney B M and Fehon R G. 1996. Distinct Cellular and Subcellular Patterns of Expression Imply Distinct Functions for the *Drosophila* Homologues of Moesin and the Neurofibromatosis 2 Tumor Suppressor, Merlin. *The Journal of Cell Biology* 133:843-852.
- McClure KD and Schubiger G. 2005. Developmental analysis and squamous morphogenesis of the peripodial epithelium in *Drosophila* imaginal discs. *Development* 132, 5033-5042.
- McCluskey J and Martin P. 1995. Analysis of the tissue movements of embryonic wound healing – DiI studies in the limb bud stage mouse embryo. *Dev. Biol.* 170:102-114
- McEwen DG and Peifer, M. 2000. Wnt signaling: moving in a new direction. *Curr. Biol.* 10:562-R564.
- Medina M, Leon P and Vallejo C.G. 1988. *Drosophila* cathepsin B-like proteinase: a suggested role in yolk degradation. *Arch. Biochem. Biophys.* 263:355-363.
- Medioni C and Noselli S. 2005. Dynamics of the basement membrane in invasive epithelial clusters in *Drosophila*. *Development* 132:3069-3077.
- Melk A. 2003. Senescence of renal cells: molecular basis and clinical implications, *Oxford Journals Medicine Nephrology Dialysis Transplantation* 18:2474-2478
- Miller AS, Cottam DM and Milner MJ. 2000. Adhesion of *Drosophila* imaginal disc cells *in vitro*. *In Vitro Cell. Dev. Biol. A.* 36:174-179.
- Miller AS, Cottam DM and Milner MJ. 2000. Cell-cell and cell-substrate adhesion in cultured *Drosophila* imaginal disc cells. *In Vitro Cell. Dev. Biol. A.* 36:180-187.
- Milner MJ. 1977. The eversion and differentiation of *Drosophila melanogaster* leg and wing imaginal discs cultured *in vitro* with an optimal concentration of beta-ecdysone. *J. Embryol. Exp. Morphol.* 37:105-117.
- Milner MJ and Dübendorfer A. 1982. Tissue-specific effects of the juvenile hormone analogue ZR 515 during metamorphosis in *Drosophila* cell cultures. *J. Insect Physiol.* 28:661-666.

Milner MJ, Bleasby AJ and Pyott A. 1983. The role of the peripodial membrane in the morphogenesis of the eye antennal disc of *Drosophila melanogaster*. Roux Arch. dev. Biol. 192:164-170.

Milner M, Bleasby A and Kelly S. 1984. The role of the peripodial membrane of leg and wing imaginal discs of *Drosophila melanogaster* during evagination and differentiation *in vitro*. Wilhelm Roux's Arch. Dev. Biol. 193:180 -186.

Milner MJ and Muir J. 1987. The cell biology of *Drosophila* wing metamorphosis *in vitro*. Roux Arch. dev. Biol. 196:191-201.

Milner MJ, Cottam DM and Miller AS. 2000. Metamorphosis during the passage of *Drosophila* imaginal disc cell lines: cell adhesion, the effect of insect hormones and ageing. *In Vitro Cell. Dev. Biol. A.* 36:13

Miranti C K and Brugge J S. 2002. Review: Sensing the environment: a historical perspective on integrin signal transduction. *Nat Cell Biol.* 4:83-90.

Mirre C, Cecchini JP, Le Parco Y. and Knibiehler B. 1988. De novo expression of a type IV collagen gene in *Drosophila* embryos is restricted to mesodermal derivatives and occurs at germ band shortening. *Development* 102:369-376.

Misquitta L and Paterson BM. 1999. Targeted disruption of gene function in *Drosophila* by RNA. *Genes & Dev.* 13:3191-3197.

Mitsuhashi J. 1969. Preliminary report on the Primary Culture of Smaller Brown Plant-hopper Cells *in vitro*. *Applied Ent. Zoology* 4:151-153

Mitsuhashi J. 1976. Primary Cultures of the Cells From Ovaries Of The Cabbage Armyworm, *Mamestra Brassicae* L. (Lepidoptera: Noctuidae). *Development, Growth and Differentiation* 18:163-166.

Mitsui T and Riddiford LM. 1976. Pupal cuticle formation by *Manduca sexta* epidermis *in vitro*. *Developmental Biology* 68:172-186,

Montgomery M K, Xu S, Fire A. 1998. RNA as a target of double-stranded RNA mediated genetic interference in *Caenorhabditis elegans*. *Proc Natl Acad Sci* 95:15502–15507.

Morris JZ, Navarro C, Lehmann R. 2003. Identification and analysis of mutations in bob, Doa and eight new genes required for oocyte specification and development in *Drosophila melanogaster*. *Genetics* 164:1435-1446.

Muller HAJ. 2000. Genetic control of epithelial cell polarity: lessons from *Drosophila*. *Dev. Dynamics* 218:52-67.

Munoz NM, Upton M, Rojas A, Washington MK, Lin L, Chytil A, Sozmen EG, Madison BB, Pozzi A, Moon RT, Moses HL and Grady WM. 2006. Transforming growth factor beta receptor type II inactivation induces the malignant transformation of intestinal neoplasms initiated by Apc mutation. *Cancer Res.* 66:9837-44.

Muro I, Hay BA and Clem RJ. 2002. The *Drosophila* DIAP1 protein is required to prevent accumulation of a continuously generated, processed form of the apical caspase DRONC. *J. Biol. Chem.* 277:49644-49650.

Murray MA, Fessler LI and Palka J. 1995. Changing distributions of extracellular matrix components during early wing morphogenesis in *Drosophila*. *Dev. Biol.* 168:150-165.

Nardi JB, Miklasz SD. 1989. Hemocytes contribute to both the formation and breakdown of the basal lamina in developing wings of *Manduca sexta*. *Tissue & Cell* 21:559-567

Navarro PM, Gomez A, Pizarro C, Gamallo A, Quintanilla A and Cant A. 1991. A role for E-cadherin cell-cell adhesion molecule during tumor progression of mouse epidermal carcinogenesis. *J. Cell Biol.* 110:349-357

Nelson RE, Fessler LI, Takagi Y, Blumberg B, Keene DR, Olson PF, Parker CG, Fessler JH. 1994. Peroxidase: A novel enzyme-matrix protein of *Drosophila* development. *EMBO J.* 13:3438-3447.

Nusse RA, Ooyen van Cox D, Fung YK and Varmus HE. 1984. Mode of proviral activation of a putative mammary oncogene (int-1) on mouse chromosome 15. *Nature* 307:131-136.

Oberlander H. 1982. The hormonal control of development of imaginal disks. *Ursprung Nothiger* 55-172.

Oberlander H, Leach CE, Lanka S and Willis JH. 1987. Ecdysteroid Action on Moth Epithelial Tissues and Cell Lines. *Archives of Insect Biochemistry and Physiology* 5:81-89

Oberdörster E, Cottam DM, Wilmot FA, Milner MJ and McLachlan JA. 1999. Interaction of PAHs and PCBs with Ecdysone-Dependent Gene Expression and Cell Proliferation. *Toxicology and Applied Pharmacology* 160:101-108.

Oberdörster E, Clay MA, Cottam DM, Wilmot FA, Milner MJ and McLachlan JA. 2001. Common phytochemicals are ecdysteroid agonists and antagonists: a possible evolutionary link between vertebrate and invertebrate steroid hormones. (in press).

Oberlander H. 1985. The imaginal disc; in *Comprehensive insect physiology, biochemistry and pharmacology* (eds) Kerkut GA and Gilbert LI 2:151-182.

- Oda H and Tsukita S. 1999. Dynamic features of adherens junctions during *Drosophila* embryonic epithelial morphogenesis revealed by a D-alpha-catenin-GFP fusion protein. *Dev Genes Evol* 209:218–225.
- Oda H, Uemura T, Harada Y, Iwai Y and Takeichi M. 1994. A *Drosophila* homolog of cadherin associated with armadillo and essential for embryonic cell-cell adhesion. *Dev. Biol.* 165:716-726.
- O'Kane CJ, Gehring WJ. 1987. Detection in situ of genomic regulatory elements in *Drosophila*. *Proc Natl Acad Sci U S A.* 84:9123-7.
- Olson PF, Fessler, LI, Nelson RE, Sterne R, Campbell AG and Fessler JH. 1990. Glutactin, a novel *Drosophila* basement membrane-related glycoprotein with sequence similarity to serine esterases. *EMBO J.* 9:1219-1227.
- Orford K, Orford CC and Byers SW. 1999. Exogenous expression of beta-catenin regulates contact inhibition, anchorage-independent growth, anoikis, and radiation-induced cell cycle arrest. *J Cell Biol.* 146:855-68.
- Ovcharenko D, Jarvis R, Hunicke-Smith S, Kelnar K and Brown D. 2005. High-throughput RNAi screening *in vitro*: From cell lines to primary cells. *RNA.*11:985-993
- Paddison PJ, Caudy AA, Bernstein E, Hannon GJ and Conklin DS. 2002. Short hairpin RNAs (shRNAs) induce sequence-specific silencing in mammalian cells. *Genes and Development* 16:8:948-958.
- Page-McCaw A, Serano J, Sante JM, Rubin GM. 2003. *Drosophila* matrix metalloproteinases are required for tissue remodeling, but not embryonic development. *Dev. Cell* 4:95-106.
- Pai LM, Kirkpatrick C, Blanton J, Oda H, Takeichi M and Peifer M. 1996. *Drosophila* -catenin and E-cadherin bind to distinct regions of *Drosophila* Armadillo. *J. Biol. Chem.* 271:32411-32420.
- Pan W. 2002. A comparative review of statistical methods for discovering differentially expressed genes in replicated microarray experiments. *Bioinformatics.*18:546-54.
- Papa FR and Hochstrasser M. 1993. The yeast *doa4* gene encodes a deubiquitinating enzyme related to a product of the human *tre-2* oncogene. *Nature* 366:313-319
- Park M and Moon RT. 2002. The planar cell-polarity gene *stbm* regulates cell behaviour and cell fate in vertebrate embryos. *Nat Cell Biol.* 4:20-5.
- Parrinello S, Coppe JP, Krtolica A and Campisi J. 2005. Stromal-epithelial interactions in aging and cancer: senescent fibroblasts alter epithelial cell differentiation. *J Cell Sci.* 1:485-96.

Pastor-Pareja JC, Grawe F, Martín-Blanco E and García-Bellido A. 2004. Invasive Cell Behavior during *Drosophila* Imaginal Disc Eversion Is Mediated by the JNK Signaling Cascade. *Developmental Cell* Volume 7 :387-399

Peel DJ and Milner MJ. 1990. The diversity of cell morphology in cloned cell lines derived from *Drosophila* imaginal discs. *Roux's Archives of Developmental Biology* 198:479-482

Peel DJ and Milner MJ. 1992. The expression of PS integrins in *Drosophila melanogaster* imaginal disc cell lines. *Roux Arch. dev. Biol.* 201:120-123.

Peel DJ and Milner MJ. 1992. The response of *Drosophila* imaginal disc cell lines to ecdysteroids. *Roux Arch. dev. Biol.* 202:23-35.

Pino-Heiss SA and Schubiger G. 1989. Extracellular protease production by *Drosophila* imaginal discs. *Dev. Biol.* 132:282-291.

Priddle H, Hemmings L, Monkley S, Woods A, Patel B, Sutton D, Dunn GA, Zicha D and Critchley DR. 1998. Disruption of the talin gene compromises focal adhesion assembly in undifferentiated but not differentiated embryonic stem cells. *J Cell Biol.* 142:1121-33.

Pöschl E, Schlötzer-Schrehardt U, Brachvogel B, Saito K, Ninomiya Y and Mayer U. 2004. Collagen IV is essential for basement membrane stability but dispensable for initiation of its assembly during early development. *Development* 131:1619-1628.

Riddiford LM, Kiguchi K, Roseland CR, Chen AC and Wolfgang WJ. 1980. Cuticle formation and sclerotization *in vitro* by the epidermis of the tobacco hornworm, *Manduca Sexta*. *Invertebrate Systems In Vitro*, Eds: Kurstak, E. Maramorosch K and Dubendorfer A. Elsevier North Holland 10:103-116

Riddiford LM. 1993. Hormone receptors and the regulation of insect metamorphosis. *Receptor* 3:203-209.

Rizki MTM. 1957. The nature of the crystal cells of *Drosophila melanogaster*. *Anat. Rec.* 128:608.

Rizki MTM. 1961. Experimental analysis of haemocyte morphology. *Am. Zool.* 1:383.

Robertson CW. 1936. The metamorphosis of *Drosophila melanogaster*, including an accurately timed account of the principal morphological changes. *J Morphol.* 59:351-99.

Robinow S and White K. 1991. Characterization and spatial distribution of the ELAV protein during *Drosophila melanogaster* development. *J. Neurobiol.* 22:443-461.

- Robles SJ and Adamia GR. 1998. Agents that cause DNA double strand breaks lead to p16INK4a enrichment and the premature senescence of normal fibroblasts. *Oncogene* 16:1113-1123
- Rogalskia TM, Mullena GP, Gilberta MM, Williams BD and Moermana DG. 2000. The UNC-112 Gene in *Caenorhabditis elegans* Encodes a Novel Component of Cell–Matrix Adhesion Structures Required for Integrin Localization in the Muscle Cell Membrane. *Journal of Cell Biology* 150:253-264
- Rogers SL, Rogers GC, Sharp DJ and Vale RD. 2002. *Drosophila* EB1 is important for proper assembly, dynamics, and positioning of the mitotic spindle. *J. Cell Biol.* 158:873-884.
- Roignant JY, Carre C, Mugat B, Szymczak D, Lepesant JA and Antoniewski C. 2003. Absence of transitive and systemic pathways allows cell-specific and isoform-specific RNAi in *Drosophila*. *RNA N.Y.* 9:299-308.
- Rolls MM, Albertson R, Shih HP, Lee CY, Doe CQ. 2003. *Drosophila* aPKC regulates cell polarity and cell proliferation in neuroblasts and epithelia. *J. Cell Biol.* 163:1089-1098.
- Rorth P. 2002. Initiating and guiding migration: lessons from border cells. *Trends Cell Biol.* 12:325-331.
- Rosset R. 1978. Effects of ecdysone on a *Drosophila* cell line. *Exp Cell Res* 111:31–36
- Saburi S and McNeill H. 2005. Organising cells into tissues: new roles for cell adhesion molecules in planar cell polarity. *Curr. Opin. Cell Biol.* 17:482-488.
- Sameni M, Dosescu J, Moin K and Sloane BF. 2003. Functional imaging of proteolysis: stromal and inflammatory cells increase tumor proteolysis. *Mol Imaging.* 2:159-75.
- Sang JH and Shields G. 1973. Development of embryonic *Drosophila* cells in culture. *Genetics* 74:238-239.
- Sang JH. 1981. *Drosophila* Cells and Cell Lines. In *Advances in Cell Culture* pp125-182
- Santini T, Rainaldi G and Indovina PL. 2000. Apoptosis, cell adhesion and the extracellular matrix in the dimensional growth of multicellular tumor spheroids. *Hematology* 36:75–87
- Scarborough JA, Cottam DM and Milner MJ. 2003. *Drosophila* Primary Embryonic Cultures Revisited. *Europ. Dros. Res. Conf.* 18 : H28.
- Schnaper HW, Kopp JB, Poncelet AC, Hubchak SC, Stetler-Stevenson WG, Klotman PE and Kleinman HK. 1996. Increased expression of extracellular matrix proteins and

- decreased expression of matrix proteases after serial passage of glomerular mesangial cells. *J Cell Sci.*109:2521-8
- Schneider I. 1971. The Culture of Cells from Insects and Ticks. *Current Topics in Microbiology and Immunology* 55:1-12
- Schneider I. 1972. Cell lines derived from late embryonic stages of *Drosophila melanogaster*. *J. Embryol. exp. Morphol.* 27:353-365.
- Schubiger M and Truman JW. 2000. The RXR ortholog USP suppresses early metamorphic processes in *Drosophila* in the absence of ecdysteroids. *Development* 127:1151-1159.
- Schubiger M, Wade AA, Carney GE, Truman JW and Bender M. 1998. *Drosophila* EcR-B ecdysone receptor isoforms are required for larval molting and for neuron remodeling during metamorphosis. *Development* 125:2053-2062.
- Seecof RL and Donady JJ. 1972. Factors Affecting *Drosophila* Neuron and Myocyte Differentiation *In Vitro*. *Mechanisms of Ageing and Development* 1: 165-174
- Seecof RL, Alleaume N, Teplitz RL and Gerson I. 1971. Differentiation of Neurons and Myocytes in Cell Cultures made from *Drosophila* Gastrulae. *Experimental Cell Research* 69:161-173
- Seecof RL, Gerson I, Donady JJ and Teplitz RL. 1973. *Drosophila* Myogenesis *in vitro*: The Genesis of 'Small' Myocytes and Myotubes. *Developmental Biology* 35:250-261
- Shi L, Sawada M, Sester U and Carlson JC. 1994. Alterations in free radical activity in aging *Drosophila*. *Exp. Gerontol.* 29:575-584.
- Shields G and Sang JH. 1970. Characteristics of five cell types appearing during *in vitro* culture of embryonic material from *Drosophila melanogaster*. *Journal Embryology and Experimental Morphology* 23:53-69
- Shields G, Dübendorfer A and Sang JH. 1975. Differentiation *in vitro* of larval cell types from early embryonic cells of *Drosophila melanogaster*. *Journal of Experimental Morphology* 33:159-175
- Shields G and Sang JH. 1977. Improved medium for culture of *Drosophila* embryonic cells. *D.I.S.* 52:161.
- Shulman JM, Perrimon N, Axelrod JD. 1998. Frizzled signaling and the developmental control of cell polarity. *Trends Genet.* 14:452-458.
- Sloane BF, Moin K, Sameni M, Tait LR, Rozhin J and Ziegler G. 1994. Membrane association of cathepsin B can be induced by transfection of human breast epithelial cells with c-Ha-ras oncogene. *J. Cell Sci.* 107:373-384

- Sloane BF, Yan S, Podgorski I, Linebaugh BE, Cher ML, Mai J, Cavallo-Medved D, Sameni M, Dosescu J, Moin K. 2005. Cathepsin B and tumor proteolysis: contribution of the tumor microenvironment. *Semin Cancer Biol.*15:149-57.
- Sonoda J and Wharton RP. 2001. *Drosophila* Brain Tumor is a translational repressor. *Genes Dev.* 15:762-773.
- Stevens B, Alvarez CM, O'Connor JD. 1980. Acquisition of resistance to ecdysteroid induced differentiative responses in Kc cells. *J. Cell Biol.* 87:30a.
- Strutt DI. 2001. Asymmetric localization of frizzled and the establishment of cell polarity in the *Drosophila* wing. *Molec. Cell* 7:367-375.
- Stupack DG, Puente XS, Boutsaboualoy S, Storgard CM and Cheresch DA. 2001. Apoptosis of adherent cells by recruitment of caspase-8 to unligated integrins. *J. Cell Biol.* 155:459-470.
- Stupack DG and Cheresch DA. 2003. Apoptotic cues from the extracellular matrix: regulators of angiogenesis *Review Oncogene* 22:9022-9029
- Sun B, Xu P and Salvaterra PM. 1999. Dynamic visualization of nervous system in live *Drosophila*. *Proc. Natl. Acad. Sci. USA* 96:10438-10443.
- Sun Q and Zinn K. 1998. Genetic studies of receptor tyrosine phosphatases and other molecules involved in *Drosophila* embryonic CNS development. *Abstr. Soc. Neurosci.* 24:1284.
- Sun YH, Jaw T, Jang CC, Chao YL, Yao LC and Pai CY. 1999. Positive and negative nuclear regulators of eye formation. *Europ. Dros. Res. Conf.* 16:174.
- Talbot WS, Swyryd EA and Hogness DS. 1993. *Drosophila* tissues with different metamorphic responses to ecdysone express different ecdysone receptor isoforms. *Cell* 73:1323-1337.
- Tepass U, Fessler LI, Aziz A and Hartenstein V. 1994. Embryonic origin of hemocytes and their relationship to cell death in *Drosophila*. *Development* 120 7:1829-1837.
- Tepass U and Knust E. 1990. Phenotypic and developmental analysis of mutations at the crumbs locus, a gene required for the development of epithelia in *Drosophila melanogaster*. *Roux Arch. dev. Biol.* 199:189-206.
- Tepass U, Theres C and Knust E. 1990. crumbs encodes an EGF-like protein expressed on apical membranes of *Drosophila* epithelial cells and required for organization of epithelia. *Cell* 61:787-799.

- Thummel CS, Burtis KC, Hogness D.S. 1990. Spatial and temporal patterns of E74 transcription during *Drosophila* development. *Cell* 61:101-111.
- Thummel C.S. 1992. Mechanisms of transcriptional timing in *Drosophila*. *Science* 255:39-40.
- Thummel C.S. 1994. Temporal coordination of regulatory gene expression by the steroid hormone ecdysone. *J. Cell. Biochem. Suppl.* 18B:385.
- Thummel C.S. 2001. Steroid-triggered death by autophagy. *BioEssays* 23:677-682.
- Tirnauer J S and Bierer BE. 2000. EB1 Proteins Regulate Microtubule Dynamics, Cell Polarity, and Chromosome Stability MiniReview -The Journal of Cell Biology 761-766.
- Tissot M and Stocker RF. 2000. Metamorphosis in *Drosophila* and other insects: the fate of neurons throughout the stages. *Prog. Neurobiol.* 62:89-111.
- Truman J.W. 1990. Metamorphosis of the central nervous system of *Drosophila*. *J. Neurobiol.* 21:1072-1084.
- Truman JW, Talbot WS, Fahrbach SE and Hogness DS. 1994. Ecdysone receptor expression in the CNS correlates with stage-specific responses to ecdysteroids during *Drosophila* and *Manduca* development. *Development* 120:219-234.
- Tucker JB, Mackie JB, Cottam DM, Rogers-Bald MM, Macintyre J, Scarborough JA and Milner MJ. 2004. Positioning and capture of cell surface-associated microtubules in epithelial tendon cells that differentiate in primary embryonic *Drosophila* cell cultures. *Cell Motil Cytoskeleton* 57:175-185.
- Tuschl T, Zamore PD, Lehmann R, Bartel DP and Sharp PA. 1999. Targeted mRNA degradation by double-stranded RNA *in vitro*. *Genes Dev.* 13:3191-7.
- Tusher VG, Tibshirani R and Chu G. 2001. Significance analysis of microarrays applied to the ionizing radiation response. *Proc Natl Acad Sci U S A.* 98:5116-21.
- Usui K and Simpson P. 2000. Cellular basis of the dynamic behavior of the imaginal thoracic discs during *Drosophila* metamorphosis. *Dev. Biol.* 225:13-25.
- Vega-Salas DE, Salas PJ and Rodriguez-Boulan. 1988. Exocytosis of vacuolar apical compartment (VAC): a cell-cell contact controlled mechanism for the establishment of the apical plasma membrane domain in epithelial cells. *J Cell Biol.* 107:1717-28.
- Vieira AV, Lamaze C and Schmid SL. 1996. Control of EGF receptor signalling by clathrin-mediated endocytosis. *Science* 274:2086-2089.

Wallingford J B. 2004. Closing in on vertebrate planar polarity. *Nature Cell Biology* 6:687-689

Ward EJ, Thaipisuttikul I, Terayama M, French RL, Jackson SM, Cosand KA, Tobler KJ, Dorman JB and Berg B. 2002. GAL4 enhancer trap patterns during *Drosophila* development. *Genesis* 34:46-50.

Watts RJ, Hoopfer ED and Luo L. 2003. Axon pruning during *Drosophila* metamorphosis: evidence for local degeneration and requirement of the ubiquitin-proteasome system. *Neuron* 38:871-885.

Watts RJ, Schuldiner O, Perrino J, Larsen C and Luo L. 2004. Glia engulf degenerating axons during developmental axon pruning. *Curr. Biol.* 14:678-684.

Wigglesworth VB. 1937. Wound healing in an insect (*Rhodnius prolixus* Hemiptera). *J Exp Biol* 14:364-381.

Williams BD and Waterston RH. 1994. Genes critical for muscle development and function in *Caenorhabditis elegans* identified through lethal mutations. *J. Cell Biol.* 124:475-490.

Williams DW and Shepherd D. 2000. The role of persistent larval neurons in the assembly of the adult sensory system of *Drosophila*. *Europ. J. Neurosci.* 12:499.

Williams DW, Tyrer M and Shepherd D. 2000. Tau and tau reporters disrupt central projections of sensory neurons in *Drosophila*. *J. comp. Neurol.* 428:630-640.

Williams KD, Helin AB, Posluszny J, Roberts SP and Feder ME. 2003. Effect of heat shock, pretreatment and hsp70 copy number on wing development in *Drosophila melanogaster*. *Molec. Ecol.* 12:1165-1177.

Williams-Masson EM, Malik AN and Hardin J. 1997. An actin-mediated two-step mechanism is required for ventral enclosure of the *C. elegans* hypodermis. *Development* 124:2889-2901.

Windham TC, Parikh NU, Siwak DR, Summy JM, McConkey DJ, Kraker AJ and Gallick GE. 2002. Src activation regulates anoikis in human colon tumor cell lines. *Oncogene* 21:7797-7807.

Wood W, Jacinto A, Grose R, Woolner S, Gale J, Wilson C and Martin P. 2002. Wound healing recapitulates morphogenesis in *Drosophila* embryos. *Nat. Cell Biol.* 4:907-912

Wood W, Jacinto A, Wilson C and Martin P. 2003. Wound healing recapitulates morphogenesis - dynamic studies of epithelial repair in *Drosophila* embryos. *A. Dros. Res. Conf.* 44:231C.

- Woodhouse E, Hersperger E and Shearn A. 1998. Growth, metastasis, and invasiveness of *Drosophila* tumors caused by mutations in specific tumor suppressor genes. *Dev. Genes Evol.* 207:542-550.
- Woods DF, Hough C, Peel D, Callaini G and Bryant PJ. 1996. Dlg protein is required for junction structure, cell polarity, and proliferation control in *Drosophila* epithelia. *J. Cell Biol.* 134:1469-1482.
- Woods DF, Hough CD, Bryant PJ. 1997. Linking cell-cell signaling to cytoarchitecture: Dlg function at the septate junction. *A. Dros. Res. Conf.* 38:34C.
- Wu C, Fritsch M, Hosokawa N, Jedlicka P, Kim SJ, Orosz A, Wisniewski J. 1995. Transcriptional regulation of heat shock genes. *J. Cell. Biochem. Suppl.* 19:190.
- Wu Z, Q Li, M Fortini, and Fischer JA. 1999. Genetic analysis of the role of the *Drosophila* fat facets gene in the ubiquitin pathway. *Dev. Genet.* 25:312-320
- Wyatt SS. 1956. Culture *in vitro* of tissue from the silkworm, *Bombyx mori*. *Insect Gen. Physiology* 39:841-852
- Yan S, Berquin IM, Troen BR, Sloane BF. 2000. Transcription of human cathepsin B is mediated by Sp1 and Ets family factors in glioma. *DNA Cell Biol.* 19:79-91.
- Yan N, Huh JR, Schirf V, Demeler B, Hay BA, Shi Y. 2006. Structure and activation mechanism of the *Drosophila* initiator caspase Dronc. *J. Biol. Chem.* 281:8667-8674.
- Yang CH, Axelrod JD, Simon MA. 2002. Regulation of frizzled by fat-like cadherins during planar polarity signaling in the *Drosophila* compound eye. *Cell* 108:675-688.
- Yang EJ, Zha J, Jockel LH, Boise, Thompson CB and Korsmeyer SJ. 1995. Bad, a heterodimeric partner for Bcl-XL and Bcl-2, displaces Bax and promotes cell death. *Cell* 80:285-291.
- Yao TP, Forman BM, Jiang Z, Cherbas L, Chen JD, McKeown M, Cherbas P and Evans RM. 1993. Functional ecdysone receptor is the product of EcR and Ultraspiracle genes. *Nature* 366:476 -479
- Yawata A, Adachi M, Okuda H, Naishiro Y, Takamura T, Hareyama M, Takayama S, Reed JC and Imai K. 1998. Prolonged cell survival enhances peritoneal dissemination of gastric cancer cells. *Oncogene* 16:2681-2686.
- Ye B, Grueber W, Yan LY and Jan YN. 2005. Genetic analysis of the differential development of dendrite and axon in *Drosophila* peripheral neurons. *FASEB J.* 19(4 Suppl. S P1)
- Yin VP and Thummel CS. 2005. Mechanisms of steroid-triggered programmed cell death in *Drosophila*. *Semin. Cell Dev. Biol.* 16:237-243.

- Young PE, Richman AM, Ketchum AS and Kiehart DP. 1993 Morphogenesis in *Drosophila* requires nonmuscle myosin heavy chain function. *Genes Dev.* 7:29–41
- Yun K, Fidler AE, Eccles MR and Reeve AE. 1993. Insulin-like growth factor II and WT1 transcript localization in human fetal kidney and Wilms' tumor. *Cancer Res.* 53:5166-71.
- Yun B, Farkas R, Lee K, Rabinow L. 1994. The Doa locus encodes a member of a new protein kinase family and is essential for eye and embryonic development in *Drosophila melanogaster*. *Genes Dev.* 8:1160-1173
- Zamore PD, Tuschl T, Sharp PA and Bartel DP. 2000. RNAi: Double-stranded RNA directs the ATP-dependent cleavage of mRNA at 21 to 23 nucleotide intervals. *Cell* 101:25-33.
- Zamore PD. 2001. RNA interference: listening to the sound of silence. *Nat Struct Biol. Review* 8:746-50.
- Zamore PD. 2002. Ancient pathways programmed by small RNAs. *Science* 296:1265-1269.
- Zinke I, Schutz CS, Katzenberger JD, Bauer M and Pankratz MJ. 2002. Nutrient control of gene expression in *Drosophila*: microarray analysis of starvation and sugar-dependent response. *EMBO J.* 21:6162-6173.

Appendices

Chapter 2

Culture medium for Clone 8+ cell lines, primary cultures and imaginal disc cultures systems

*MM3 for Imaginal disc cell cultures (g for 2 litre)

*Aspartic acid	0.6
Threonine	1
Serine	0.7
Asparagine	0.6
Glutamine	1.2
Alanine	3
Valine	0.8
Methionine	0.5
Isoleucine	0.5
Leucine	0.8
Tyrosine	0.5
Phenylalanine	0.5
b -Alanine	0.5
Histidine	1.1
Tryptophan	0.2
Arginine	1
Lysine HCl	1.7
Cysteine HCl	0.4
Proline	0.8
Glycine	1
KCl	5.2
MgSO ₄ .7H ₂ O	8
Na glutamate	15.72
Na ₂ H ₂ PO ₄ .2H ₂ O	0.88
CaCl ₂ .2H ₂ O	1.864
Glucose	20
TC Yeastolate	2
BIS-TRIS	2.1
PenGNa	0.064
Strep. sulph.	0.2
Oxaloacetic acid	0.5
Choline chloride	0.1

Adjust to pH 6.8 with 1%NaOH

*MM3 for Primary Embryonic Cell Culture (g for 2 litre)

*Aspartic acid	0.6
Threonine	1.0
Serine	0.7
Asparagine	0.6
Glutamine	1.2
Alanine	3.0
Valine	0.8
Methionine	0.5
Isoleucine	0.5
Leucine	0.8
Tyrosine	0.5
Phenylalanine	0.5
b -Alanine	0.5
Histidine	1.1
Tryptophan	0.2
Arginine	1.0
Lysine HCl	1.7
Cysteine HCl	0.4
Proline	0.8
Glycine	1.0
MgSO ₄ .7H ₂ O	8.8
Na glutamate	13.06
K glutamate.H ₂ O	15.76
Na ₂ H ₂ PO ₄ .2H ₂ O	1.76
CaCl ₂ .2H ₂ O	0.438
Glucose	20
TC Yeastolate	2
BIS-TRIS	2.1
Oxaloacetic acid	0.5
Choline chloride	0.1
PenGNa	0.064
Strep. sulph.	0.2

Adjust to pH 6.6 with 1%NaOH

KHCO ₃	1.0
-------------------	-----

Should now be pH 6.8.

Insulin

Sigma I1882. To make up to 12.5 IU/ml stock solution put 10mg in universal, add 0.5ml 0.01N HCl to dissolve add 19.5ml D = or PBS, and mix on vortex mixer. Leave it to stand until it clears then filter-sterilise the solution through a 0.22µm filter. Store at 4 deg. C for up to 1 month. This is added at 1ml per 100ml CSM.

Chapter 4

PBS

Per litre	
140 mM NaCl	8g
2.7 mM KCl	0.2g
1.5 mM KH ₂ PO ₄	0.2g
8.1 mM Na ₂ HPO ₄	1.15g

Chapter 6

TRIzol, GibcoBRL cat.no. 15596-018

1.5 ml microfuge tubes + pestle, Anachem, cat. no. K-749520-0090

Table 6a: Genes increased in YCl.8+ after ecdysone, no/small change in Cl8R cells

Pairwise comparison of Young Clone 8+ and Clone 8R before and after ecdysone

Table 6a: Genes upregulated in YCl.8+ after ecdysone, no/small change Cl.8R cells

Gene	Gene product: location and role
BEST:CK02318	Saccharopine dehydrogenase (NAD+, Llysine forming)
CG1090	Calcium, potassium:sodium antiporter
CG1648	Not known
fax	Axonogenesis
Glt	Basement membrane, calcium ion binding

Table 6a: Genes upregulated in YCl.8+ after ecdysone, no/small change Cl.8R cells. 5 genes were found which were positively expressed after ecdysone.

Table 6b: Genes downregulated in YCl.8+ after ecdysone, no/small change Cl8.R cells

Gene	Gene product: location and role
<i>bif</i>	cytoplasm, actin & microtubule binding, protein phosphatase 1 binding
<i>Cg25C</i>	Basement membrane, collagen type IV,
<i>CG3273</i>	Actin filament reorganisation (aka scrambled (sced))
<i>CG3380</i>	Sodium independent organic anion transporter
<i>CG3906</i>	Not known
<i>CG7224</i>	Not known
<i>CG9089</i>	Not known
<i>Chd64</i>	Actin binding
<i>cul-2</i>	Nuclear ubiquitin ligase complex
<i>Doa</i>	Cytoplasm, nucleus, protein kinase, protein amino acid phosphorylation
<i>ERR</i>	Ligand dependent nuclear receptor
<i>Ggamma30A</i>	Cytoplasm, GTPase, Gprotein coupled receptor protein signalling pathway
<i>Hex-A</i>	Hexokinase
<i>Idgf3</i>	Extracellular, imaginal disc growth factor ,
<i>Jafrac1</i>	Cytosol, antioxidant, thioredoxin peroxidase, redox homeostasis
<i>roX1</i>	Dosage compensation complex
<i>Trx-2</i>	Cellular component unknown, redox homeostasis

Table 6b: Genes downregulated in YCl.8+ after ecdysone, no/small change Cl8.R cells

17 genes were identified which had little or no change was found in the Clone 8R raw data after ecdysone

Chapter 8

Tables: 8.4a,b, 8.5a,b, 8.6a,b, 8.7a,b, 8.8a,b, 8.9a,b, 8.10a,b, 8.13c.

Table 8.4a: Genes of Interest upregulated in YCl.8+ cells after ecdysone

Gene	Gene product: Location and function
<i>Abl</i>	Adherens junction, nonmembrane spanning protein tyrosine kinase
<i>Act57B</i>	Actin filament, cytoskeleton
<i>ap</i>	Nucleoplasm and nucleus, Specific RNA polymerase II transcription factor
<i>ATPsyn-b</i>	Mitochondrion, protontransporting ATP synthase complex
<i>bt</i>	Cytoplasm, structural constituent of cytoskeleton, phosphorylation
<i>Cdc42</i>	GTPase, actin filament polymerization, TGFbeta receptor signalling p/way
<i>CG16974</i>	Not known
<i>CG32245</i>	Not known
<i>CG4532</i>	Actin binding
<i>CG7635</i>	Not known
<i>CG7874</i>	Not known
<i>CG9279</i>	Dynactin complex, microtubule based movement
<i>chic</i>	Actin binding, actin polymerization and/or depolymerization
<i>did</i>	Not known
<i>Dyb</i>	Dystrobrevin complex, cytoskeleton protein binding
<i>en</i>	Nucleus, specific RNA polymerase II transcription factor, repressor
<i>fat-spondin</i>	Extracellular
<i>Fim</i>	Actin binding
<i>GstS1</i>	Cellular component unknown, glutathione peroxidase
<i>Hsp23</i>	Actin binding, heat shock protein
<i>Hsp27</i>	Heat shock protein
<i>klg</i>	Not known
<i>Kr-h1</i>	Nucleus, transcription factor, metamorphosis
<i>LanB2</i>	Basement membrane, histogenesis, organogenesis
<i>lola</i>	Nucleus, RNA polymerase II transcription factor, axonogenesis
<i>lolal</i>	Nucleus, specific RNA polymerase II transcription factor
<i>osa</i>	Nucleus, DNA binding
<i>tomosyn</i>	Synaptic vesicle, syntaxin1 binding, neurotransmitter secretion
<i>trol</i>	Basement membrane, extracellular matrix

Table 8.4a: Genes of Interest upregulated in YCl.8+ cells after ecdysone.

29 genes of interest were identified as upregulated in the YCl.8+ cells after ecdysone when compared to the YCl.8+ cells. 6 genes which were upregulated 1.5 fold or more are indicated in red type.

The genes have been listed alphabetically.

Table 8.4b: Genes of Interest downregulated in YCl.8+ cells after ecdysone

Gene	Gene product: Location and function
<i>Ank</i>	Plasma membrane, cytoskeletal protein binding, cytoskeletal anchoring
<i>Ank2</i>	Plasma membrane, cytoskeletal protein binding, cytoskeletal anchoring
<i>bt</i>	Cytoplasm, structural constituent of cytoskeleton
<i>CalpA</i>	Cytoplasm, actin cytoskeleton organization and biogenesis
<i>CG14762</i>	Not known
<i>CG2955</i>	Structural constituent of cytoskeleton
<i>CG32600</i>	Not known
<i>CG4655</i>	Integral to plasma membrane, calciumdependent cell adhesion molecule
<i>Chd64</i>	Actin binding
<i>Chi</i>	Nucleus, transcription, axon guidance, wing morphogenesis
<i>Chit</i>	Extracellular, chitinase, cuticle chitin catabolism
<i>Cyp4ae1</i>	Membrane, microsomes, cytochrome P450
<i>Cyp9c1</i>	Membrane, microsomes, cytochrome P451
<i>E2f2</i>	Nucleus, RNA polymerase II transcription factor, -ve regulation of DNA
<i>glec</i>	Not known
<i>Hn</i>	Phenylalanine 4monooxygenase, phenylalanine catabolism
<i>ldgf1</i>	Extracellular, imaginal disc growth factor, NOT chitinase
<i>ldgf3</i>	Extracellular, imaginal disc growth factor, NOT chitinase
<i>LamC</i>	Lamin filament, nuclear envelope reassembly
<i>mnd</i>	Amino acid transporter
<i>p53</i>	RNA polymerase II transcription factor, DNA damage response
<i>RhoL</i>	Rho GTPase, fz receptor signalling pathway, cell differentiation
<i>sp1</i>	Nucleus, RNA polymerase II transcription factor
<i>spz</i>	Extracellular, Toll binding, defense response
<i>Strn-Mlck</i>	Calcium/calmodulin dependent protein kinase, cytoskeleton
<i>tgo</i>	nucleus, RNA polymerase II transcription factor, metabolism
<i>toy</i>	Nucleus, specific RNA polymerase II transcription factor
<i>DNasell</i>	Deoxyribonuclease II
<i>fz</i>	Integral to membrane, receptor, Wnt protein binding, epithelial cell polarity
<i>klar</i>	Microtubule associated complex, dynein ATPase, m/tubule movement
<i>ninaA</i>	Cytoplasmic vesicle, integral to plasma membrane
<i>Rca1</i>	Not known
<i>RN-tre</i>	Not known
<i>rux</i>	Nucleus, regulation of cell cycle, regulation of mitosis

Table 8.4b: Genes of Interest downregulated in YCl.8+ cells after ecdysone.

34 genes of interest were identified as downregulated in the YCl.8+ cells after ecdysone when compared to the YCl.8+ cells no ecdysone. 5 genes were downregulated 1.5 fold or more, indicated in red type.

The genes have been listed alphabetically.

Table 8.5a: Genes of Interest upregulated in OCI.8+ cells after ecdysone

Gene	Gene product: Location and function
<i>Abl</i>	Adherens junction, nonmembrane spanning protein tyrosine kinase
<i>Act57B</i>	Actin filament, cytoskeleton
<i>Ank</i>	Plasma membrane, cytoskeletal protein binding, cytoskeletal anchoring
<i>ATPsyn-b</i>	Mitochondrion, protontransporting ATP synthase complex
<i>bnl</i>	Extracellular, FGF receptor binding, FGF receptor signalling
<i>brat</i>	rRNA metabolism
<i>bt</i>	Cytoplasm, structural constituent of cytoskeleton, phosphorylation
<i>CG32245</i>	Not known
<i>CG7800</i>	Not known
<i>CG7874</i>	Not known
<i>Chd64</i>	Actin binding
<i>ct</i>	Nucleus, specific RNA polymerase II transcription factor, cell fate commitment
<i>Cyp6a8</i>	Membrane, microsomes, cytochrome P450
<i>dlg1</i>	Membrane, cytoskeleton, cell proliferation
<i>Dr</i>	Nucleus, specific RNA polymerase II transcription factor,
<i>Eip63F-1</i>	Cytoplasm, nucleus, plasma membrane, calcium ion binding
<i>en</i>	Nucleus, RNA polymerase II transcription factor, transcriptional repressor
<i>eya</i>	Nucleus, hydrolase, transcription, eyeantennal disc metamorphosis
<i>fat-spondin</i>	Extracellular
<i>Fim</i>	Actin binding
<i>fln</i>	Muscle fiber, striated muscle thick filament
<i>fz</i>	Transmembrane receptor, Wnt protein binding, fz receptor signalling p/way
<i>gl</i>	Nucleus, RNA polymerase II transcription factor, photoreceptor development
<i>glec</i>	Not known
<i>Glt</i>	Basement membrane, calcium ion binding
<i>GstS1</i>	Cellular component unknown, glutathione peroxidase
<i>Hsp23</i>	Actin binding, heat shock protein
<i>Hsp27</i>	Heat shock protein
<i>Idgf3</i>	Extracellular, imaginal disc growth factor, NOT chitinase
<i>klg</i>	Not known
<i>Kr-h1</i>	Nucleus, transcription factor, metamorphosis
<i>lolal</i>	Nucleus, specific RNA polymerase II transcription factor
<i>mnd</i>	Amino acid transporter
<i>osa</i>	Nucleus, DNA binding
<i>Pvf1</i>	Cytoplasm, extracellular, receptor binding
<i>Pxn</i>	Extracellular matrix, peroxidase
<i>Rapgap1</i>	RAS GTPase activator
<i>sda</i>	Membrane, alanyl aminopeptidase
<i>Sh</i>	Integral to membrane, voltage gated potassium channel complex,
<i>spz</i>	Extracellular, Toll binding, defense response
<i>sqd</i>	Chromatin, nucleus, ribonucleoprotein complex
<i>stil</i>	Oogenesis

<i>Tak1</i>	MAP protein kinase, JNK cascade, signal transduction, apoptosis
<i>tomosyn</i>	Synaptic vesicle, syntaxin1 binding, neurotransmitter secretion
<i>trol</i>	Basement membrane, extracellular matrix

Table 8.5a: Genes of Interest upregulated in OCl.8+ cells after ecdysone.

46 genes of interest were identified as upregulated in the OCl.8+ cells after ecdysone when compared to the OCl.8+ cells no ecdysone. 13 genes which were upregulated 1.5 fold or more are indicated in red type.

Table 8.5b: Genes of Interest downregulated in OCl.8+ cells after ecdysone

Gene	Gene product: Location and function
<i>Ank</i>	Plasma membrane, cytoskeletal protein binding, cytoskeletal anchoring
<i>CG7800</i>	Not known
<i>Chd64</i>	Actin binding
<i>ct</i>	Nucleus, specific RNA polymerase II transcription factor, cell fate
<i>Cyp6a8</i>	Membrane, microsomes, cytochrome P450
<i>Eip63F-1</i>	Cytoplasm, nucleus, plasma membrane, calcium ion binding
<i>fln</i>	Muscle fiber, striated muscle thick filament
<i>fz</i>	Transmembrane receptor, Wnt protein binding, epithelial cell polarity
<i>glec</i>	Not known
<i>ldgf3</i>	Extracellular, imaginal disc growth factor, NOT chitinase
<i>mnd</i>	Amino acid transporter
<i>Pvf1</i>	Cytoplasm, extracellular, receptor binding
<i>sda</i>	Membrane alanyl aminopeptidase
<i>Sh</i>	Integral to membrane, voltage gated potassium channel complex
<i>spz</i>	Extracellular, Toll binding, defense response
<i>stil</i>	Oogenesis
<i>Tak1</i>	MAP protein kinase, JNK cascade, signal transduction, apoptosis

Table 8.5b: Genes of Interest downregulated in OCl.8+ cells after ecdysone.

17 genes of interest were identified as downregulated in the OCl.8+ cells after ecdysone when compared to the OCl.8+ cells no ecdysone. Only 3 genes were downregulated 1.5 fold or more, indicated in red type.

Table 8.6a: Genes of Interest upregulated in ZfeCl.8+ cells after ecdysone

Gene	Gene product: Location and function
<i>Abl</i>	Adherens junction, nonmembrane spanning protein tyrosine kinase
<i>Act57B</i>	Actin filament, cytoskeleton
<i>Antp</i>	Nucleus, regulation of transcription, segment specification
<i>ap</i>	Nucleoplasm and nucleus. RNA polymerase II transcription factor
<i>ATPsyn-b</i>	Mitochondrion, proton transporting ATP synthase complex
<i>brat</i>	rRNA metabolism
<i>bt</i>	Cytoplasm, structural constituent of cytoskeleton, phosphorylation
<i>cdi</i>	Protein kinase
<i>cg</i>	Nucleus, transcription factor, wing morphogenesis
<i>CG16974</i>	Not known
<i>CG17184</i>	Not known
<i>CG1826</i>	Not known
<i>CG3210</i>	Microtubule associated complex
<i>CG32245</i>	Not known
<i>CG4532</i>	Actin binding
<i>CG7466</i>	Not known
<i>CG9279</i>	Dynactin complex, microtubule based movement
<i>CLIP-190</i>	Cell cortex, microtubule associated complex, actin and microtubule binding
<i>cry</i>	Cytoplasm, nucleus, Gprotein coupled receptor protein signalling pathway
<i>did</i>	Not known
<i>disco</i>	Nucleus, transcription factor
<i>dlg1</i>	Plasma membrane, cytoskeleton, cell proliferation
<i>Dr</i>	Nucleus, specific RNA polymerase II transcription factor, imaginal disc
<i>E2f</i>	Nucleus, transcription factor, +ve regulation of proliferation
<i>en</i>	Nucleus, specific RNA polymerase II transcription factor, repressor
<i>eya</i>	Nucleus, hydrolase, transcription, eyeantennal disc metamorphosis
<i>fat-spondin</i>	Extracellular
<i>gl</i>	Nucleus, specific RNA polymerase II transcription factor
<i>GstS1</i>	Cellular component unknown, glutathione peroxidase
<i>Gug</i>	Cytoplasm, nucleus, transcription co-repressor, leg morphogenesis
<i>Hsp23</i>	Actin binding, heat shock protein
<i>Hsp27</i>	Heat shock protein
<i>klar</i>	Microtubule associated complex, dynein ATPase, m/t based movement
<i>klg</i>	Not known
<i>Klp31E</i>	Cytoplasm, kinesin complex, microtubulebased movement
<i>Kr-h1</i>	Nucleus, transcription factor, metamorphosis
<i>Lap1</i>	RAS interactor
<i>lola</i>	Nucleus, RNA polymerase II transcription factor, axonogenesis
<i>lolal</i>	Nucleus, specific RNA polymerase II transcription factor
<i>Med</i>	Cytoplasm, nucleus, DNA binding, TGFbeta receptor, cell proliferation
<i>N</i>	Transmembrane receptor, transcriptional activator, cell adhesion
<i>osa</i>	Nucleus, DNA binding
<i>phl</i>	Cytoplasm, diacylglycerol binding, RAS protein signal transduction

<i>Rapgap1</i>	RAS GTPase activator
<i>Rbf</i>	Nucleus, DNA binding, cell cycle, negative regulation of cell proliferation
<i>rdgB</i>	Integral to p. membrane, calcium ion binding, calcium transporting ATPase
<i>ssh</i>	MAP kinase phosphatase, dephosphorylation, actin poly/depolymerization
<i>Su(dx)</i>	Ubiquitin protein ligase, N receptor signalling pathway, ubiquitin cycle
<i>Toll-6</i>	Integral to membrane, transmembrane receptor, signal transduction
<i>Toll-7</i>	Integral to membrane, transmembrane receptor, signal transduction
<i>tomosyn</i>	Synaptic vesicle, syntaxin1 binding, neurotransmitter secretion
<i>Tor</i>	Phosphatidylinositol 3kinase, positive regulation of cell growth & size
<i>trol</i>	Basement membrane, extracellular matrix
<i>ttk</i>	Nucleus, polytene chromosome, transcriptional repressor
<i>usp</i>	Nucleus, DNA binding, ecdysteroid hormone receptor, transcription factor

Table 8.6a: Genes of Interest upregulated in ZfeCl.8+ cells after ecdysone.

55 genes of interest were identified as upregulated in the ZfeCl.8+ cells after ecdysone when compared to the ZfeCl.8+ cells no ecdysone. 17 genes which were upregulated 1.5 fold or more are indicated in red type.

Table 8.6b: Genes of Interest downregulated in ZfeCl.8+ after ecdysone

Gene	Gene product: Location and function
<i>bt</i>	Cytoplasm, structural constituent of cytoskeleton, phosphorylation
<i>CG10824</i>	Not known
<i>CG12009</i>	Not known
<i>CG3121</i>	Microtubule associated complex, microtubule binding
<i>CG4655</i>	Integral to plasma membrane, calciumdependent cell adhesion molecule
<i>CG5308</i>	Not known
<i>CG6059</i>	Not known
<i>CG7051</i>	Cytoplasmic dynein complex, microtubule based movement
<i>CG7252</i>	Structural constituent of peritrophic membrane
<i>CG7298</i>	Structural constituent of peritrophic membrane
<i>Chd64</i>	Actin binding
<i>Chit</i>	Extracellular, chitinase, cuticle chitin catabolism
<i>Cyp4d8</i>	Membrane, microsomes, cytochrome P450
<i>Cyp6a8</i>	Membrane, microsomes, cytochrome P450
<i>Cyp9c1</i>	Membrane, microsomes, cytochrome P450
<i>DNasell</i>	Deoxyribonuclease II
<i>Gug</i>	Cytoplasm, nucleus, transcription co-repressor, leg morphogenesis
<i>Hn</i>	Phenylalanine 4monooxygenase, phenylalanine catabolism
<i>ldgf1</i>	Extracellular, imaginal disc growth factor, NOT chitinase
<i>ImpL1</i>	Extracellular
<i>mnd</i>	Amino acid transporter

<i>Oda</i>	Ornithine decarboxylase inhibitor, cell differentiation
<i>Prm</i>	Striated muscle thick filament
<i>rux</i>	Nucleus, regulation of cell cycle, regulation of mitosis
<i>sp1</i>	Nucleus, RNA polymerase II transcription factor
<i>Stim</i>	Plasma membrane, cell adhesion

Table 8.6b: Genes of Interest downregulated in ZfeCl.8+ cells after ecdysone

26 genes of interest were identified as downregulated in the ZfeCl.8+ cells after ecdysone when compared to the ZfeCl.8+ cells no ecdysone. 5 genes were downregulated 1.5 fold or more, indicated in red type.

Table 8.7a: Genes of Interest upregulated in Cl.8R cells after ecdysone

Gene	Gene product: Location and function
<i>Abl</i>	Adherens junction, nonmembrane spanning protein tyrosine kinase
<i>Antp</i>	Nucleus, regulation of transcription, segment specification
<i>ATPsyn-b</i>	Mitochondrion, protontransporting ATP synthase complex
<i>bt</i>	Cytoplasm, structural constituent of cytoskeleton, phosphorylation
<i>cdi</i>	Protein kinase
<i>cg</i>	Nucleus, transcription factor, wing morphogenesis
<i>CG11870</i>	protein serine/threonine kinase, protein amino acid phosphorylation
<i>CG16974</i>	Not known
<i>CG17184</i>	Not known
<i>CG3210</i>	Microtubule associated complex
<i>CG32245</i>	Not known
<i>CG9279</i>	Dynactin complex, microtubule based movement
<i>CLIP-190</i>	Cell cortex, microtubule associated complex, actin & microtubule binding
<i>crb</i>	Integral to membrane, zonula adherens assembly and maintenance
<i>did</i>	Not known
<i>dlg1</i>	Plasma membrane, cytoskeleton, cell proliferation, epithelial morphogenesis
<i>Dr</i>	Nucleus, specific RNA polymerase II transcription factor
<i>en</i>	Nucleus, specific RNA polymerase II transcription factor, repressor
<i>eya</i>	Nucleus, hydrolase, transcription, eyeantennal disc metamorphosis
<i>Gasp</i>	Chitin binding, structural constituent of peritrophic membrane
<i>klar</i>	Microtubule associated complex, dynein ATPase, m/t based movement
<i>klg</i>	Not known
<i>Klp31E</i>	Cytoplasm, kinesin complex, microtubulebased movement
<i>Lap1</i>	RAS interactor
<i>lola</i>	Nucleus, RNA polymerase II transcription factor, axonogenesis
<i>mask</i>	Structural constituent of cytoskeleton, cell growth/ maintenance, proliferation
<i>osa</i>	Nucleus, DNA binding
<i>Pbprp2</i>	extracellular, phenylalkylamine binding

<i>PeritrophinA</i>	Chitin binding, structural constituent of peritrophic membrane
<i>phl</i>	Cytoplasm, diacylglycerol binding, RAS protein signal transduction
<i>pnut</i>	Apical plasma membrane, actin and microtubule binding, cytokinesis
<i>Pxn</i>	extracellular matrix, peroxidase
<i>Rbf</i>	Nucleus, DNA binding, cell cycle, negative regulation of cell proliferation,
<i>rho</i>	Golgi apparatus, positive regulation of EGF receptor signaling pathway
<i>Toll-7</i>	Integral to membrane, transmembrane receptor, signal transduction
<i>tomosyn</i>	Synaptic vesicle, syntaxin1 binding, neurotransmitter secretion
<i>Tor</i>	Phosphatidylinositol 3kinase, positive regulation of cell growth and cell size
<i>trol</i>	Basement membrane, extracellular matrix
<i>ttk</i>	Nucleus, polytene chromosome, RNA polymerase II transcription factor

Table 8.7a: Genes of Interest upregulated in Cl.8R cells after ecdysone

39 genes of interest were identified as upregulated in the Cl.8R cells after ecdysone when compared to the Cl.8R cells no ecdysone. 13 genes which were upregulated 1.5 fold or more are indicated in red type.

Table 8.7b: Genes of Interest downregulated in Cl.8R cells after ecdysone

Gene	Gene product: Location and function
<i>blot</i>	Integral to membrane, n-transmitter transporter, epithelial morphogenesis
<i>CG5308</i>	Not known
<i>CG7051</i>	Cytoplasmic dynein complex, microtubule based movement
<i>DNasell</i>	Deoxyribonuclease II
<i>EcR</i>	Nucleus, ecdysteroid hormone receptor, RNA polymerase I transcription factor
<i>Hn</i>	Phenylalanine 4monooxygenase, eye pigment
<i>so</i>	Nucleus, RNA polymerase II transcription factor

n=neurotransmitter

Table 8.7b: Genes of Interest downregulated in Cl.8R cells after ecdysone

7 genes of interest were identified as downregulated in the Cl.8R cells after ecdysone when compared to the Cl.8R cells no ecdysone. No genes were downregulated 1.5 fold or more.

Table 8.8a: Genes of Interest upregulated in OCl.8+ cells after ecdysone

Gene	Gene product: Location and function
<i>Abl</i>	Adherens junction, nonmembrane spanning protein tyrosine kinase

Act57B	Actin filament, cytoskeleton organization
ago	Ubiquitinprotein ligase, regulation of mitosis
AGO2	Translation initiation factor
arr	Plasma membrane, receptor, Wnt receptor signalling pathway
ATPsyn-b	Mitochondrion, hydrogen transport
bt	Cytoplasm, myosin light chain kinase, phosphorylation
CAP	Focal adhesion, vinculin binding
caps	Membrane, cell adhesion molecule
cg	Nucleus, transcription factor, wing morphogenesis
CG10971	Actin binding
CG11870	protein serine/threonine kinase, phosphorylation
CG17184	Not known
CG3210	Microtubule associated complex
CG32245	Not known
CG3622	Metalloendopeptidase
CG4532	Actin binding
CG6522	Not known
CG7466	Not known
CG9248	Not known
CG9279	Dynactin complex, microtubule based movement
CLIP-190	Cell cortex, Golgi apparatus, actin and microtubule binding
cry	Cytoplasm, G protein coupled receptor protein signalling pathway
Cyp1	Nuclear cyclin dependent kinase holoenzyme complex, protein folding
Cyp6a22	Membrane, microsomes, cytochrome P450
Ddc	Aromatic L-amino acid decarboxylase, eclosion rhythm
did	Not known
DI	Integral to membrane, Notch binding, signal transducer, cell adhesion
dlg1	Plasma membrane, cytoskeleton, proliferation, epithelial morphogenesis
dp	Extracellular matrix
Dr	Nucleus, specific RNA polymerase II transcription factor
en	Nucleus, RNA polymerase II transcription factor, transcriptional repressor
eya	Nucleus, hydrolase, transcription, eye antennal disc metamorphosis
Fmr1	Cytoplasm, mRNA binding, negative regulation of translation
Gasp	Chitin binding, structural constituent of peritrophic membrane
Glt	Basement membrane, calcium ion binding
hdc	Cytoplasm, cell differentiation
heix	Integral to membrane
Hr39	Nucleus, DNA binding, liganddependent nuclear receptor
Hsp23	Actin binding, heat shock protein
Hsp26	Heat shock protein
Hsp27	Heat shock protein
Idgf1	Extracellular, imaginal disc growth factor, NOT chitinase
Idgf2	Extracellular, imaginal disc growth factor, NOT chitinase
klg	Not known
Klp61F	Cytoplasm, kinesin complex, microtubule based movement
Lap1	RAS interactor
LIMK1	Serine/threonine kinase, actin cytoskeleton organization & biogenesis

<i>Lnk</i>	Not known
<i>lola</i>	Nucleus, RNA polymerase II transcription factor, axonogenesis
<i>lolal</i>	Nucleus, specific RNA polymerase II transcription factor
<i>mask</i>	Structural constituent of cytoskeleton, cell proliferation
<i>Med</i>	Nucleus, TGFbeta receptor, transcription factor, cell proliferation
<i>N</i>	Transmembrane receptor, transcriptional activator, cell adhesion
<i>Nup154</i>	Nuclear pore
<i>osa</i>	Nucleus, DNA binding
<i>Pbprp2</i>	Extracellular, phenylalkylamine binding
<i>Peritrophin-A</i>	Chitin binding, structural constituent of peritrophic membrane
<i>phl</i>	Cytoplasm, extrinsic to plasma membrane, RAS protein signal transduction
<i>Phm</i>	peptidylglycine monooxygenase
<i>pnut</i>	Apical plasma membrane, actin/microtubule binding, cytokinesis
<i>Prm</i>	Striated muscle thick filament
<i>Pxn</i>	Extracellular matrix, peroxidase
<i>raw</i>	Elongation of leading edge cells, regulation of JNK cascade
<i>Rbf</i>	Nucleus, DNA binding, negative regulation of cell proliferation, cell cycle
<i>RfaBp</i>	Structural molecule, fatty acid binding, microtubule binding
<i>RhoL</i>	Rho small monomeric GTPase
<i>rols</i>	Cytoplasm, myoblast fusion
<i>shi</i>	Plasma membrane, actin/microtubule binding, synaptic vesicle endocytosis
<i>Toll-7</i>	Integral to membrane, receptor, signal transduction, defense response
<i>Tom</i>	Cell fate specification, N receptor signaling pathway
<i>tomosyn</i>	Synaptic vesicle, syntaxin1 binding, neurotransmitter secretion
<i>trol</i>	Basement membrane, extracellular matrix
<i>Tsp86D</i>	Integral to membrane
<i>Tsp96F</i>	Integral to membrane
<i>ttk</i>	Nucleus, RNA polymerase II transcription factor, transcriptional repressor
<i>tty</i>	Not known
<i>usp</i>	Nucleus, DNA binding , Ecdysteroid hormone receptor, transcription factor

Table 8.8a: Genes of Interest upregulated in OCl.8+ cells after ecdysone.

78 genes of interest were identified as upregulated in the OCl.8+ cells after ecdysone when compared to the YCl.8+ cells after ecdysone . 41 genes which were upregulated 1.5 fold or more are indicated in red type.

Table 8.8b: Genes of Interest downregulated in OCl.8+ cells after ecdysone

Gene	Gene product: Location and function
<i>asp</i>	Microtubule associated complex, microtubule binding
<i>blot</i>	Integral to membrane, neurotransmitter transporter
<i>brat</i>	rRNA metabolism
<i>CG14991</i>	Not known
<i>CG5308</i>	Not known
<i>CG7298</i>	Structural constituent of peritrophic membrane
<i>CG7366</i>	Not known
<i>CG7874</i>	Not known
<i>cul-2</i>	Nuclear ubiquitin ligase complex
<i>Cyp4d8</i>	Membrane, microsomes, cytochrome P450
<i>dm</i>	Nucleus, transcription factor, +ve regulation of cell growth, cell cycle
<i>Doa</i>	Cytoplasm, nucleus, bristle morphogenesis,
<i>EcR</i>	Nucleus, DNA binding, ecdysteroid hormone receptor, transcription factor
<i>Egfr</i>	Integral to plasma membrane, EGF receptor, antiapoptosis
<i>Hn</i>	Phenylalanine 4monooxygenase, phenylalanine catabolism
<i>ImpL1</i>	Extracellular
<i>ImpL2</i>	Extracellular, cell adhesion molecule
<i>Lac</i>	Extrinsic to membrane
<i>mth</i>	Integral to membrane, Gprotein coupled receptor, synaptic vesicle
<i>mts</i>	Protein phosphatase type 2A complex, microtubule/chromatin interaction
<i>mus209</i>	deltaDNA polymerase cofactor complex, mitotic spindle assembly
<i>Orc1</i>	Nucleus, DNA replication initiation, gene silencing
<i>p53</i>	DNA binding, RNA polymerase II transcription factor, apoptosis
<i>snf</i>	Nucleus, small nuclear ribonucleoprotein complex, RNA interactions
<i>Tektin-A</i>	Microtubule associated complex, microtubule binding

Table 8.8b: Genes of Interest downregulated in OCl.8+ cells after ecdysone.

25 genes of interest were identified as downregulated in the OCl.8+ cells after ecdysone when compared to the YCl.8+ cells after ecdysone. 9 genes were downregulated 1.5 fold or more, indicated in red type.

Table 8.9a: Genes of Interest upregulated in ZfeCl.8 cells after ecdysone

Gene	Gene product: Location and function
<i>Abl</i>	Adherens junction, nonmembrane spanning protein tyrosine kinase
<i>Act57B</i>	Actin filament, cytoskeleton
<i>Ank2</i>	Plasma membrane, cytoskeletal protein, cytoskeletal anchoring
<i>ATPsyn-b</i>	mitochondrion, hydrogen transport
<i>bt</i>	Cytoplasm, structural constituent of cytoskeleton, phosphorylation
<i>Cg25C</i>	Basement membrane, collagen type IV
<i>CG32245</i>	Not known
<i>CG9279</i>	dynactin complex, microtubule based movement
<i>cul-2</i>	nuclear ubiquitin ligase complex
<i>disco</i>	nucleus, transcription factor
<i>Dr</i>	Nucleus, specific RNA polymerase II transcription factor
<i>Eip74EF</i>	nucleus, specific RNA polymerase II transcription factor, autophagy
<i>en</i>	Nucleus, specific RNA polymerase II transcriptional regulator
<i>eya</i>	Nucleus, hydrolase, transcription, eyeantennal disc metamorphosis
<i>Flo-2</i>	flotillin complex, structural molecule, cell adhesion
<i>ImpL2</i>	extracellular, cell adhesion molecule
<i>klg</i>	Not known
<i>N</i>	Integral to membrane, receptor, transcriptional activator, cell adhesion
<i>osa</i>	nucleus, DNA binding
<i>Pbprp2</i>	extracellular, phenylalkylamine binding
<i>phl</i>	Extrinsic to plasma membrane, protein kinase, RAS signal transduction
<i>Rbf</i>	Nucleus, DNA binding, negative regulation of cell proliferation & cell cycle
<i>rho</i>	Golgi apparatus, regulation EGF receptor signalling pathway & EGF receptor
<i>thr</i>	mitotic chromosome segregation, mitotic sister chromatid separation
<i>tomosyn</i>	synaptic vesicle, syntaxin1 binding, neurotransmitter secretion
<i>trol</i>	basement membrane, extracellular matrix
<i>Unc-76</i>	cytoskeleton, microtubule

Table 8.9a: Genes of Interest upregulated in ZfeCl.8+ cells after ecdysone.

28 genes of interest were identified as upregulated in the ZfeCl.8+ cells after ecdysone when compared to the OCl.8+ cells after ecdysone. 5 genes which were upregulated 1.5 fold or more are indicated in red type.

Table 8.9b: Genes of Interest downregulated in ZfeCl.8 cells after ecdysone

Gene	Gene product: Location and function
<i>Ank</i>	Plasma membrane, spectrosome, cytoskeletal protein binding, anchoring
<i>blot</i>	Membrane, neurotransmitter transporter, epithelial morphogenesis
<i>bun</i>	Cytoplasm, nucleus, RNA polymerase II transcription factor, cell fate
<i>cdc2</i>	Nucleus, cyclindependent protein kinase regulation of cell cycle
<i>CG14762</i>	Not known
<i>CG4655</i>	Integral to plasma membrane, calciumdependent cell adhesion molecule
<i>CG6059</i>	Not known
<i>CG7051</i>	Cytoplasmic dynein complex, microtubule based movement
<i>CG7298</i>	Structural constituent of peritrophic membrane
<i>CG7635</i>	Not known
<i>CG7800</i>	Not known
<i>CG7874</i>	Not known
<i>CG8177</i>	Anion exchanger
<i>CG9313</i>	Cytoplasmic dynein complex, dynein ATPase, microtubule based movement
<i>Chit</i>	Extracellular, chitinase, cuticle chitin catabolism
<i>Cyp4d8</i>	Membrane, microsomes, cytochrome P450
<i>Cyp6a8</i>	Membrane, microsomes, cytochrome P451
<i>dlg1</i>	Membrane, cytoskeleton, proliferation, establishment/maintenance of ecp
<i>DNasell</i>	Deoxyribonuclease II
<i>dp</i>	Extracellular matrix
<i>EcR</i>	Nucleus, ecdysteroid hormone receptor, transcription factor
<i>flw</i>	Protein serine/threonine phosphatase, cell adhesion
<i>fz</i>	Membrane, receptor, Wnt protein binding, establishment of ecp
<i>Gel</i>	Actin filament, actin binding
<i>gro</i>	Nucleus, NOT DNA binding, transcription corepressor
<i>GstS1</i>	Cellular component unknown, glutathione peroxidase
<i>Gug</i>	Cytoplasm, nucleus, transcription co-repressor, leg morphogenesis
<i>Hsp23</i>	Actin binding, heat shock protein
<i>Hsp27</i>	Heat shock protein
<i>Idgf1</i>	Extracellular, imaginal disc growth factor, NOT chitinase
<i>Idgf3</i>	Extracellular, imaginal disc growth factor, NOT chitinase
<i>ImpL1</i>	Extracellular
<i>Jra</i>	Cytoplasm, nucleus, specific RNA polymerase II transcription factor
<i>kal-1</i>	Extracellular matrix
<i>mth</i>	Integral to membrane, receptor, synaptic vesicle exocytosis
<i>mts</i>	Protein phosphatase type 2A complex, microtubule/chromatin interaction
<i>ninaA</i>	Cytoplasmic vesicle, integral to plasma membrane, cyclosporin A binding
<i>Oda</i>	Ornithine decarboxylase inhibitor, cell differentiation
<i>Prm</i>	Striated muscle thick filament
<i>Pvf1</i>	Cytoplasm, extracellular, receptor binding
<i>Rca1</i>	Not known
<i>sax</i>	Membrane, receptor, BMP & TGFbeta and receptor signalling p/way
<i>scb</i>	Membrane, laminin receptor, calcium dependent cell adhesion receptor
<i>scra</i>	Cytoplasm, nucleus, actin & microtubule binding, cellularization, cytokinesis
<i>vanin-like</i>	Extrinsic to membrane, hydrolase, pantetheinase

Table 8.9b: Genes of Interest downregulated in ZfeCl.8+ cells after ecdysone. 45 genes of interest were identified as downregulated in the ZfeCl.8+ cells after ecdysone when compared to the OCl.8+ cells after ecdysone. 11 genes were downregulated 1.5 fold or more, indicated in red type.

Table 8.10a: Genes of Interest upregulated in Cl.8R cells after ecdysone

Gene	Gene product: Location and function
<i>Abl</i>	Adherens junction, nonmembrane spanning protein tyrosine kinase
<i>bt</i>	Cytoplasm, myosin light chain kinase, phosphorylation
<i>bun</i>	Cytoplasm, nucleus, RNA polymerase II transcription factor, cell fate
<i>Cg25C</i>	Basement membrane, collagen type IV
<i>Chd64</i>	Actin binding
<i>Chit</i>	Extracellular, chitinase, cuticle chitin catabolism
<i>disco</i>	Nucleus, transcription factor, brain development, eclosion rhythm,
<i>Doa</i>	Cytoplasm, nucleus, bristle morphogenesis,
<i>Eip55E</i>	Sulphur amino acid metabolism
<i>en</i>	Nucleus, RNA polymerase II transcription factor, transcription regulator
<i>Gel</i>	Cytosol, extracellular, actin filament, actin binding
<i>hdc</i>	Cytoplasm, cell differentiation
<i>ldgf1</i>	Extracellular, imaginal disc growth factor, NOT chitinase
<i>ldgf2</i>	Extracellular, imaginal disc growth factor, NOT chitinase
<i>ldgf3</i>	Extracellular, imaginal disc growth factor, NOT chitinase
<i>ldh</i>	Isocitrate dehydrogenase (NADP+)
<i>klg</i>	Not known
<i>lola</i>	Nucleus, specific RNA polymerase II transcription, axonogenesis
<i>osa</i>	Nucleus, DNA binding
<i>Ppn</i>	Basement membrane, extracellular matrix
<i>Pxn</i>	Extracellular matrix, peroxidase
<i>rho</i>	Golgi apparatus, positive regulation of EGF receptor signalling pathway
<i>RhoL</i>	Rho small monomeric GTPase
<i>stg</i>	Regulation of mitosis
<i>tomosyn</i>	Synaptic vesicle, syntaxin1 binding, neurotransmitter secretion
<i>trol</i>	Basement membrane, extracellular matrix

Table 8.10a: Genes of Interest upregulated in Cl.8R cells after ecdysone

26 genes of interest were identified as upregulated in the Cl.8R cells after ecdysone when compared to the YCl.8+ cells after ecdysone. 12 genes which were upregulated 1.5 fold or more are indicated in red type.

The genes have been listed alphabetically.

Table 8.10b: Genes of Interest downregulated in Cl.8R cells after ecdysone

Gene	Gene product: Location and function
<i>Arc-p34</i>	Arp2/3 protein complex, regulation of actin polymerization
<i>Arp66B</i>	Arp2/3 protein complex, actin filament, cell cycle dependent
<i>blot</i>	Membrane, neurotransmitter transporter, epithelial morphogenesis
<i>Cdc42</i>	GTPase, actin filament polymerization
<i>CG31619</i>	Procollagen Nendopeptidase
<i>CG3960</i>	Cytoskeleton, actin binding
<i>CG6933</i>	Structural constituent of peritrophic membrane
<i>CG7635</i>	Not known
<i>CG7874</i>	Not known
<i>dpld</i>	Not known
<i>drpr</i>	Cell adhesion molecule
<i>Egfr</i>	Integral to plasma membrane, EGF receptor, Antiapoptosis
<i>Eip63E</i>	Cyclindependent protein kinase
<i>emc</i>	Nucleus, negative regulation of transcription, wing vein morphogenesis
<i>fat-spondin</i>	Extracellular
<i>GstS1</i>	Cellular component unknown, glutathione peroxidase
<i>Gug</i>	Cytoplasm, nucleus, transcription co-repressor
<i>Hem</i>	Cytoplasm, plasma membrane, cytoskeleton organization & biogenesis
<i>HLHmbeta</i>	Nucleus, specific transcriptional repressor, N receptor signalling pathway
<i>Hsp23</i>	Actin binding, heat shock protein
<i>Hsp27</i>	Heat shock protein
<i>Impl2</i>	Extracellular, cell adhesion molecule
<i>kek1</i>	Plasma membrane, negative regulation of EGF receptor signalling p/way
<i>mts</i>	Protein phosphatase type 2A complex, mitosis, spindle assembly
<i>Nc</i>	Cytoplasm, caspase2, signalling (initiator) caspase, apoptosis
<i>Nrt</i>	Basolateral plasma membrane, integral to membrane
<i>p120ctn</i>	Adherens junction
<i>poe</i>	Calmodulin binding
<i>Rapgap1</i>	RAS GTPase activator
<i>rux</i>	Nucleus, regulation of cell cycle, regulation of mitosis
<i>spen</i>	Nucleus, axon guidance, glia cell migration
<i>trio</i>	Plasma membrane, Rho protein signal transduction, actin cytoskeleton

Table 8.10b: Genes of Interest downregulated one fold or more in Cl.8R cells after ecdysone

32 genes of interest were identified as downregulated in the Cl.8R cells after ecdysone when compared to the YCl.8+ cells after ecdysone. 14 genes were downregulated 1.5 fold or more.

The genes have been listed alphabetically.

Table 8.13c: Ambiguous gene expression in Cl.8+ cells

Gene	OCI.8+	ZfeCl.8+	Cl.8R
<i>bt</i>	u	amb	amb
<i>CG9279</i>	u	u	amb
<i>Cyp1</i>	u	nc	amb
<i>dlg1</i>	u	nc	amb
<i>Grip84</i>	u	amb	amb
<i>klar</i>	u	amb	amb
<i>lola</i>	u	amb	amb
<i>sqd</i>	u	amb	amb
<i>Su(dx)</i>	u	amb	amb
<i>Tor</i>	u	nc	amb
<i>lolal</i>	u	amb	d
<i>pnut</i>	u	amb	d
<i>Toll-7</i>	u	u	nc zero
<i>CG32245</i>	u	amb	u
<i>for</i>	u	amb	u
<i>Tsp96F</i>	u	nc	us
<i>RhoL</i>	u	d	us
<i>HLHmbeta</i>	nc	d	amb
<i>r</i>	nc	amb	d
<i>CG3960</i>	d	amb	d
<i>CG7298</i>	d	amb	d
<i>mus304</i>	d	amb	d s
<i>Rca1</i>	d	d	na
<i>EcR</i>	d	amb	amb
<i>mnd</i>	amb	d	amb
<i>sno</i>	amb	d	amb
<i>dpld</i>	amb	amb	d
<i>ap</i>	amb	u	u
<i>rho</i>	amb	u	u
<i>Thor</i>	amb	amb	u

Table 8.13c: Ambiguous gene expression in Clone 8+ cells

30 genes of interest were identified where the microarray data was ambiguous or not available in all three cell lines.

amb, ambiguous; d, downregulated; ds, small negative change; nc, no change;

u, upregulated; us, small positive change; N/D, no data

Chapter 9

x-gal staining

Staining solutions for X-gal

X-gal solution (5-bromo-4-chloro-3-indolyl- β -D-galctopyranoside)

8%: 8mg /100 μ l dimethylformamide

(kept refrigerated for up to 3 days in glass container)

Fe/Na P staining buffer

	g/100ml
1.8ml 0.2M Na ₂ HPO ₄	2.84
0.7 ml 0.2M NaH ₂ PO ₂	2.4
1.5ml 5M NaCl	29.22
50 μ l 1MgCl ₂	20.33
305 μ l 500mM K ₃ Fe(CN) ₆	16.46
305 μ l 500mM K ₄ Fe CN ₆	21.12
45.34ml distilled H ₂ O	

Staining solution

25 μ l X-gal solution was added to 1ml of staining buffer.